ORNL
MASTER COPY

EXTERNAL TRANSMITTAL AUTHORIZED

ORNL
Central Files Number
60-10-63

100

PRELIMINARY DESIGN OF A 10-Mw(t) PEBBLE-BED REACTOR EXPERIMENT

NOTICE

This document contains information of a preliminary nature and was prepared primarily for internal use at the Oak Ridge National Laboratory. It is subject to revision or correction and therefore does not represent a final report. The information is not to be abstracted, reprinted or otherwise given public dissemination without the approval of the ORNL patent branch, Legal and Information Control Department.

OAK RIDGE NATIONAL LABORATORY
operated by
UNION CARBIDE CORPORATION
for the
U.S. ATOMIC ENERGY COMMISSION

LEGAL NOTICE

This report was prepared as an account of Government sponsored work. Neither the United States, nor the Commission, nor any person acting on behalf of the Commission:

A. Makes any warranty or representation, expressed or implied, with respect to the accuracy, completeness, or usefulness of the information contained in this report, or that the use of any information, apparatus, method, or process disclosed in this report may not infringe privately owned rights; or

B. Assumes any liabilities with respect to the use of, or for damages resulting from the use of any information, apparatus, method, or process disclosed in this report.

As used in the above, "person acting on behalf of the Commission" includes any employee or contractor of the Commission, or employee of such contractor, to the extent that such employee or contractor of the Commission, or employee of such contractor prepares, disseminates, or provides access to, any information pursuant to his employment or contract with the Commission, or his employment with such contractor.

ORNL
Central Files Number
60-10-63

External Distribution Authorized

Contract No. W-7405-eng-26

PRELIMINARY DESIGN OF A 10-Mw(t) PEBBLE-BED REACTOR EXPERIMENT

Staff

Oak Ridge National Laboratory

DATE ISSUED
NOV - 1 1960

OAK RIDGE NATIONAL LABORATORY
Oak Ridge, Tennessee
operated by
UNION CARBIDE CORPORATION
for the
U. S. ATOMIC ENERGY COMMISSION

CONTENTS

1. SUMMARY 1.1
2. INTRODUCTION 2.1
3. SELECTION OF REACTOR CORE GEOMETRY 3.1
4. SELECTION OF PLANT CONFIGURATION 4.1
   Plant Requirements 4.1
      Horizontal Versus Vertical Position for Core and Steam Generators 4.2
      Pressure Vessel Envelope Integrity 4.5
      Access for Operation, Inspection, and Maintenance 4.6
      Construction Costs 4.8
   Proposed Configurations 4.8
5. PROPOSED REACTOR 5.1
   Graphite Structure 5.1
   Control Rods 5.4
   Pressure Vessel and Support Structure 5.4
   Viewing Provisions 5.6
   Pressure-Vessel Cooling and Thermal Insulation 5.6
   Shield Plugs 5.7
   Closure Flanges 5.7
6. PROPOSED PLANT 6.1
   Design Data 6.1
   Site Selection 6.3
   Plant Layout 6.5
      Reactor Area 6.5
      Turbine-Generator Bay 6.11
      Main Control Room 6.13
      Administrative Wing and Service Bay 6.14
      Holding Pond for Low-Activity-Level Waste 6.14
   System Leaktightness Requirements 6.15
   Shielding 6.16
7. REACTOR PHYSICS 7.1
   Core Dimensions and Fuel Loading 7.1
   Fast Flux Distribution 7.3

Reactivity Effects 7.4

Control Blades 7.7

Power and Flux Distributions 7.9

Reflector Heat Load 7.9

Gamma Heating in Pressure Vessel 7.11

Neutron Lifetime 7.11

8. FUEL ELEMENTS AND GRAPHITE COMPONENTS 8.1

Fuel Elements 8.1

Sanderson & Porter Program 8.2

Property Evaluations and Effects of Irradiation 8.4

Fission-Gas Retention 8.17

Graphite Components 8.33

Pebble-Bed Container 8.33

Reflector 8.35

Reflector Perimeter 8.35

Conclusions 8.35

9. STRUCTURAL ANALYSIS OF GRAPHITE REFLECTOR 9.1

Stress Analysis 9.1

Interpretation of the Results 9.3

Estimated Friction Forces and Sleeve Interferences for Various Modes of Deformation and Fracture 9.10

10. CORE HEAT TRANSFER, PRESSURE DROP, AND TEMPERATURE DISTRIBUTION 10.1

Nomenclature 10.1

Basic Relations 10.2

Typical Values 10.3

Simplified Approach to Investigation of the Hot-Spot Problem 10.5

Relations Between Maximum Surface Temperature, Power Density, and Pumping Power Requirements 10.11

Cores with Constant Voidage 10.11

11. NUCLEAR CONTROL AND SAFETY SYSTEMS 11.1

Safety System 11.1

Nuclear Control System 11.5

Further Analysis 11.6

12. STEAM GENERATOR 12.1

General Considerations in the Selection of a Heat-Removal System 12.1

Design Requirements 12.2

Steam Conditions and Steam Generator Type 12.3

Steam Generator Geometry 12.5

Detail Design Considerations 12.8

Leak Detection and Maintenance Procedures 12.12

Costs 12.14

13. BLOWERS 13.1

14. FUEL-HANDLING SYSTEM 14.1

Design Precepts 14.1

Fuel-Discharge System 14.2

Fuel-Loading System 14.11

15. SERVICING EQUIPMENT AND PROCEDURES 15.1

Design Precepts 15.2

Servicing Equipment 15.5

Servicing Operations 15.6

Cost Estimates 15.9

16. HELIUM PURIFICATION SYSTEM 16.1

System Components 16.1

Fission-Product Delay Trap 16.1

Chemical Purification Train 16.1

Particle Filters 16.2

System Flowsheet 16.3

Operation and Maintenance 16.7

17. DECONTAMINATION PROCEDURES AND FACILITIES 17.1

Chemical Treatment 17.1

Decontamination Procedures 17.2

Equipment Required 17.4

18. STEAM SYSTEM 18.1

Used Equipment Available 18.1

Arrangements Considered 18.1

Recommended System 18.2

19. HAZARDS ANALYSIS 19.1
Escape of Fission-Product Activity from the Fuel Element 19.1
Hazards Associated with Gas Leakage 19.11
Hazard Associated with Rupture of Primary System 19.14
Radiation Level with Shielding 19.17
Radiation Level Without Shielding 19.19
Natural-Circulation Cooling 19.20
Heat Exchanger Tube Rupture 19.23
Hazards Summary and Conclusion 19.24
Maximum Credible Accident 19.24
Normal Activity Release 19.24
Direct Radiation Dose Rates from Reactor Components 19.26
Other Conditions 19.26
20. RESEARCH AND DEVELOPMENT 20.1
Fuel Element Development 20.1
Coated Particle Evaluation 20.2
Fuel Sphere Fabrication and Evaluation 20.3
Fuel Reprocessing 20.4
Development of Graphite Components 20.5
Graphite Shrinkage Cracking 20.5
Core Cooling Problems 20.5
Helium Containment and Fuel Handling 20.6
Helium Purification 20.7
Maintenance Procedures 20.8
Summary of Research and Development Costs 20.9
21. CONSTRUCTION COSTS 21.1
Reactor Building 21.1
Reactor 21.5
Possible Reductions in Construction Costs 21.6
Fuel Fabrication Costs 21.9
BIBLIOGRAPHY

1. SUMMARY

The objectives of this study have been to examine the problems of the pebble-bed reactor concept and to conceive a design of a facility for investigating the feasibility of this type of reactor. The design must provide for adequate leaktightness of the contaminated-gas system and adequate maintenance of contaminated components, the most vital feasibility questions of the concept. At the outset it was established that the facility should be as inexpensive as possible consistent with the requirements that it should provide for thorough testing of the fuel elements, fuel-handling equipment, and cooling-gas cleanup equipment under conditions suitable for a prototype plant. The facility should further provide for inspection and maintenance operations, including core graphite replacement and decontamination of components, such as blowers, even after substantial amounts of contamination had been distributed throughout the system. Means for carrying out inspection and maintenance are considered essential, since otherwise an unforeseen difficulty might arise which could not even be diagnosed, let alone repaired or corrected.

Only seven weeks were available to examine the problems, conceive a design, and prepare this report. The solution of many problems could not even be attempted, and it is difficult to say with confidence to what extent the proposed design could be improved, whether space allocations are adequate or overly generous, or what the costs would be. Thus the design must be considered as tentative and likely to be subject to extensive revision.

The proposed design is for a reactor which could be operated at a thermal power generation level of up to 10 Mw. It has a core diameter of 18 in., a core height of 8 ft, and a 3-ft-thick graphite reflector surrounding the core at the sides and at the ends. The core consists of 1 1/2-in.-diam balls containing about the same total concentration of uranium plus thorium as that required for a full-scale reactor, but

the proportion of uranium is higher to sustain criticality in the smaller core. Since the graphite shrinkage-cracking problem is severe in high-power-density cores, the pressure vessel has been designed to allow replacement of that portion of the graphite most subject to radiation damage. This graphite is in the form of concentric cylindrical sleeves 2 in. thick which enclose the core and constitute the inner 6 in. of the reflector. The gas system is designed to supply helium at a pressure of 1000 psi with a core inlet temperature of 550°F and a core outlet temperature of 1250°F. The gas system configuration was chosen to assure removal of afterheat by thermal convection and to provide good cooling of the entire pressure envelope so as to maintain its temperature between 550 and 650°F under all conditions of operation.

A steam generator designed to deliver steam at 1000°F and 1000 psi is provided to remove heat. Consideration was given to the alternatives of employing the steam for driving a 3-Mw turbine generator or dumping the heat to a water-cooled or air-cooled condenser. It was apparent early in the study that the generation of electricity could not be justified economically.

Full-pressure containment of the reactor gas is provided. In addition, gas-tight rooms surround all flanged joints in the gas system to minimize dispersal of activity in the event of a leak and during servicing operations.

The tentative reactor site chosen for this study to facilitate cost estimates is close to the present Experimental Gas-Cooled Reactor (EGCR) at Oak Ridge, Tennessee, so that advantage can be taken of the road and services provided for the EGCR.

During the course of the study it became apparent that a number of important research and development problems would have to be solved before a firm Title I design for a pebble-bed reactor experiment could be prepared. For example, no fuel element has been adequately demonstrated to date. A considerable amount of research is still required on fuel-ball design and fabrication, including (1) the determination of the

magnitude and character of fission-product release rates at high burnups and at a temperature at least 500°F higher than the 1500°F used for the single fuel element that has been extensively tested, (2) the development and testing of other fuel compositions, for example, high-temperature pyrolytic graphite-coated particles instead of the Al_2O_3 or the low-temperature pyrolytic carbon-coated particles used to date, (3) the evaluation of various means for coating the fuel elements to inhibit oxidation, and (4) the establishment of reasonable fuel-ball integrity (resistance to impact and abrasion) under the conditions of temperature, gas flow, ball movement, and ball handling to be expected in the reactor. The nature and extent of fission-product deposition on the pipe walls and equipment making up the helium-circulation system must be determined, along with decontamination procedures for removing the activity. Greater knowledge is needed with respect to ball movement, gas flow distribution, and temperature distribution in the reactor core. Much work will be required to develop a fuel-handling system capable of reliable remote operation. In addition, a system of valves or locks is required which will allow fuel movement in and out of the high-pressure reactor while maintaining extreme tightness with respect to outleakage of activity. The system also must be amenable to reasonable dismantling and decontamination procedures. The cost of a minimal research and development program will probably be between $5,000,000 and $8,000,000. Development of a fuel reprocessing facility, if desired, would cost between $1,000,000 and $3,000,000 additional.

It is difficult to estimate the construction cost for any reactor, and in this instance the uncertainties are compounded by the absence of detailed designs for the important items of equipment and by major uncertainties associated with the results to be expected from the research and development program. The reactor construction cost was estimated by listing the major cost items for both the EGCR and the proposed Pebble-Bed Reactor Experiment (PBRE); assigning weight, volume, capacity, or area values to each component of the two reactors; and scaling the PBRE costs from the EGCR costs. With the above qualifications, these preliminary estimates indicate that the cost of construction of the proposed PBRE might be between $8,000,000 and $9,000,000.

2. INTRODUCTION

Sanderson & Porter have carried out a series of design studies over the past four years which indicate that the pebble-bed reactor concept may be an attractive way to obtain low-cost power. Recent in-pile tests of 1 1/2-in.-diam spherical fuel elements irradiated at temperatures from 1300 to 1500°F have indicated that the fission-product release from the fuel elements may be considerably lower than previously expected. At the request of the AEC, ORNL has, with the assistance of Sanderson & Porter, studied the problems of a small reactor experiment which would permit the evaluation of this concept.

The design proposed is aimed at a system which should permit higher operating temperature and better conversion ratio than in the EGCR at the cost of accepting a contaminated-cooling-gas system. It would differ from the Dragon and the HTGR in that it would offer a simplified fuel-handling system with a good potential for on-stream loading, and it would not have a complex system for aspiration of the fuel elements to reduce fission-product contamination of the cooling gas. The PBRE would differ from the Turret reactor experiment in that the fuel-handling operation would be simplified, and moving parts would be eliminated from the core. The proposed operating temperature is lower than that for the Turret experiment, and the anticipated gas-contamination level would be about that expected in the Dragon and HTGR reactors rather than that expected for the Turret experiment.

The Sanderson & Porter work was reviewed carefully, with particular attention to results of studies on ball fabrication and testing, ball flow through core models, reactor designs, core configurations, core heat transfer and gas pressure drop, and system configurations. On the basis of this work and in consultation with Sanderson & Porter, the reactor inlet and outlet gas temperatures, power density, ball size, core geometry, gas system pressure level, and gas system pressure envelope operating temperature were established.

The extensive ORNL advanced design work on all-ceramic gas-cooled reactors was reviewed in the light of the Sanderson & Porter studies.

It was found that estimates of the uranium and thorium concentrations in the core and the core pressure drop were consistent with those of Sanderson & Porter. ORNL analyses indicated that the hot-spot problem is likely to be more serious than Sanderson & Porter had expected. The Sanderson & Porter studies had not proceeded to the point where they had included in their designs allowances for the problems imposed by graphite shrinkage-cracking, graphite oxidation (particularly in the event of a rupture in the pressure envelope), fast-neutron damage to the pressure vessel, thermal convection removal of afterheat, accommodation of differential thermal expansion without excessive stresses, vibration excitation by the blower, leaktightness at flanged joints and in valves, and access for inspection and repair of contaminated equipment, all of which have proved difficult to cope with in ORNL advanced design studies.

In designing a reactor experiment it is important that the power density be close to that of a typical full-scale reactor. Sanderson & Porter have commonly used 25 w/cm^3. Two studies made at ORNL show the effects of power density on both capital charges and fuel cycle costs. Both of these studies are in agreement with the Sanderson & Porter estimates in that a power density of 25 w/cm^3 does indeed give low power costs. However, these studies also show that reducing the power density to, say, 10 w/cm^3 will cause relatively little increase in over-all costs. This comes about because, although the capital costs increase with reductions in power density, the protactinium losses decrease and the conversion ratio increases sufficiently to cut the fuel cycle costs and thus partially compensate for changes in capital costs over than range from 10 to 50 w/cm^3.

The experimental reactor system was designed so that is would eventually be capable of operating at about the Sanderson & Porter design power density, but it seems likely that further studies will indicate that at least the first few years of operation of the PBRE should be at much lower power densities.

After a careful review of the available material, a set of design precepts was established on September 13, 1960, and adopted as a basis for evolving the design of a pebble-bed reactor experiment. These design precepts are outlined in the following statements.

1. The major objectives of the 10-Mw PBRE are to study the structural stability and fission-product retention characteristics of fueled-graphite spheres, deposition of fission-product activity throughout the system, means of dealing with problems posed by this activity (e.g., gas leaks, equipment decontamination for maintenance, etc.), and a fuel-handling system suitable for this type of fuel.

2. The design should not be compromised by requirements for tests not concerned with the pebble-bed concept.

3. The size of the fuel spheres, the power density, operating temperature, temperature distribution, and stack height should be the same as for a full-scale core.

4. In order to simplify the system and cut costs, no thorium blanket will be employed in the small experimental reactor.

5. The fuel-handling system requirements will be studied and selected to provide for one of the following: (a) charging at full power, (b) charging at zero power but full pressure and temperature, or (c) charging at zero power, atmospheric pressure, and the temperatures characteristic of full-power operation.

6. A fast gas system pump-down (not more than 1 hr) is essential to reduce the hazards if a small leak develops suddenly.

7. The fuel element should be of a type shown by in-pile testing to give a fission-product release rate of less than 10^{-4} times the rate of fission-product generation at full power.

8. Provisions for coping with the fission products released should include means for handling the isotopes characteristically released from UO_2 and those to be expected from UC and UC_2 fuels.

9. The gas system configuration should give satisfactory removal of afterheat by thermal convection if practicable.

10. The means of coping with differential thermal expansion in the system configuration for the small experimental reactor should be consistent with means that would be suitable for a full-scale plant.

11. The moving parts of the blowers must be replaceable.

12. Provisions should be made to permit decontaminating the blowers and the fuel-handling system before the initiation of maintenance work. These should include means for hydraulically isolating the component affected to permit spraying or flooding it with a cleaning solution.

13. Provisions for maintenance of the main heat exchanger need include only access to tube headers outside the shield to permit plugging of a leaky tube and an access opening in the pressure vessel for inspection with a periscope or TV camera and removal of samples.

14. The fuel-handling system must be designed to permit cleaning out a region of jammed balls.

15. The graphite core structure should be accessible for inspection and maintenance. If possible, parts in the high fast-neutron flux region should be replaceable, preferably through an access opening about 2 ft in diameter.

16. The temperature of the structural envelope should not exceed 650°F.

17. Full pressure containment should be provided.

3. SELECTION OF REACTOR CORE GEOMETRY

Two types of reactor core have been considered; (1) a short, squat, 30-in.-diam by 30-in.-high cylinder and (2) a tall, thin, 18-in.-diam by 8-ft-high cylinder. Both would require a 3-ft-thick graphite reflector to keep fast-neutron damage to the reactor pressure vessel to an acceptable level. This reflector would be sufficiently effective so that the differences in fuel concentration in the two types of core would not be important, except that control rods operated in the reflector just outside the core would have a greater reactivity effect for the tall, thin core.

The most important requirement of the experimental core is that it give a power density and a temperature distribution similar to that of a full-scale reactor. The gas inlet temperature should be roughly 550°F to give as high a gas temperature as is compatible with SA-212, grade B, pressure-vessel steel, and the reactor gas outlet temperature for this type of reactor should be at least 1250°F to give a significant improvement over that obtainable with stainless-steel-clad UO_2 fuel elements. The required gas temperature rise could be obtained with a nominal 200°F temperature difference between the fuel and the cooling gas in a long, thin core, whereas a nominal temperature difference of about 500°F between the fuel element and the gas would be required to achieve the same temperature rise with a short, squat core. The fueled balls within the reactor core will be arranged randomly and will be rather loosely packed, but in some regions there may be clusters of closely packed balls. Since the pressure-loss coefficient for the closely packed arrays might be as much as a factor of 10 greater than for the randomly packed regions, the local mass flow rates through the tightly packed clusters might be only one-third the average value for the core. This could lead to local temperature differences between the fuel element and the gas that were substantially larger in the wakes of the closely packed clusters than for the core as a whole. The maximum temperature in a closely packed cluster might be, perhaps, 400°F above

the local gas temperature for the tall, thin core and as much as 900°F above the local gas temperature for the short, squat core. This and related effects appear to give peak surface and internal temperatures, respectively, of 1800 and 2200°F for the tall, thin core as compared with corresponding values of ~2600 and ~3000°F for the short, squat core. In view of the likelihood that the graphite fuel spheres will be damaged by temperatures above 2200°F, it appears that the short, squat core is definitely less desirable than the tall, thin core and that the latter will more nearly simulate the temperature distribution in a full-scale reactor for the same power density and the same inlet and outlet gas temperatures.

The distance which the balls will drop during loading into the core, the static head on the balls that tends to increase local contact pressures and possibly leads to sintering, and the possibility of ratcheting and consequent damage to the core structure all seem to be directly proportional to the height of the core, and the tall, thin core appears to simulate better the conditions to be expected in a full-scale reactor.

The problems arising from graphite shrinkage under irradiation and the possibilities of cracking as a result indicate that the graphite should be employed in the form of cylindrical sleeves having a thickness of not more than 2 in. Experience with ceramic cylinders has indicated that the thickness-to-diameter ratio should not be less than 0.1. Since the thickness is fixed, the tall, slender core gives a more favorable geometry from the standpoint of the graphite structural design. Further, pressure vessel considerations make it reasonable to consider putting in access tubes having diameters of up to 24 in. and, possibly, as much as 30 in., but the larger diameter access tubes pose rapidly increasing problems, particularly in the design of the closure flanges and provisions for handling them remotely. With the smaller diameter cores, the inner graphite sleeves can readily be removed and replaced if radiation damage leads to shrinkage cracks. Further, in the event that sintering occurred to such a degree that the balls could not be readily removed from the

core, it would be possible to remove the entire inner graphite sleeve and the complete bed of balls with a tall, slender core.

An important disadvantage of the tall, slender core is that the ratio of ball diameter to core diameter would be only 12, and therefore the ball flow distribution would be quite different from that for a full-scale reactor. This would not be important if the fuel were loaded and unloaded in batches, but it could lead to substantial differences in the degree of burnup from one ball to another in the smaller diameter cores if these could not be designed to match the ball flow distribution to the reactor power distribution. Another disadvantage of the tall, slender core is that it would yield a much higher pressure drop and hence require a greater vertical distance between the core and the steam generator to give adequate cooling flow by thermal convection to remove the afterheat.

It is important to obtain a uniform gas temperature distribution across the outlet face of the reactor. This implies that the gas flow distribution should be matched to the power distribution. Examination of the characteristic curves for both the power distribution and the flow distribution to be expected indicates that better matching of the two can probably be obtained with the tall, slender core. These considerations, which have been summarized in Table 3.1, led to the selection of the 18-in.-diam, 8-ft-tall core as the basis for the design study.

Sanderson & Porter have considered both upflow and downflow cores. The downflow cores have the advantage that no structure is required over the top of the ball bed to hold the balls in place at power densities above about 15 w/cm^3, where the aerodynamic updraft loads become large enough to begin to float the bed of balls. However, if fast-neutron damage to the pressure vessel is to be avoided, some sort of heavy graphite or steel structure must be used over the top of the core, and the accessibility seems to be little affected if this thermal shield is also made to serve to hold the ball bed in place against a strong vertical updraft force. It should be noted that experience with ball

Table 3.1. Relative Advantages and Disadvantages of 30-in.-diam, 30-in.-High and 18-in.-diam, 8-ft-High Cores

	Short, Squat Core	Long, Thin Core
Simulation of full-scale reactor	Good	Good
Power density	Good	Good
Temperature distribution	Fair	Good
Hot spots	Poor	Good
Ball flow	Fair	Poor
Ball-contact pressures	Fair	Good
Ball-drop distance	Fair	Good
Accessibility for maintenance	Fair	Good
Suitability for control rods	Fair	Good

beds indicates that the bed will begin to float at a pressure drop equal to about 87% of the weight of the bed, in this instance about 57 lb/ft^2 pressure drop per foot of height of the bed. This tendency of the aerodynamic loads to float the bed may prove advantageous in that it can be used to agitate the bed slightly to break up incipient sintering. Since the pressure drop to be expected at 25 kw/liter is about double that required to float the bed, it might be desirable to idle the reactor down to perhaps half power once a day and thus allow the bed to settle and shift a little to break up incipient sintering.

Sanderson & Porter have found data indicating that an upflow bed would be likely to give trouble with bed "chugging" or local ball "spinning" or "dancing" even at pressure drops equal to double the weight of the bed. This comes about because the flow rate required to float a single ball is about seven times that required to float a randomly packed bed so that, while the bed as a whole might be lifted against the upper grate, some individual balls or groups of balls might be free to flutter. A solution to this problem may lie in the shaping of the upper grate. If it is made conical or an irregular hexagonal pyramid with, perhaps, a 60-deg included angle at the top where the balls would be admitted and if the flow passages through the grate permit the greater part of the gas flow to leave the core near the base of this

region, the gas flow through the balls near the apex will be less than that required to cause them to float. That portion of their weight not balanced by the pressure drop would act to tamp the balls into the base of the core where they could bridge to carry the upflow gas load. A static head of balls in the supply tube would assist this tamping action. The effectiveness of this approach can be determined only by experiment.

A major problem is posed by the core support structure. If the structure is at the reactor inlet temperature, the problems associated with differential thermal expansion between the graphite and the steel support structure will be minimized, and the heavy gravity loads will be carried by structure operating at a temperature such that its strength is high. If the downflow core were used, the core support structure would have to be made of stainless steel or graphite, and serious differential thermal expansion problems would result. These would greatly complicate the design and increase the cost relative to that of an upflow core. It would also limit the allowable reactor outlet gas temperature for special experiments or during accidental transients to a lower value than would be permissible with an upflow core.

The upflow core appears to be better from the thermal-convection standpoint. While a configuration such as that proposed by Sanderson & Porter (see Fig. 4.10 of chap. 4, this report) can be made so that after-heat removal can be effected by thermal convection in the event of loss of power to the blowers, it cannot be built so that the system could be started cold simply by thermal convection and without blowers. This possibility might prove advantageous for small reactors located in remote areas where it would be difficult to supply electricity to the blowers for startup.

The relative advantages and disadvantages of updraft and downdraft cores have been summarized in Table 3.2. In reviewing this information, it appears that an updraft core is definitely preferable to the downdraft type. The only disadvantage of the updraft core is that it may give trouble with ball floating at high power densities. This shortcoming does not appear to be as serious as the hot spot or maintenance problems

Table 3.2. Relative Advantages of Updraft and Downdraft Cores

	Downdraft Core	Updraft Core
Thermal convection		
Pressure drop	Fair	Good
Installation height	Fair	Good
Startup	Poor	Good
Core support structure	Poor	Good
Ball retention at high power density	Good	Fair
Ball agitation to inhibit sintering	Poor	Good

of the short, squat core (see chaps. 5 and 10), especially since cost studies indicate that there is no great incentive to go to power densities above that at which ball floating may prove to be a problem. Further, the most severe test to date of a fuel ball has been at a power density of about 25 w/cm^3, or about that which would prevail in the peak power density zone of the proposed tall, thin core if it were operated just below the region in which ball floating might begin to be troublesome.

Experimental data on the effects of power density on the fuels considered are not available, but thermal stress considerations indicate that 25 w/cm^3 is close to the value for incipient cracking of both the alumina-coated fuel particles and the 1.5-in.-diam graphite balls. These problems should be given much further attention before a final design is chosen, but, for the purposes of this study, an upflow core seems to be the best choice and should give the least expensive and most flexible system.

4. SELECTION OF PLANT CONFIGURATION

If ceramic fuel elements without metallic cladding are employed in gas-cooled reactors, an appreciable amount of fission-product contamination will be distributed around the system, including the steam generator and blowers. Not only will shielding of these components be required, but it will be necessary to provide a containment vessel around the entire reactor coolant gas system. In order to minimize the size of the primary gas system which must be both shielded and enclosed in a containment vessel, it seems desirable to develop a plant configuration that is considerably more compact than that used for Calder Hall, which has served as the model for most gas-cooled reactor designs. A series of typical configurations of reactor, steam generator, and blower suitable for a 300-Mw(e) power plant has therefore been studied, and each has been evaluated from the standpoint of the many requirements which must be met.

Insofar as possible, these configurations have been made directly comparable by using the same design power output, the same gas conditions, and the same steam conditions throughout. It appears that the results of the study would not be changed in an important fashion by variations in the design power level or the gas and steam conditions over the ranges of interest. It was taken as axiomatic that the maximum pressure vessel thickness that could be used was 8 in. and that there was a strong incentive to keep the pressure vessel thickness to 4 in. except in the vicinity of penetrations.

Plant Requirements

There are many requirements imposed on the design of a given reactor system, and, although some may take precedence over others, most must be satisfied reasonably well, and compromises must be made to keep the costs from becoming excessive. Unfortunately, while capital costs are difficult to estimate, estimates of operating costs are even more

difficult to make; for example, it is very difficult to estimate the cost of remote-handling operations simply from paper studies.

The design of the PBRE must provide for:

1. adequate support of the moderator while allowing for thermal expansion and growth or shrinkage from irradiation and assuring integrity of the passages for the fuel elements and control rods,
2. flow stability on the water side of the steam generator,
3. removal of afterheat by thermal convection,
4. movement of the spherical fuel elements in the pebble bed,
5. integrity of the primary pressure envelope,
6. accommodating differential thermal expansion,
7. accommodating seismic loads,
8. maintaining the pressure envelope at the reactor inlet temperature,
9. leaktightness of all flanged joints and maintenance of both flanged joints and flexible elements, such as bellows in ducts,
10. minimizing vibration excitation by the blowers,
11. fuel handling,
12. installation, operation, and removal of control rods and their drive mechanisms,
13. access to the blowers for inspection, maintenance, and replacement,
14. access to the headers of the steam generator for inspection and plugging of leaking tubes,
15. access to the core for inspection and maintenance,
16. good access to major components for installation and maintenance by overhead crane,
17. minimum size and complexity of shield,
18. minimum size of containment vessel.

Horizontal Versus Vertical Position for Core and Steam Generators

The requirements outlined above impose such a complex set of problems that it is best to consider them one by one. Probably the first consideration in the design is that of the support for the graphite moderator and core structure, which has a coefficient of thermal expansion substantially less than that of steel. In order to make the most of the

reactor output, the temperature rise in the gas flowing through the various fuel passages should be the same across the entire core, thus favoring a core in the form of a cylinder with the gas flow parallel to the axis. The design must be such as to support the weight of the moderator and at the same time insure that the passages for both the fuel and the control rods will remain straight and of the proper cross section so that there will be no interference with coolant flow, control rod operation, or fuel charging or discharging operations. Some notion of the problem is given by the fact that the differential thermal expansion between graphite and carbon steel at the temperature range from room temperature to the operating temperature will be about 1.0 in. in 10 ft. This makes it very difficult to provide good support for a cylindrical core if its axis is horizontal. It was this consideration that led to the choice of a vertical core axis in both the Calder Hall reactor and the EGCR. While a reactor core with horizontal passages was considered (see Fig. 4.8 in later section of this chapter), no suitable structure for supporting the moderator in such a core appears to be available.

It is not sufficient that the reactor core support its own weight; it must withstand the large forces associated with the gas pressure drop across the core as well as the horizontal shaking forces that might be imposed by an earthquake. Several methods of holding the core together have been proposed. These include circumferential hoops, such as those used in the Calder Hall and later British reactors; tubular springs that can be placed between the pressure vessel and the core, as proposed for a Maritime gas-cooled reactor,[1] and are suitable for cores having diameters up to about 12 ft; graphite columns located by steel grids, as used in the EGCR; and utilization of the pressure differential across the core to squeeze the core together through the use of seals between the tiers of blocks around the outer perimeter, as in the Dragon reactor.

---

[1]A. P. Fraas, "Nuclear Gas Engine," ORNL CF-58-9-12, Nov. 28, 1958.

In all cases, the adverse effects of differential thermal expansion and graphite shrinkage under irradiation make it progressively more difficult to obtain a satisfactory moderator support structure as the reactor core size is increased, even in a cylindrical core with its axis vertical.

Much practical experience in the boiler field, as well as analytical work, indicates that the steam generator should be mounted so that the water will move upward through the tubes. The more nearly vertical the movement and the greater the height of the tubes the better will be the water flow stability and distribution between parallel tubes. Further, experience has shown that horizontal runs of tubes may give difficulty with corrosion if they tend to run partly full of water. Thus steam boiler experience strongly favors tall vertical tubes in the boiler portion of the steam generator.

An important consideration in the design of the heat exchanger is provision for the support of the heat exchanger tubes. In this respect vertical tubes have a marked advantage over horizontal tubes in that relatively small forces are required because the tubes are stable if hung from their upper ends in the vertical condition. Further, there is little tendency for the tubes to warp between supports if they are hung vertically so that the tube spacing can be maintained accurately with a minimum of structure.

The greater the vertical distance between the center lines of the reactor and the steam generator, the greater the driving force for thermal convection. In most of the configurations studied, this difference in elevation must be about 50 ft to insure afterheat removal by thermal convection.

Further, studies of ball movement in beds of spheres have indicated that the reactor core axis should be vertical if the fuel charge is to be changed in small increments rather than in a single batch. Thus it appears that the first four of the 18 requirements listed above are best met by making the reactor core and steam generator axes vertical, with the steam generator well above the reactor.

Pressure Vessel Envelope Integrity

Requirements 5 through 10 are concerned with the integrity of the pressure envelope. In a gas-cooled reactor this is of the highest importance, particularly for contaminated systems in which the gas may contain many thousands of curies of activity. Experience with steam boilers and other pressure vessels used at elevated temperatures indicates that the envelope components should be cylindrical or spherical, with as little variation in section thickness and operating temperature as possible. For the high reactor outlet temperatures contemplated in this study, it seems best to maintain the entire pressure envelope close to the reactor inlet temperature both to minimize thermal stresses and to permit the use of a single alloy, SA-212, grade B steel, throughout the system. This will help keep costs down and will avoid the danger of cracking at welds between dissimilar materials. The size and number of penetrations should be minimized, and bellows joints should be avoided if possible.

The mounting must be sufficiently rigid to withstand the severe lateral shaking forces of an earthquake, and yet it must accommodate differential thermal expansion between the vessel and the concrete support structure. The latter requirement is commonly met either by mounting one point of the structure rigidly and allowing two or more other points in the same plane to float on rollers, or by mounting major components on support skirts in which the temperature distribution is carefully controlled. If the latter approach is used, ducts between major components must be made long and flexible or must be fitted with flexible elements such as bellows.

Experience with both the Calder Hall reactors and the Zenith critical experiment has shown the extreme difficulty of getting a leak-tight system. Oak Ridge experience indicates that this can be done best if all flanged joints are located in cool, well-shielded zones so that elastomers can be employed. ORNL tests have indicated that for diameters over 12 in., Conoseal joints probably do not have the degree

of integrity required. Seal-welded, brazed, or soldered joints can be used if they are in zones where they can be inspected and checked for leaktightness. This requires that the radiation dose level be less than about 1 r/hr during a shutdown after extended operation. Since even a small leak would necessitate shutdown of a plant with a contaminated-gas system, there should be a minimum number of flanged joints, and the design of these must be based on thoroughly proven types.

Much experience with rotating machinery indicates that the blowers should be supported by heavy concrete structure as close to the shaft bearings as possible. Above about 100 hp the shafts should be horizontal to avoid difficulties with "whirl."

Access for Operation, Inspection, and Maintenance

Requirements 11 through 15 are concerned with factors that will greatly influence operating costs and have long been considered as presenting such difficulties that there have been major doubts as to the feasibility of a reactor with a contaminated-gas system.

The fuel-handling system must provide for adding and removing fuel without permitting a serious amount of activity to escape into the fuel-handling area. Particulate activity is especially objectionable. In this connection, the activity level in rooms frequented by personnel must be kept below 10^{-10} $\mu c/cm^3$. Assuming a room volume of 1000 m^3 and a fission-product concentration in the gas system of 100 $\mu c/cm^3$, this implies that less than 0.001 cm^3 of gas may escape into a room containing personnel when a flange is broken.

Control rods should operate vertically suspended on cables from above or driven by ball screws from below the reactor. In either case, the shorter the distance between the drive units and the core the better, particularly from the standpoint of the damage that might result from an accidental rod drop.

Access to the blowers for maintenance will be greatly facilitated if they can be isolated from both the reactor and the steam generator by about 5 ft and 3 ft, respectively, of concrete shielding. This should permit limited contact maintenance during a shutdown. Similarly, the tube headers for the steam generator should be shielded from the steam generator proper to permit direct access for inspection and tube plugging.

The information available on the effects of irradiation on graphite indicates that it would be desirable to design the reactor core so that the moderator could be replaced if difficulties should arise after a few years of reactor operation. This might be done in any one of several ways. A removable pressure vessel head with a flanged joint could be employed, or the pressure vessel could be cut with a torch and rewelded after installation of a new core. The latter approach does not seem promising in view of the difficulties associated with carrying out the welding and inspection operations, since the activity level in and around the pressure vessel would probably require that this work be carried out by remote control. A more promising approach would be an access tube, perhaps 2 ft in diameter, extending through the shield from the top or the bottom of the reactor. In the latter case, a hole could be placed in the center of the core support grid and covered with a plug which could be held in place with a large snap ring. By removing this plug, the moderator, or at least a portion of it, could be allowed to tumble out into a cask, and the balance could be pushed out with remote-handling equipment. After removal of the old moderator blocks, that region of the core could be washed down with an oxalic acid solution to decontaminate it insofar as possible. It could then be sprayed with a thin coating of lacquer to hold any remaining particulate matter in place on the surfaces and to minimize airborne contamination during the installation of fresh moderator blocks.

Large assemblies of fresh moderator blocks could be glued together with a cement such as a low-ash methylmethacryate to facilitate their installation. After stacking these large sections in the core, the cement could be removed by baking at low temperature.

Construction Costs

Requirements 16 through 18 have been included because of their pronounced effects on construction costs. The best system is likely to be that which best meets these requirements while at the same time meeting the other 15 requirements.

Proposed Configurations

The configurations considered in this study are shown schematically in Figs. 4.1 through 4.9. The various configurations are drawn to the same scale, with the major components sized to give a reactor thermal power output of 800 Mw, with a gross electrical output of 300 Mw, for the system. The gas temperature was taken to be 550°F at the entrance to the core and 1250°F at the exit. The steam leaving the superheater was taken as being at 2400 psia and 1050°F, with reheat to 1000°F and 400 psi. In all cases the gas was taken as being helium, although the substitution of CO_2 would have relatively little effect on the size of the various components. In each case the proposed configuration has been proportioned to satisfy the fundamental requirements which are either inherent in the application or arise from considerations of problems of construction or operation.

Figure 4.1 shows the Calder Hall configuration modified to provide shielding around the heat exchangers and blowers. The reactor core size was also reduced in keeping with the 1000-psi gas system pressure level and the higher gas temperatures, and axial tubes have been employed in the steam generator. The system has two important weaknesses in that provision for thermal expansion requires the use of bellows joints, and these must be located in regions where, in a contaminated-gas system, it would be extremely difficult to replace them in the event a defect developed. Further, the system inherently requires hot gas ducts, thus reducing the integrity of the primary pressure envelope and limiting the peak reactor outlet temperature to about 1250°F for a reasonable duct wall thickness. The system also suffers from a cost disadvantage

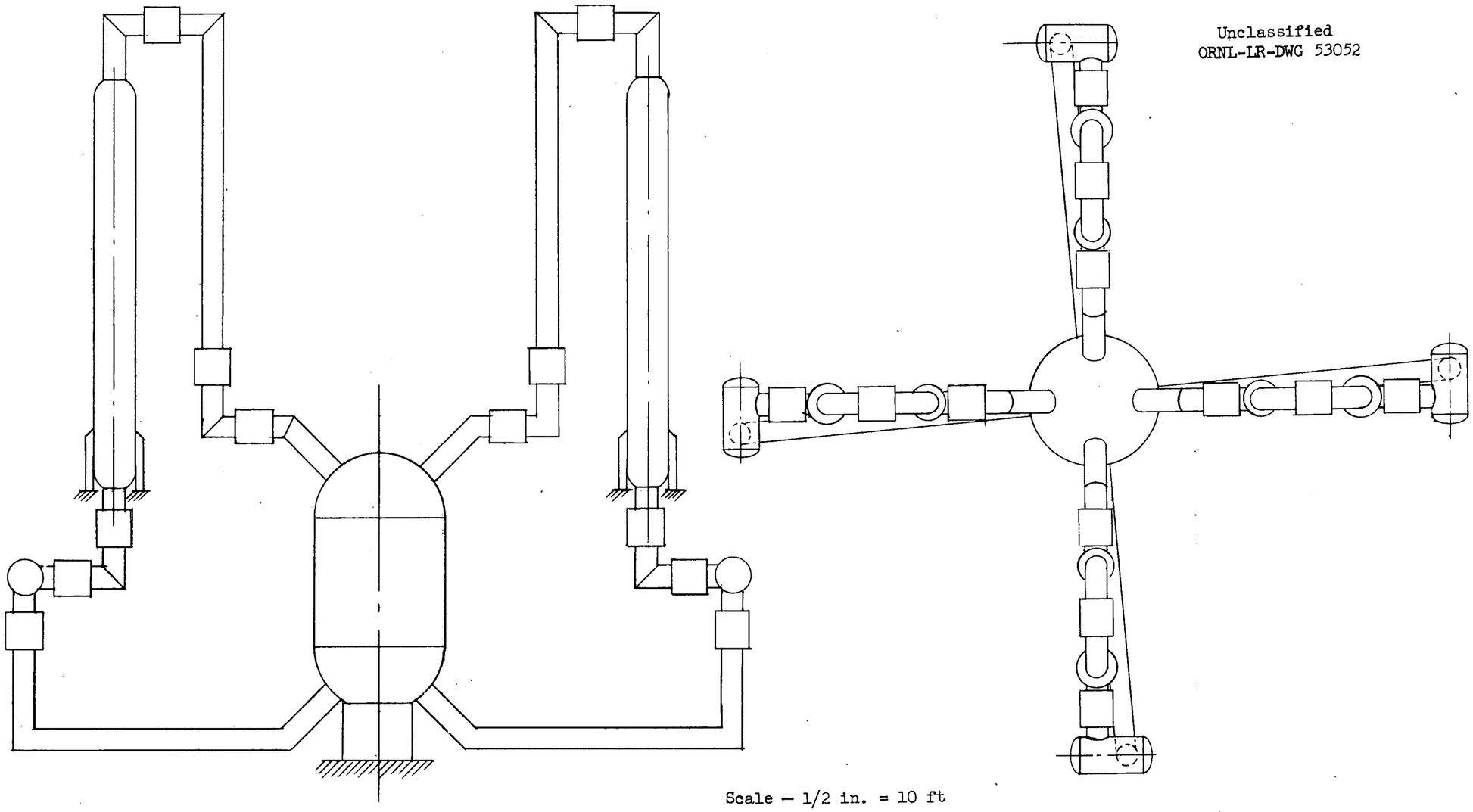

Fig. 4.1. The Calder Hall Layout Modified to Provide Extra Shielding.

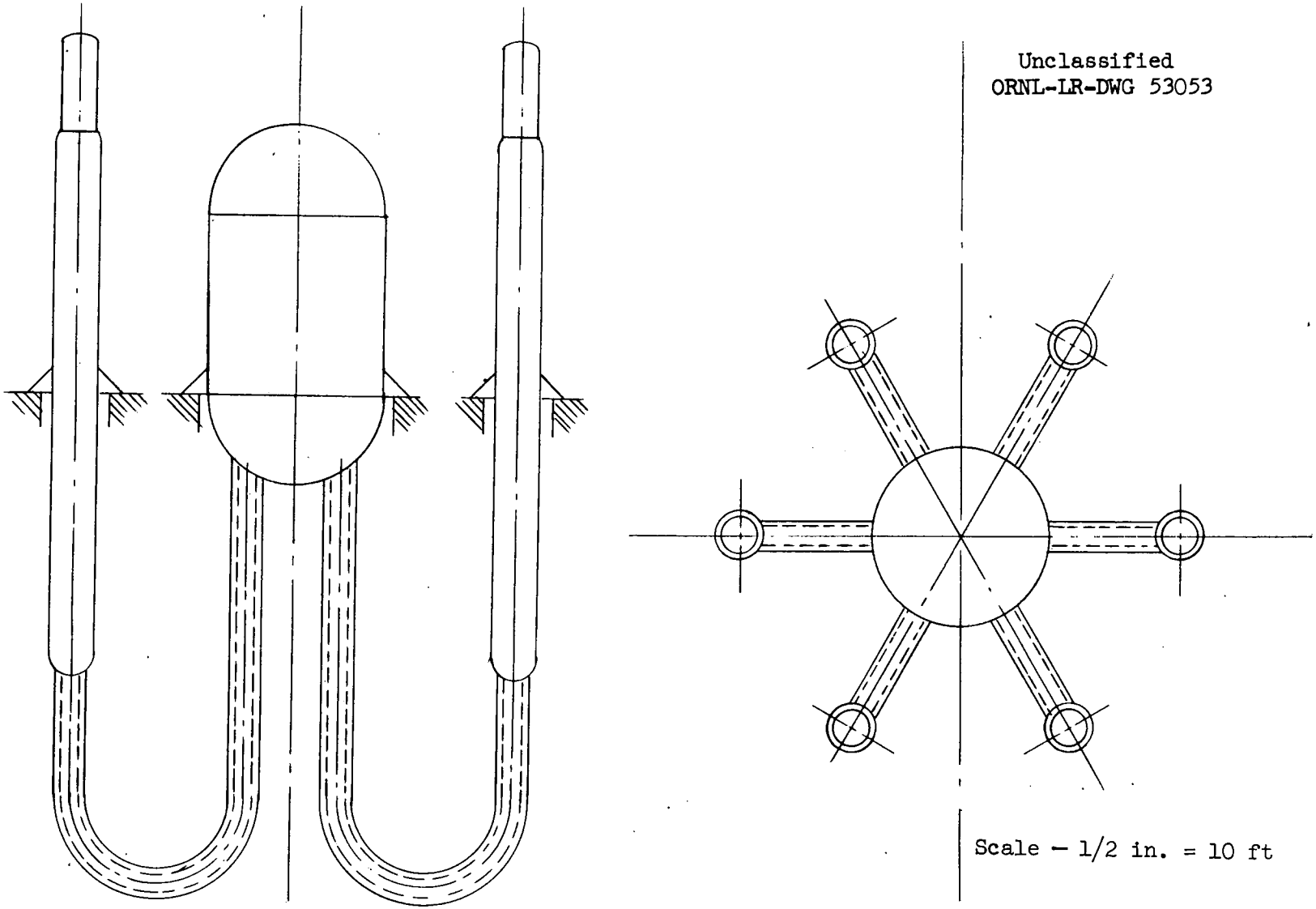

Fig. 4.2. Sanderson & Porter Layout with Flexible Pipes.

Unclassified
ORNL-LR-DWG 53054

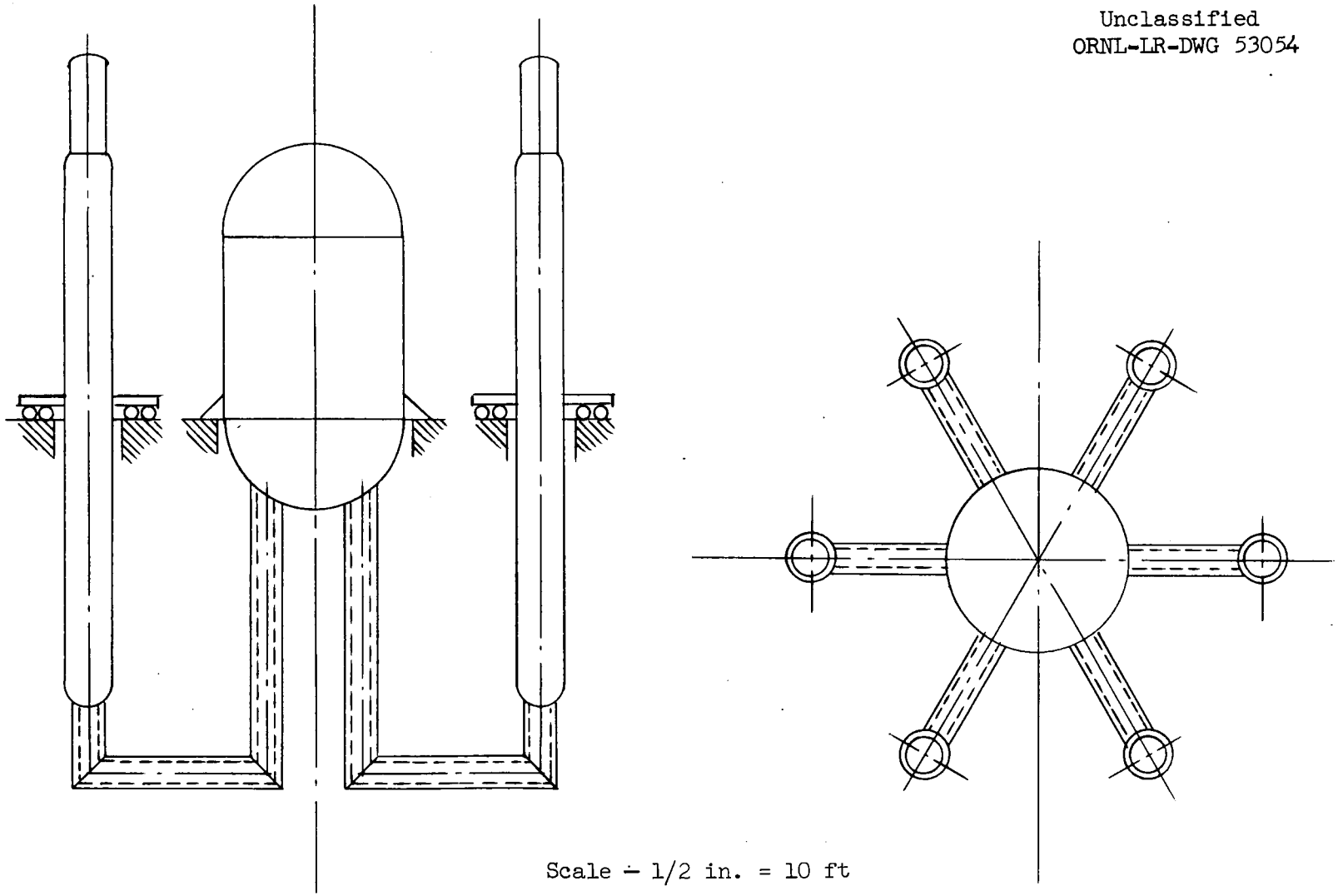

Fig. 4.3. Sanderson & Porter Layout with Rollers Under the Steam Generator.

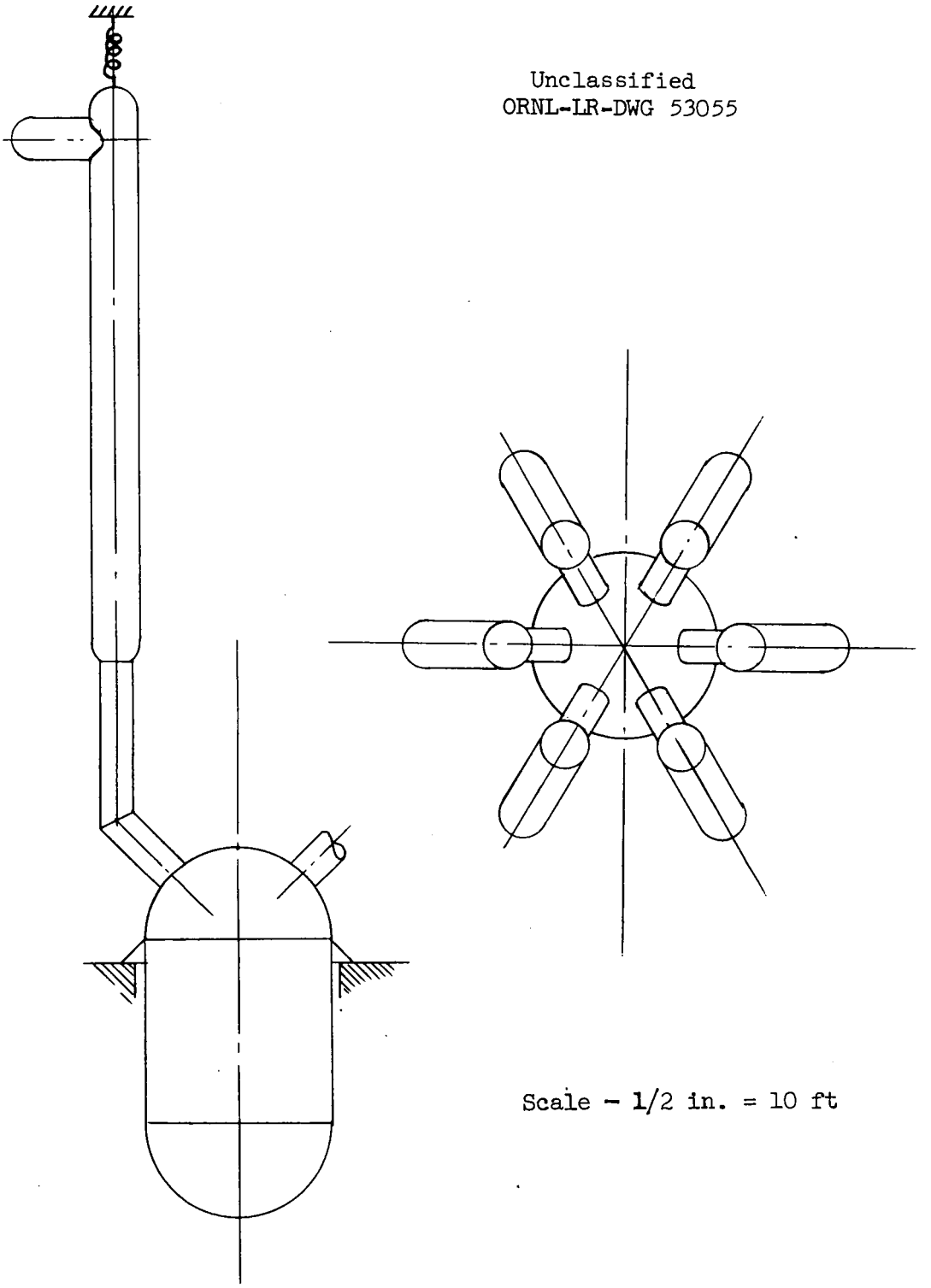

Fig. 4.4. The Dragon Layout.

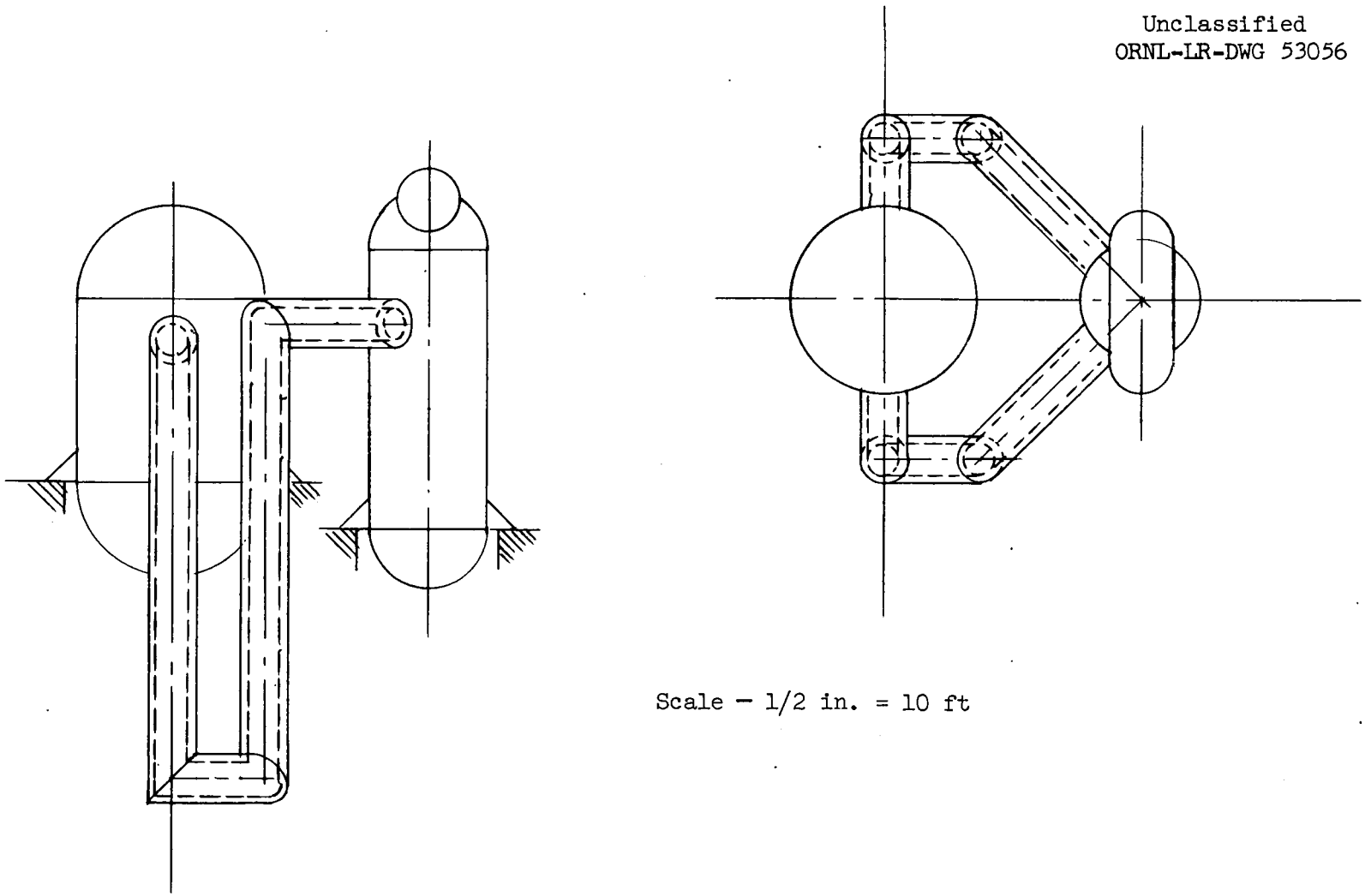

Fig. 4.5. Peach Bottom Plant Layout.

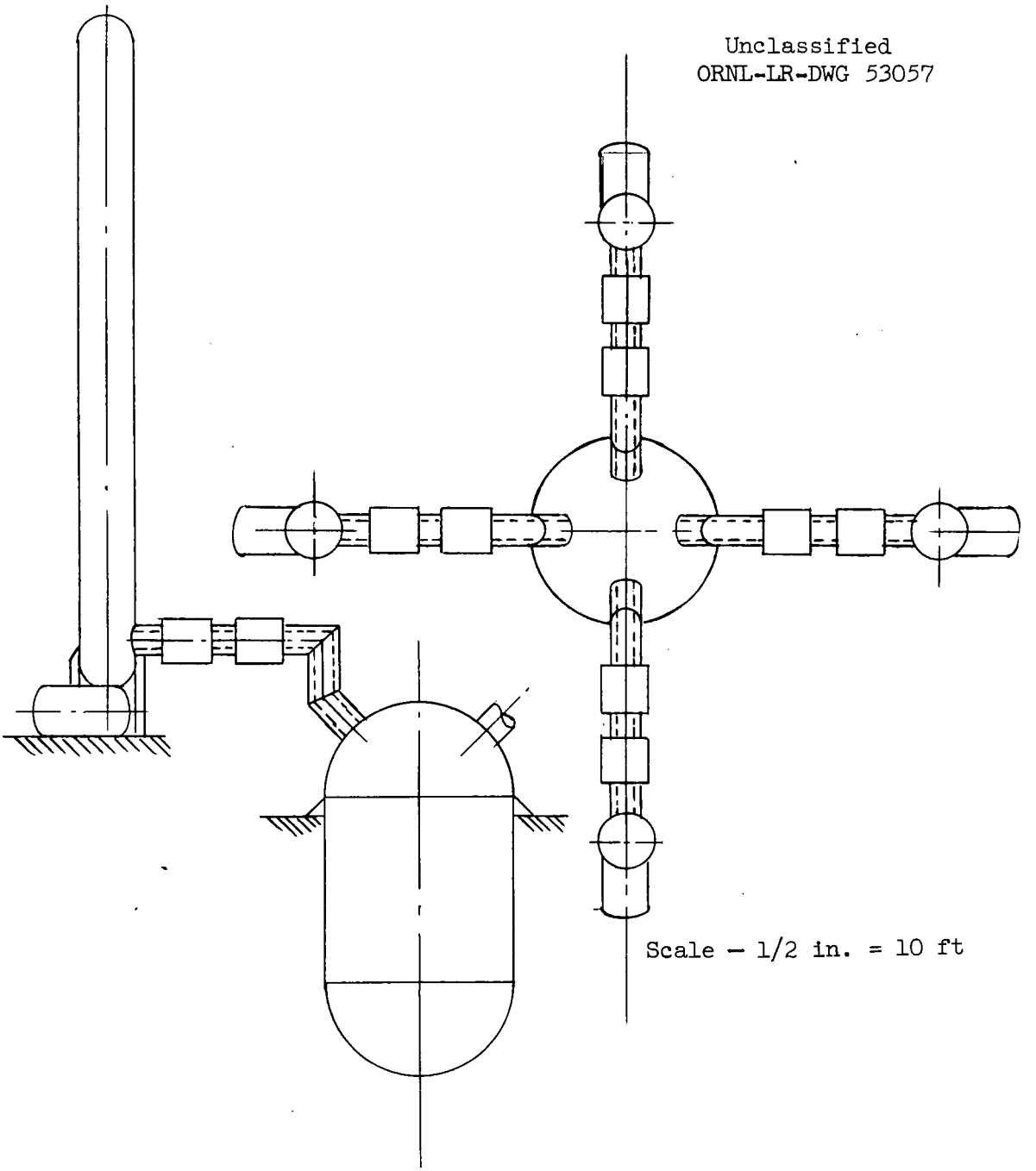

Fig. 4.6. Modified Calder Hall Layout with Concentric Ducts and the Blowers Housed in the Steam Generator Pressure Vessels.

Unclassified
ORNL-LR-DWG 53058

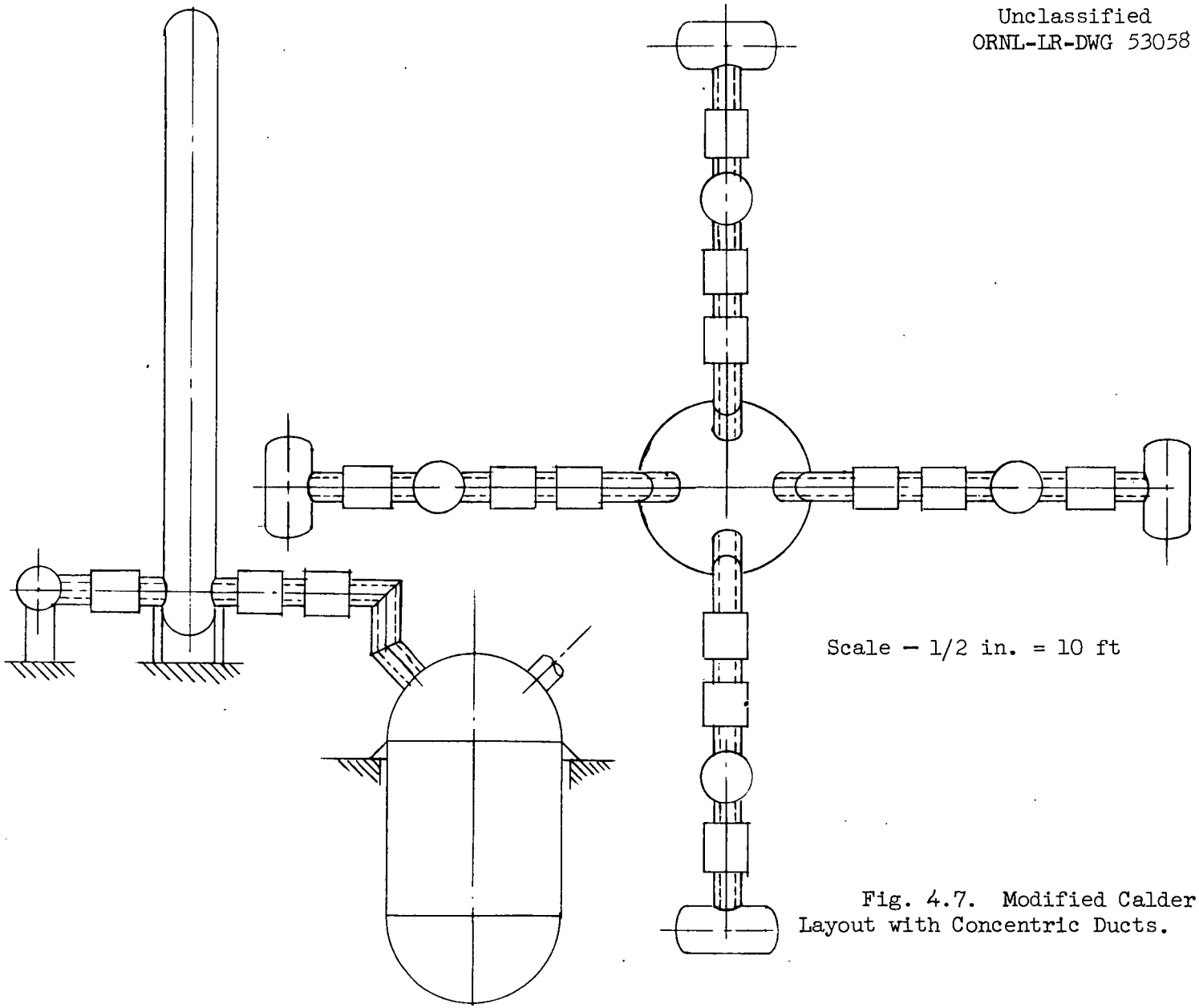

Fig. 4.7. Modified Calder Hall Layout with Concentric Ducts.

Unclassified
ORNL-LR-DWG 53059

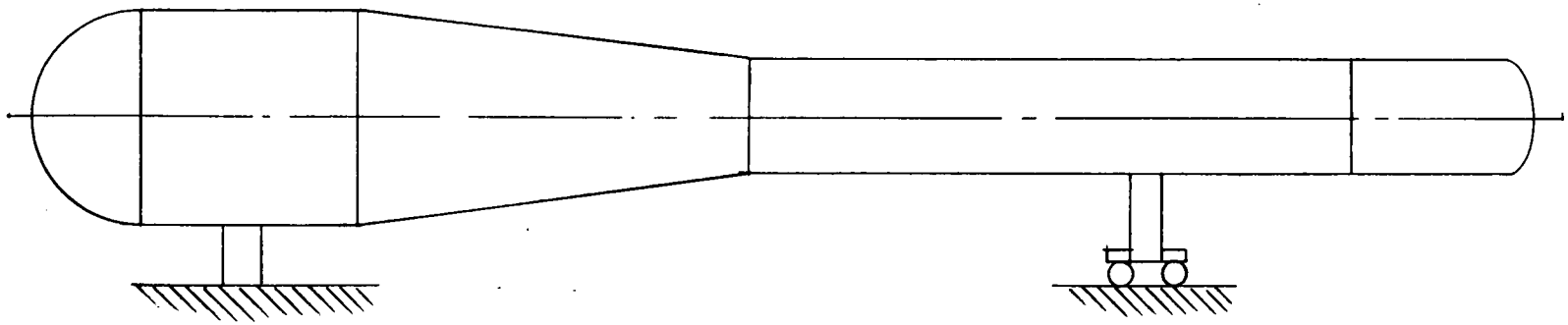

Scale — 1/2 in. = 10 ft

Fig. 4.8. Layout Used in ORNL Small Core Study.

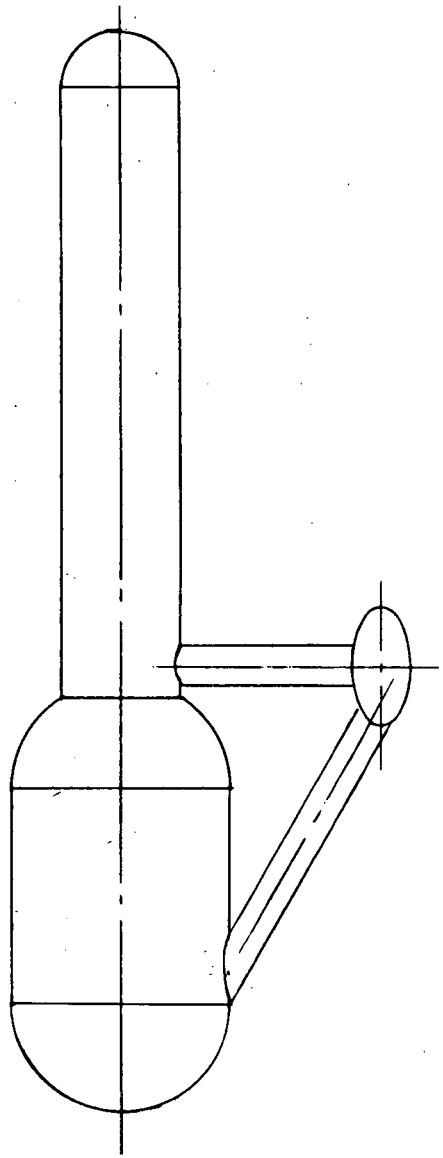

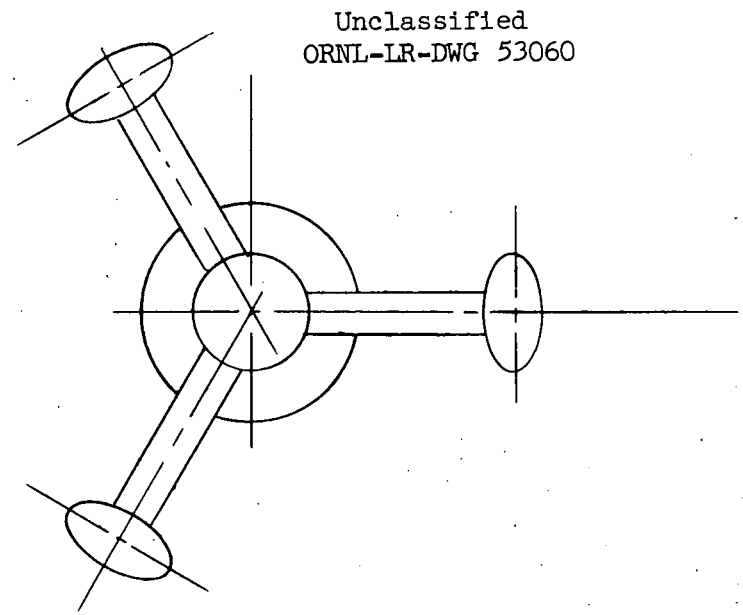

Scale — 1/2 in. = 10 ft

Fig. 4.9. Unified Core and Steam Generator Configuration.

in that the volume and complexity of the shielding would increase the shielding costs, and the over-all configuration would require a large containment vessel.

The second configuration (Fig. 4.2) considered was that proposed by Sanderson & Porter. This makes use of a long concentric-duct loop extending 75 ft below the reactor vessel to accommodate thermal expansion in the ducts. While adequate flexibility can be provided in the pipes in this fashion, the large bending moments in the pipes give reaction loads at both the steam generators and the reactor (which are rigidly attached to the concrete) that will lead to large bending moments in the shells, and there is some doubt as to whether these can be accommodated satisfactorily. The arrangement also has the disadvantage that the flanged joint for the attachment of the blower will not have the degree of leak-tightness desired, and, since the blowers are not mounted at an anchoring point, they may induce serious vibrations in the structure, particularly since vertical shaft motors have a bad tendency to whirl. This configuration does not provide shielding to isolate the blowers from the steam generator, and hence will greatly increase blower maintenance problems. The long piping loop between the steam generator and reactor will increase the size of the shield and containment vessel substantially.

A modification of the Sanderson & Porter layout of Fig. 4.2 is shown in Fig. 4.3. This design avoids the serious stress problem where the ducts enter the pressure vessels by mounting the steam generators on rollers so that they can move radially outward from the reactor. Unfortunately, this arrangement appears to be completely unsatisfactory in its ability to withstand the lateral shaking forces which might be induced in an earthquake.

Figure 4.4 shows the configuration employed for the British Dragon reactor. This configuration was worked out primarily for a small experimental reactor and is not considered by the British to be a model for a large-scale reactor. However, it has been included here to indicate the problems which would arise if such a layout were attempted. Its principal

feature is that the six blowers and steam generators are mounted at the top of concentric ducts which extend radially outward and upward from the pressure vessel of the reactor. The bending moments in both the ducts and the pressure vessel wall associated with the weight of the steam generator and blowers are relieved by supporting most of this weight on constant-tension spring hangers. Such an arrangement would be clearly unsuitable for a full-scale plant. It also would have very poor characteristics in the event of an earthquake. Provisions for both maintenance and vibration isolation of the blowers leave much to be desired.

Figure 4.5 shows the configuration developed for the HTGR reactor system of the Peach Bottom plant. Thermal expansion of the concentric ducts will induce large reaction loads at the reactor and steam-generator pressure vessels. These will induce troublesome local bending moments in the vessel shells. The blower mounting at the top of the steam generator may give vibration difficulties, and the blowers are not isolated by shielding from the activity deposited in the steam generator. Thermal convection will not be effective in removing after-heat in the event of a power failure.

Figure 4.6 presents a modified Calder Hall configuration which employs concentric ducts to provide good cooling of all the pressure envelope and thus avoid both hot ducts and the necessity to weld dissimilar metals together in large heavy sections. Unfortunately, it is hard to see how a defective bellows joint could be replaced in the event of a leak. The configuration does provide good mounting for the blower in the sense that there should not be a vibration problem, but replacement of a blower would be difficult, since it would not be isolated from the steam generator by shielding.

Figure 4.7 shows a further modification of this basic layout designed to provide a more favorable configuration for blower maintenance. Unfortunately, this gives more bellows joints, although it should be a somewhat better system from the standpoint of vibration isolation of the blower.

Figure 4.8 shows a configuration evolved two years ago in an ORNL study of a small reactor core that was designed for a high-pressure gas system. This arrangement would present very serious problems in the support of the moderator and reactor core structure and would make after-heat removal by thermal convection out of the question. It would also present a serious problem in getting adequate leaktightness of the flanged joints for the blower attachments, and it does not give good vibration isolation of the blower. The fuel-handling problem would leave something to be desired because the flow characteristics of balls through a horizontal cylinder would not be naturally favorable for loading in small increments. The control rods would have to operate horizontally, a less satisfactory arrangement than vertical operation. Similarly, maintenance of the reactor core would be more difficult with the horizontal-core axis. The water flow in the steam generator would be inherently much less favorable than for a vertical axis system. The containment vessel would have to be relatively large in diameter rather than relatively tall and slender, and hence would be more expensive.

Figure 4.9 shows a configuration developed about a year ago for a beryllium oxide all-ceramic reactor. This configuration was evolved after many layout studies, which were made in an effort to satisfy as well as possible all the 18 requirements being used as criteria in this study. Its principal disadvantage is the absence of direct vertical access to the top of the reactor core. This will require that the control rods be operated by ball screws from below, as in the Maritime gas-cooled reactor, or that they be suspended on quite long cables from the top of the steam generator. The absence of direct vertical access to the top of the reactor core would also make maintenance and inspection of the reactor core more difficult, since it would have to be carried out from beneath. In other respects, however, the layout seems to be the best of all the configurations considered. It will yield a minimum size of containment vessel and a minimum shield volume and complexity. The blowers are well isolated from the rest of the structure, both by shielding and from the standpoint of vibration. The pressure envelope

is inherently simple in shape, so it should have high integrity. After-heat removal by thermal convection is the most favorable of any of the systems considered. The differential thermal expansion problem is accommodated with a simple rugged system. Enclosing the steam generator and reactor in a common pressure vessel eliminates one of the steam-generator-vessel closure heads, thus effecting an important saving in cost.

The layouts considered in Figs. 4.1–4.9 were intended primarily for full-scale plants. In re-examining these with a view toward their applicability to a 10-Mw(t) reactor experiment, it appeared that most of the designs were applicable and that the relative advantages and disadvantages of the nine configurations considered would be almost the same. The principal changes required for the PBRE stem from the greatly reduced diameter of the heat exchanger relative to the reactor and the much smaller diameter of the gas piping. The latter suggested that the Sanderson & Porter configuration of Fig. 4.3 could be modified to provide afterheat removal by thermal convection by using the configurations of Figs. 4.10 and 4.11. In Fig. 4.10, concentric ducts are used as in the Sanderson & Porter design, whereas, in Fig. 4.11, separate hot and cold ducts are used as in the Calder Hall plant. The configuration of Fig. 4.12, a modification of that of Fig. 4.9, was also considered in an effort to provide direct vertical access to the center of both the top and the bottom of the reactor. The latter configuration seemed to possess all the advantages of the configuration of Fig. 4.9, together with the improved access. This was considered particularly desirable from the control-rod standpoint, since it showed promise of making possible the use of control rod drives essentially similar to those of the EGCR. The control rods themselves could be in the form of segments of a cylinder having a diameter a little less than the inside diameter of the large access tube at the top of the reactor. Most servicing operations could be carried out through the charge tube at the bottom of the reactor. This could be enclosed in a hydraulically tight steel-lined room which would lend itself readily to washdown and decontamination

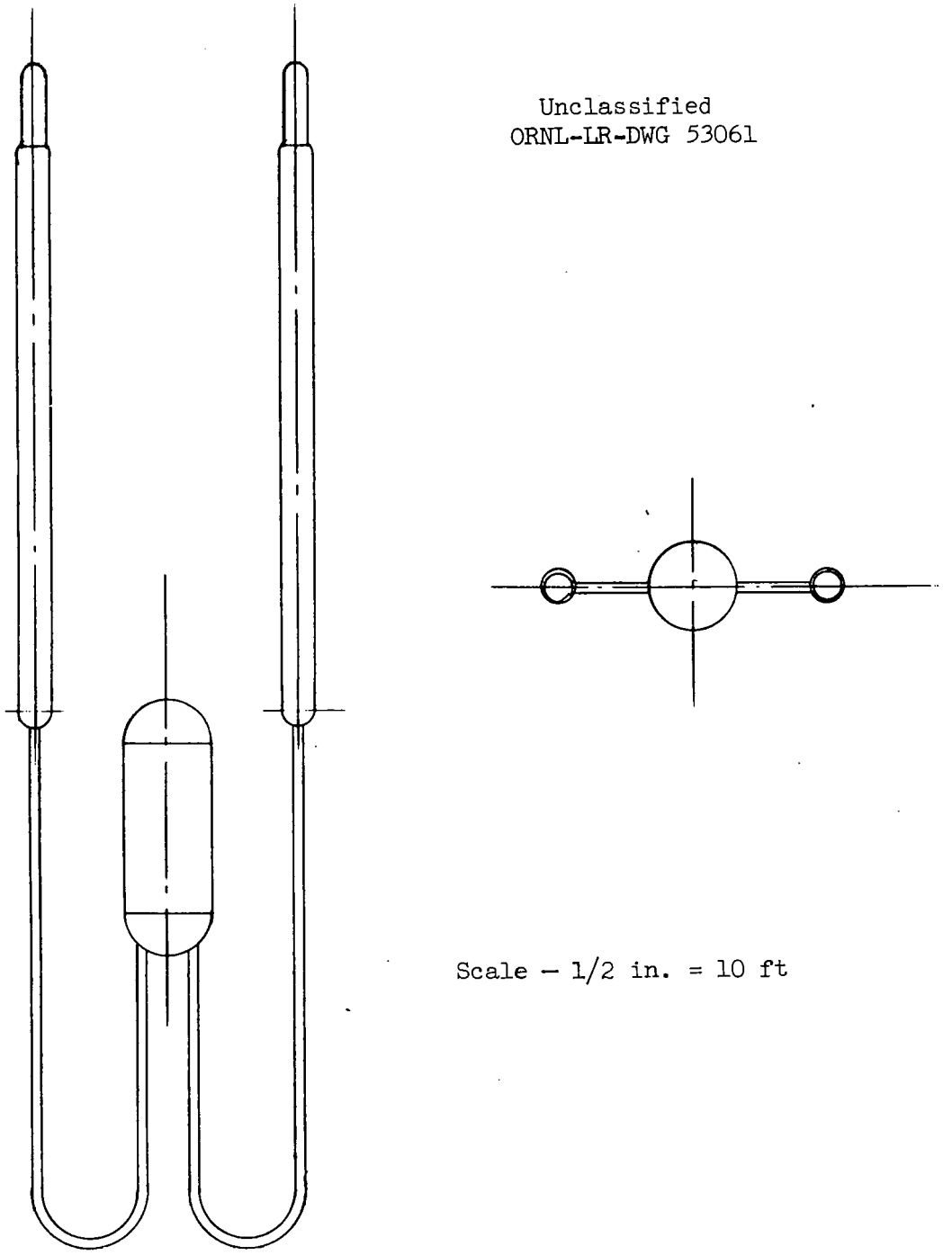

Fig. 4.10. Sanderson & Porter Layout Modified for a 10 Mw(t) Reactor Experiment.

Unclassified
ORNL-LR-DWG 53062

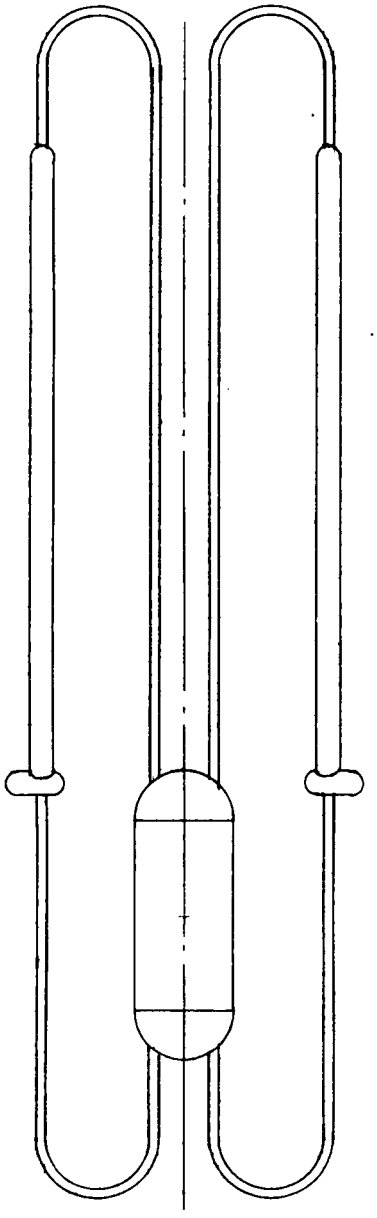

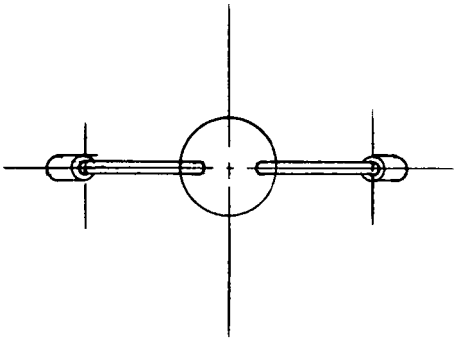

Scale — 1/2 in. = 10 ft

Fig. 4.11. Calder Hall Layout Modified for a 10 Mw(t) Reactor Experiment.

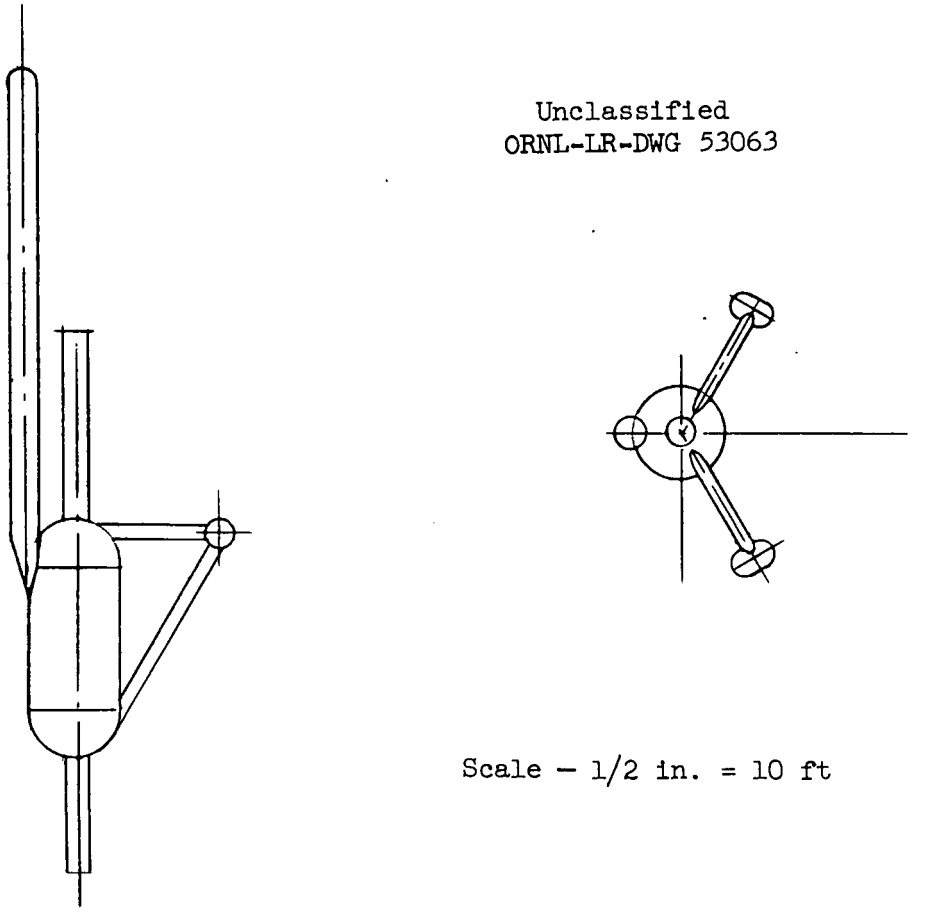

Fig. 4.12. Unified Configuration with Steam Generator Offset to Improve Access to Top of Core for a 10 Mw(t) Reactor Experiment.

and could be hermetically sealed from the rest of the building to prevent the spread of particulate activity.

The long, slender flexible pipes of configurations 4.10 and 4.11 require a very substantial amount of space and would impose serious bending moments in the pressure vessels, as mentioned above. While 2 in. of thermal insulation could be provided inside the hot duct, this would serve to reduce the duct wall temperature only about 250°F, and therefore a chrome-moly or stainless steel would be required. Further, strength considerations for these ducts would impose serious limitations on permissible reactor gas outlet temperatures. This might be very important during a temperature transient of the type that might occur following an accident or in the event that a higher reactor gas outlet temperature might be desired for some experimental testing.

5. PROPOSED REACTOR

The design of the proposed pebble-bed reactor experiment is shown in Fig. 5.1, and the various regions and their particular design problems are discussed below. A brief summary of the research and development program required to substantiate the design is given in Chapter 20.

Graphite Structure

The three principal regions in the graphite reflector are indicated in section B-B of Fig. 5.1. The central region consists of four concentric sleeves, the inner three of which are removable as a unit through the lower access tube. The outer of the four sleeves is too large to be removed through the access tube, and hence it is split axially into four segments to facilitate installation and removal. The top end is held in place by a steel retainer ring while the bottom rests in a groove in the core support plate. The intermediate graphite region consists of wedge-shaped pieces 4 in. high and approximately 26 in. long. The outer region consists of a 4-in.-thick layer of borated graphite blocks.

All the reflector graphite would be coated with silicon carbide to inhibit oxidation. This should serve to reduce graphite weight losses during normal operation, as well as to keep the oxidation rate low enough that in the event of a major system rupture the graphite would not support combustion.

The inner three graphite sleeves are laminated to increase resistance to shrinkage cracking under irradiation. The lower ends of these graphite sleeves are threaded into steel sockets with internal threads in the steel to avoid cracking of the graphite because of differential thermal expansion during heating. This arangement will give a snug fit of the graphite in the steel socket during installation and removal operations when the graphite and steel will be at a relatively low temperature. Looseness at operating temperature should not pose a problem, since there will be no forces tending to cause the graphite

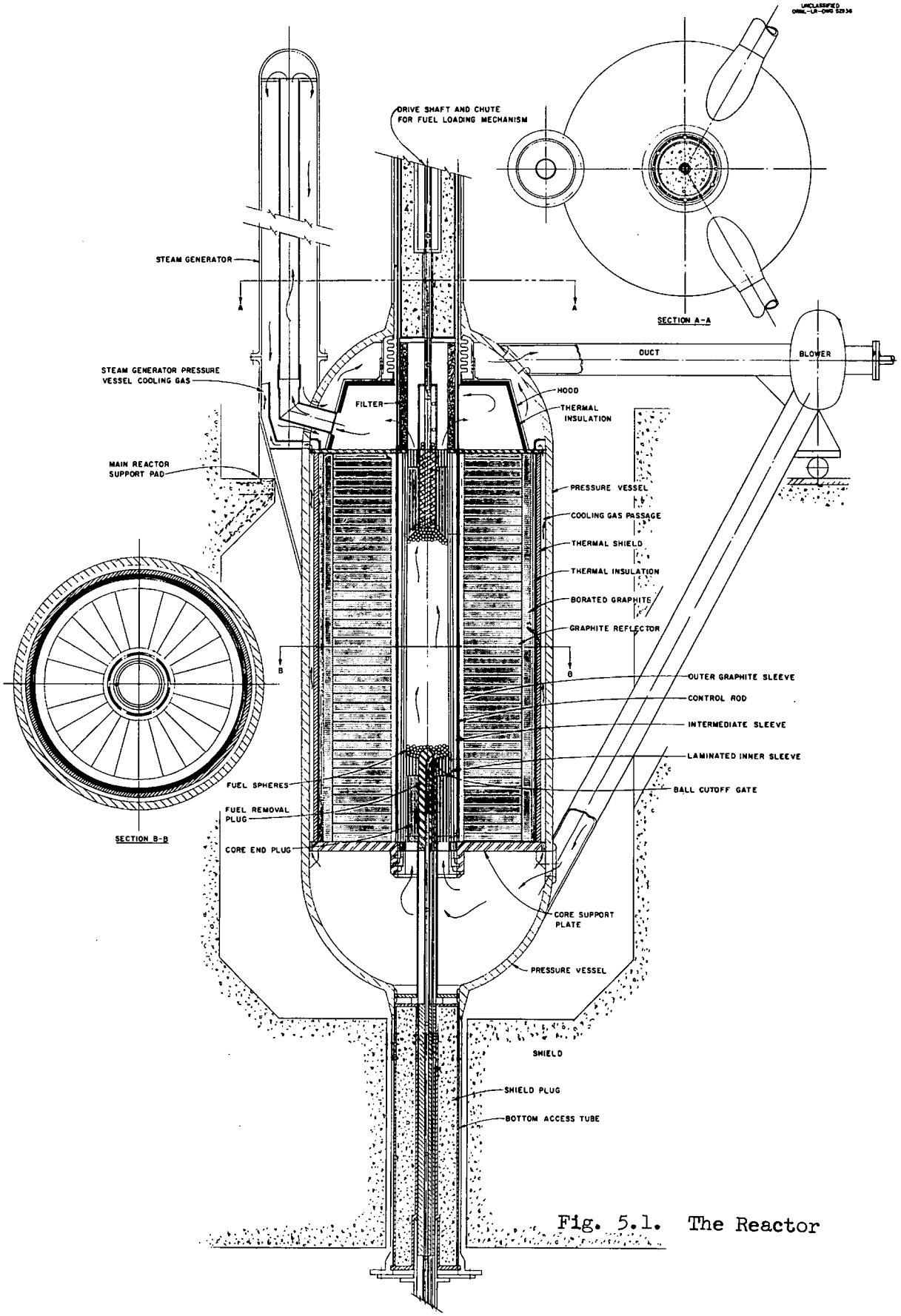

Fig. 5.1. The Reactor

to turn relative to the steel socket. The inner steel socket is fitted with external lugs so that it can be bayoneted into the socket of the intermediate graphite sleeve, and that in turn has similar lugs that can be bayoneted into the core support plate. The core support plate consists of a steel plate 3 in. thick welded into the pressure vessel. The two inner graphite sleeves have a taper of 1 in. in their length from top to bottom of the core, or 1 3/4-in. taper over their entire length. This taper insures freedom from bridging of the balls in the core and should aid in separating adjacent sleeves when one is withdrawn for maintenance or replacement.

The graphite is separated from the 2-in.-thick steel thermal shield by 2 in. of reflective insulation. Except for the two inner graphite sleeves, the graphite in the reflector would be retained at the top by a segmented grid bolted to the thermal shield. This grid is intended to hold the graphite in place only in the event of some peculiar accident, since the gas pressure drop across the reflector will occur largely across orifices in the bottom support plate. Cooling passages rising vertically from these orifices will be sufficiently large so that the pressure drop through the graphite reflector will be less than one-half that through the core. Orifice plugs would be installed in the support plate in much the same way as jets in a carburetor, so the reflector cooling gas flow distribution can be modified readily if shakedown tests indicate that this is advisable.

The diametral clearance between concentric sleeves was chosen tentatively as 1/8 in. This clearance may have to be increased to provide more cooling gas flow after a detailed analysis of the reflector cooling requirements is made. Shrinkage under irradiation will be greatest on the inner sleeves and hence will tend to cause the clearances to increase with operating time. While the axial variation in fast flux will tend to give approximately 0.4 in. greater shrinkage at the center than at the ends, this will not present a problem with the amounts of clearance and taper that have been provided.

Control Rods

The control rods are in the form of curved plates of Inconel which slide in an annulus between the intermediate and outer graphite sleeves of the reflector. Ridges protrude radially inward from the outer graphite cylinder to control the thickness of the annulus in which the control rods, or blades, move. As discussed in Chapter 7, the blades are so effective in poisoning the reactor that a blade thickness of only about 0.062 in. will suffice. In order to improve the blade stiffness and at the same time provide plenty of gas flow cross-sectional area into the filter at the top of the reactor, the blades will be of thick, perforated material and will be surrounded by a tubular frame. A honeycomb structure or three alternate layers of flat and corrugated sheet will also be considered for this application.

The control rods operate through an annulus provided between the shield plug and the top reactor access tube. A small pressure vessel attached to the top flange of this access tube houses the control-rod drive assemblies. These may be units similar to those planned for the EGCR; indeed, it may be possible to use the same design.

Pressure Vessel and Support Structure

The reactor pressure vessel is cylindrical with hemispherical heads and is made of SA-212, grade B carbon steel. There is a 28-in.-i.d. vertical access tube in the center of each head of the vessel. The thermal insulation surrounding these tubes and the shield plugs is designed to provide a uniform temperature gradient from the reactor gas inlet at the pressure vessel to the flange at the outer end of the tube, which will operate at room temperature. The steam generator is attached to the side of the pressure vessel in such a way that its base also serves as a major mounting foot for the support of the reactor-steam generator assembly. Much of the weight load of the reactor is transmitted in shear to the conical base of this steam generator, from which it is transmitted in turn to the mounting foot having its load-bearing surface in the form of an element of a sphere. Ports in the reactor vessel wall provide for gas flow between the reactor and the steam generator.

The reactor, steam-generator, and blower assembly is supported on a three-point suspension so that the load distribution is determinate. In addition to the fixed mounting foot under the steam generator, an additional mounting foot is located under each of the two blowers. Thus the ducts to the blowers also serve as elements of the reactor vessel support structure. To increase their stiffness, they are larger in diameter than is essential from the standpoint of fluid pressure drop considerations, and their wall thickness is double that required to withstand the internal pressure. Actually, the stresses imposed by the weight of the reactor assembly are much less than the pressure stresses. A vertical splitter web has been provided through the ducts at the blower to transmit the load in shear from the horizontal to the diagonal duct and thus avoid inducing serious bending moments in the shell surrounding the blower. The blowers are mounted on rollers to provide for differential thermal expansion relative to the concrete supporting structure. The static weight loads are far more than necessary to prevent relative movement of the blower, rollers, and base plate under any lateral shaking forces likely to be set up by small amounts of blower rotor unbalance.

The end plugs for the inner reflector graphite sleeve are made of sets of concentric graphite sleeves 1 in. thick. Gas flow passages through these sleeves are provided by allowing 1/8-in. radial clearances between sleeves. The upper ends of the lower sleeves are stepped slightly toward the center to avoid possible difficulty with balls catching in the circumferential gaps between concentric sleeves. Two sets of sleeves are provided in each of these end plugs so that their cooling gas annuli can be staggered to inhibit fast-neutron streaming toward the ends of the pressure vessel. Two parallel cylindrical cross bars, one above the other, retain each set of concentric sleeves, while a third cross bar at right angles to the other two keeps them centered relative to each other. One end of each cross bar is threaded into the laminated core-retaining sleeve.

Viewing Provisions

Two 6-in.-diam access tubes are provided for viewing the interior of the reactor during shutdown conditions. These tubes penetrate the shield horizontally nearly in the plane of the mounting foot under the steam generator to minimize relative movement between these tubes and the shield. The viewing equipment consists of a TV camera kept well buried in the shield so that the radiation dose to its lense will be low. A mirror and arc-light assembly extend into the space above or below the reactor core where the assembly can be rotated to inspect most of the interior at either end of the core. A unit of this type is under development for the Dragon reactor.

Pressure-Vessel Cooling and Thermal Insulation

The unfavorable surface-to-volume ratio in a small power reactor makes pressure-vessel cooling somewhat more of a problem than it would be in a full-scale plant. About 10% of the blower output bypasses the reactor core to cool the pressure vessel, thermal shield, and the steam generator pressure vessel. (The cooling provisions for the latter are described in the section on the steam generator.) The cool gas returning from the steam generator to the blowers is directed around a hood which separates it from the hot gas coming out of the top of the reactor core. In this manner the entire reactor pressure vessel is supplied with a forced flow of cooling gas at essentially the reactor inlet temperature, i.e., 550°F. The borated graphite in the outer portion of the reflector serves to keep the heat generation in the thermal shield and pressure vessel fairly low so that these members will be at temperatures less than 50°F above the cooling gas temperature in spite of the unusually high power density of the reactor. Three inches of reflective insulation on the inner surface of the hood over the top of the reactor will serve to reduce heat losses from the hot reactor outlet gas to the cool gas going to the blowers. Zirconium oxide may be considered for this application in place of reflective insulation, since it would give a

substantially lower thermal conductivity. However, cost and outgassing problems may be disadvantages of zirconium oxide.

The hot duct leading out of the reactor is connected to the steam generator by a short quill equipped with slip joints at either end to accommodate differential thermal expansion. Gas leakage through these joints is to be minimized with piston rings made of a material chosen to avoid difficulty with galling, chaffing, or seizing. The hot ducts will be made of an 18-8 stainless steel to provide good strength at 1500°F in the event of a reactor temperature overshoot and to permit special experiments at gas outlet temperatures in the 1250 to 1500°F range.

Shield Plugs

Heavy shield plugs are installed in the access tubes at the upper and lower ends of the reactor. These plugs not only provide shielding but also incorporate elements of the fuel-handling system. Ceramic filters may also be installed on each of the plugs to minimize the dispersal of particulate activity from the core. This will be particularly important at the reactor outlet, where a filter should be especially effective. The upper shield plug includes an outer annulus through which the control rods operate.

Closure Flanges

The reactor is designed with all the closure flanges in well-shielded cool zones so that O-ring seals can be employed. Each flange is provided with two O-rings, and the space between the O-rings is buffered with clean helium at a pressure a little above the reactor operating pressure. Each flange is also fitted with a cylindrical surface to facilitate attachment of an axially collapsible plastic bag into which the shield plug or other element can be drawn and the bag pinched off to minimize the dispersal of particulate activity.

Pressure vessel fabrication experience indicates that the weight and cost of these flanges increase rapidly with their diameter. The

access tubes were made 28 in. in diameter because this seemed to be close to the upper size limit for units that could be handled fairly well with remote-handling equipment without a serious cost penalty.

6. PROPOSED PLANT

Design Data

The reactor is designed to produce a gross thermal power output of 10 Mw. Although addition of a turbine generator plant to produce a gross electrical power of approximately 3 Mw was considered, the cost of the addition appeared prohibitive since the plant is primarily a reactor experiment. The basic design data of the plant follow:

Over-all power generation data	
Reactor thermal output, Btu/hr	34.1×10^6
Reactor thermal output, Mw	10
Gross electrical output, Mw	3
Fuel element characteristics	
Sphere outside diameter, in.	1.5
Sphere thermal stress (for ideal rigid body), psi	2500
Sphere surface, ft^2/ft^3 of fuel	48
Sphere surface, ft^2/reactor (39% voidage assumed)	418
Sphere average surface temperature, °F	~1200
Sphere maximum design surface temperature in hot zone, °F	2000
Sphere maximum allowable internal temperature (including hot spots), °F	2200
Number of spheres per reactor (39% voidage assumed)	8500
Average power density in core, w/cm^3	25
Average surface heat flux, $Btu/hr \cdot ft^2$	81 500
Reactor core material and dimensions	
Material	Graphite
Core height, ft	8.1
Core diameter, ft	1.5
Core face area, ft^2	1.77
Height of core plus reflector, ft	14
Diameter of core plus reflector, ft	7.5

Machined weight of graphite, tons	32
Core density, g/cm^3	1
Total graphite volume, ft^3	600
Number of fuel channels	1
Number of fuel charge tubes	1
Pressure vessel dimensions	
Shape	Cylinder
Outside diameter, ft	9.25
Material	SA-212, grade B steel
Vessel height, ft	25
Thickness, in.	3.25
Working pressure, psig	1000
Design stress, psi	15 000
Maximum temperature, °F	600
Volume, ft^3	1300
Gross vessel weight (including vessel and core supports, thermal barriers, nozzles, steam generator, and insulation), lb	~200 000
Coolant characteristics	
Gas	Helium
Working pressure, psia	1000
Total flow (normal), lb/sec	12.0
Reactor inlet temperature, °F	550
Reactor outlet temperature, °F	1250
Number of inlet pipes	2
Number of outlet pipes	1
Inside diameter of pipe, ft	1
Mean coolant velocity in cool pipe, ft/sec	20.7
Mean coolant velocity in hot pipe, ft/sec	71
Total volume occupied by coolant, ft^3	950
Circuit pressure drop, psi	30
Specific heat capacity of coolant, Btu/lb·°F	1.24

Coolant blowers	
Type	Centrifugal
Number per reactor	2
Adiabatic efficiency, %	70
Compression power, Bhp	127
Power, kw (at 90% motor efficiency and 70% adiabatic efficiency)	150 each
Blower drive motor power, Bhp	182 each
Steam Generator	
Type of generator	Natural recirculation
Number per reactor	1
Number of steam generator sections	2
Shell height between heads, ft	43
Shell height including heads, ft	45
Shell inside diameter, ft	2
Shell thickness, in.	1
Gas inlet inside diameter, ft	0.75

Site Selection

The site chosen for this PBRE study is close to the EGCR to take advantage of common services, such as transmission lines, highway, sanitary water, and the possibility of using some of the EGCR personnel for occasional auxiliary help in handling unusual operations. Also, the site has already been approved for reactors.

At the site, a layer of loose soil (clay, sand, silt, and gravel) covers an irregular layer of weathered and deeply folded shale. This shale is found at an elevation of approximately 850 ft and is quite close to the Clinch River. With the construction of the Melton Hill Dam, the elevation of the river can be expected to fluctuate between a minimum of about 795 ft to a maximum probable flood of about 805 ft. The general topography of the site is indicated by the contour lines in Fig. 6.1.

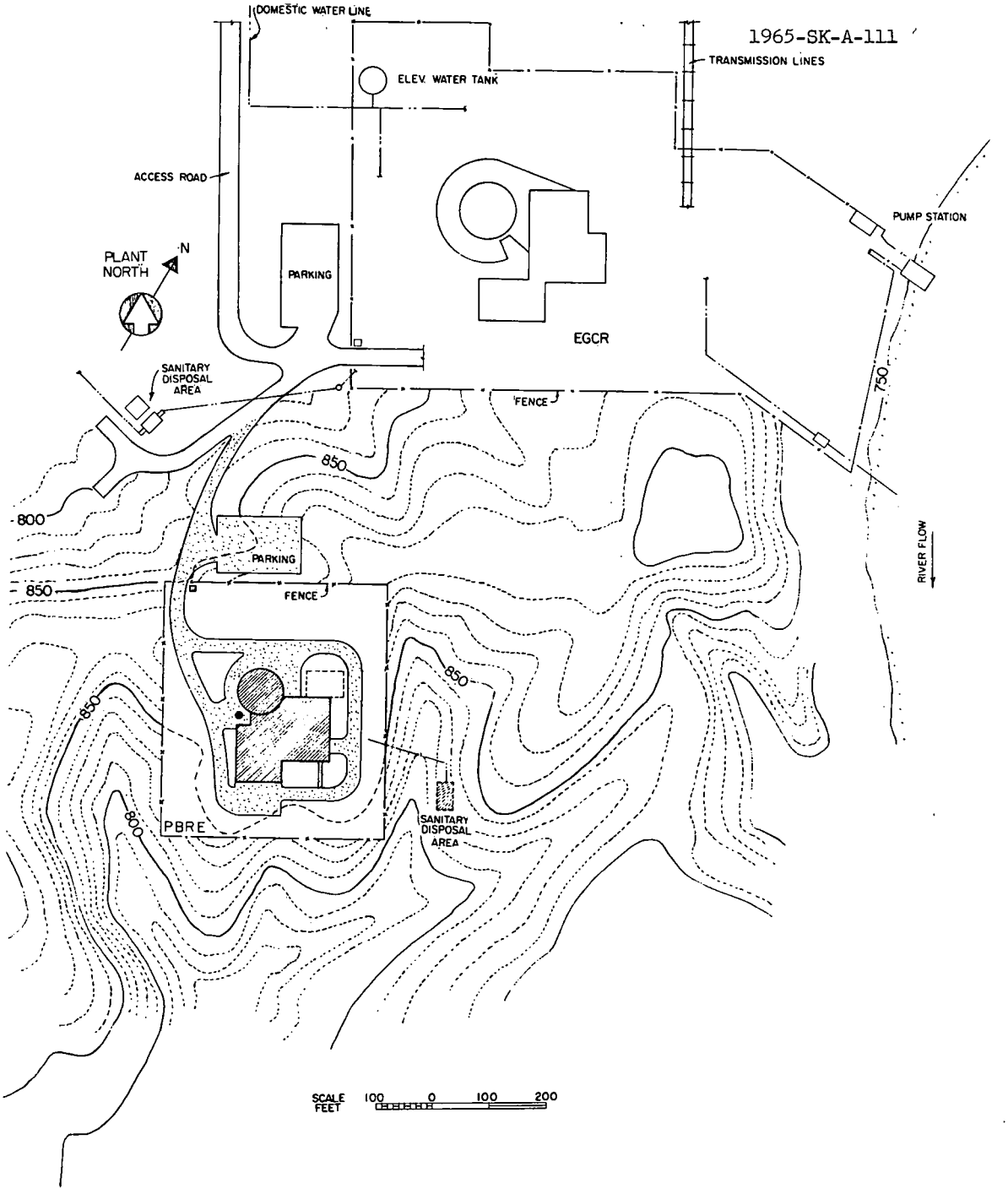

Fig. 6.1. PBRE Site Plan.

Plant Layout

A plan view of the plant is shown in Fig. 6.2. The reactor complex is located near the river, and the ground floor of the building is located at an elevation of about 845 ft. With the exception of the reactor area, which is enclosed in a containment shell, the entire plant is located on the ground floor in various interconnected rooms forming an outlying building adjacent to the containment shell. Approximately 0.1 mile of access highway will be required to provide access to the service bay loading dock and the fuel storage area.

Reactor Area

The reactor area is enclosed in a hermetically sealed containment shell that is approximately 80 ft in diameter and 200 ft high. An elevation section through the containment vessel and building is shown in Fig. 6.3. As shown in the figure, the bottom of the containment shell is located 104 ft below ground, bringing the reactor pressure vessel about 10 ft below ground level. The upper opening to the reactor vessel is located at ground level, and the steam generator is mounted integrally with the reactor vessel and extends vertically upward about 60 ft. Since it is possible for the steam generator to accumulate activity in the course of time, it is shielded on three sides with concrete and on the fourth side with cast iron slabs to avoid interference with the upper closure. This equipment and all that in the floors below is serviced from a bridge crane running on a circular track in the upper part of the containment shell. The control rod drives at the top of the upper access tube to the pressure vessel are enclosed in a tank fitted with its own hoist for removing and installing equipment as a further precaution against spreading contamination. The ground floor plan (Fig. 6.2) indicates the relationship between the major parts of the circulating system and the various services. An equipment air lock leading out of the containment shell into the maintenance area is shown to the south, and to the east is a personnel air lock for access to and from the rest of the plant. The helium circulates in two parallel loops placed 120 deg apart from the heat

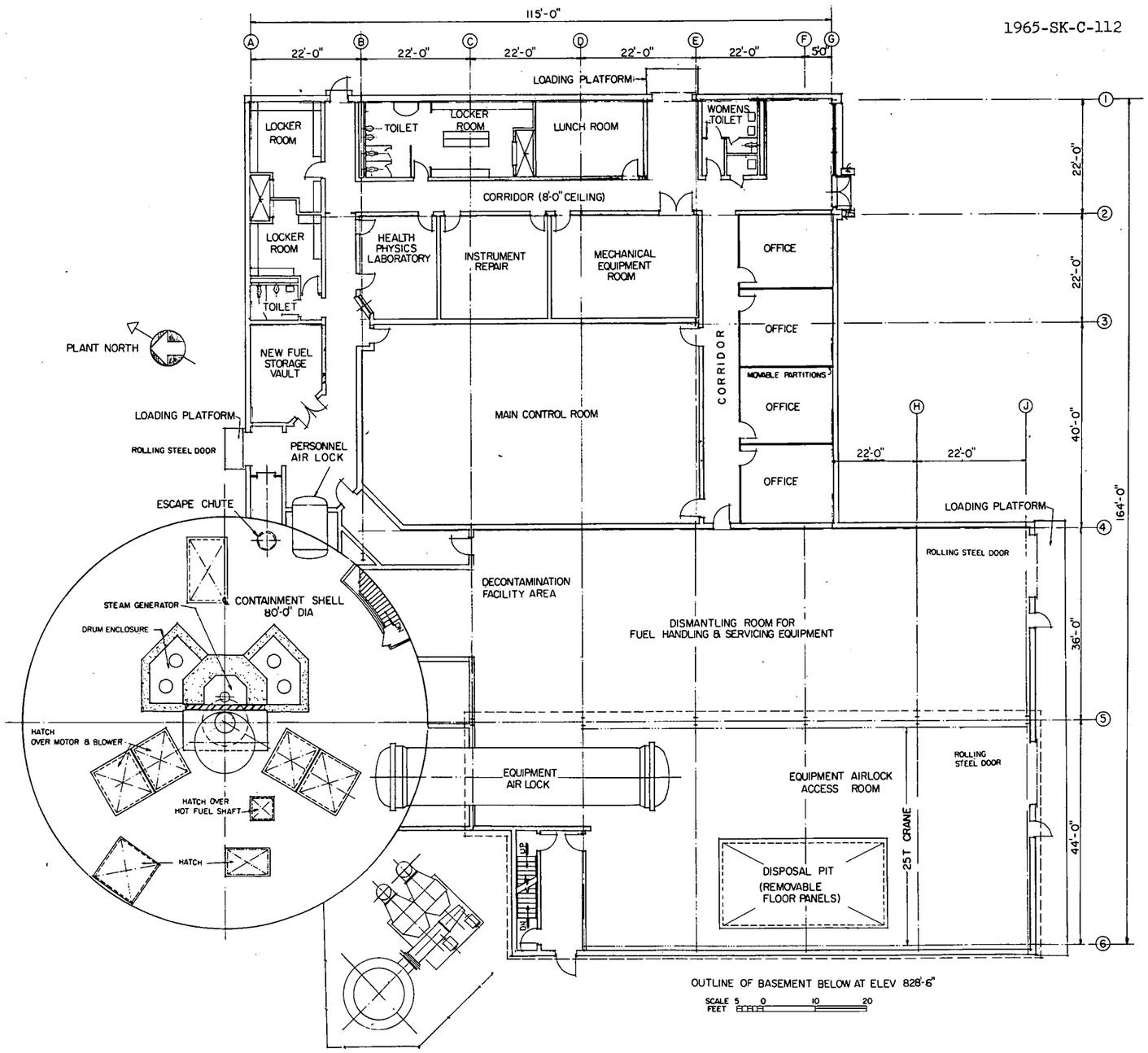

Fig. 6.2. Ground Floor Plan of Building and Containment Vessel.

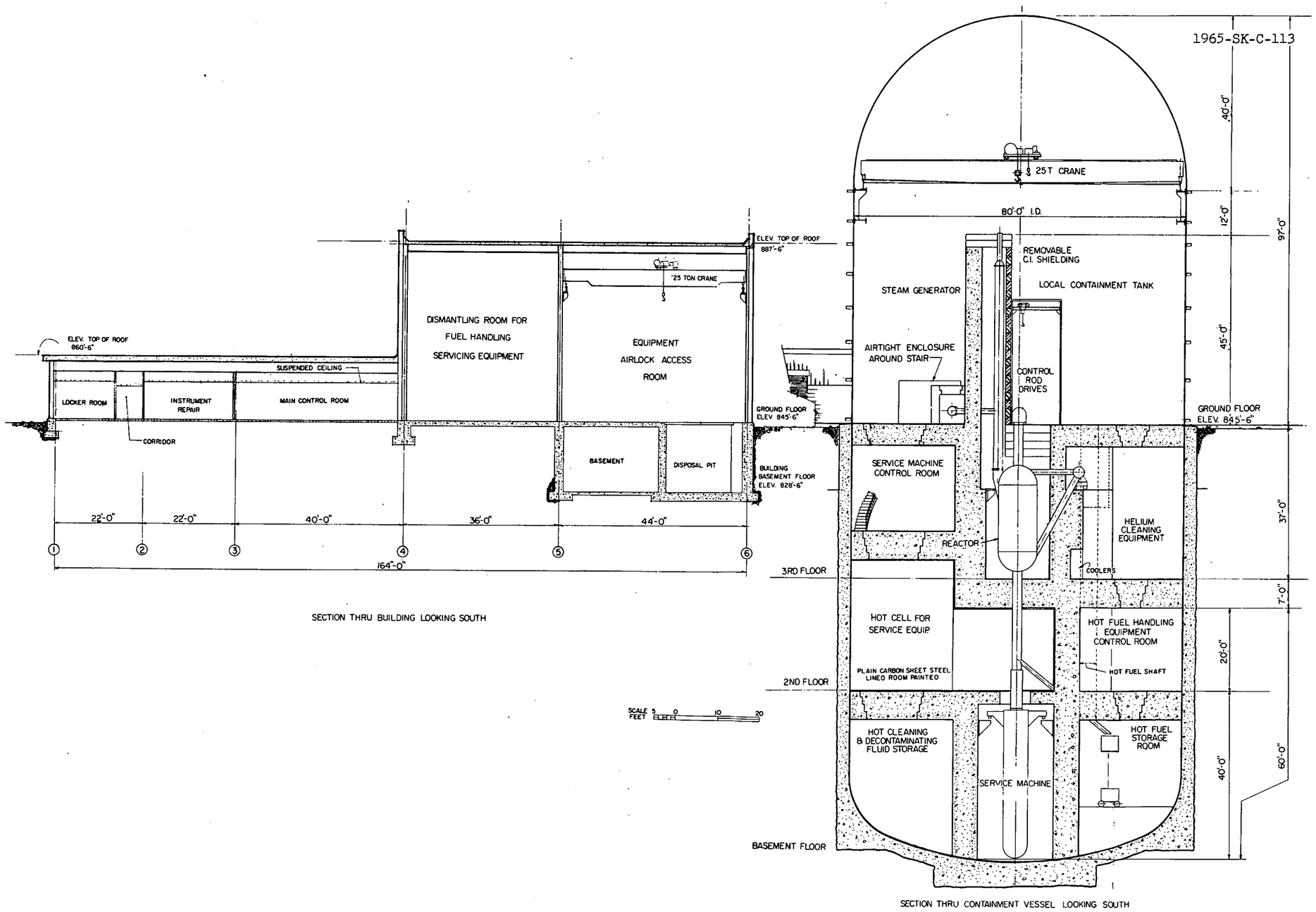

Fig. 6.3. Section Through Containment Vessel and Building.

exchanger, and above each of the blowers there are removable floor panels for maintenance purposes. A small covered shaft is located between the blower panels to provide access for raising spent fuel, suitably contained in shielded caskets, to the ground floor for transportation to reprocessing facilities.

The third floor (first floor below ground) is shown in plan view in Fig. 6.4. On the east is the service machine control room, which is completely shielded from the reactor and from other parts of the containment area. In this room are located all the instruments and remote-control mechanisms, as well as viewing mechanisms, for the transfer of spent fuel from the reactor to the hot fuel storage room and for remote replacement of a control rod and drive. Just west of the center the circulating loops are shown, and, as may be seen in Fig. 6.2, the blowers are supported on rollers on a mezzanine in the helium cleanup room. In the helium cleanup room are located the shield cooling blowers and heat exchangers, helium compressors, vacuum pumps, and the chemical cleanup system for a bypass stream of helium. The cleanup system includes coolers, heaters, oxidizers, and molecular sieves.

On the second floor, shown in plan view in Fig. 6.5, the large room on the east is the hot cell for servicing equipment. In this room, which is connected with the rooms above and below it through hatchways shielded by large concrete blocks, are provisions for the final cleaning or storage of equipment that has been decontaminated in the room below and also provision for uncoupling the fuel discharge equipment from the lower end of the reactor vessel closure in the event that it is necessary to do maintenance on the contaminated fuel-handling system. This room, which may become contaminated at various times, is lined with sheet steel which is covered with a good grade of chemical-resistant paint. On the west side is the contaminated fuel-handling equipment control room which is likewise connected with the rooms above and below it through hatchways containing appropriate shielding plugs. The plan view of this room shows the four tanks used for the storage of contaminated helium. Two of these vessels are designed for 500 psi, one for 100 psi, and one for 20 psi. The charcoal traps of the helium cleanup system are also located in this area.

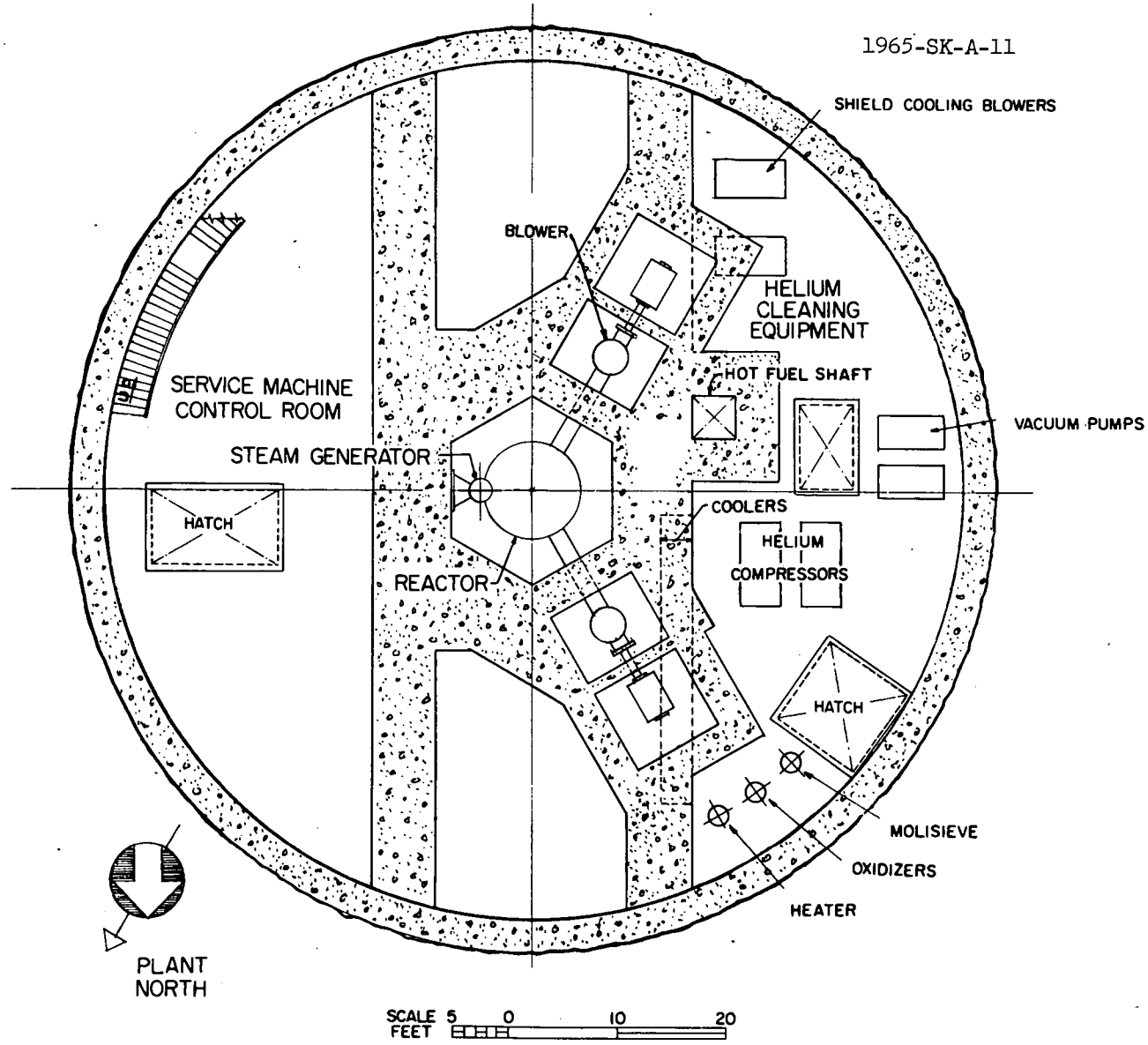

Fig. 6.4. Third Floor Plan — Containment Vessel.

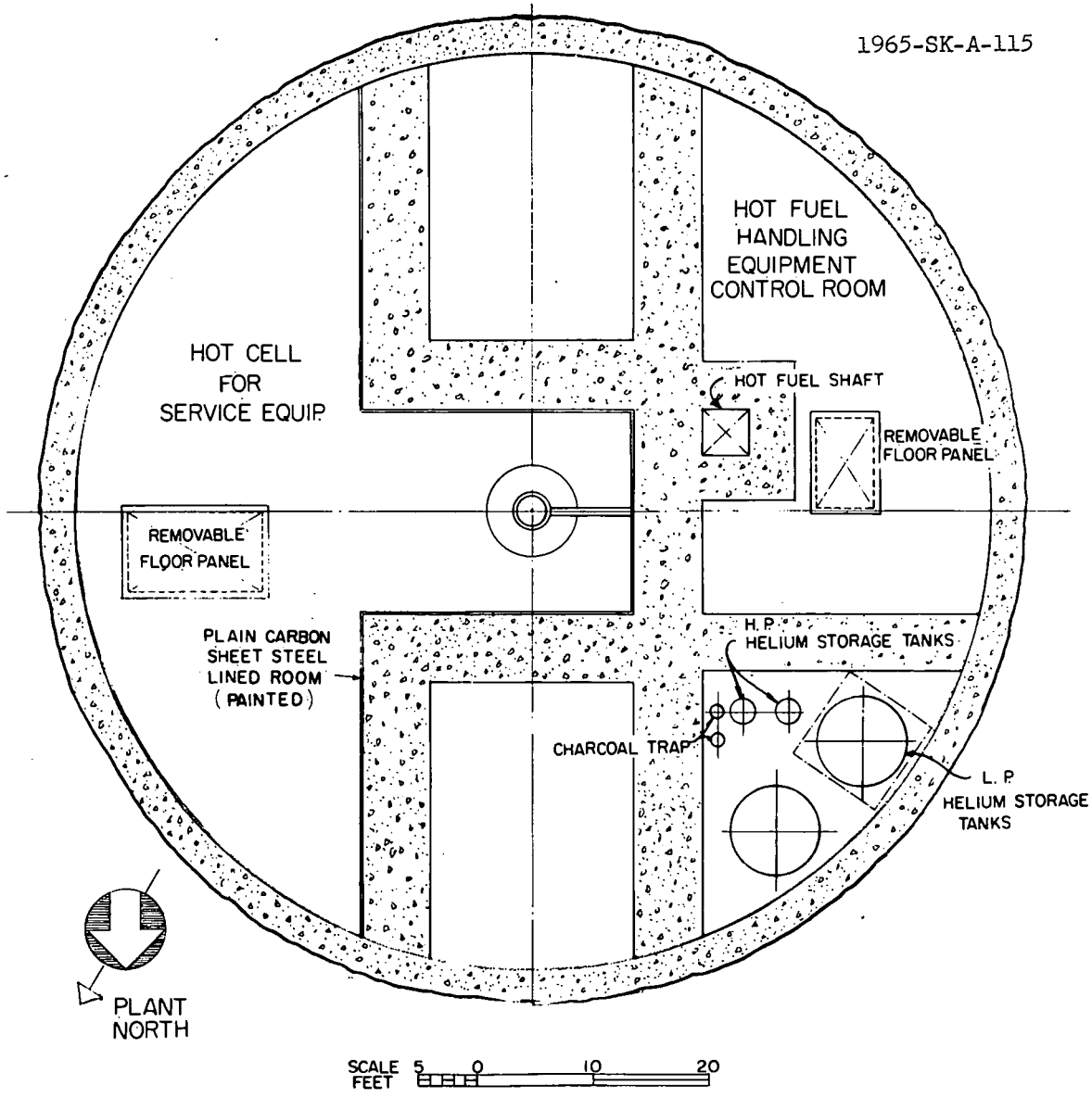

Fig. 6.5. Second Floor Plan — Containment Vessel.

The basement floor, shown in plan view in Fig. 6.6, contains the cleaning and decontaminating fluid storage tanks. In the service canyon, which runs across the diameter of the containment vessel and directly under the reactor, is located a ram and drive assembly that is capable of reaching up to remove the shield plug, elements of the fuel-handling mechanism, the graphite sleeve assemblies surrounding the core, or other components. On the west side of the floor is shown a room for the storage of contaminated fuel as it comes out of the fuel-unloading tube and is stored in appropriate baskets. Since the fuel will be cooled by thermal convection within the room, water-cooled pipes will be required on the walls. After appropriate cooling, the fuel will be loaded by remote means into shielded casks and withdrawn up the shaft to the ground floor for transportation elsewhere for reprocessing.

The ventilation requirements for the rooms in the reactor area are given in Table 6.1. All the air within the containment shell is circulated through filters to remove any particulate activity that might accidentally escape into the rooms, and part of this air is discharged regularly through the stack.

Turbine-Generator Bay

The AEC requested that this study include consideration of both a simple heat dump and a turbine-generator to convert a substantial part of the heat generated in the reactor to electrical power. The cost of the latter appears to be out of proportion to the advantages obtained. Even though a turbine generator of 3-Mw capacity can be obtained at no cost from another AEC facility, the cost of the installation for delivery of 60-cycle power to the electrical grid is estimated to be about $400 000 more than the cost of a heat dump utilizing river water. Therefore, the turbine room is shown only in outline to indicate the approximate size that it would have to be in the event that a decision were made to install

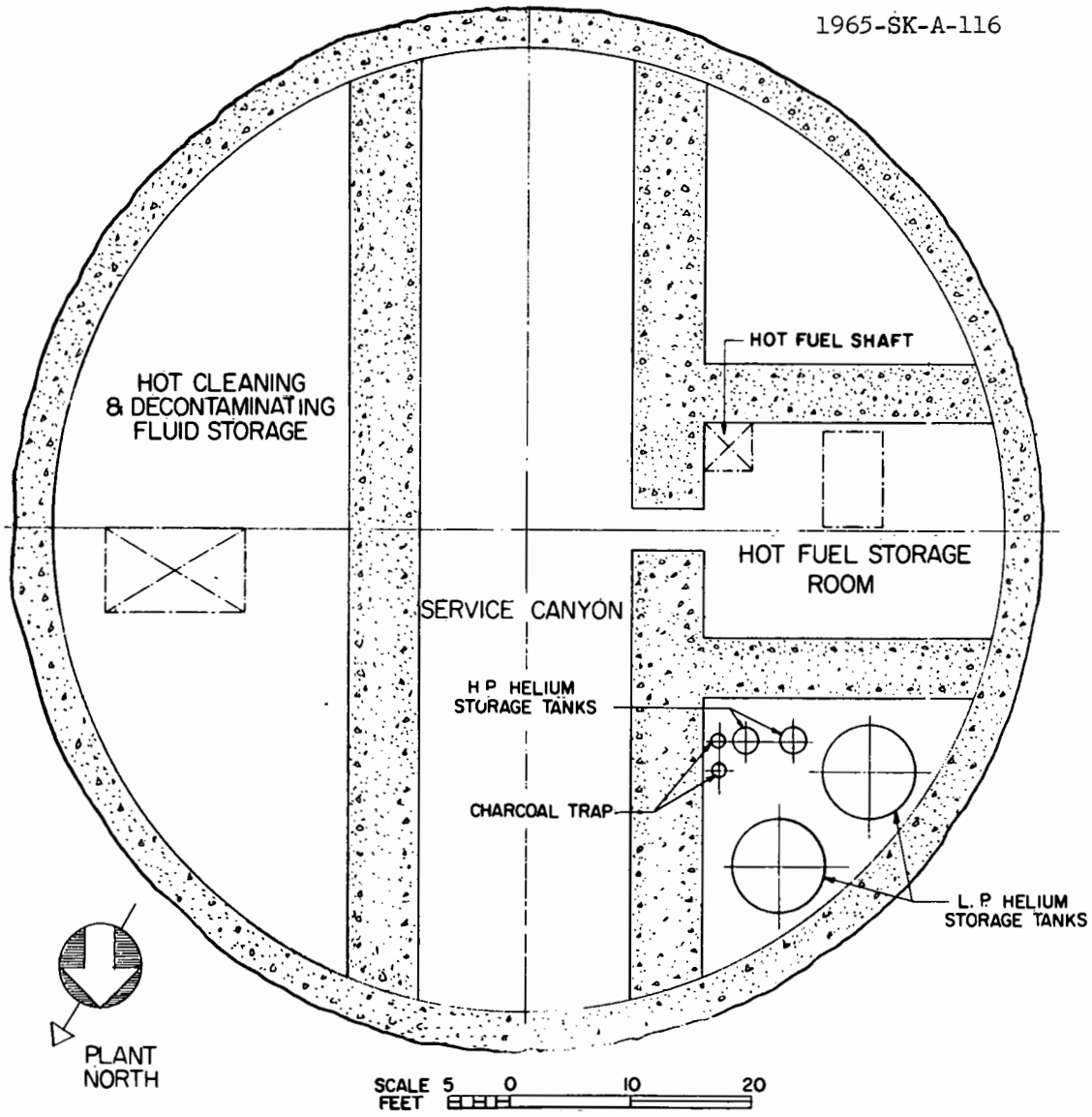

Fig. 6.6. Basement Floor Plan — Containment Vessel.

Table 6.1. Ventilation Requirements of Rooms in Reactor Area

Floor	Room	Ventilation Requirements
Ground	Fuel-loading, control-rod, and steam-generator maintenance	Forced-air circulation through filters, partial exhaust to stack via third floor
Third	Service machine control room	Air conditioning, separate exhaust to reactor vessel cell
	Blower mezzanine and helium cleanup room	Filtered air, exhaust to reactor vessel cell and thence to stack
Second	Hot cell for service equipment	Filtered air, separate exhaust
	Contaminated fuel-handling control room	Filtered air, exhaust to reactor vessel cell
Basement	Hot cleaning and fluid storage room	Filtered air, direct exhaust to stack
	Service canyon	Filtered air, direct exhaust to stack
	Contaminated fuel storage	Filtered air, separate exhaust
	Helium storage area	Filtered air, exhaust to reactor vessel cell

this facility. It is proposed instead that the steam from the reactor steam generator be discharged through appropriate expansion valves and desuperheaters directly to one or more condensers without attempting to utilize the heat. In this way the operator will be free to run the reactor in the most expeditious manner for determining its characteristic behavior rather than having to consider the coupling problems associated with integration with a power grid.

Main Control Room

The main control room is the monitoring and control center for the entire plant. In Fig. 6.2 it is shown as the central room of the ground-level building just outside the containment shell. It contains the reactor panel and bench boards. From this position the entire reactor

system, except the fuel charging and discharging equipment, can be operated. It will be unnecessary for personnel to be within the containment shell during the time that the reactor is at power, since it is proposed that the charging and discharging of fuel be done when the reactor is shut down and depressurized until sufficient experience has been gained to undertake this operation with confidence, probably after considerable equipment development.

Administrative Wing and Service Bay

The administrative wing, consisting of various offices, a change house, store rooms, and locker rooms, is shown wrapped around the main control room on three sides. On the fourth side of the main control room and also adjacent to the containment shell is the dismantling room for fuel-handling and servicing equipment. Next to this room is the room which communicates with the equipment air lock from the containment shell. In the access room is a disposal pit covered by removable floor panels and filled with water for shielding so that contaminated equipment other than fuel can be submerged safely for temporary storage. A loading dock is located at the end of the dismantling and access rooms for the transportation of equipment and accessories, as needed. There is another loading dock of smaller size off the corridor to the left of the main control room and adjacent to the containment shell for the purpose of bringing in fresh fuel for placement in the fuel storage vault. All these areas are accessible to people dressed in clothing appropriate for work in contaminated areas without having to go through the main control room or the administrative area.

Holding Pond for Low-Activity-Level Waste

The water in the disposal pit and the used decontamination solutions located or stored in tanks in the bottom of the containment shell can be discharged from time to time, if the activity is low enough, to a holding pond located some distance from the reactor, prior to slow drainage into the river. In the event that the activity from any of these sources is too high to permit discharge to the holding pond or river, the liquid

will be pumped into suitable portable tanks and transferred to regular high-level waste storage elsewhere in the ORNL area.

System Leaktightness Requirements

Since the helium circulation system is designed to operate at pressures as high as 1000 psi and is subject to contamination from fission products, the leaktightness requirements of both the circulation system and the containment shell are of paramount importance. Since noticeable leakage from the high-pressure system simply cannot be tolerated, it is felt that all connections in the high-temperature region must be welded. Bellows connections are not reliable if used in the high-temperature region and, where used, must be suitably backed up by pressure buffering. Where mechanical closures are required, it is believed that they must be placed in regions of low enough temperature to permit the use of elastomeric gaskets, since this type of seal is the only one known to be both reliable and relatively easily made leaktight.

The shaft seals on the circulating blowers are, of course, potentially serious points of leakage. Following, in general, the practice for the EGCR design, the proposed design calls for a sleeve-type seal that is pressure buffered with oil. The atmospheric side of this seal must be provided with means to draw off oil that leaks through and also to draw off any helium leakage that may occur in the event of oil system pressure failure for a sufficient length of time to permit shutting down the reactor and depressurizing enough to bring the leakage rate to tolerable proportions.

Since an absolutely leaktight system is not attainable, the problem becomes one of how much leakage can be tolerated. It is believed that for a system of this size and operating conditions, a helium leakage rate not exceeding about 0.1% of the helium inventory in the system per day is attainable. This corresponds to about 35 std ft^3 of helium per day. It is not probable that particulate fission products could escape a system of this leaktightness, but fission gases would

be present to some extent. The containment shell ventilation system is designed to sweep this activity out of the shell and up the stack, as indicated in Table 6.1.

The most likely occasions for fission-product escape into the containment shell are believed to be those when the helium circulating system or the reactor must be opened. Barring a major breakdown, there are only three points at which the system would be opened, and then only occasionally. These three points are (1) the blowers, (2) the upper closure containing the control rods and fuel-feed mechanisms, and (3) the lower closure containing the fuel-discharge mechanism. The upper closure for the control-rod system has its own containment enclosure within the containment shell, the blowers are located in separately shielded compartments, and, of course, the fuel-discharge system is in its own separately shielded room which can be washed down with decontaminating solutions. The area is flushed out by remote control.

Shielding

Several basic precepts were followed in laying out the shielding for the reactor. First, each component was isolated from the others insofar as possible to facilitate maintenance. It was assumed that this isolation should be sufficient so that, with no decontamination except of the component in question, the dose in the immediate vicinity of a component such as a blower would not exceed 100 mr/hr with the fuel removed from the reactor. In each instance at least 3 ft of space was provided between the permanent concrete shielding and the component in question to provide space for personnel to work on the equipment.

Where construction problems make close clearances between permanent shielding and the reactor pressure vessel or other components difficult or out of the question, removable block shielding was provided. Four major areas in which this was done include isolation of the blowers from the blower drive motors, isolation of the reactor from the heat exchanger by shielding at the base of the heat exchanger vessel, isolation

of the steam generator from the ground floor of the containment vessel, and enclosure of the coolers for the helium cleanup system. In addition, removable concrete block access hatches were provided over the blowers and blower drive motors, the steam generator header drums, the service room, and the contaminated fuel-handling area. Removable block shielding could also be provided around the fuel discharge chute leading from the bottom access tube to the contaminated fuel storage room if this proved desirable. Analyses may indicate that it will be necessary to include a thick annular layer of shielding around the duct leading into the steam generator to minimize fast-neutron leakage from the reactor. Such a shield annulus could also serve as thermal insulation if made of zirconium oxide.

All the components requiring shielding are below ground level. Further, most of the maintenance and servicing operations where shielding is necessary (except control-rod removal) can be carried out in areas below ground level. The shielding column around the heat exchanger was designed to provide shadow shielding of the office area during such operations as removal and replacement of the control rods. A rough estimate of control rod activation indicates that a single rod will involve about 1000 curies of activity. This would give a dose just outside the reactor containment vessel of about 2 r/hr if no shielding other than the containment vessel wall itself were provided. The shielding for the heat exchanger should cut off the direct beam dose so that scattered radiation would probably give a dose of less than 20 mr/hr in the office area if the rod were withdrawn into the open enclosure instead of into a lead coffin.

7. REACTOR PHYSICS

Core Dimensions and Fuel Loading

In the full-scale power reactor described by Sanderson & Porter,[1] the fuel balls consist of 90.0 wt % graphite, 9.17 wt % ThO_2, and 0.83 wt % UO_2. The average power density is 23.7 w/cm^3, and the specific power is 3900 kw/kg of uranium. A core height of 8.1 ft is used. The core burnup (% of total atoms) is 0.021.

A 10-Mw reactor experiment cannot, of course, have the same values for all these parameters as a 350-Mw power reactor. In order to provide the most meaningful experiment, values were chosen so that the experimental reactor would be the same as the power reactor in core height, core power density, weight percentage of oxides in the fuel balls, and fraction of total atoms burned in the fuel. By keeping the power density and core height the same as in the reference case, the gas flow rate and temperature distribution approximate those which will be found in a full-scale reactor. By keeping the power density the same as in the reference case, the fuel balls are subjected to the same internal temperature gradients and thermal stresses. The total oxide content of the fuel balls is the primary factor in determining their physical properties, and the fractional burnup of the atoms in the fuel balls determines the radiation damage to the balls and the fission-product release.

The critical concentrations of U^{235}-Th mixtures are shown in Fig. 7.1 for various core diameters and various values of the thorium-to-uranium atom ratio in the fuel. The computations were made with a one-dimensional diffusion-theory code employing 27 energy groups (the General Motors GNU code for IBM-704). The calculational model assumed a homogeneous core with atomic densities reduced to correspond to a 39% void fraction. A 3-ft-thick radial reflector of graphite with an average density of 1.49 gm/cm^3 was used, and an axial buckling corresponding to a core 8.1 ft long with 3-ft-thick axial reflectors was assumed. The uranium was assumed

---

[1]Sanderson & Porter, "Pebble-Bed Reactor," Part 2, System Analysis, Table 1.4-3, S & P 1963.

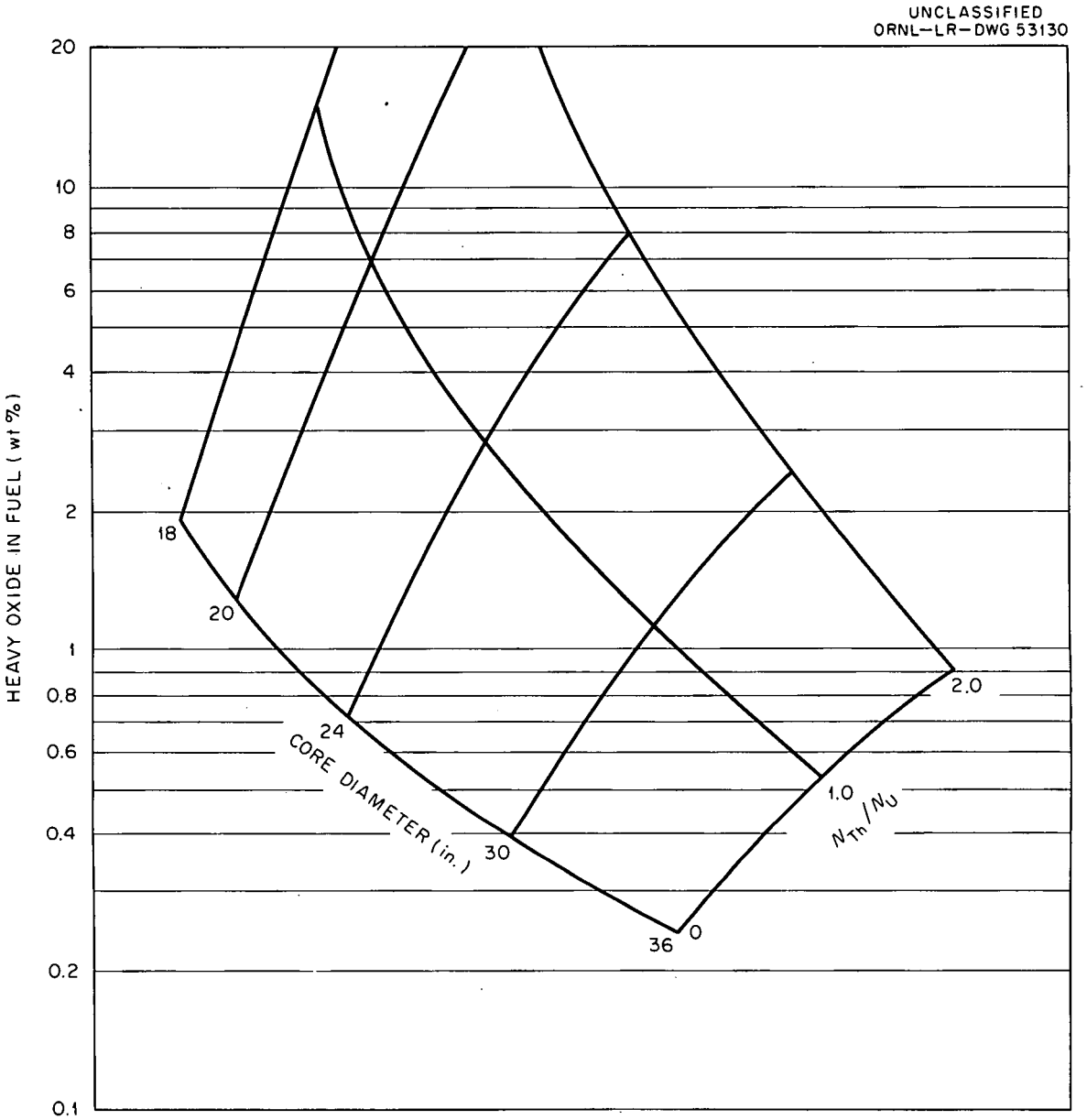

Fig. 7.1. Critical Concentrations of U^{235}-Th Mixture as a Function of Core Diameter and Total Oxide Content of the Fuel in the PBRE.

to be 93% U^{235} and 7% U^{238}. Equilibrium quantities of xenon and samarium were used, together with fission products appropriate to 5% U^{235} burnup.

From the criteria stated above (power density, core height, and weight percentage oxide) it may be seen that the point of particular interest in Fig. 7.1 is that for a core having an 18-in. diameter and 10 wt % oxide in the fuel. This point, corresponding to a fuel element containing slightly less thorium than uranium, was taken as the design value for the reactor experiment. A summary of the characteristics of the reactor is given below:

Core	
Diameter, in.	18
Height, ft	8.1
Fuel element volume fraction	0.61
Void volume fraction	0.39
Fissionable material inventory, kg	21
Specific power, kw/kg	476
Fuel	
Weight fraction	
Graphite	0.9000
U^{235} O_2	0.0513
U^{238} O_2	0.0036
ThO_2	0.0451
U^{235} burnup, %	10
Average fuel residence time in core, days	246
Conversion ratio	0.084

As a consequence of the low total power output and small core diameter (compared with a 350-Mw electrical power plant), the reactor experiment has a much higher ratio of uranium to thorium, a much lower specific power, and a much lower conversion ratio.

Fast Flux Distribution

In determining the graphite reflector thickness, neutron economy is not of primary importance, since a high conversion ratio is not one of the goals of the reactor experiment. The power distribution could

be improved (flattened) slightly by reducing the thickness of the reflector. However, the radiation damage to the pressure vessel becomes excessive if the fast flux incident upon the vessel is allowed to exceed a value of approximately 2×10^{10} neutrons/cm^2·sec above 0.1 Mev. The fast flux at the inside surface of the pressure vessel, as determined by the thickness of graphite between the pressure vessel and the core, is given in Fig. 7.2. In each case attenuation by a 1-in.-thick steel thermal shield was also included. The useful life of the pressure vessel in years of full power operation is also plotted in Fig. 7.2. The actual life of the vessel would be somewhat longer, since the reactor would not operate at full power all the time. It was felt that it would be unwise to design for a total life less than 20 years. Hence the reflector thickness was fixed at 3 ft.

The fast flux in the inner portions of the reflector is a matter of concern with respect to differential shrinkage of the graphite reflector pieces. The data in Fig. 7.3 were used to determine the reflector thickness which could be used without cracking from the stresses imposed by shrinkage.

Reactivity Effects

The total burnup in a fuel ball will be 0.10 fissions/initial fissionable atom. The corresponding decrease in fission cross section is

$$\frac{\Delta\Sigma}{\Sigma} = 0.10\ (1 + \alpha)\ (1 - R_c) \quad ,$$

where the capture-to-fission ratio α is 0.29 and the conversion ratio R_c is 0.08. Hence $\Delta\Sigma/\Sigma = 0.117$. The multigroup calculations show that $(\Delta\Sigma/\Sigma)/(\Delta k/k) = -10.0$. The reactivity change associated with a core which is batch loaded is therefore 1.17%. In practice it would probably prove advantageous to refuel only a small portion of the core at one time so that a pseudoequilibrium axial distribution of burnup would be achieved after a period of time, and the power distribution would therefore not vary with time. If the first refueling were done after the fuel in the region of maximum power had reached a burnup of 5%, the maximum reactivity change

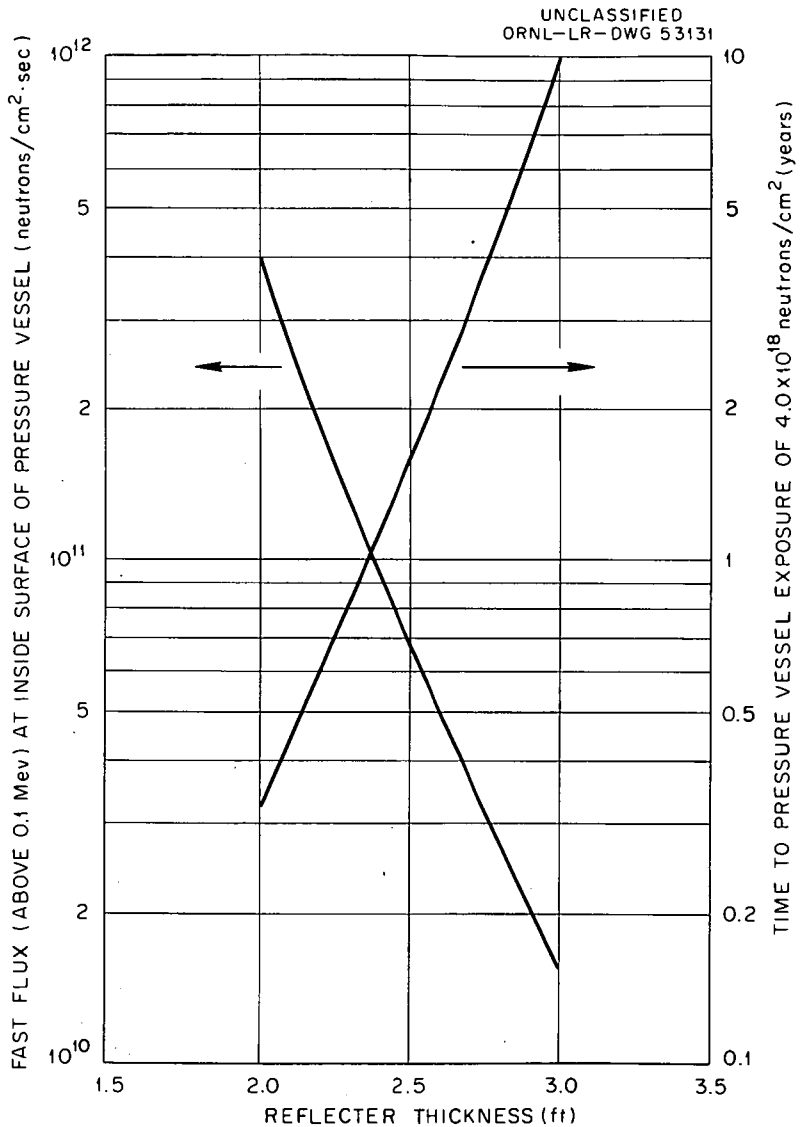

Fig. 7.2. Exposure of PBRE Pressure Vessel.

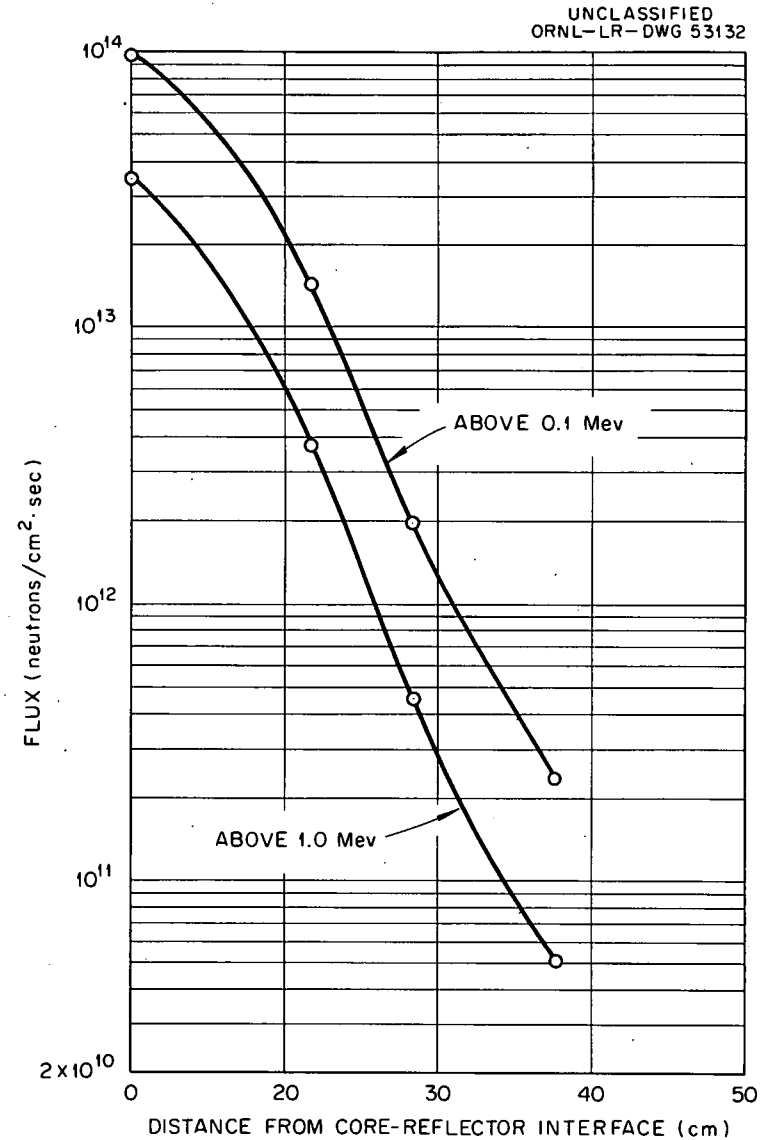

Fig. 7.3. Fast Flux in PBRE Reflector as a Function of Distance from Core-Reflector Interface.

due to burnup would be the one which occurred during this period and would be somewhat less than 0.58%.

The reactivity loss due to equilibrium xenon poisoning at full power operation is 2.71%. This loss can rise to a maximum of 3.60% if the reactor is shut down and then brought to power at the time when the xenon concentration has reached a maximum. Thus the amount of reactivity control needed for "xenon override" is 0.89%. The reactivity loss as a result of equilibrium samarium poisoning is 1.16%.

In considering the effects of temperature on reactivity, it is necessary to keep in mind that neutron moderation occurs primarily in the reflector rather than in the core. For example, one finds that over 90% of the thermal neutrons absorbed in the core attain thermal energies in the reflector and then migrate to the core, whereas less than 10% attain thermal energies while in the core. Hence it is to be expected that the moderator temperature coefficient will depend mainly on reflector conditions. There are three noticeable contributions of temperature to reactivity. In changing the temperature of the entire system from 68 to 900°F, the decrease in core and reflector density gives a reactivity loss of 0.16%, the change in effective nuclear cross sections gives a reactivity gain of 0.06%, and the Doppler broadening in the thorium resonance integral gives a reactivity loss of 0.42%. The first two of these effects are obtained directly from the multigroup calculations, while the Doppler broadening is computed from the thorium resonance parameters. The over-all temperature coefficient from the three effects together is

$$\frac{1}{k}\frac{dk}{dT} = -0.4 \times 10^{-5}/°F \quad .$$

Since the dominant contributor to the negative temperature coefficient is the thorium resonance integral, it follows that the presence of thorium

in the core is important in providing a stable reactor, as well as in providing a fuel ball of the desired physical properties.

Control Blades

For mechanical reasons it is most appropriate to locate the control devices in the reflector where the fuel balls will not interfere with their operation. With the inner portion of the reflector arranged in concentric annuli, the control devices can be located in a ring between two graphite sleeves. Absorber blades which surround the core in a nearly continuous ring were chosen in preference to rods in order to avoid undesirable "scalloping" effects on the circumferential power distribution when the rods are partially inserted. The various items affecting reactivity, as discussed in the previous section, are indicated below:

	$\Delta k/k$
Uranium burnup	0.0058
Equilibrium xenon	0.0271
Xenon override	0.0089
Samarium	0.0116
Temperature defect	0.0052
Total	0.0586

Figure 7.4 presents the worth of control blades of various thicknesses of type 316 stainless steel when located in a 27-in.-diam circle concentric with the core. A strong reactivity effect is noted with comparatively thin layers of absorber because of the high importance of the reflector region. A thickness equivalent to 1/16 in. of stainless steel was chosen, giving a total reactivity control of 0.140 $\Delta k/k$ from full insertion to full withdrawal of the blades. As may be seen from the tabulation above, the maximum control needed in changing from a cold, clean core to a hot core with equilibrium burnup and maximum xenon is 0.0586 $\Delta k/k$. Thus 0.0814 $\Delta k/k$ is available for shutdown margin.

The reactivity control of the blades which were chosen is shown in Fig. 7.5 as a function of the depth of insertion into the core. The blades

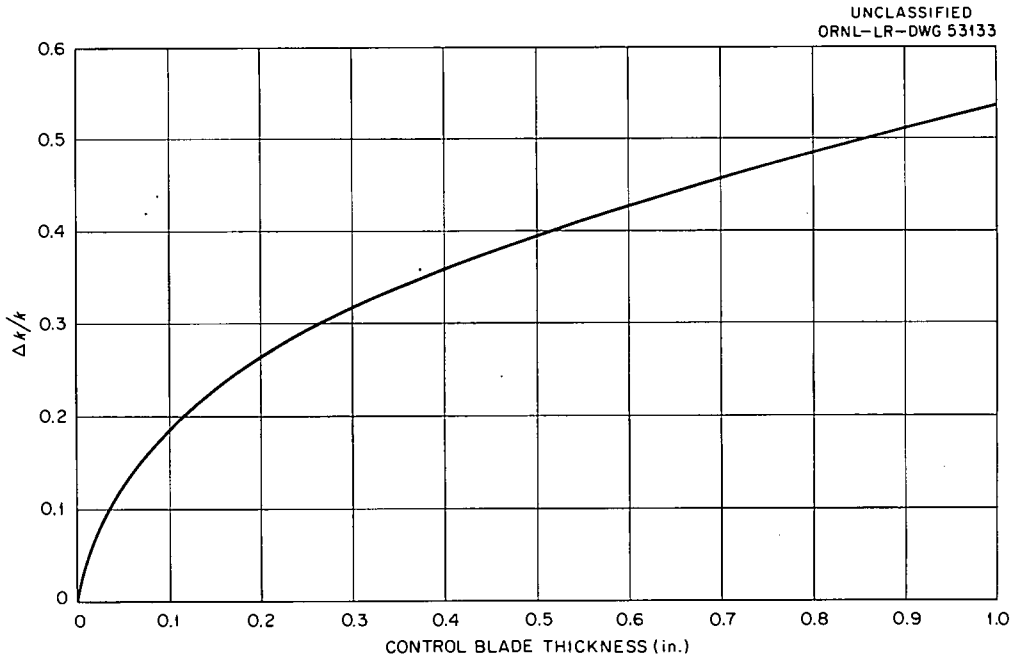

Fig. 7.4. Total Reactivity Worth Versus Control Blade Thickness.

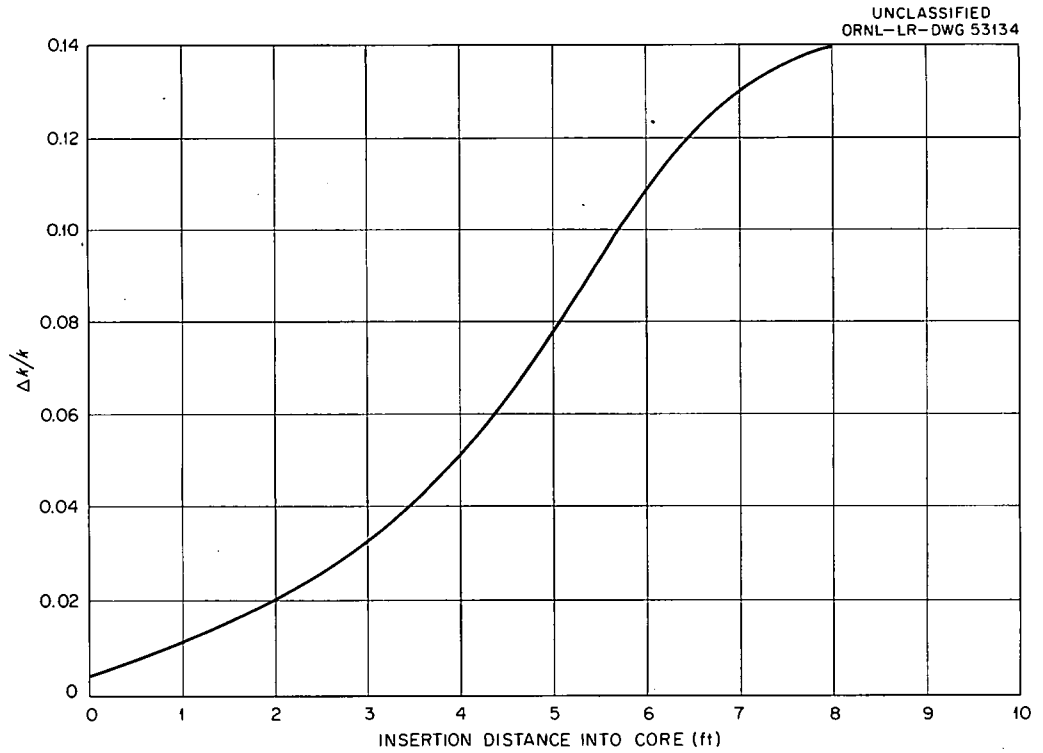

Fig. 7.5. Differential Worth of a 1/16-in.-Thick Control Blade.

are fully withdrawn (from the upper reflector, as well as from the side reflector) when the reactor is hot and contains the equilibrium fuel burnup and the maximum xenon poisoning. When the xenon poisoning is reduced to the equilibrium value, the control blades are inserted 0.7 ft into the core. This position is the normal one during operation after equilibrium burnup distribution has been achieved. For a hot, clean core with equilibrium xenon the control blades are inserted to a depth of 2.6 ft (0.0263 $\Delta k/k$), corresponding to initial power operation. The position of the control blades at which the reactor first attains criticality (cold, clean core) is insertion to a depth of 4.4 ft.

Power and Flux Distributions

The power distribution in the operating reactor depends on the position of the control blades. Two representative cases are given in Figs. 7.6 and 7.7. Figure 7.6 gives the power distribution when the control blades are completely withdrawn (approximately the condition for the hot core with equilibrium burnup). The peak power density is 2.08 times the average, while the minimum is 0.417 of the average. Figure 7.7 shows the power distribution when the control blades are inserted 2.7 ft into the core, corresponding approximately to the hot core under initial operating conditions. The peak power density is raised to 2.38 times the average and occurs 1 ft below the center of the core instead of at the center, as before. These power distributions were computed with the two-dimensional four-group PDQ code. The normalization is to an average of 1.0 in the core.

Flux traverses in the radial direction at the mid-plane are shown in Fig. 7.8. The prominent peak of thermal flux in the reflector, characteristic of a reflector-moderated reactor may be seen, as well as the relatively high ratio of epithermal to thermal flux in the core, indicating an "under-moderated" reactor. Only 56% of the fissions occur at thermal energies.

Reflector Heat Load

The neutron heating in the reflector was computed from the fast fluxes and the scattering cross section. The gamma heating was computed by summation

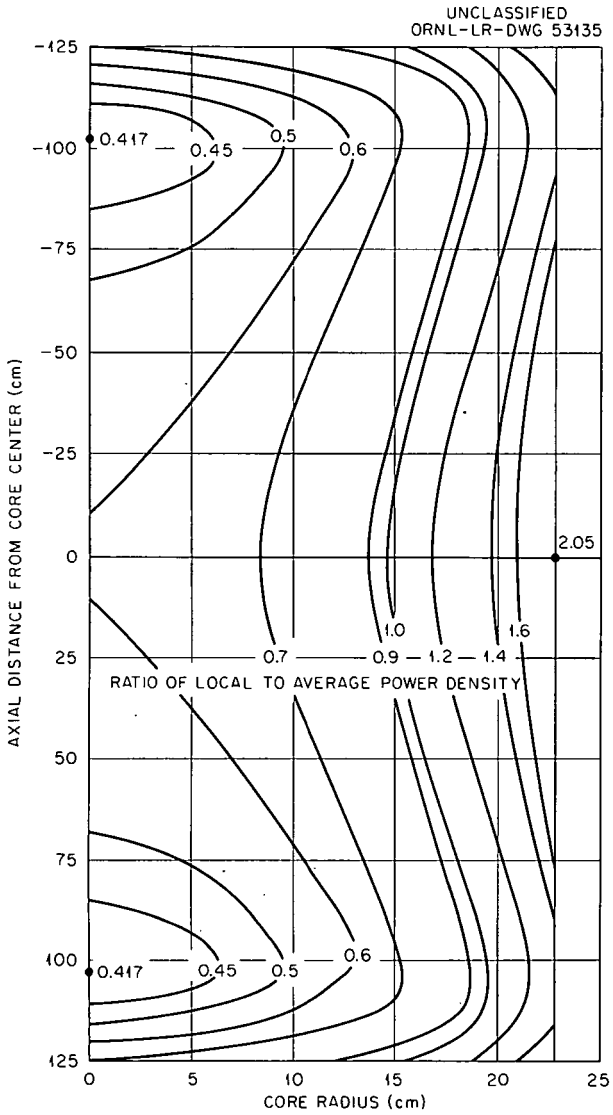

Fig. 7.6. Power Distribution with Control Blades Withdrawn.

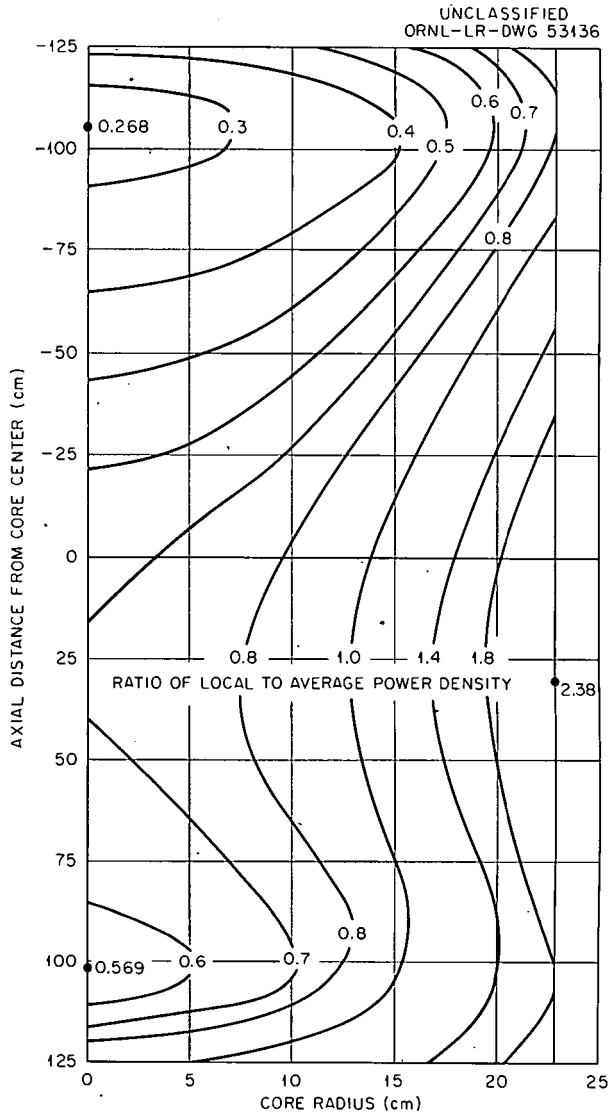

Fig. 7.7. Power Distribution with Control Blades Inserted 2.7 ft.

of the contributions from the source points in each of six energy groups. The results of the calculations are given in Fig. 7.9.

Gamma Heating in Pressure Vessel

The gamma heating in the pressure vessel was assumed to be due primarily to the capture gammas in the steel and thus proportional to the thermal flux in the steel. A series of plane sources was computed, and the contribution from each to the heating at the inner surface of the pressure vessel was determined. The calculation gives 0.26 w/cm^3 as the peak heating density. This heat generation can be reduced substantially, if necessary, by impregnating the outer portion of the reflector with boron. Assuming a simple exponential attenuation of the thermal flux in the borated graphite, it is found that 1% by weight of boron in the outer 2 in. of graphite gives a factor of 7 reduction in the pressure vessel heating, while 2% boron in the outer 2 in. of graphite gives a factor of 50 reduction.

Neutron Lifetime

From the fluxes of the multigroup calculations, the average prompt neutron lifetime is determined to be 1.5×10^{-3} sec. Approximately 99% of the lifetime occurs in the reflector.

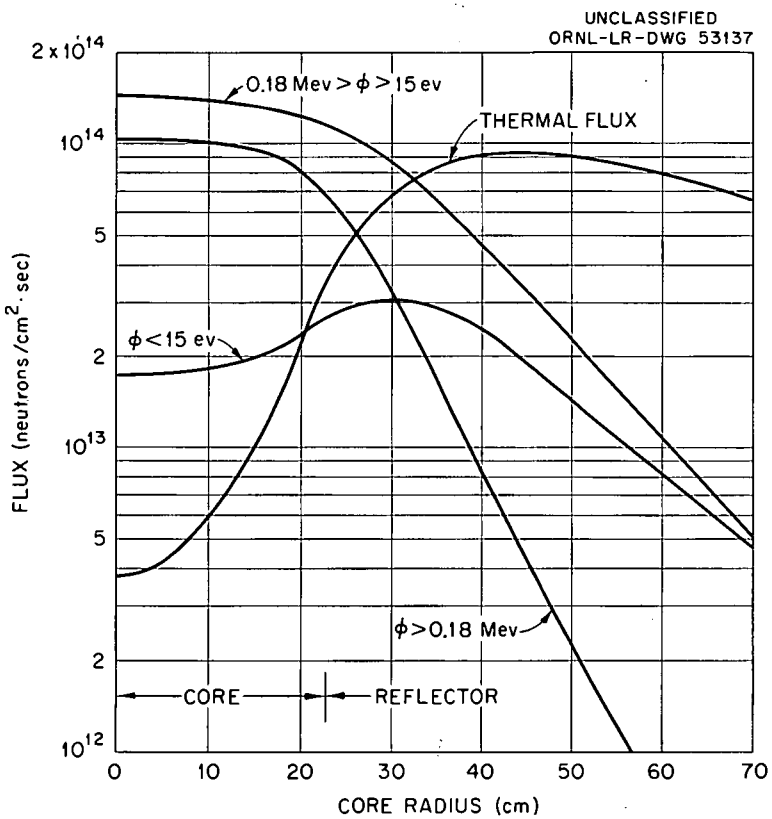

Fig. 7.8. Radial Flux Traverse at the Reactor Mid-Plane.

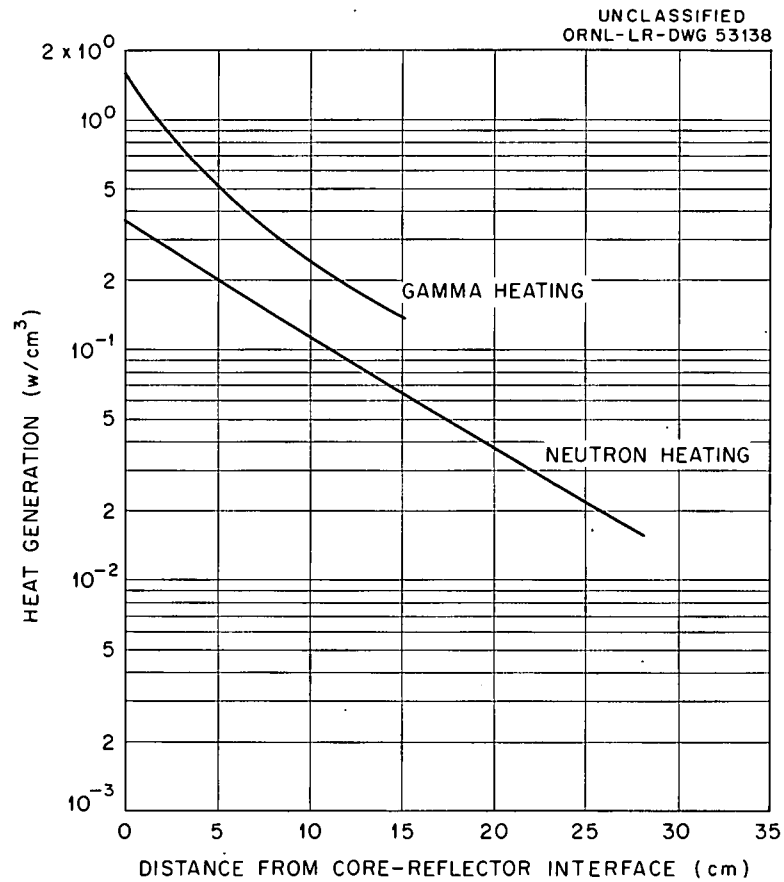

Fig. 7.9. Reflector Heating in PBRE.

8. FUEL ELEMENTS AND GRAPHITE COMPONENTS

This chapter is devoted primarily to a review and evaluation of existing information on fueled-graphite elements of the type under consideration for use in the PBRE. An evaluation is also included of the requirements and fabrication limitations applicable to graphite components to be used in the bed container, the reflector, and the reflector perimeter.

Fuel Elements

The proposed PBRE fuel element is a graphite sphere containing a fuel-particle dispersion of UO_2, UC_2, or UC. The required fuel element characteristics and the proposed operating conditions are summarized below:

Configuration	Sphere
Sphere diameter, in.	1 1/2
Fuel loading	Equivalent to 0.164 g of uranium per cm^3 of total fuel element volume
Carbon density	1.70 g per cm^3 of net graphite volume
Sphere operating temperatures, °F	
Average surface	1200
Maximum surface	2000
Maximum allowable internal (including hot spots)	2200
Number of spheres per reactor (assuming 39% void volume in core)	8500
Average power density in core, w/cm^3	25
Average surface heat flux, $Btu/hr \cdot ft^2$	81 500
Maximum irradiation exposure, kwhr/sphere	5500

In service the fuel spheres will be subjected to impact loads during the charging and unloading operations, compressive loads primarily from differential thermal expansion between the ball bed and its container

wall, abrasive action from ball agitation during power cycling or ball spinning under aerodynamic forces, thermal stresses arising from temperature gradients within the fuel sphere, oxidation by impurities in the helium coolant, and radiation damage from both neutron- and fission-fragment bombardment. Under these conditions, the fuel elements must maintain structural integrity, must retain a large proportion of the fission products generated, and must not self-weld to adjacent spheres.

The data on the ability of the fueled-graphite matrix to withstand the mechanical and thermal stresses anticipated under operating conditions are encouraging, although not extensive. Self-welding is a problem only in the case of Si-SiC coated spheres. Even with this type of fuel sphere, self-welding should not occur at the presently anticipated maximum surface temperature of 2000°F. However, additional tests will be required to define more clearly the temperature, time, and contact pressure conditions under which self-welding will occur. The major uncertainty at present is fission-product release from the spheres at high temperatures and high burnups.

Sanderson & Porter Program

Much of the available information on the performance of graphite fuel elements under PBRE operating conditions was developed by Sanderson & Porter in connection with a design study of a 125-Mw(e) pebble-bed reactor and steam power plant, and a detailed description of the Sanderson & Porter fuel-sphere testing program has been published.[1]

The specimens are obtained from various companies and are evaluated at Battelle Memorial Institute. At Battelle, the fuel-sphere specimens are inspected visually for flaws and then weighed and measured dimensionally. The specimen density is calculated from these measurements. Representative samples of a given lot of spheres are examined metallographically. Next, additional samples are subjected to the following tests:

[1]"Pebble Bed Reactor Program Progress Report for Period June 1, 1958, to May 31, 1959," NYO-2373.

1. Impact. A 1-lb steel weight is dropped onto the fuel sphere from increasing heights, and the sphere is rotated between impacts to simulate anticipated service conditions. With coated specimens, a "hot oil" permeability test is used after each impact to determine whether fracture has occurred.

2. Compression. The fuel sphere is loaded at a rate of 200 lb/min in a Universal Testing Machine. Coated specimens are compression tested under hot oil.

3. Abrasion. The test sphere and a number of dummy elements are tumbled together in an 8-in.-diam, 4 3/4-in.-high drum rotated at a speed of 52 rpm. Evaluation is based on weight change and visual appearance.

4. Self-Welding. A vertical row of specimens is subjected to an axial load (typically 50 lb) for 100 hr while in a furnace capable of heating them to 2500°F. Visual examination and "hot oil" testing are used to determine self-welding tendencies of the sphere. This test is, of course, applied only to coated spheres.

5. "Hot Oil" Permeability. Coated specimens are immersed in silicone oil at 400°F. Faults in the coatings are revealed by a stream of bubbles of adsorbed gases released from the substrate graphite.

6. Surface Contamination. Uranium contamination in the surface of fuel specimens is determined by counting the gross alpha activity in a flow-type alpha proportional counter.

Fuel elements that look promising after undergoing these tests are evaluated under irradiation. The testing program is designed to yield data on fission-product retention and the effect of irradiation on physical characteristics and mechanical properties of the fuel sphere. The following types of irradiation tests are used:

1. Neutron Activation. The fuel spheres are irradiated at low temperatures to a low dose (up to 6×10^{15} neutrons/cm^2) in order to generate a measurable amount of fission products. After a 3- to 7-day decay period, the specimens are heated in flowing helium that is analyzed with an on-stream gamma-ray spectrometer.

2. Furnace Capsule. The fuel sphere is irradiated at a low flux but at high temperatures maintained by electrical heaters. The isotopes Xe^{133}, Xe^{135}, Kr^{87}, Kr^{88}, and Kr^{85} are measured in the exit helium sweep gas. The ratio of the rate at which fission products are released to the rate at which fission products are generated (R/B) is determined for each isotope.

3. Sweep Capsule. The fuel sphere is irradiated at a high flux at high temperatures maintained by nuclear heating alone. Helium gas is passed over the sphere during irradiation and analyzed as in the furnace capsule tests. Radiation damage data are obtained in postirradiation examinations.

4. Static Capsule. The fuel sphere is irradiated in a capsule under conditions which, except for the absence of gas flow, are similar to the sweep capsule tests. This test is designed primarily for radiation damage evaluation, although fission-product-release data can also be obtained by collecting the gases from the sealed container at the end of the test.

The characteristics of the various types of fuel elements procured for evaluation are summarized in Table 18.1 (refs. 1–4), and the types which were ultimately evaluated under irradiation are listed in Table 8.2.

Property Evaluations and Effects of Irradiation

Data on the effects of irradiation on dimensional distortion, weight change, impact resistance, compressive strength, and abrasion resistance were obtained in capsule tests SP-1, SP-3, and SP-4 at Battelle. Additional information on dimensional change under irradiation was obtained

---

[2] "Fuel Element Development Program for the Pebble Bed Reactor, Phase I Progress Report for Period May 1, 1959, to October 31, 1959," NYO-2706.

[3] "Fuel Element Development Program for the Pebble Bed Reactor, Quarterly Progress Report for Period November 1, 1959, to January 31, 1959," S & P 1964-14.

[4] "Current Fuel Element Developments and Their Effects on the Pebble Bed Reactor Program, May 10, 1960," S & P 1965-17.

Table 8.1. Characteristics of Fueled-Graphite Elements Studied in Sanderson & Porter Program

Element Designation	Manufacturer[a]	Fuel			Matrix				Coating		
		Loaded as	Final Form	Particle Size	Reimpregnated	Net Density (g/cm^3)	Shell Thickness (in.)	Baking Temperature (°F)	Location	Material	Thickness (in.)
					Graphite Infiltrated with Fuel						
FI-1	Syl	UNH	UO_2	1 μ	No	1.65	0	1470			
FI-6	AMP	UNH	UC_2	1 μ	Yes	1.85	0	3500	Sphere	ZrC	0.001
					Graphite Containing Lumps of Fuel						
FL-1	AMP	UC_2	UC_2	3/8 in.	Yes	1.85	0.35	3500			
FL-2	AMP	UC_2	UC_2	3/8 in.	Yes	1.85	0.35	3500	Sphere	ZrC	0.001
FL-3	BMI	UO_2	UO_2	67 μ	No	NR[b]	0.25	2000			
					Unfueled Graphite						
FX-1	Plas								Sphere	TiC	0.010
FX-2	Plas								Sphere	ZrC	0.010
FX-3	Ray								Sphere	Pyrolitic carbon	0.060
					Admixture of Fuel in Graphite						
FA-1	NC	UO_2	UO_2	100–150 μ	No	1.62	0	2560			
FA-2	BMI	UO_2	UO_2	67 μ	No	1.63	0	2000			
FA-5	3M	UO_2	UC	100–200 μ	Yes	1.80	0.15	3600			
FA-6	3M	UO_2	UC	100–200 μ	Yes	1.80	0.15	3600	Sphere	Si-SiC	0.003
FA-7	Carbo	UC_2	UC_2	100–200 μ	No	1.63	0	3600			
FA-8	Carbo	UC_2	UC_2	100–200 μ	No	1.63	0	3600	Sphere	Si-SiC	0.030
FA-9	NC	UO_2	UO_2	100–150 μ	Yes	1.68	0	2560			
FA-10	GLC	UO_2	UO_2	350–420 μ	Yes	1.80	0	2000			
FA-11	NC	UO_2	UO_2	100–150 μ	Yes	1.68	0	2560	Sphere	Pyrolitic carbon	0.005
FA-14	NC	ThO_2–UO_2	ThO_2–UO_2	100–150 μ	No	1.62	0	2560			
FA-16	3M	UO_2	UC	100–200 μ	Yes	1.75	0.060	3600	Sphere	Si-SiC	0.003
FA-17	NC	UO_2	UO_2	100–150 μ	No	1.62	0	2560	Sphere	Pyrolitic carbon	0.002
FA-19	NC	UO_2	UC_2	100–150 μ	No	1.65	0	4800			
FA-20	NC	UO_2	UC_2	100–150 μ	No	1.65	0	4800	Sphere	Pyrolitic carbon	0.002
FA-21	Ray	UO_2	UC_2	100–150 μ	No	1.65	0	4800	Sphere	Pyrolitic carbon	0.050
FA-22	NC/BMI	UO_2	UO_2	100–150 μ	No	1.57	0	2350	Particle	Al_2O_3	0.002
FA-23	3M	UO_2	UC	100–200 μ	NR	NR	NR	NR	Sphere	Si-SiC	0.008

[a]AMP – American Metal Products Co.
BMI – Battelle Memorial Institute
Carbo – The Carborundum Company
GLC – Great Lakes Carbon Corp.
3M – Minnesota Mining and Manufacturing Company
NC – National Carbon Company
Plas – Plasmakote Company
Ray – Raytheon Mfg. Co.
Syl – Sylvania-Corning Nuclear Company.

[b]Not reported.

Table 8.2. Summary of Irradiation Test Program of Sanderson & Porter on Fueled-Graphite Elements

Test Capsule No.	Type of Irradiation Test	Designations of Fuel Element Tested[a]
SP-1	Static	FA-1 (NC86) FA-1 (NC87) FL-3 (BMI-12) FL-3 (BMI-11) FI-1 (E16) FI-1 (E13)
SP-2	Sweep	FA-1 (E81) FA-1 (E84) FI-1 (E5) FI-1 (E10)
SP-3	Sweep	FA-6 (18E) FA-6 (20E) FA-8 (E4) FA-8 (E5)
SPF-1	Furnace	FA-20 (310)
SP-4	Static	FA-1 FA-8 FI-1 FA-2 FA-20 FA-10
SPF-2	Furnace	FA-16
SPF-3	Furnace	b
SP-5	Sweep	FA-22 (471) FA-23 (E8-7)
SP-5	Static	FA-20 (338) FA-20 (345) FA-22 (470) FA-23 (E8-2)

[a]For description of fuel elements see Table 8.1.

[b]Admixture type of fuel element containing Al_2O_3-coated normal UO_2.

in MTR tests conducted by ORNL[5–7] and by General Atomic[8] using cylindrical pellets of fueled graphite. The operating conditions utilized in these irradiation tests are summarized in Tables 8.3, 8.4, and 8.5.

The fuel pellets for the ORNL-MTR-48-1 test were fabricated by National Carbon Company by the admixing of UO_2 spherical shot and a carbonaceous mixture. The UO_2 was converted to UC_2 during the baking operation, which reached a temperature of approximately 5000°F.

The General Atomic irradiation test pellets were 0.220 in. in diameter, 1/4 in. long, and contained approximately 24 vol % UC or UC_2 dispersed in graphite. Four pellets contained in type 316 stainless steel constituted each irradiation test specimen.

Dimensional and Weight Changes

The dimensional and weight changes which occurred during the BMI SP-1, SP-3, and SP-4 tests are listed in Table 8.6. The effect of combined neutron and fission-fragment bombardment is shrinkage of the fueled graphite. According to the work of Nightingale et al.,[9] at Hanford, shrinkage would be expected at the irradiation temperatures of these tests from fast-neutron effects alone. In the impregnated specimens, additional shrinkage due to fission-fragement bombardment is believed to have caused the larger dimensional changes. Attenuation of essentially all fission fragments in the graphite matrix of these specimens is associated with the small fuel particle size (approximately 1 μ). There was no direct correlation between shrinkage and fuel particle size in the range from 67 to 400 μ, however, according to the data obtained in the SP-4 test.

---

[5] "GCR Quar. Prog. Rep. Dec. 31, 1959," ORNL-2888, p. 107.

[6] "GCR Quar. Prog. Rep. March 31, 1960," ORNL-2929, p. 155.

[7] "GCR Quar. Prog. Rep. June 30, 1960," ORNL-2964, pp. 160–6.

[8] D. E. Johnson and J. M. Tobin, "The Dimensional Stability on Irradiation of Al_2O_3-UO_2, BeO-UO_2, Graphite-UC, and Graphite-UC_2," ORNL Conference on Nuclear Reactor Chemistry, October 13, 1960.

[9] R. E. Nightingale, J. M. Davidson, and W. A. Snyder, "Damage Effects to Graphite Irradiated up to 1000°C," A/Conf. 15/P/14, 1958.

Table 8.3. Operating Conditions for BMI Irradiation Tests of Fueled-Graphite Specimens SP-1, SP-3, and SP-4[a]

Capsule No.	Specimen No.[b]	Operating Temperatures[c] (°F)			Heat Generation Rate[c] (kw/sphere)	U^{235} Burnup (at. %)	Total Exposure (kwhr/sphere)
		Block	Specimen Surface	Specimen Center			
SP-1	FA-1 (NC86)	940	1224	NR[d]	1.71	1.5	1150
	FA-1 (NC87)	980	1288	NR	1.81	1.6	1225
	FL-3 (BMI-11)	920	1204	NR	1.65	1.5	1120
	FL-3 (BMI-12)	800	~1070	NR	NR	NR	NR
	FI-1 (E16)	1060	1332	NR	1.88	1.9	1330
	FI-1 (E13)	1050	1317	NR	1.85	1.8	1225
SP-3	FA-6 (18E)	1000	1300	1600	1.7	NR	2400
	FA-6 (20E)	1000	1300	1600	1.7	NR	1950
	FA-8 (E4)	1200	1600	1900	2.2	NR	2400
	FA-8 (E5)	1200	1600	1900	2.2	NR	2600
SP-4	FA-1	1290	1620	1780[e]	1.95	6.7[f]	6700[f]
	FA-8	1410	1770	1830	2.24	6.7	6700
	FI-1	1400	1760	1850	2.37	6.7	6700
	FA-2	1410	1770	1910	2.27	6.7	6700
	FA-20	1250	1560	1770	1.96	6.7	6700
	FA-10	1300	1630	1730	1.75	6.7	6700

[a]See refs. 1, 2, 3, and 4.

[b]For description of fuel elements see Table 8.1.

[c]Heat generation rate was calculated from measured graphite block temperature, pool water temperature, and effective thermal-resistance properties of the capsule. Specimen temperatures were then calculated, using 20 Btu/in.·ft·°F for thermal conductivity.

[d]Not reported.

[e]Temperature measured by thermocouple inserted into fuel spheres.

[f]Average for six specimens in capsule.

Table 8.4. Test Parameters for ORNL-MTR-48-1 Fueled-Graphite Element Irradiation[a]

Test Parameters	Forward Pellet No. 85	Rear Pellet No. 91
Pellet characteristics		
Diameter, in.	0.9969	0.9965
Length, in.	1.4687	1.4682
Volume, cm^3	18.766	18.764
Total weight, g	35.4107	37.8407
Weight of UC_2, g	10.52	19.33
U^{235} content (93.12% enrichment), wt %	8.89	16.33
U^{235} concentration, g/cm^3	0.1677	0.3295
U^{235} concentration, $atoms/cm^3$	42.9×10^{19}	84.3×10^{19}
Test duration (MTR at 40 Mw), hr	1446	1446
Operating temperatures		
Graphite capsule wall less coolant water temperature (110°F), °F		
Design value	1392	1467
Average operating value	1450	1240
Interface between graphite can and fuel pellet, estimated, °F	1780	1520
Central pellet, estimated, °F	3500	3000
Thermal neutron flux, $neutrons/cm^2 \cdot sec$		
Design value	4.6×10^{13}	2.6×10^{13}
Average operating value	4.8×10^{13}	2.2×10^{13}
Fission power density, w/cm^3		
Design value	270	300
Average operating value	282	254
U^{235} atoms fissioned, $atoms/cm^3$	5.24×10^{19}	4.72×10^{19}
Percent	12.2	5.6
Burnup of fueled graphite matrix, Mwd/MT	8970	7560
Burnup of U^{235}, Mwd/MT	101 000	46 300

[a]See refs. 5 and 6.

Table 8.5. Data on General Atomic (MGCR) Fueled-Graphite Irradiation Tests[a]

Specimen No.	Material	Fuel Loading (g of U^{235})	Estimated Cladding Surface Temperature (°F)	Surface Heat Flux (Btu/hr·ft^2)	Fission-Gas Release (% of Kr^{85})	Burnup (% of U^{235} atoms)	Diametral Dimensional Change (%)[b]
5	UC_2-C	1.46	1520	204 000		1.58	
9	UC-C	1.44	1560	198 000	0.37, 0.41	1.56	−1.5
8	UC-C	1.44	1430	156 000		1.23	−1.5
4	UC_2-C	1.46	1270	132 000	0.30, 0.12[c]	1.01	−1

[a]See ref. 8.

[b]No change in the microstructure was observed for either type of fuel as a result of irradiation.

[c]The 0.12 value is considered questionable; the 0.30 value is considered reliable.

Table 8.6. Dimensional and Weight Changes in Irradiated Fueled-Graphite Spheres Tested in BMI Capsules SP-1, SP-3, and SP-4

Specimen No.[a]	Type	Weight Change (%)	Dimensional Change (%)		
			x[b]	y	z
		Capsule SP-1			
FI-1 (E13)	Impregnated	-4.48	-0.86	-0.83	-1.10
FI-1 (E16)	Impregnated	-2.88	-0.91	-1.08	-0.82
FA-1 (NC86)	Admixture	+0.03	-0.07	-0.24	-0.28
FA-1 (NC87)	Admixture	-0.08	-0.29	-0.23	-0.21
FL-3 (BMI-11)	Lumped fuel	-4.25	-0.33	-0.26	-0.27
FL-3 (BMI-12)	Lumped fuel	-0.71	-0.11	-0.28	-0.16
		Capsule SP-3			
FA-6 (18E)	Admixture, Si-SiC coating	-0.1		-0.3	
FA-6 (20E)	Admixture, Si-SiC coating	0.0		-0.0	
FA-8 (E4)	Admixture, SiC coating	-0.3[c]		+0.01	
FA-8 (E5)	Admixture, SiC coating	-0.1[c]		+0.08	
		Capsule SP-4			
			Polar	Equitorial[d]	
FI-1	Impregnated	-0.40	-0.76	-0.67	
FA-2	Admixture	-0.55	-0.03	-0.08	
FA-1	Admixture	-0.11	-0.47	-0.52	
FA-10	Admixture	-0.06	-0.69	-0.81	
FA-8	Admixture, SiC coating	+0.14	-0.16	+0.65	
FA-20	Admixture, pyrolitic carbon coating	+0.19	-0.93	-0.17	

[a]For description of fuel element see Table 8.1.

[b]x, y, and z are three mutually perpendicular diameters.

[c]Weight measured after hot-oil immersion test.

[d]Polar — parallel to cylindrical irradiation capsule axis. Equitorial — perpendicular to polar direction.

Examination of the ORNL-MTR-48-1 test capsule revealed no apparent change in the two graphite cans which contained the graphite-UC_2 fuel pellets.[7] The dimensions of the cans agreed with preirradiation values to within 0.1%. Only the rear graphite-UC_2 fuel pellet, No. 91, has been inspected to date. It was removed intact from the can and very little change in appearance was noted. The average diameter of the end of the pellet nearest the reactor core decreased 2.4% while the diameter of the other end decreased 5.1%. The length of the pellet increased 3.5%.

The micrometer measurements were reported to be difficult to make because the surfaces of the fuel pellets were friable. This difficulty could have resulted from reaction of the UC_2 with moisture in the hot-cell atmosphere.

As indicated in Table 8.5, the General Atomic graphite-UC and graphite-UC_2 pellets decreased 1.5 and 1% in diameter, respectively, during irradiation. One of the irradiated graphite-UC pellets was annealed at 2500°F for 4 hr in flowing helium (15 ft^3/hr), and it disintegrated to a "crusty lump of crumbs." However, it was believed that accidental oxidation could have caused this behavior.[8]

It may be seen in Table 8.6 that, in almost every case, the fueled graphite lost weight during irradiation and that, in capsule SP-1, three of the specimens suffered very large weight losses. The mechanism of weight loss has not yet been determined but should be investigated, because the lost material may be a potential coolant contaminant.

Impact Properties

The results of impact tests on irradiated and control specimens are presented in Table 8.7. With the one exception noted in the table, the impact tests were performed by dropping a steel weight onto the specimen from increasing heights. It is anticipated that the spheres will be subjected to impact energies resulting from a 20-ft free fall, or approximately 2.3 ft-lb during the loading operation. Although too

Table 8.7. Results of Impact Tests on Control and Irradiated Fueled-Graphite Specimens from BMI Capsules SP-1, SP-3, and SP-4

Specimen No.[a]	Type	Impact Energy at Failure (ft-lb)	
		Preirradiation	Postirradiation
	Capsule No. SP-1		
FI-1	Impregnated	13.5 11.5 12.5	10.4
FA-1	Admixture	7.3 11.5 11.5	8.35
FL-3	Lumped fuel	3.1 2.1	<1.04
	Capsule No. SP-3		
FA-6	Admixture, Si-SiC coating	1.33[b] 1.25[b] 3.00 1.9	<0.1[c]
FA-8	Admixture, SiC coating	0.5[b] 0.42[b] 1.0 0.6 0.5	0.75
	Capsule No. SP-4		
FA-1	Admixture	>11.6	9.4
FA-2	Admixture	7.5	3.0
FI-1	Impregnated	12.5	>11.6
FA-10	Admixture	10.4	>11.6

[a]For description of fuel elements see Table 8.1.

[b]Impact made on one location on sphere.

[c]Fractured in 1-ft free fall.

few tests have been performed to provide a sound statistical basis for evaluation, the impact resistance of the uncoated fueled-graphite spheres appears to be quite adequate to meet the operating requirements. The surface-coated spheres, on the other hand, show poor impact resistance. The graphite matrix of FA-6 specimens in the SP-3 capsule was believed to have contained cracks prior to the irradiation test.[2]

Compressive Strength

Based on calculations of the differential thermal expansion between the ball bed and its container wall, it was established that the spheres should be able to withstand compressive loads as high as 500 lb without fracturing. The data presented in Table 8.8 indicate that except for the specimens fueled by the "lump" technique, which developed cracks during irradiation, the graphite spheres possess adequate compressive strength and that irradiation apparently enhances this strength. More data are required to confirm this conclusion, however.

Abrasion Resistance

The results of abrasion tests, presented in Table 8.9, indicate that irradiation tends to harden the fuel spheres. The irradiated spheres either actually gained weight by picking up carbon from the dummy elements or showed a much smaller weight loss than the unirradiated specimens. No spalling or flaking of the graphite surface occurred.[1] However, the fuel temperature during exposure was considerably lower than design (i.e., a maximum of 1580°F) and the burnup did not exceed 1.8%.

Self-Welding

Self-welding tests are reported for three pairs of Si-SiC coated fuel spheres.[2] At 2000°F, neither type FA-6 nor FA-8 spheres showed a tendency to self-weld in 100 hr. The contact areas were tested by the "hot oil" permeability technique and showed no leaks.

Table 8.8. Results of Compression Tests on Control and Irradiated Fueled-Graphite Spheres from BMI Capsules SP-1 and SP-3

Specimen No.[a]	Type	Preirradiation Test		Postirradiation Test	
		Load (lb)	S (lb/in.)[b]	Load (lb)	S (lb/in.)[b]
		Capsule No. SP-1			
FI-1	Impregnated	2555	24 900	2672	39 100
FA-1	Admixture	2410	55 900	3712	65 800
		2865	56 400		
FL-3	Lumped fuel	1060[c]	43 500	258[d]	8 300
		278	40 500		
		Capsule No. SP-3			
FA-8	Admixture, SiC coating	530	NR[e]	1697	146 000
		837	NR		

[a]For description of fuel elements see Table 8.1.

[b]S stands for slope of the straight portion of the load-deflection curve.

[c]After sharp jump in deflection curve at a 1060-lb load, the specimen was unloaded and then retested. Failure occurred at 708 lb during the second test.

[d]Outer shell cracked during irradiation.

[e]Data not reported.

Table 8.9. Results of Abrasion Tests on Control and Irradiated Fueled-Graphite Spheres from BMI Capsule SP-1

Specimen No.[a]	Type	Weight Change (g)			
		Preirradiation[b]			Postirradiation[c]
		Maximum	Average	Minimum	
FI-1	Impregnated	−0.0352	−0.0156	−0.0008	
E13					+0.0025
E16					−0.0008
FA-1	Admixture	−0.0281	−0.0088	−0.0003	
NC86					+0.0026
NC87					+0.0024
FL-3	Lumped fuel	−0.3081	−0.0928	−0.0035	
BMI-11					−0.0185

[a]For description of fuel elements see Table 8.1.

[b]Tumbled 2 hr in a drum with dummy elements.

[c]Tumbled 10 min in a drum with dummy elements.

At 2500°F, in a test terminated after 66 hr because of thermocouple failure, two type FA-6 fuel spheres stuck to each other and to the graphite supports holding them in the test furnace.[3] It appears that self-welding of coated spheres may not be a problem at the temperatures and gas-purity levels under consideration for the PBRE, but confirmation of this by means of a thorough and realistic testing program is mandatory.

Fission-Gas Retention

One of the main advantages of the pebble-bed reactor concept over the fixed-fuel-element designs of the General Atomic HTGR and the OEEC Dragon is the relative ease with which fresh fuel can be added and spent fuel discharged. The cost of this fuel-handling flexibility is the preclusion of a purge-gas system as a means for handling fission products emitted from the fuel. The fuel spheres must therefore retain a large proportion of the generated fission products in order to maintain the coolant contamination at levels which will permit maintenance of components, such as blowers, at a resonable cost.

Uncoated Spheres

Both neutron-activation and sweep-capsule tests have demonstrated that fission-gas release from uncoated spheres containing uncoated fuel particles would be much too large for pebble-bed reactor application. The results of neutron-activation experiments are summarized in Table 8.10.

In sweep capsule SP-2, the release of fission gases from uncoated spheres was determined while the specimens were being irradiated. This type of test permits the measurement of the ratio of release rate to equilibrium production rate. The operating conditions for capsule SP-2 are presented in Table 8.11 and the fission-gas release factors are given in Table 8.12. The activity in the helium flowing over the impregnated specimens was too high to be handled in the available equipment.

Table 8.10. Release of Xe^{133} from Fueled-Graphite Specimens Containing Uncoated Fuel Particles[a]

Specimen No.[b]	Type	Test Temperature (°F)	Test Time (min)	Xe^{133} Released (%)
FA-1 (278)	Admixture, 100–150 μ UO_2	1000	10	0.4
		1500	20	0.9
		1900	20	0.6
FA-1 (282)	Admixture, 100–150 μ UO_2	1000	20	0.1
		1500	60	0.6
		1500	60	0.7
		1500	90	0.7
FA-1 (283)	Admixture, 100–150 μ UO_2	800	30	0.4
		1100	40	0.1
		1100	25	0.3
		1500	55	0.9
FA-14 (373)	Admixture, 100–150 μ UO_2	800	15	0.1
		1500	40	0.2
FI-1	Impregnated with ~1 μ UO_2 particles	1000	240	8.3
		1250	240	3.1
		1500	240	3.0
FA-5	Admixture, 100–200 μ UC, in shell	1000	10	0.87
		1500	10	0.08
FA-7	Admixture, 100–200 μ UC_2	1000	20	0.07
		1500	20	0.3

[a]See refs. 1 and 2.

[b]For description of fuel elements see Table 8.1.

Table 8.11. Summary of Capsule SP-2 Operating Conditions[a]

Specimen No.[b]	Type	Surface Temperature[c] (°F)		
		Cycle 1	Cycle 2	Cycle 3
FA-1 (E81)	Admixture	1050	1200	1380
FA-1 (E84)	Admixture	1040	1190	1360
FI-1 (E5)	Impregnated	1120	1220	1410
FI-1 (E10)	Impregnated	1140	1230	1420

[a]See ref. 1.

[b]For description of fuel elements see Table 8.1.

[c]Specimen power: cycle 1, 0.45 kw; cycle 2, 0.5 kw; cycle 3, 0.6 kw.

Table 8.12. Fission-Gas-Release Factors for Specimens FA-1[a] in Sweep Capsule SP-2

Gas Sample No.[b]	Release Factor, R/B	
	Kr^{85m}	Xe^{135}
1[c]	1.4×10^{-4}	2.5×10^{-4}
2	5.18×10^{-2}	6.3×10^{-3}
3	6.36×10^{-2}	1.68×10^{-2}

[a]Uncoated, admixtures.

[b]All samples taken during first cycle.

[c]Sampling apparatus leaked.

Data obtained recently at ORNL indicate that even highly impermeable graphite (admittance constant = 1.5×10^{-8} cm^2/sec) may not be an effective fission-gas barrier for a pebble-bed fuel element under high-temperature irradiation. In the ORNL-MTR-48-2 experiment, a UC_2-graphite pellet sealed in a graphite can of the above quality was irradiated in the MTR at a graphite wall temperature of approximately 1500°F. Helium was passed over the graphite can and monitored for gaseous fission products. The release factor, R/B, for Xe^{133} increased from 1.9×10^{-4} ten days after startup to approximately 0.20 after two months of operation (3.8×10^{19} atoms of U^{235} fissioned per cm^3). The R/B ratios for Kr^{85m}, Kr^{88}, and Xe^{135} at this time were 2.5×10^{-3}, 7×10^{-4}, and 3.9×10^{-5}, respectively.[10] The capsule is still operating, however, and the cause of the increase in release rate is not yet known.

Spheres with Surface Coatings

The most promising sphere coatings have been shown by "hot oil" permeability and neutron-activation tests to be Si-SiC and pyrolytically deposited carbon. Specimens coated with these materials were subjected to irradiation tests in furnace capsules, static capsules, and sweep capsules.

Spheres Coated with Pyrolytically Deposited Carbon.[2,3] The FA-20 specimens (see Table 8.1) consist of a graphite-UC_2 matrix coated with 2 to 5 mils of pyrolytically deposited carbon. The molded admixture of UO_2, graphite flour, and coal-tar pitch binder was baked at 4800°F to graphitize the matrix and convert the UO_2 to UC_2. The coating was deposited at 3100°F, and the coated sphere was then rebaked at 4800°F. These spheres had the highest impact strength, 3.6 ft-lb, among the coated specimens, and all 6 specimens tested passed the "hot oil" permeability test. Two irradiation tests have been completed on FA-20 type spheres.

---

[10]Personal communication from C. W. Cunningham, ORNL.

The results of the furnace capsule SPF-1 test are presented in Table 8.13. In postirradiation examination, pitting of the coating, which has been attributed to impurities in the helium, was observed.[11] The release factors observed in this test, may therefore be higher than this type of coating is capable of achieving. In a neutron-activation test, no detectable release was obtained in 70 min at 1700°F or 100 min at 2200°F from a pyrolytic-carbon-coated sphere. This coating was applied at a temperature 200°F higher than that on the FA-20 specimen of SPF-1, however.

Table 8.13. Summary of SPF-1 Release Rate Data[a] on Pyrolytic-Carbon-Coated Specimen FA-20 (310)

Specimen Temperature (°F)	Release Factor, R/B				
	Kr^{85m}	Kr^{87}	Kr^{88}	Xe^{133}	Xe^{135}
150	3.8×10^{-4}	1.6×10^{-4}	b	4.6×10^{-3}	1.5×10^{-3}
1000	4.3×10^{-3}	2.3×10^{-3}	3.8×10^{-3}	5.7×10^{-3}	3.9×10^{-3}
1500	1.6×10^{-2}	1.3×10^{-2}	1.6×10^{-2}	4.1×10^{-2}	9.0×10^{-3}
1900	2.6×10^{-2}	1.07×10^{-2}	2.4×10^{-2}	6.7×10^{-2}	1.9×10^{-2}

[a]See ref. 3, p. 15.

[b]No detectable release.

A second FA-20 type specimen was irradiated in static capsule SP-4, the irradiation conditions for which are listed in Table 8.3. Post-irradiation examination revealed five closely spaced, parallel, great-circle cracks that leaked profusely in the "hot oil" test. Two additional FA-20 specimens are included in a static atmosphere compartment of the SP-5 capsule, which is still in test.

---

[11]Personal communication from G. Raines, Battelle Memorial Institute.

Spheres with Si-SiC Coatings Applied Directly to Fueled Matrix.[2] The FA-8 specimens (see Table 8.1) were fabricated by admixing UC_2, isotropic-grade graphite (Speer 901S), and resin-type binder. The spheres were molded at 1000 psi and baked at 3600°F. The 0.03-in. coating of SiC containing excess silicon was applied directly to the fueled-graphite matrix. Coatings applied in this way are subject to uranium contamination by the reaction of silicon with UC_2 during the coating operation. In preirradiation tests, specimens showed an average surface contamination of 0.3 wt % of the total uranium in the sphere. The impact strengths of the FA-8 specimens were also low, below 1 ft-lb, and only 7 of 17 specimens tested passed the "hot oil" test.

Two FA-8 specimens were tested in one compartment of capsule SP-3 under the conditions listed in Table 8.3. After two days of operation at surface temperatures of 1300 to 1500°F, it was found that the activity in the gas lines was too high to permit sampling. The irradiation was continued to the burnup given in Table 8.3, with the gas lines sealed. In the postirradiation examination, the two FA-8 spheres appeared to be in good condition. One specimen exhibited no leakage during immersion in hot silicone oil for 17 min, and the other emitted only a single stream of bubbles after 52 sec of immersion in hot oil. The high activity levels which prevented sampling during irradiation are believed to have resulted from uranium contamination in the coating surface. No uranium contamination measurement was made prior to the irradiation test, but later measurement of other samples from the same lot showed excessive contamination, as discussed above.

An FA-8 specimen, irradiated in static capsule SP-4 (see Table 8.3), had a 0.2-in. crack in its coating after irradiation. The "hot oil" immersion test indicated a major leak. Metallographic examination revealed no apparent change in the microstructure of the coating.

Coating of Si-SiC Applied to Unfueled Graphite Shell on Sphere. In the FA-6, FA-16, and FA-23 specimens, the fueled matrix and the Si-SiC coating were separated by a shell of unfueled graphite. The graphite

matrix was made by mixing UO_2, Graphite Specialties Grade W filler, and pitch binder, molding isostatically at 5000 psi, and reimpregnating several times. The final graphite density was 1.80 g/cm^3. Baking at 3600°F converted the UO_2 to UC, according to x-ray analysis.

The FA-6 specimens were fabricated with a 0.15-in.-thick unfueled shell and coated with 0.003-in.-thick Si-SiC. The UO_2 used was contaminated by 3.24 wt % iron, and 5.57 g of fuel particles was added to get the 5.19 g of UO_2 desired. Metallography showed small cracks in the fueled-graphite matrix.

The FA-16 specimens were made with improved techniques to avoid the flaws shown in the FA-6 matrix. The unfueled shell was decreased to 0.060 in., but the Si-SiC coating was the same as on the FA-6 specimens. No cracks were found by metallographic examination. The Si-SiC coating was increased to 0.008 in. in the FA-23 specimens, which were the latest tested in this series.

The use of the unfueled graphite shell made possible uranium contamination levels of the order of 0.001 wt %, or less, of the total contained uranium. The impact resistance of these specimens was also low, however, and only 11 of 23 FA-6 specimens passed the "hot oil" test.

The FA-6 type specimens were irradiated in sweep capsule SP-3 and static capsule SP-4, the FA-16 specimens in furnace capsule SPF-3, and the FA-23 specimens in sweep and static compartments in capsule SP-5.

The helium flowing through the compartment containing the FA-6 specimen in capsule SP-3 (see Table 8.3) was first sampled after two days of operation at surface temperatures of 1300 to 1500°F. After three additional days of operation at the same temperature and power level, an attempt was made to obtain a second sample. It was found, however, that the activity in the gas lines was too high to be handled in the available equipment. The reactor power level was then reduced to 100 kw to reduce the activity level so that the sample could be taken. The fission-gas-release data from the two samples are given in Table 8.14.

Table 8.14. Fission-Gas-Release Data for Si-SiC Coated Specimen FA-6 Irradiated in Capsule SP-3

	Sample 1	Sample 2
Date sample was taken[a]	May 8	May 18
Reactor power	2 Mw	100 kw
Specimen power	2 kw	100 w[b]
Specimen temperature	1300°F	170°F
Fission-gas-release factor, R/B		
Kr^{85m}	2×10^{-7}	8×10^{-5}
Xe^{135}	3×10^{-8}	3×10^{-6}

[a]Startup date was May 6.

[b]Activity was too high for sample 2 to be taken at full power.

Irradiation was continued until a total of 61 days at full reactor power (2 Mw) was accumulated. During this time, the gas lines were modified to provide double containment so that high activity levels in the gas could be handled safely. A leak developed, however, and prevented further sampling.

In postirradiation examination, numerous cracks were observed in the coatings of the specimens. However, the coating itself and the graphite-coating interface did not appear to have been affected. No separation of the unfueled shell from the fueled matrix was observed.

An FA-16 specimen was irradiated in furnace capsule SPF-2 with the results shown in Table 8.15. The release factors were extremely low and did not appear to be a function of temperature in the range from 1500 to 1900°F under the low-flux conditions prevailing in this test.

Specimen FA-23 (E8-7) is being irradiated in capsule SP-5. The fission-gas-release rate data for this specimen are presented in Table 8.16. Very low release rates were observed during the first two reactor cycles with sphere surface and center temperatures of 1300 and 1500°F, respectively, and a fission heat-generation rate of 1.6 kw. During startup of the third cycle, an increase of approximately 10^5 in R/B occurred. Coating failure was undoubtedly the cause of the large increase in R/B. However, the

Table 8.15. Summary of SPF-2 Release Rate Data on Si-SiC Coated Specimen FA-16[a]

Sample Collection Date (1960)	Irradiation Temperature (°F)	Flux (neutrons cm^{-2} sec^{-1})	Release Factor, R/B				
			Xe^{133}	Xe^{135}	Kr^{85m}	Kr^{87}	Kr^{88}
2-10[b]	200	1.7×10^{10}					
2-11[b]	1000	1.7×10^{10}					
2-12[b]	1000	3×10^{11}					
2-15[b]	1000	3×10^{11}					
2-17[b]	1000	3×10^{11}					
2-19	1500	3×10^{12}	6.1×10^{-6}	6.1×10^{-7}	5.1×10^{-7}	$<1.3 \times 10^{-7}$	3×10^{-7}
2-22	1500	3×10^{12}	2.8×10^{-6}	2.0×10^{-7}	8.1×10^{-7}	$<1.3 \times 10^{-7}$	2.7×10^{-7}
2-26	1500	3×10^{12}	2.1×10^{-6}	1.6×10^{-7}	3.1×10^{-7}	$<1.3 \times 10^{-7}$	1.7×10^{-7}
2-20	1500	3×10^{12}	1.7×10^{-6}	1.1×10^{-7}	3.1×10^{-7}	$<1.3 \times 10^{-7}$	1.7×10^{-7}
3-2	1900	3×10^{12}	2.6×10^{-6}	3.8×10^{-7}	6.7×10^{-7}	$<1.3 \times 10^{-7}$	1.5×10^{-7}
3-3	1900	3×10^{12}	4.5×10^{-6}	4.2×10^{-7}	4.1×10^{-7}	$<1.3 \times 10^{-7}$	1.2×10^{-7}
3-14	1900	3×10^{12}	8.2×10^{-6}	2.0×10^{-7}	7.0×10^{-7}	$<1.3 \times 10^{-7}$	3.0×10^{-7}
3-15	1900	3×10^{12}	4.3×10^{-6}	2.5×10^{-7}	4.7×10^{-7}	$<1.3 \times 10^{-7}$	1.0×10^{-7}

[a]C. R. Tipton, Jr. and R. W. Dayton, "Progress Relating to Civilian Applications During March, 1960," BMI-1430.

[b]Very low releases prevented species identification; therefore, no R/B values were reported.

Table 8.16. Summary of Fission-Gas-Release Data for SP-5 Capsule Test of Si-SiC Coated Specimen FA-23[a]

Sample Collection Date (1960)	Release Factor, R/B				
	Kr^{85m}	Kr^{87}	Kr^{88}	Xe^{133}	Xe^{135}
4/27[b]	Nil[c]	Nil	Nil	Nil	Nil
4/22	Nil	Nil	Nil	Nil	Nil
4/26-27	2.6×10^{-9}	Nil	1.5×10^{-9}	5.7×10^{-9}	1.5×10^{-9}
5/4	d	d	d	7.9×10^{-3}	d
5/4	6.6×10^{-4}	2.0×10^{-4}	1.7×10^{-4}	3.0×10^{-3}	1.1×10^{-4}
5/4	3.8×10^{-3}	1.2×10^{-3}	6.6×10^{-4}	6.3×10^{-3}	9.3×10^{-4}
5/19	3.8×10^{-4}	1.3×10^{-4}	2.0×10^{-4}	5.2×10^{-4}	1.0×10^{-4}

[a]C. R. Tipton, Jr. and R. W. Dayton, "Progress Relating to Civilian Applications During May 1960," BMI-1442.

[b]Startup date was April 6, 1960.

[c]Below sensitivity of fission-gas analysis.

[d]These species decayed out during long cooling period.

failure in this case may have been of the pinhole type, since the release rate was not so great as would be expected from a crack, and the rate did not increase further during the two weeks of operation after the initial increase. The specimen has continued to be irradiated as a static specimen to an estimated burnup of 5.3 at. % of the uranium (as of October 3, 1960). Another gas sampling is planned but has not yet been accomplished.[11]

Shortly after the FA-23 (E8-7) coating failure occurred, the helium sweep gas was passed for 2 hr through a "daughter trap" for detection of the isotopes Sr^{89}, Be^{140}, Ce^{141}, and Cs^{137}. These four species give information on the release from the sphere of their precursors, 3.2-min Kr^{89}, 16-sec Xe^{140}, 1.7-sec Xe^{141}, and 3.9-min Xe^{137}. The "daughter trap" data are summarized in Table 8.17.

Comparison of the data of Tables 8.16 and 8.17 shows that the R/B values determined in the "daughter trap" for the 3.2-min Kr^{89} and

Table 8.17. Summary of Daughter Trap Results for SP-5 Capsule Test of Si-SiC Coated Specimen FA-23(E8-7)[a]

Trap Species	Radioactivity (μc)			Precursor				
	Trap[b]	Total[c]	In Specimen	Species	Radioactivity in Specimen (μc)	R (atoms/sec)	B[d] (atoms/sec)	R/B
Sr^{89}	17.5	50.0	14×10^6	Kr^{89}	65×10^6	1.7×10^9	2.4×10^{12}	7.2×10^{-4}
Ba^{140}	7.5	8.2	57×10^6	Xe^{140}	54×10^6	6.7×10^7	2.0×10^{12}	3.4×10^{-5}
Ce^{141}	0.070	0.16	29×10^6	Xe^{141}	19×10^6	3.2×10^6	7.0×10^{11}	4.6×10^{-6}
Cs^{137}	0.045	0.15	0.12×10^6	Xe^{137}	87×10^6	1.3×10^9	3.2×10^{12}	4×10^{-4}

[a] C. R. Tipton, Jr. and R. W. Dayton, "Progress Relating to Civilian Applications During July 1960," BMI-1455.

[b] Amount collected in trap during 2-hr period.

[c] Amount in trap corrected for precursor delay prior to trap and precursor breakthrough.

[d] Equilibrium production rate in sphere.

3.9-min Xe^{137} are similar to the R/B values previously determined for the longer lived isotopes Kr^{85m}, Kr^{87}, Kr^{88}, Xe^{133}, and Xe^{135}. On the other hand, the R/B values for the 16-sec Xe^{140} and 1.7-sec Xe^{141} are lower and decrease in the order of decreasing half-life. It was estimated from these data that hold-up time in the graphite sphere is not more than a few minutes.

Si-SiC Coated Graphite Cans Containing Oxide Fuel Pellets. Two tests of Si-SiC coated graphite cans containing oxide fuel pellets have been run in the B-9 facility in the Oak Ridge Research Reactor at ORNL.[12,13] The first test capsule contained two 95.5 wt % ThO_2–4.5 wt % UO_2 pellets which were fabricated at ORNL. The pellets were encapsulated in the graphite can by the Minnesota Mining and Manufacturing Company, who also applied the Si-SiC coatings. The preirradiation test of coating integrity consisted of heating for 400 hr at 1800°F in air. The specimen apparently failed during the first startup, since high activity levels were detected immediately in the nitrogen flowing over the capsule. The activity increased gradually during the 440-hr duration of the test which was operated at 1500°F. The test was terminated when the increase in activity became rapid. Postirradiation examination has not been completed, but the failure has been attributed to differential expansion of the UO_2-ThO_2 pellet and the graphite can. No clearance was provided between the pellet and the can.

In order to prevent recurrence of this type of failure in the second test, 8-mils diametral clearance was provided between the pellet and the can. This test specimen operated satisfactorily for more than 720 hr at 1800°F and withstood 15 thermal cycles caused by fluctuations in the reactor operating conditions. A high activity level was present on the gas lines from the previous test, but this level did not increase during the second test. However, when the test capsule was reinserted

---

[12] "GCR Quar. Prog. Rep. Dec. 31, 1959," ORNL-2888, pp. 125–7.

[13] "GCR Quar. Prog. Rep. June 30, 1960," ORNL-2967, pp. 166–7.

in the reactor after it had been removed following the 720 hr of operation, a coating or can failure must have occurred because the activity increased soon after the operating temperature had been reached.

Since postirradiation examination has not been performed on either of these specimens, the exact cause of failure in each case is not yet known. However, the first specimen probably failed because of thermal expansion of the fuel pellet, and the second failure could have been caused by a racheting effect as a result of fragmentation of the fuel pellet.

Spheres With Coated Particles

Surface coatings of the Si-SiC type have exhibited excellent fission-gas retention properties initially, but coated graphite components have not given reliably satisfactory service under long term, high-flux, high-temperature irradiation. In most cases, failure cannot be attributed to the coating itself, and it is possible that continued development and testing can result in more reliably coated components. Nevertheless, the serious consequences of a single failure militate against the use of sphere surface coatings as the sole fission-product diffusion barrier. Because of the porous nature of graphite, almost all the fission gases would escape through a surface crack.

The coating of individual fuel particles with an impervious material as a means for retaining fission gases in the fuel elements offers many advantages. A 1-1/2-in. fuel sphere may contain several hundred thousand fuel particles; consequently, occasional failure of individual coatings should not be serious. Even if many of the coatings developed cracks, the majority of the recoils might still be retained in the sound portion of the coating, and a substantial reduction in both the fission-gas release and the irradiation damage to the graphite matrix would be realized. In addition, pyrolytic-carbon coatings on UC_2 particles would ease the handling problem by protecting the particles from atmospheric attack during fabrication.

Metallic coatings were tried but found to be unsuitable because of the carburization problem. Sintered Al_2O_3 coatings could not be applied

with the required degree of control of thickness, density, and continuity. In January 1960, Battelle found that uniform, high-density Al_2O_3 coatings could be vapor deposited on UO_2 particles by hydrolysis of $AlCl_3$ in a fluidized bed of the fuel particles. Encouraging results in neutron-activation tests led to the coating of fully enriched UO_2 particles for more rigorous radiation tests.

The Al_2O_3 coating was applied to the enriched, high-fired UO_2 shot in five successive operations at a fluidized bed temperature of 1000°C. Photomicrographs showing the microstructures of typical coated particles from this batch are shown in Fig. 8.1. The apparently low-density layer resulted from a slight variation in coating conditions during one of the early cycles.

Fuel spheres incorporating these coated particles were fabricated by the National Carbon Company. On April 6, 1960, irradiation of one of these spheres, FA-22 (471), was started in sweep capsule No. 5. Data on R/B values measured in this test are plotted in Fig. 8.2.

The gradual increase in R/B with time indicates that the coatings are leaking, but the mechanism of coating failure is not yet known. The behavior shown could result either from occasional failure of an individual coating or from a gradual deterioration of the Al_2O_3 structure, which could be caused by radiation-accelerated reaction with the graphite or by fission-fragment damage. Berman, Bleiberg, and Yeniscairch[14] found gross swelling and destruction of the crystal structure of Al_2O_3 when Al_2O_3–21 wt % UO_2 platelets were irradiated to burnups of 0.9 to 10.8×10^{20} fissions/cm^3 at approximately 550°F. This behavior was attributed to an anisotropic effect of fission-fragment bombardment on the crystal structure, which was thereby distorted and rendered unstable. However, Johnson and Tobin[15] irradiated Al_2O_3–20 vol % UO_2 and BeO–20 vol % UO_2 at 1300 to 1500°F to burnups of 0.45×10^{20} fissions per cm^3

---

[14]R. M. Berman, M. L. Bleiberg, and W. Yeniscairch, "Fission Fragment Damage to Crystal Structures," J. Nuclear Materials 2(2), 129–40 (1960).

[15]D. A. Johnson and J. M. Tobin, "The Dimensional Stability on Irradiation of Al_2O_3-UO_2, BeO-UO_2, Graphite-UC, and Graphite-UC_2," ORNL Conference on Nuclear Reactor Chemistry, Oct. 13, 1960.

UNCLASSIFIED
PHOTO 51978

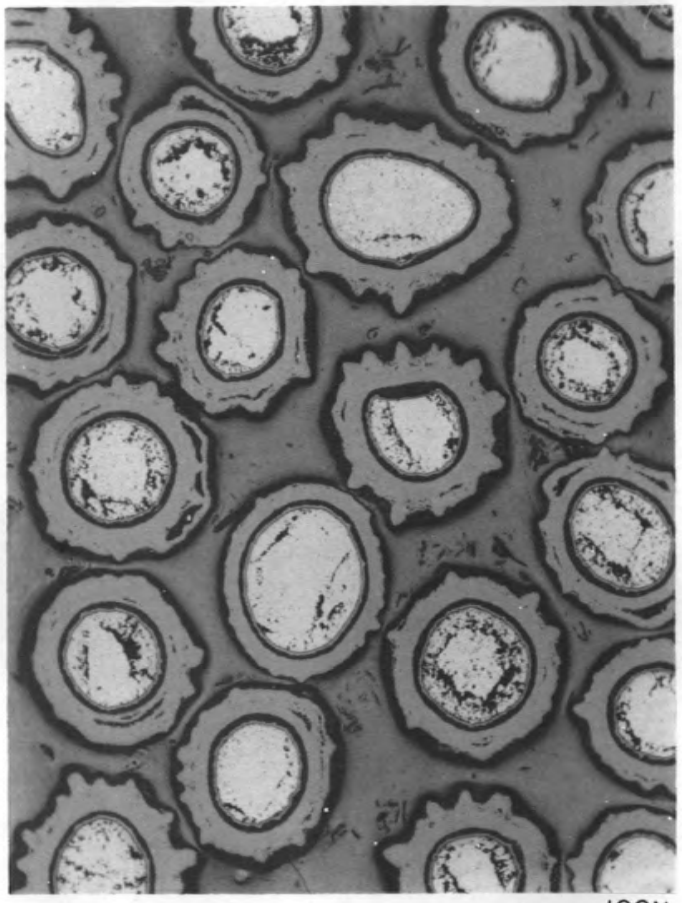

100X

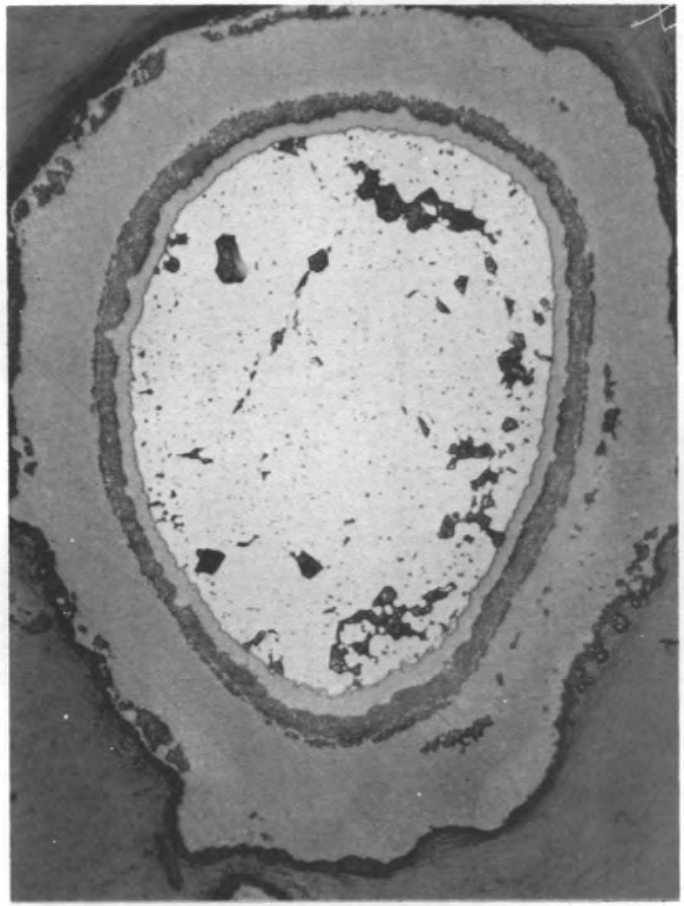

500X

Fig. 8.1. Vapor-Deposited Al_2O_3 on Enriched UO_2 Used to Fabricate Fuel Sphere Irradiated in Sweep Capsule SP-5.

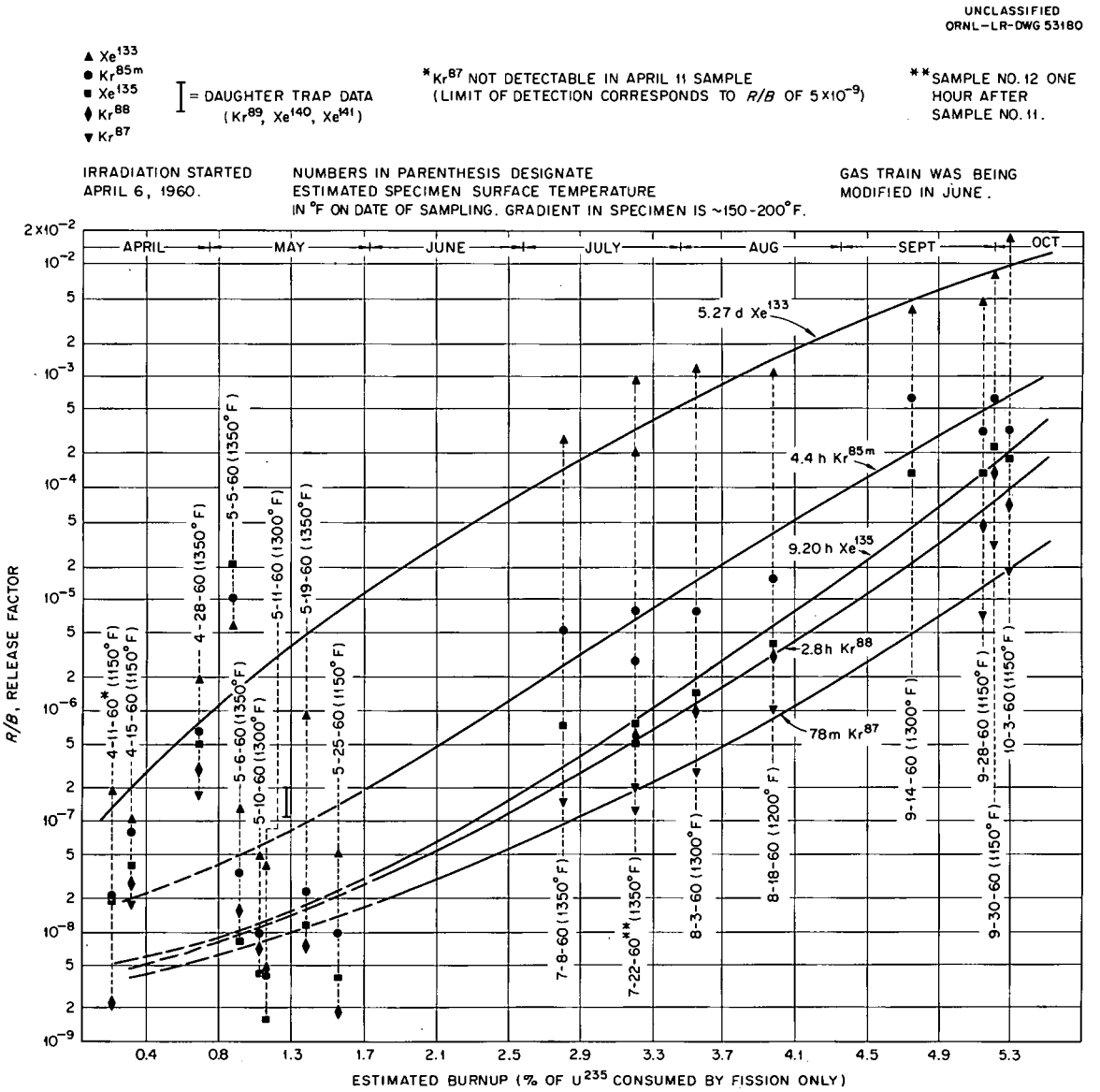

Fig. 8.2. Release Factors Versus Time and Burnup for Specimen FA-22 Irradiated in Sweep Capsule SP-5. Specimen fueled with Al_2O_3-coated UO_2.

of pellet (or 2.25×10^{20} fissions per cm^3 of UO_2) and found that the pellets maintained excellent dimensional and structural stability.

Furnace capsule SPF-3 was used in a study of the effect of temperature on R/B values for Al_2O_3-coated UO_2 particles dispersed in a graphite matrix. The data from this experiment are summarized in Table 8.18. Since these data were obtained, the temperature has been increased to 1900°F and a slight tendency toward higher release rates has been observed.[16]

Graphite Components

Pebble-Bed Container

The pebble-bed container is to be a cylindrical graphite assembly 18 in. in inside diameter, 26 in. in outside diameter, and 14 ft long. The assembly will be made up of concentric graphite cylinders, with wall thicknesses of 1 to 2 in.

The fabrication of graphite cylinders of these dimensions has not been attempted previously, but it does not appear to be an impossible task. The main difficulty in fabricating a shape of this length would be in the machining operation. At the present time, graphite shapes of this type can be machined in lengths up to 8 ft to a wall-thickness tolerance of ±0.01 to 0.015 in.

Coating the cylinders with an oxidation-resistant material, such as SiC or Si-SiC, would require a very large scaleup of existing processes. The present coating capability restricts the size to less than 6 in. in diameter and 10 ft in length.

If the coating must be completely protective, special grades of graphite must be used. These grades have not been produced in large cylinders. The largest cylinder produced to date is roughly 5 in. in diameter and about 10 ft in length. The production of a 20-in.-diam cylinder suitable for coating would require a considerable development

[16]Personal communication from G. Raines, Battelle Memorial Institute.

Table 8.18. Summary of SPF-3 Fission-Gas Data for Sphere Containing Al_2O_3-Coated UO_2 Particles[a]

Collection Date (1960)	Temperature (°F)	Flux (neutrons/cm^2 sec)	Release Factor, R/B				
			Xe^{133}	Xe^{135}	Kr^{85m}	Kr^{87}	Kr^{88}
3/17	1000	1.8×10^{12}	1.2×10^{-6}	1.7×10^{-7}	5.6×10^{-7}	4.2×10^{-7}	2.6×10^{-7}
3/18	1500	1.8×10^{12}	5.8×10^{-6}	1.7×10^{-6}	2.0×10^{-6}	1.0×10^{-6}	3.2×10^{-7}

[a]C. R. Tipton, Jr. and R. W. Dayton, "Progress Relating to Civilian Applications During March 1960," BMI-1430.

effort by the graphite manufacturers but at present does not seem to be out of the question.

Reflector

The reactor core is surrounded by a 26-in.-thick graphite reflector comprised of a stack of graphite wedges approximately 4 in. × 4 in. on one end, 12 in. × 4 in. on the outer end, and 26 in. long. There is no foreseeable difficulty in the fabrication of graphite shapes of this type.

Coating these wedges with an oxidation-resistant material would require a scaleup of the existing coating processes. However, this scaleup is not as large as that discussed for the pebble-bed container. The grades of graphite necessary for complete protection are available in this size.

Reflector Perimeter

The graphite industry is presently able to produce boron-loaded graphite materials in reasonable sizes. The amount of boron in the graphite is most easily controlled when the piece is not heated to graphitization temperatures. However, it is reasonable to expect that the boron content could be controlled to ±1/2% even in graphitized material.

Conclusions

The following conclusions are drawn from this discussion:

1. Based on the large amount of data that has been obtained primarily in the development program being carried out by Sanderson & Porter and Battelle Memorial Institute, it is clear that if ceramic fuel elements are to be used in the PBRE, coated fuel particles dispersed in graphite will be required.

2. Fission-gas-release data for Al_2O_3-UO_2 particles in graphite indicate that an improvement in performance will be required.

3. Data on the ability of the fueled-graphite matrix to withstand the anticipated mechanical and thermal stresses are encouraging, although not extensive.

4. The merit of using sphere-surface coatings in addition to coated particles should be evaluated. Coatings of Si-SiC appear to be far more attractive than pyrolytically-deposited carbon coatings for protection against both fission-gas release and oxidation. Clarification is required, however, concerning the failures of Si-SiC coatings in irradiation tests. Other possible limiting factors in this concept are the possibility of self-welding at maximum fuel element surface temperatures and the possible loss of protection as a result of cracks developed upon free fall of greater than approximately 10 ft.

5. Fabrication of the large graphite components for the bed container, the reflector, and the reflector perimeter appears to be technically feasible, although a large scaleup of existing fabrication techniques by the industry would be required. The production of an Si-SiC coated pebble-bed container would involve a particularly large scaleup of existing fabrication and coating techniques, but an accomplishment of this magnitude does not appear to be out of the question.

9. STRUCTURAL ANALYSIS OF GRAPHITE REFLECTOR

Stress Analysis

The graphite reflector is 14 ft high, 90 in. in outside diameter, and 18 in. in inside diameter. Because of the steep gradient in the fast-neutron flux in the inner portion of the reflector, it has been proposed that the inner 6-in. thickness of the reflector be made as a composite structure of concentric sleeves. Further, the first 4-in. thickness of the reflector may be supported in a manner that will permit the removal of the composite sleeve cylinders making up this portion of the reflector.

The fast-neutron exposure distribution in the reflector for one year of full power operation is shown in Fig. 9.1. The exposure is expressed in megawatt days per adjacent tonne of fuel in the Hanford reactors (Mwd/AT), since shrinkage data are ordinarily given in terms of this unit. The distribution shown represents that at the mid-plane of the reactor. In the stress analysis of the reflector, only the concentric-sleeve region was examined. An anisotropic elastic analysis was used to predict the axial, circumferential, and radial stress distributions in each sleeve for three combinations of thicknesses. Each sleeve was treated as a thick-walled member with free ends. The differences in mechanical properties and shrinkage rates perpendicular and parallel to the extrusion axis were taken into consideration. Since the longitudinal axis will coincide with the direction of extrusion, the properties are the same in the radial and tangential directions.

The mean temperature of the reflector at the mid-plane of the reactor was assumed to be 1000°F. Based on this temperature, the shrinkage rates for the needle-coke AGOT graphite were taken as -3.4×10^{-7} (in./in.)/(Mwd/AT) and -1.4×10^{-7} (in./in.)/(Mwd/AT) in the axial and perpendicular directions, respectively.[1] The modulus of elasticity was

[1]Private communication from D. R. deHalas, Hanford, October 30, 1959, to W. F. Banks, Allis-Chalmers Manufacturing Company.

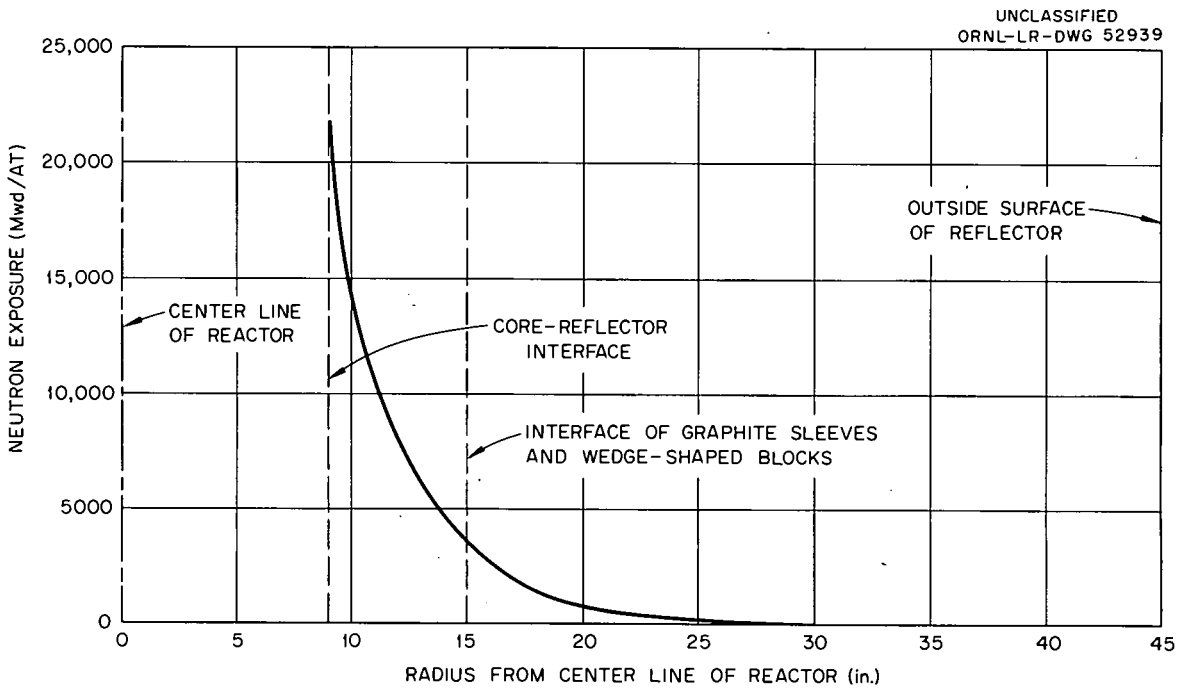

Fig. 9.1. Fast-Neutron Exposure in Pebble-Bed Reactor Reflector After One Year of Full Power Operation.

taken as 1.53×10^6 psi in the axial direction and 1.13×10^6 psi in the perpendicular direction.

The first combination examined was three concentric sleeves, each having a thickness of 2.0 in. The results of the calculations are presented in Fig. 9.2, where the axial, radial, and tangential stresses, designated as σ_z, σ_r, and σ_θ, are plotted for each sleeve as a function of radius from the core centerline. The stresses shown represent those occurring after one year of full power operation of the reactor. It may be seen that in each case the maximum stress is σ_z and that the maximum value occurs at the inner surface of the sleeve. Figure 9.3 represents the stress distributions for the case where the first 2-in.-thick sleeve is replaced by two 1-in.-thick sleeves. The outer two sleeves are the same as in Fig. 9.2. It may be seen that by dividing the first 2-in.-thick sleeve into two smaller sleeves, the maximum stress is appreciably reduced. The third combination examined represents the case of three sleeves proportioned in such a manner that the maximum stresses in all three sleeves are equal. In this case the thicknesses are 1, 1 3/4, and 3 1/4 in., respectively, and Fig. 9.4 shows the stress distributions in the three sleeves after one year of full power operation.

Interpretation of the Results

On the basis of available shrinkage and rupture-elongation data and the present knowledge concerning graphite behavior, it must be concluded that strains induced by fast-neutron irradiation will cause failure in some exposure interval. This interval depends on the ability of the graphite to withstand deformation without rupture. Specific examples of failure from this cause have not been documented, although some evidence does exist in graphite-moderated reactors now in operation. However, in a Russian article[2] that discusses the disassembly of a

[2]B. B. Brohovich et al., "Disassembly of an Experimental Uranium-Graphite Isotope Reactor After Four Years of Operation," Second United Nations International Conference on the Peaceful Uses of Atomic Energy 7, 241 (1958).

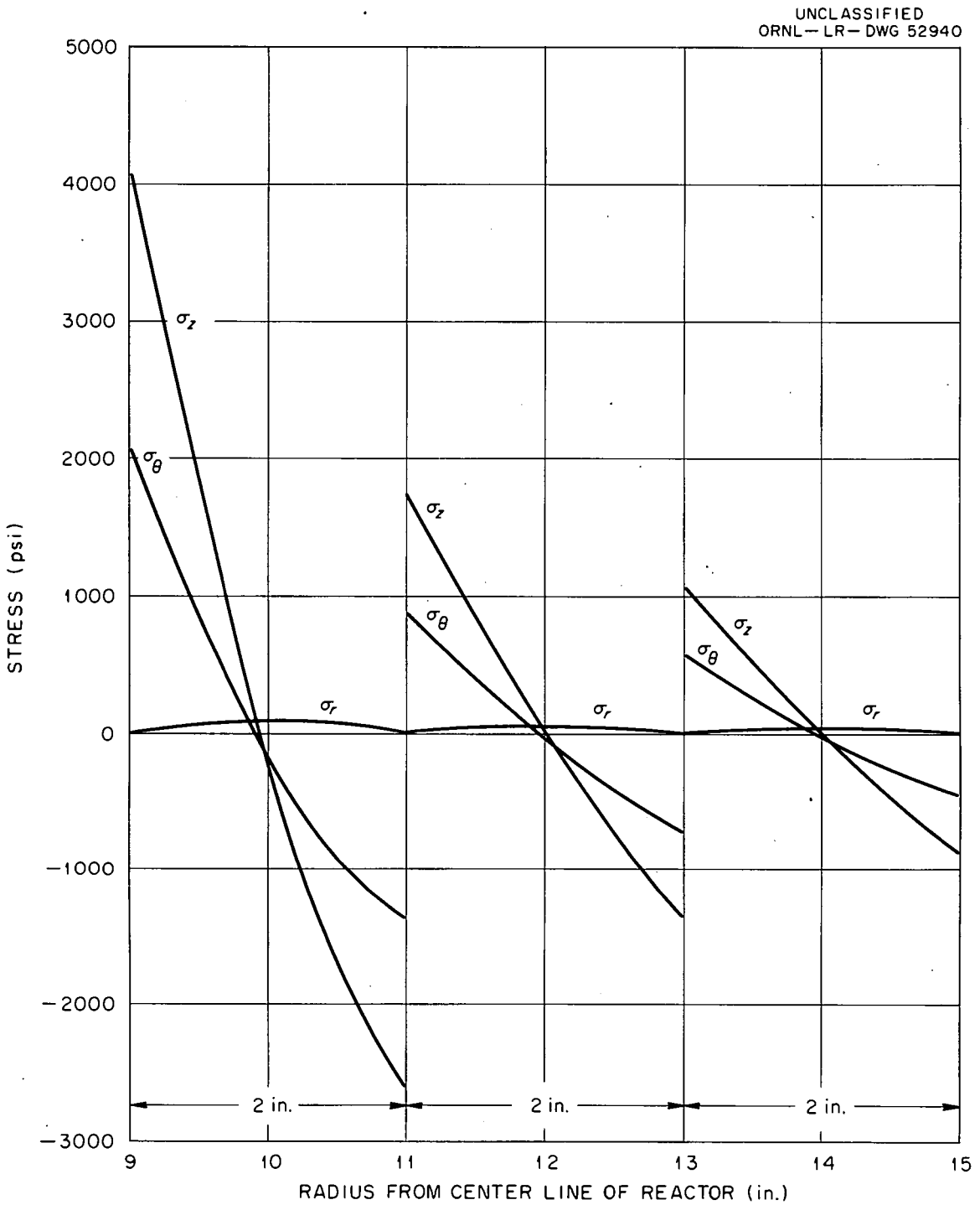

Fig. 9.2. Stresses in First 6 in. of Pebble-Bed Reactor Reflector After One Year of Full Power Operation, Assuming Three Cylinders of Equal Thickness.

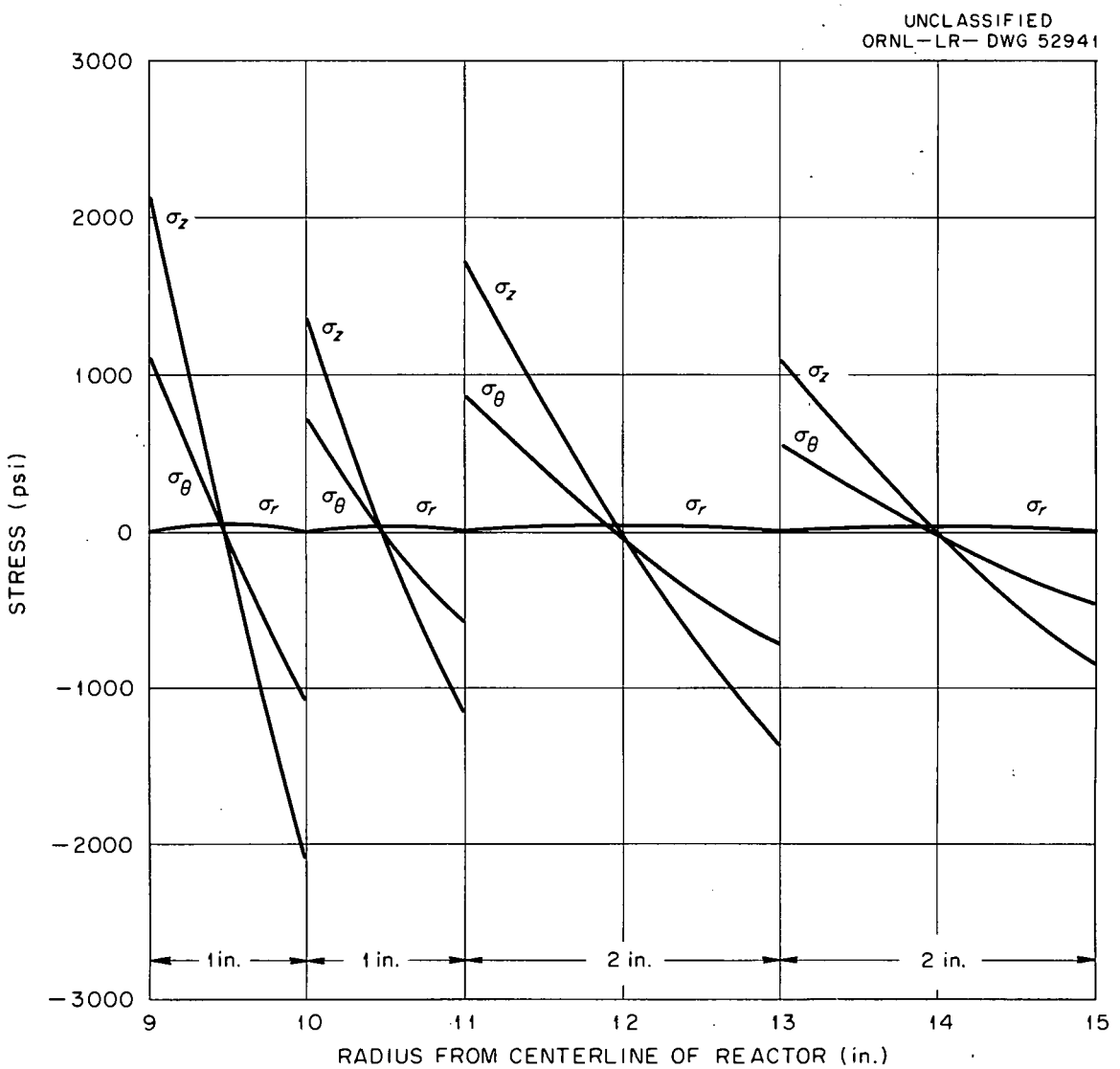

Fig. 9.3. Stresses in First 6 in. of Pebble-Bed Reactor Reflector After One Year of Full Power Operation, Assuming Four Cylinders of Thicknesses 1, 1, 2, and 2 in.

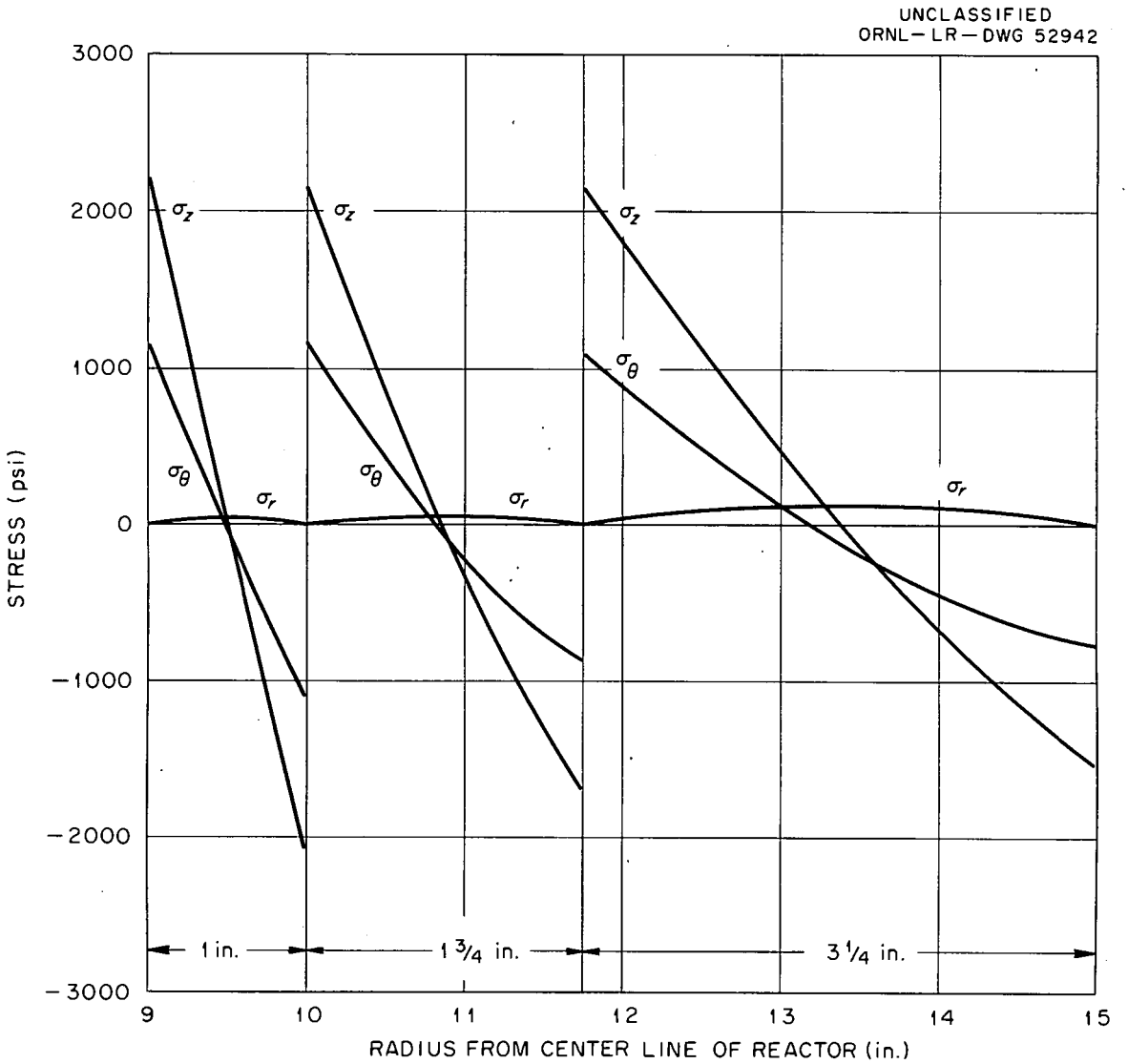

Fig. 9.4. Stresses in First 6 in. of Pebble-Bed Reactor Reflector After One Year of Full Power Operation, Assuming Three Cylinders of Thicknesses 1, 1 3/4, and 3 1/4 in.

uranium-graphite reactor after four years of operation, the condition of the graphite lattice is discussed. The lattice was constructed in the form of rectangular bricks. The author states that "the internal stresses associated with the uneven changes in brick dimensions caused the distortion of the bricks and even, in some cases, the appearance of longitudinal cracks. The cracks were formed in those bricks which were in the zone of maximum swelling" (the cooler regions of the reactor).

The results from various mechanical properties tests may be used to predict the exposure times at which cracking will occur. However, an accurate prediction is not possible because the strength properties vary widely from specimen to specimen and even within the same specimen. The most applicable available data are the results of the brittle-ring tests performed at ORNL on specimens taken from EGCR fuel element sleeves.[3] The sleeves were manufactured from Texas-coke graphite instead of needle-coke graphite. However, the strength properties of needle-coke graphite and Texas-coke graphite are approximately equal. Rings were cut from several sample sleeves with defect areas on the inner surfaces. Some rings had no defects; in others, artificial defects were produced. The specimens were loaded to rupture by diametrically opposed compressive forces which gave rise to tensile stresses on the inner surface directly under the points of load application. These tests allowed the determination of the tensile strength of the graphite in the defect zone. The rupture values obtained represent the strength in the direction perpendicular to the extrusion axis. A total of 31 tests was reported. For these 31 tests the lowest, average, and highest calculated rupture stresses were 1480, 1880, and 2780 psi, respectively.

The results of uniaxial tensile tests on needle-type AGOT graphite at ORNL[4] are given in Table 9.1. Minimum, average, and maximum values of rupture strength and fracture strain in the directions parallel and perpendicular to the extrusion axis are presented. Since the maximum

---

[3] Internal memorandum from F. L. Carlsen, Jr., ORNL. Data to be published in "GCR Quar. Prog. Rep. Sept. 30, 1960," ORNL-3015 (in press).

[4] "GCR Quar. Prog. Rep. June 30, 1960," ORNL-2964, p. 99.

Table 9.1. Uniaxial Tensile Data for Needle-Type AGOT Graphite

	Rupture Stress (psi)	Fracture Strain (%)
Axial direction		
Minimum	2270	0.163
Average	2310	0.188
Maximum	2360	0.205
Perpendicular direction		
Minimum	1650	0.299
Average	1790	0.351
Maximum	1890	0.406

stress in each cylinder is an axial stress, only the strength properties in the axial direction are of interest in predicting failure times. This is because the maximum principal stress establishes the rupture criterion. In order to convert the results of the brittle-ring tests for application to stresses in the axial direction, the results were multiplied by the ratio of the average rupture stress in the axial direction to the average rupture stress in the perpendicular direction as obtained from Table 9.1. Thus, the minimum, average, and maximum rupture stresses in the axial direction are 1870, 2380, and 3520 psi, respectively.

The rupture stresses obtained from the brittle-ring tests as converted to stresses in the axial direction are directly comparable with the calculated stress values, and thus allowances are made for defects in the material. The rupture stress values obtained from the tensile tests are not directly comparable with the calculated stresses because the calculated stresses were determined on the basis that the material follows a linear elastic law. Actually, the stress-strain curves for graphite exhibit some nonlinearity even at low stresses. Comparative stresses may be obtained by multiplying the fracture strains by the modulus of elasticity corresponding to the slope of the stress-strain curve at zero stress, since this value was used when the stresses in the cylindrical model were calculated. The above procedure gives minimum,

average, and maximum stress values of 2490, 2880, and 3140 psi, respectively. These values fall within the range given by the brittle-ring tests.

Table 9.2 gives the predicted time to cracking for each of the sleeves represented in Figs. 9.2, 9.3, and 9.4 based on the minimum and maximum rupture stresses from the brittle-ring tests and the minimum and maximum values of stress obtained from the axial fracture strains. The results are given in three groups corresponding to the thickness combinations examined. The first number in each sleeve designation represents the position of the sleeve with respect to the core centerline. The second number represents the thickness of the sleeve. The values given in Table 9.2 should be taken as representing ranges of times at which cracking would be expected to occur.

The combination of two 1.0-in.-thick and two 2.0-in.-thick sleeves appears to be the most desirable. If the inner two sleeves are supported on a common base and the third is supported separately on a second base, the first two sleeves can be removed together,

Table 9.2. Predicted Time to Cracking for Various Sleeve Thicknesses

Sleeve		Predicted Time to Cracking (weeks)			
Position	Thickness (in.)	Based on Minimum Brittle-Ring Strength	Based on Maximum Brittle-Ring Strength	Based on Minimum Fracture Strain	Based on Maximum Fracture Strain
1	2	24	46	32	40
2	2	57	108	76	96
3	2	91	172	122	154
1	1	44	84	60	75
2	1	71	133	94	118
3	2	57	108	76	96
4	2	91	172	122	154
1	1	44	84	60	75
2	1 3/4	44	84	59	74
3	3 1/4	46	86	61	77

while the third can be removed either with the first two or separately. The fourth sleeve cannot be removed as a single unit.

The lifetimes of the graphite sleeves may be increased by reducing the flux gradient or by any of several other devices, e.g., applying an axial compressive force to counteract the large tensile stresses. The latter appers to offer an attractive solution. Since the compressive strength of graphite is three or four times the tensile strength, large axial compression forces may be applied without exceeding acceptable limits for the compressive stresses. If forces were applied to the ends of a cylinder so that when the maximum tangential stress became 1500 psi the maximum axial stress would also be 1500 psi, the life of the cylinder could be increased by a factor of 1.94. As an example, the forces necessary for the proposed sleeve combination are 21 000 lb for the inner sleeve, 23 000 lb for the second sleeve, 53 000 lb for the third sleeve, and 62 000 lb for the fourth sleeve.

Estimated Friction Forces and Sleeve Interferences for Various Modes of Deformation and Fracture

In order to gain a knowledge of the difficulty which might be encountered in removing a sleeve from the reflector, the frictional force between the outer 2-in.-thick sleeve and the assembly of inner sleeves was calculated for various diametral interferences. It was assumed that the outer sleeve deforms to an elliptical shape so that interference occurs at diametrically opposite points. The coefficient of static friction for graphite on graphite at room temperature was taken as 0.34.[5] Since the friction coefficient is highly dependent on surface conditioning, the friction coefficient might be considerably higher than this value. A plot of the friction force per inch of cylinder length versus diametral interference is presented in Fig. 9.5.

---

[5]P. Wagner et al., "Some Mechanical Properties of Graphite in the Temperature Range 20 to 3000°C," Second United Nations International Conference on the Peaceful Uses of Atomic Energy 7, 379 (1958).

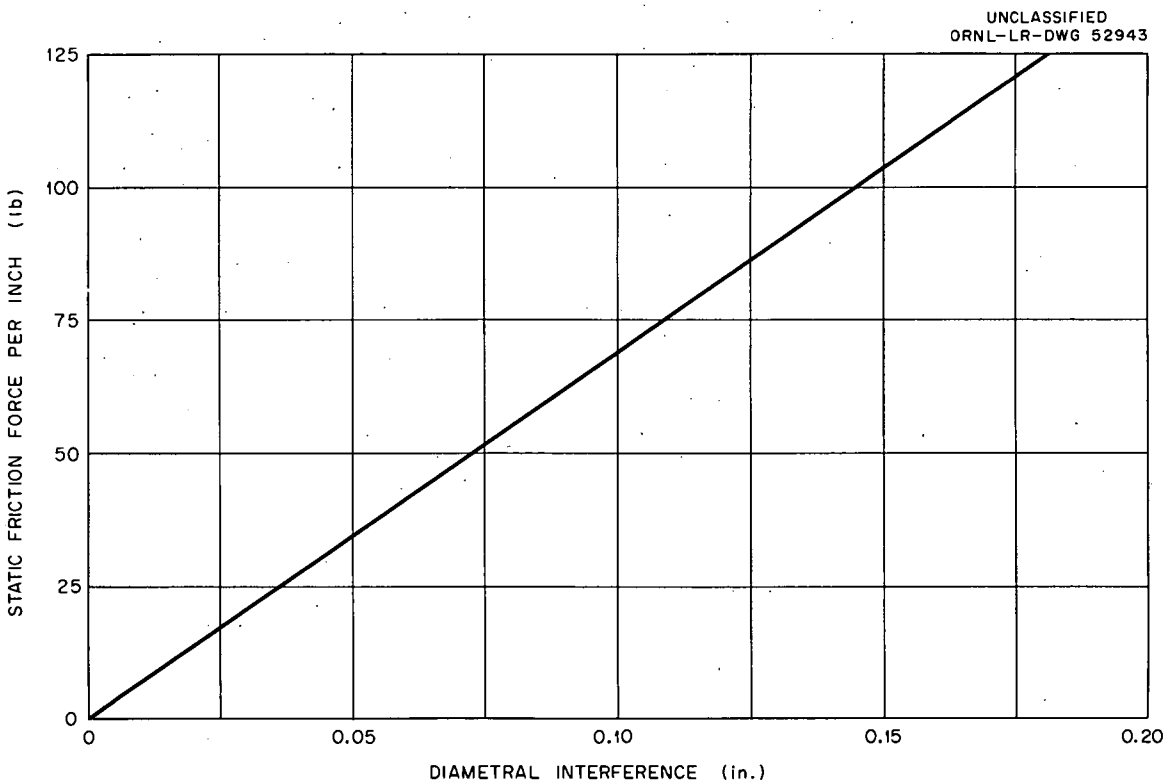

Fig. 9.5. Static Friction Force Per Inch Versus Diametral Interference Between Outer 2-in. Cylinder and Inner 2-in. Cylinder.

If a complete circumferential break should occur, the ends of the cylinder at the break will tend to curl radially inward because of the axial stress distribution across the thickness. For the proposed sleeve combination, the amount of radial deflection that will occur because of this curling has been calculated for the two 2-in. sleeves. For the inner 2-in. sleeve, the radial deflection at the break will be 0.0074 in./yr of exposure. The amount of deflection depends only on the total exposure time and is independent of when the break occurs. For the outer 2-in. cylinder, the deflection will be 0.0054 in./yr of exposure. From the above values it may be seen that a small initial clearance between the outer 2-in. cylinder and the middle 2-in. cylinder and between the middle 2-in. cylinder and the 1-in. cylinders will eliminate any problem produced by curling of the ends of a broken cylinder.

10. CORE HEAT TRANSFER, PRESSURE DROP, AND TEMPERATURE DISTRIBUTION

Fluid flow and heat transfer relations are among the most important considerations in the design of a pebble-bed reactor. This chapter presents the basic relations employed in the analyses, a simplified approach to the hot spot problem, and the results of a parametric survey of the effects of the principal factors on the peak temperature to be expected in a pebble-bed reactor core.

Nomenclature

The symbols used in this analysis are defined below:

A = core face area, ft^2,

a = area of a circular ring, ft^2,

C = a constant,

C_p = specific heat, Btu/lb·°F,

D_s = diameter of sphere, ft,

f = friction factor, dimensionless,

F_{st} = hot-spot factor for gas temperature rise due to radial variation of voidage in the core, dimensionless,

$F_{\Delta t}$ = hot-spot factor for film temperature drop due to radial variations in the core voidage, dimensionless,

G = mass flow rate of gas per unit core face area, lb/ft^2,

g = acceleration due to gravity, ft/hr^2,

h = heat transfer coefficient, $Btu/hr \cdot ft^2 \cdot °F$,

k = thermal conductivity, $Btu/hr \cdot °F \cdot (ft^2/ft)$,

K = power density, $Btu/hr \cdot ft^3$,

K^* = power density, kw/liter,

$\overline{K}^*$ = average core power density, kw/liter,

L = core length, ft,

M = molecular weight of gas,

P = pressure, lb/ft^2 absolute,

ΔP = pressure drop, lb/ft^2 absolute,

Pr = Prandtl number,

Q = heat generation rate per unit core face area, Btu/hr·ft^2,

γ_{ax} = axial peak-to-average core power density ratio,

γ_{rad} = radial peak-to-average core power density ratio,

Re = Reynolds number,

S = heat transfer area per unit core volume, ft^2/ft^3,

T = temperature, °R,

t = temperature, °F

t_i = inlet temperature, °F,

δt = gas temperature rise in core, °F,

$\overline{\delta t}$ = average gas temperature rise in core, °F,

Δt = film temperature drop from the surface of sphere to the gas in the hot region, °F,

$\overline{\Delta t}$ = average film temperature drop for the core, °F,

W = pumping power per unit core face area, Btu/hr·ft^2,

ϵ = void fraction,

$\psi(\epsilon)$ = $\epsilon^{1.73}/(1 - \epsilon)^{0.735}$,

$\phi(T)$ = a function representing $(\rho/\mu)^{0.577}$ as a function of temperature,

μ = viscosity, lb/ft·hr,

ρ = density, lb/ft^3.

Subscripts

e = equivalent (e.g., if the variable voidage of the core were replaced by an equivalent uniform voidage),

i = portion of core subtended by the circular ring i,

m = maximum.

Basic Relations

A careful review of the literature indicated that the empirical relations employed by Sanderson & Porter for the pressure drop, heat transfer coefficient, and ball internal temperature differential describe the situation as well as any information available. These relations are as follows:

1. Bed pressure drop

$$\Delta P = 2f \frac{G^2}{\rho g} \frac{L}{D_s} ,$$

where

$$f = 7.5 \frac{(1 - \epsilon)^{1.27}}{\epsilon^3} Re^{-0.27} .$$

2. Heat transfer coefficient

$$h = 0.5 (1 - \epsilon)^{0.3} GC_p Pr^{-0.66} Re^{-0.3} .$$

3. Heat transfer area per unit core volume

$$S = \frac{6 (1 - \epsilon)}{D_s} .$$

4. Average film temperature drop

$$\overline{\Delta t} = \frac{K}{Sh} .$$

5. Ball internal temperature drop

$$\Delta t_s = \frac{\overline{K}}{(1 - \epsilon)} \frac{D_s^2}{24k} .$$

Typical Values

In applying the foregoing relations to the PBRE for the design conditions chosen, the core pressure drop, the average film temperature drop from the spheres to the cooling gas, and the average ball internal temperature difference can be evaluated.

The properties of helium at 1000 psia and a 900°F mean temperature are

$$\mu = 0.0955 \text{ lb/ft}\cdot\text{hr},$$
$$C_p = 1.241 \text{ Btu/lb}\cdot{}^\circ\text{F},$$
$$Pr = 0.7265 \text{ (dimensionless)},$$
$$\rho = \frac{PM}{1544T} = \frac{1000 \times 144 \times 4}{1360 \times 1544} = 0.274 \text{ lb/ft}^3 .$$

The mass flow rate is thus

$$G = \frac{\text{core power}}{\text{core area} \times C_p \times \overline{\delta t}} = \frac{10 \times 10^3 \times 3413}{\left[\frac{\pi}{4} \times (1.5)^2\right] \; 1.241 \times 700}$$
$$= 2.22 \times 10^4 \text{ lb/ft}^2\cdot\text{hr} .$$

The Reynolds number is

$$Re = \frac{G_s D_s}{\mu} = \frac{(2.22 \times 10^4) \times 0.125}{0.0955} = 2.9 \times 10^4 .$$

Using a core void fraction of 0.4, the friction factor becomes

$$f = 7.5 \frac{(0.6)^{1.27}}{(0.4)^3} (2.9 \times 10^4)^{-0.27} = 3.83 .$$

The core pressure drop is

$$\Delta P = 2 \times 3.83 \frac{(2.22 \times 10^4)^2}{0.274 \; [32.2 \times (3600)^2]} \frac{8}{0.125}$$
$$= 2115 \text{ psia} = 14.7 \text{ psig} .$$

The average heat transfer coefficient is

$$h = \frac{0.5\ (0.6)^{0.3}\ (2.22 \times 10^4)\ 1.241}{(0.7265)^{0.66}\ (2.91 \times 10^4)^{0.3}} = 675\ \text{Btu/hr}\cdot\text{ft}^2\cdot{}^\circ\text{F} \quad .$$

The surface area per cubic foot of bed is

$$S = \frac{6 \times 0.6}{0.125} = 28.8\ \text{ft}^2/\text{ft}^3 \quad .$$

The power density is

$$\bar{K} = \frac{\text{core power}}{\text{core volume}} = \frac{10 \times 10^3 \times 3412}{\frac{\pi}{4} \times 1.5^2 \times 8} = 24.1 \times 10^5\ \text{Btu/hr}\cdot\text{ft}^3$$

$$= 25\ \text{w/cm}^3 \quad .$$

The average film temperature drop is

$$\overline{\Delta t} = \frac{\bar{K}}{Sh} = \frac{24.1 \times 10^5}{28.8 \times 675} = 124^\circ\text{F} \quad .$$

The average temperature drop from the center to the surface of a ball having a thermal conductivity of 15 Btu/hr·ft^2·°F/ft is

$$\Delta t_s = \frac{\bar{K} D_s^2}{24\ (1 - \epsilon)\ k} = \frac{(24.1 \times 10^5)(0.125)^2}{24 \times 0.6 \times 15} = 170^\circ\text{F} \quad .$$

Simplified Approach to Investigation of the Hot-Spot Problem

The first step in studying the hot-spot problem was a careful review of some recent Canadian work (see Bibliography) on the local heat transfer coefficient over the surface of a sphere in a closely packed bed. In connection with this work, a number of tests were made in which

balls were dumped at random into containers. These tests showed that, under some conditions, clusters of closely packed spheres appeared in randomly packed beds. The pressure drop test data shown in Fig. 10.1 indicate that the pressure drop through such closely packed regions would be much higher than the average value for randomly packed beds. Much of the flow will tend to bypass such closely packed clusters, so the flow rate in the closely packed regions will be only about 35% of the average for the bed as a whole. Since such closely packed clusters are likely to be associated with the hottest regions in a pebble-bed reactor, attention was directed solely to beds of closely packed spheres in the Canadian experiments. The experimental results disclosed that the local heat transfer coefficient in the vicinity of points of contact between balls and in the stagnation region on the downstream surface of the ball was only about one-half the average heat transfer coefficient.

In examining the particular case at hand, the writers concluded that local variations in heat transfer coefficient over the surface of a ball would result in some increase in local surface temperatures, but that thermal conduction within the ball would largely alleviate these hot regions; therefore the principal effect would be an increase in the internal temperature difference within the ball. A rough estimate of this increase indicated that it would be about 25% of the internal temperature difference for a ball having a uniform heat flux over its outer surface.

The next step in the analysis of the hot-spot problem was to estimate the average gas and ball surface temperatures as a function of axial position, with allowances for the axial power distribution. The resulting temperature distribution curves are shown in Fig. 10.2. Experience with other types of gas-cooled reactor has shown that the most severe hot spots ordinarily occur approximately 70% of the distance through the core where the gas temperature has risen most of the way and yet the power densities are nearly as high as at the center of the

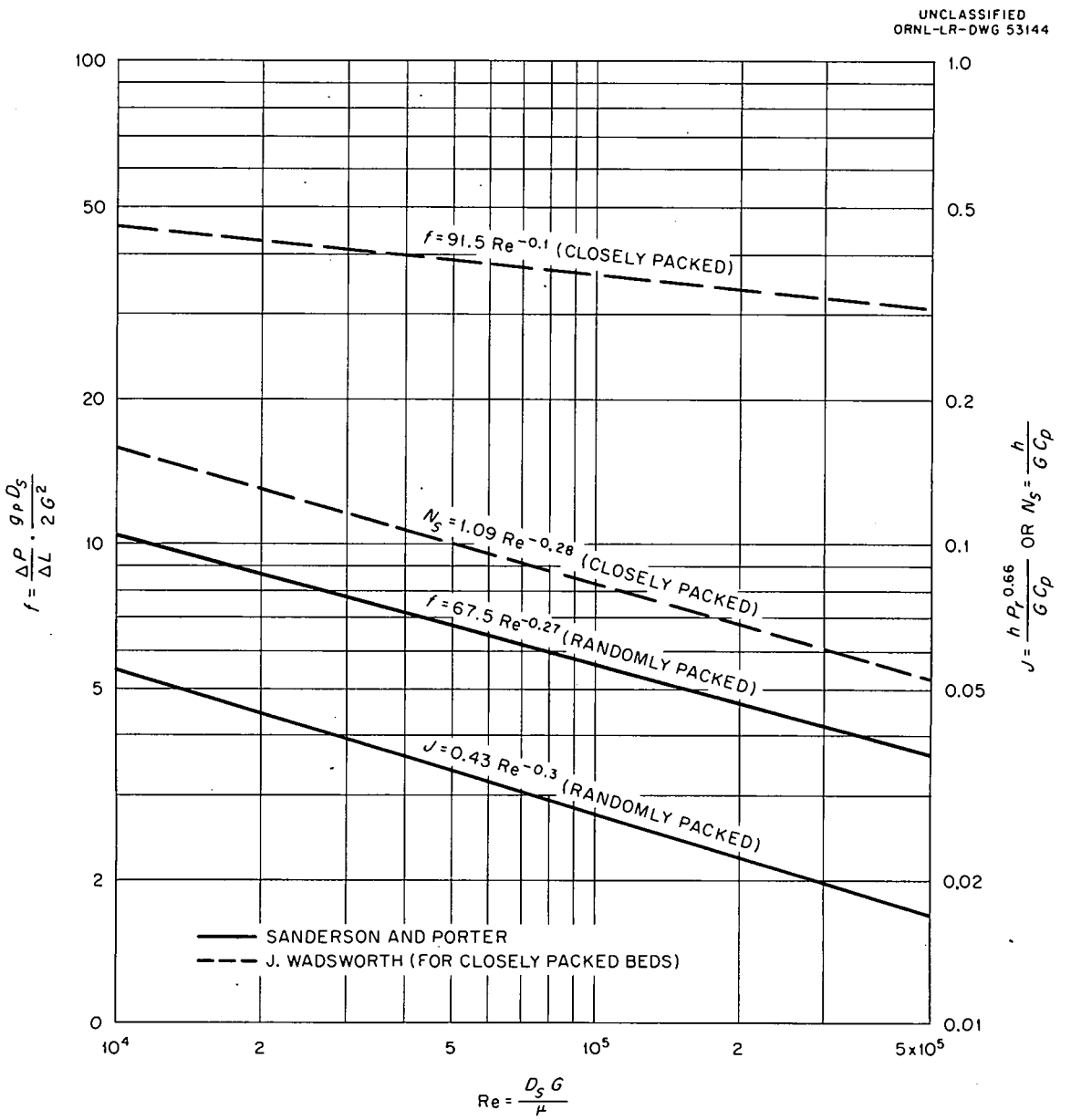

Fig. 10.1. Friction Factor, f, and Heat Transfer Correlations for Beds of Spheres.

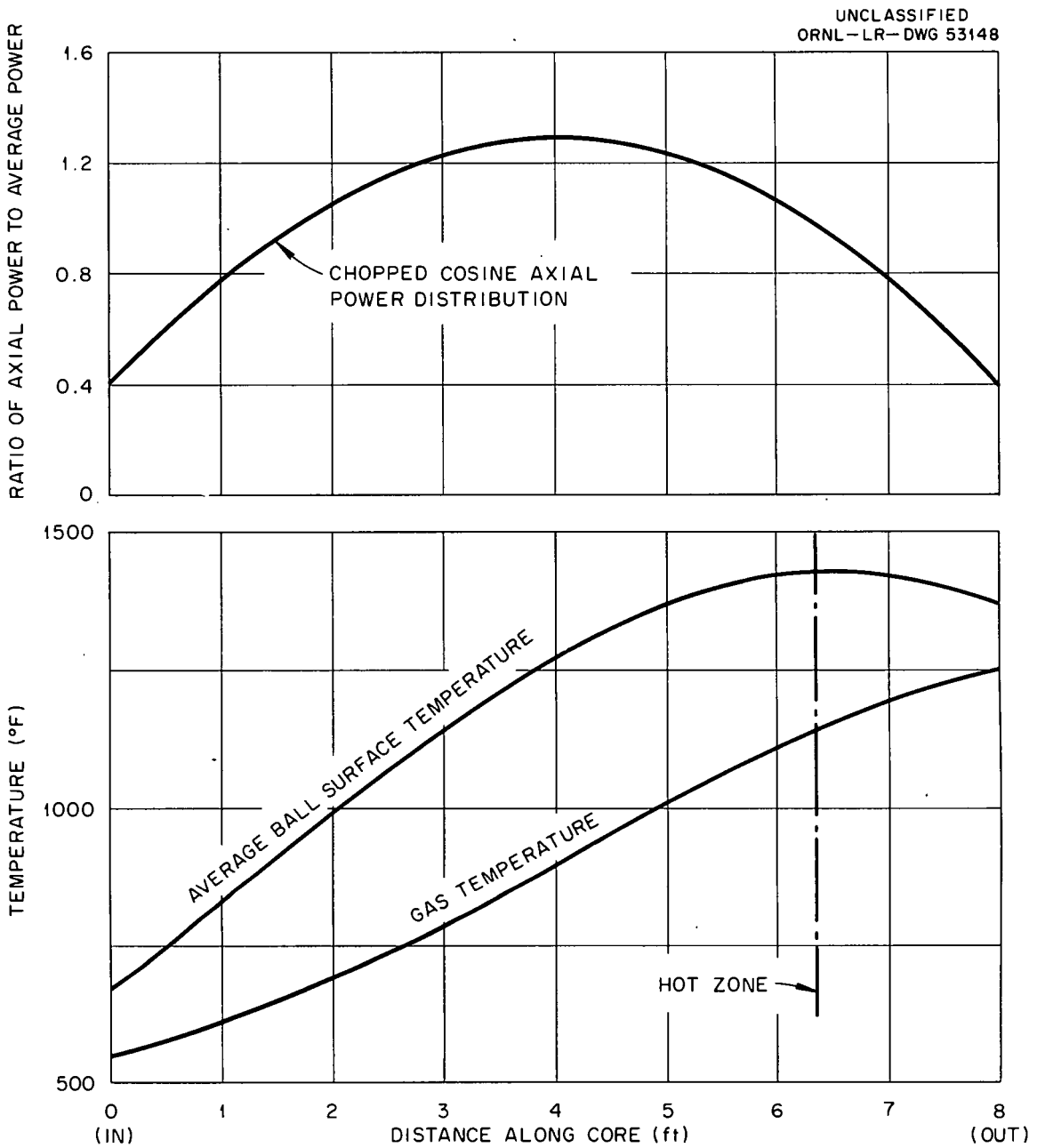

Fig. 10.2. Gas Temperatures and Ball Surface Temperatures in a Large Pebble Bed Assuming a Chopped Cosine Axial Power Distribution and a Uniform Radial Power Distribution.

core. This region has been referred to as the hot zone in the subsequent discussion.

The combined effects of both axial and radial variations in power density will give local regions in the hot zone in which the power density will be about double the average for the core. Thus, although the average film drop for the core was estimated above to be 124°F, the film drop in the hot zone will be about 250°F for random packing. If a closely packed cluster that is several ball diameters across develops in this zone, the gas velocity within the closely packed cluster will be about the same as in the randomly packed surrounding bed, and hence the local heat transfer coefficient will differ little from the average value, even though the gas flow rate per unit of bed cross-sectional area is reduced by a factor of 3. However, the reduced local gas flow rate in the wake of the cluster will reduce the heat transfer coefficient in that region by a factor of about 2.2, and this will give local values for the film drop of approximately 550°F. Further, the temperature rise per unit of core length in the closely packed cluster will be triple that of the surrounding bed.

The same sort of reasoning can be applied to the ball internal temperature drop. The average value for the core of 170°F should be multiplied by a factor of 1.25 to allow for the increase resulting from variations in local heat transfer coefficients over the surface of the sphere. This, coupled with a local power density twice the average, gives a temperature drop of roughly 420°F within a ball in the hot zone.

The gas temperature rise through the reactor will not be the same in all annular regions because of variations in both the radial power distribution and the radial gas flow distribution. While a great effort may be made to match the radial gas flow distribution to the radial power distribution, this matching will not be perfect, and, even with the benefits provided by radial mixing between adjacent annuli, it seems likely that the gas temperature distribution in a radial direction in the hot zone will lead to gas temperatures in some annuli perhaps 200°F above the average. This, coupled with the extra gas temperature rise

in a hot cluster, is likely to give a local gas temperature in the wake of a closely packed cluster in the hot zone of about 1350°F, as compared with the average gas temperature in the hot zone of 1050°F. These rough estimates have been summarized in Table 10.1, where the cumulative effects give a hot ball surface temperature of 1850°F and a hot ball internal temperature of 2270°F.

Table 10.1. Factors in a Simplified Hot-Spot Temperature Estimate

Hot-Spot Factor	Temperature Estimate (°F)	
	For 18-in.-diam by 8-ft-High Core	For 30-in.-diam by 30-in.-High Core
Average film temperature drop for entire core	124	270
Average film temperature drop for hot zone	250	540
Film drop in the wake of closely packed cluster in the hot zone	550	1200
Temperature drop within an average ball uniformly cooled and operating at the average core power density	170	170
Same as above but with allowances for irregularities in heat transfer coefficient over the surface of the sphere	210	210
Same as above but for the peak power density in hot zone	420	420
Average gas temperature in hot zone	1050	1050
Peak gas temperature in hot cluster	1300	1400
Hot ball surface temperature	1850	2600
Hot ball internal temperature	2270	3020

As a point of interest, a similar set of estimates was prepared for a 30-in.-diam, 30-in.-high reactor core. These estimates have also been included in Table 10.1. The hot ball surface temperature for this core might be as much as 2600°F, while the hot ball internal temperature might reach 3000°F. It was for this reason that the tall, slender core was chosen for the proposed design.

The estimates of Table 10.1 are a bit shocking to one whose first estimate of the hot test surface temperature would be the gas temperature at the core outlet plus the average film temperature drop, i.e., 1250 + 124 = 1374°F. The values are not surprising, however, if one reviews the struggles to flatten the core power density and match the coolant flow distribution to the power density in such reactors as those at Calder Hall, the EGCR, and various air-cooled reactors built for military applications. It is quite possible that a more favorable power distribution can be obtained than that assumed in the preparation of Table 10.1. A great deal of transverse mixing may occur as the gas moves from one layer of balls to the next, and this will reduce the gas temperature in the hot zone. This effect will be particularly beneficial in a tall, thin core where the core length will be 64 ball diameters, while the core radius will be only six ball diameters, giving a mixing length-to-diameter ratio of about 10. The corresponding ratio for the short, squat core would be only 2; hence, in this core, transverse mixing would be only 20% as effective in alleviating a "hot stream" effect as in the tall, thin core.

Relations Between Maximum Surface Temperature, Power Density, and Pumping Power Requirements

Cores with Constant Voidage

Studies have shown that it is especially useful in a parametric survey of reactor fuel element heat transfer performance to relate the maximum ball surface temperature to the core power density and the pumping power-to-heat removal ratio. The general analytical equation

relating the core power density for a gas-cooled pebble-bed reactor to the principal variables can be derived readily if a uniform voidage throughout the core is assumed. First, consider an axial element of a reactor in the region where the radial power density is maximum. If this core element has a cross-sectional area of 1.0 ft^2, the heat transfer and pumping power relations for this volume are

$$Q_m = G_s C_p \, \delta t_m \quad , \tag{1}$$

and

$$Q_m = hSL \frac{\Delta t_m}{\gamma_{ax}} \quad . \tag{2}$$

Assuming that the gas pressure drop is the same everywhere across the core,

$$W = \frac{\Delta P \, G_s}{778 \, \rho} \quad . \tag{3}$$

The core power density for the core volume considered can be defined as follows:

$$K_m = \frac{Q_m}{L} \quad . \tag{4}$$

From Eqs. (1) and (3),

$$\frac{W}{Q_m} = \frac{1}{778} \frac{\Delta P}{\rho C_p \, \Delta t_m} \quad . \tag{5}$$

The relations used earlier in this section may be restated as follows:

$$h = 0.5 \, (1 - \epsilon)^{0.3} \, G_s C_p Pr^{-0.66} Re^{-0.3} \quad , \tag{6}$$

$$\Delta P = 2f \frac{G_s^2}{\rho g} \frac{L}{D_s} \quad , \tag{7}$$

$$f = 7.5 \frac{(1-\epsilon)^{1.27}}{\epsilon^3} Re^{-0.27} \quad , \tag{8}$$

$$Re = \frac{G_s D_s}{\mu} \quad , \tag{9}$$

$$S = \frac{6(1-\epsilon)}{D_s} \quad . \tag{10}$$

Substituting Eqs. (8) and (9) into (7),

$$\Delta P = \frac{2 \times 7.5}{g} \frac{(1-\epsilon)^{1.27}}{\epsilon^3} \frac{G_s^{1.73}\mu^{0.27}L}{\rho D_s^{1.27}} \quad . \tag{11}$$

Substituting Eq. (11) into (5),

$$\frac{W}{Q_m} = \frac{15}{778\ g} \frac{(1-\epsilon)^{1.27}}{\epsilon^3} \frac{G_s^{1.73}\mu^{0.27}}{\phi^2 C_p D_s^{1.27}} \left(\frac{\delta t_m}{L}\right)^{-1} \quad . \tag{12}$$

From Eqs. (1) and (4),

$$K_m = G_s C_p \frac{\delta t_m}{L} \quad . \tag{13}$$

Eliminating G_s between Eqs. (12) and (13),

$$K_m = \left(\frac{778\ g}{15}\right)^{0.577} \frac{\epsilon^{1.27}}{(1-\epsilon)^{0.735}} \frac{C_p^{1.577}\rho^{1.54}}{\mu^{0.156}} D_s^{0.735} \times$$

$$\times \left(\frac{\delta t_m}{Q_m}\right)^{1.577} \left(\frac{W}{Q_m}\right)^{0.577} \quad . \tag{14}$$

Let

$$\rho = \frac{P}{T}\,\frac{M}{1544} \quad . \tag{15}$$

Substituting Eq. (15) into (14),

$$K_m = 192\,\frac{\epsilon^{1.73}}{(1-\epsilon)^{0.735}}\,\frac{C_p^{1.577}}{\mu^{0.156}}\left(\frac{PM}{T}\right)^{1.154} D_s^{0.735} \times$$

$$\times\left(\frac{\delta t_m}{L}\right)^{1.577}\left(\frac{W}{Q_m}\right)^{0.577} \quad . \tag{16}$$

Equation (16) includes all of the principal reactor parameters, except for the film temperature drop, Δt_m. An analytical equation relating the film temperature drop to the other parameters can be obtained in the following manner.

From Eqs. (1) and (2):

$$G_s C_p\,\delta t_m = hSL\,\frac{\Delta t_m}{\gamma_{ax}} \quad . \tag{17}$$

Substituting Eqs. (6), (9), and (10) into (17),

$$G_s C_p\,\delta t_m = \left[0.5\,(1-\epsilon)^{0.3}\,G_s C_p Pr^{-0.66}\left(\frac{G_s D_s}{\mu}\right)^{-0.3}\right] \times$$

$$\times\left[\frac{6\,(1-\epsilon)}{D_s}\right] L\,\frac{\Delta t_m}{\gamma_{ax}} \quad ,$$

or

$$G_s^{0.3} = 3\,(1-\epsilon)^{1.3}\,Pr^{-0.66}\mu^{0.3}D_s^{-1.3}\left(\frac{\delta t_m}{L}\right)^{-1}\left(\frac{\Delta t_m}{\gamma_{ax}}\right) \quad . \tag{18}$$

Solving Eq. (12) for $G_s^{0.3}$,

$$G_s^{0.3} = \left(\frac{778\ g}{15}\right)^{0.173} \frac{\epsilon^{0.52}}{(1-\epsilon)^{0.22}} \left(\frac{W}{Q_m}\right)^{0.173} \times$$

$$\times \frac{\rho^{0.346} C_p^{0.173} D_s^{0.22}}{\mu^{0.046}} \left(\frac{\delta t_m}{L}\right)^{0.173} . \qquad (19)$$

Substituting Eq. (15) into (19),

$$G_s^{0.3} = \left(\frac{778\ g}{15}\right)^{0.173} \frac{\epsilon^{0.52}}{(1-\epsilon)^{0.22}} \left(\frac{W}{Q_m}\right)^{0.173} \frac{1}{1544^{0.346}} \times$$

$$\times \left(\frac{PM}{T}\right)^{0.346} \frac{C_p^{0.173}}{\mu^{0.046}} D_s \left(\frac{\delta t_m}{L}\right)^{0.173} . \qquad (20)$$

Eliminating G_s between Eqs. (18) and (20) and solving for Δt_m,

$$\Delta t_m = 1.60\ \gamma_{ax} \frac{\epsilon^{0.52}}{(1-\epsilon)^{1.52}} D_s^{1.52} \left(\frac{W}{Q_m}\right)^{0.173} \frac{C_p^{0.173} Pr^{0.66}}{\mu^{0.346}} \times$$

$$\times \left(\frac{PM}{T}\right)^{0.346} \left(\frac{\delta t_m}{L}\right)^{1.173} . \qquad (21)$$

Equations (16) and (21) give the core power density and the film temperature drop for the core radius at which the power density is a maximum. The average values for the entire core can be defined as follows:

$$\begin{aligned} \overline{K} &= K_m/\gamma_{rad} \quad , \\ \overline{Q} &= Q_m/\gamma_{rad} \quad , \\ \overline{\delta t} &= \delta t_m/\gamma_{rad} \quad , \\ \overline{\Delta t} &= \Delta t_m/\gamma_{rad} \quad . \end{aligned} \tag{22}$$

Substituting (22) into Eqs. (16) and (21), it can be seen that the term γ_{rad} cancels out, and

$$\overline{K} = 192 \frac{\epsilon^{1.73}}{(1-\epsilon)^{0.735}} \frac{C_p^{1.577}}{\mu^{0.156}} \left(\frac{PM}{T}\right)^{1.154} D_s^{0.735} \times \left(\frac{\overline{\delta t}}{L}\right)^{1.577} \left(\frac{W}{\overline{Q}}\right)^{0.577} , \tag{23}$$

and

$$\overline{\Delta t} = 1.60\, \gamma_{ax} \frac{\epsilon^{0.52}}{(1-\epsilon)^{1.52}} \frac{C_p^{0.173} Pr^{0.66}}{\mu^{0.346}} \left(\frac{PM}{T}\right)^{0.346} \times D_s^{1.52} \left(\frac{\overline{\delta t}}{L}\right)^{1.173} \left(\frac{W}{\overline{Q}}\right)^{0.173} \tag{24}$$

For Eqs. (23) and (24), it is probably best to evaluate the gas properties at the mean temperature of the gas in the core. The temperature T, however, entered the equation because the gas density appears in Eqs. (3) and (7) for the pumping power and the pressure drop, respectively. It should be pointed out that as the gas in the core is heated, it expands and contributes to the pumping process. In order to allow for that portion of the pumping accomplished by expansion of the gas during the heating process, where the temperature enters the equation via the gas density in the expression for the pump work, it should be evaluated at the

gas inlet temperature, while, where it enters via the gas density in the expression for the pressure drop, the mean temperature of the gas in the core should be used.

In applying these relations to the helium-cooled pebble-bed reactor experiment, the properties of helium in the temperature range of interest can be taken as follows:

$$\mu = 0.00145\ T^{0.58} \quad ,$$
$$C_p = 1.24 \quad ,$$
$$Pr = 0.727 \quad .$$

The dimensions of the reactor are

$$L = 8 \text{ ft} \quad ,$$
$$D_s = 0.125 \text{ ft } (1.5 \text{ in.}) \quad ,$$
$$\epsilon = 0.39 \quad .$$

Substituting these values in Eqs. (23) and (24), and in order to simplify the results, evaluating T at the arithmetic mean temperature of gas in the core, gives

$$\overline{K} = 8.46 \left(\frac{W}{\overline{Q}}\right)^{0.577} P^{1.154} \frac{\overline{\delta t}^{1.577}}{\left(460 + t_i + \frac{\overline{\delta t}}{2}\right)^{0.244}} \quad , \tag{25}$$

and

$$\overline{\Delta t} = 0.103\ \gamma_{ax} \left(\frac{W}{\overline{Q}}\right)^{0.173} P^{0.346} \frac{\overline{\delta t}^{1.173}}{\left(460 + t_i + \frac{\overline{\delta t}}{2}\right)^{0.547}} \quad . \tag{26}$$

These equations are extremely useful, since $\overline{K}$ and $\overline{\Delta t}$ can easily be calculated for any given values of $W/\overline{Q}$, P, and $\overline{\delta t}$.

The range of interest for these parameters is usually rather limited. Previous studies of gas-cooled reactors have shown that pumping costs will be excessive if W/Q, the pumping power-to-heat removal ratio, is greater than 1 or 2%, while capital costs begin to rise sharply if W/Q is less than 0.5%. Similarly, pressure vessel fabrication and cost problems limit the maximum gas system pressure to about 1000 psi, while capital charges for the reactor core begin to rise steeply as the system pressure is dropped below about 300 psia. The cost and strength of alloy steels limit the maximum gas temperature of real interest to 1200 to 1500°F, while plant thermal efficiency considerations make it desirable to keep the gas temperature leaving the steam generator above 500°F.

The equations derived above were applied to investigate the effects of the principal design parameters on the ball surface temperature in the hot zone of a large reactor core having a ball diameter of 1.5 in., a uniform voidage of 0.39, a core length of 8 ft, a core inlet gas temperature of 550°F, a helium system pressure of 1000 psi, and a power density in the hot zone equal to twice the average power density for the core as a whole. Allowances were made for the effects of a low heat transfer coefficient in the wakes of closely packed clusters. The results have been plotted in Fig. 10.3 to show that increasing the power density gives a rapid increase in ball surface temperature if the pumping power-to-heat removal ratio is held constant but increases relatively slowly if the pumping power-to-heat removal ratio is increased and the reactor gas outlet temperature is held constant.

The same basic analytical technique was applied to estimate the temperature distribution to be expected in the PBRE core using the power density distribution presented in Fig. 7.6. The core was divided into both annuli and vertical layers. Allowances were made for the effects of the higher void fraction near the walls on the gas flow distribution. The first estimate was made for no radial mixing to relieve the effects of poor matching between the flow distribution and the power distribution,

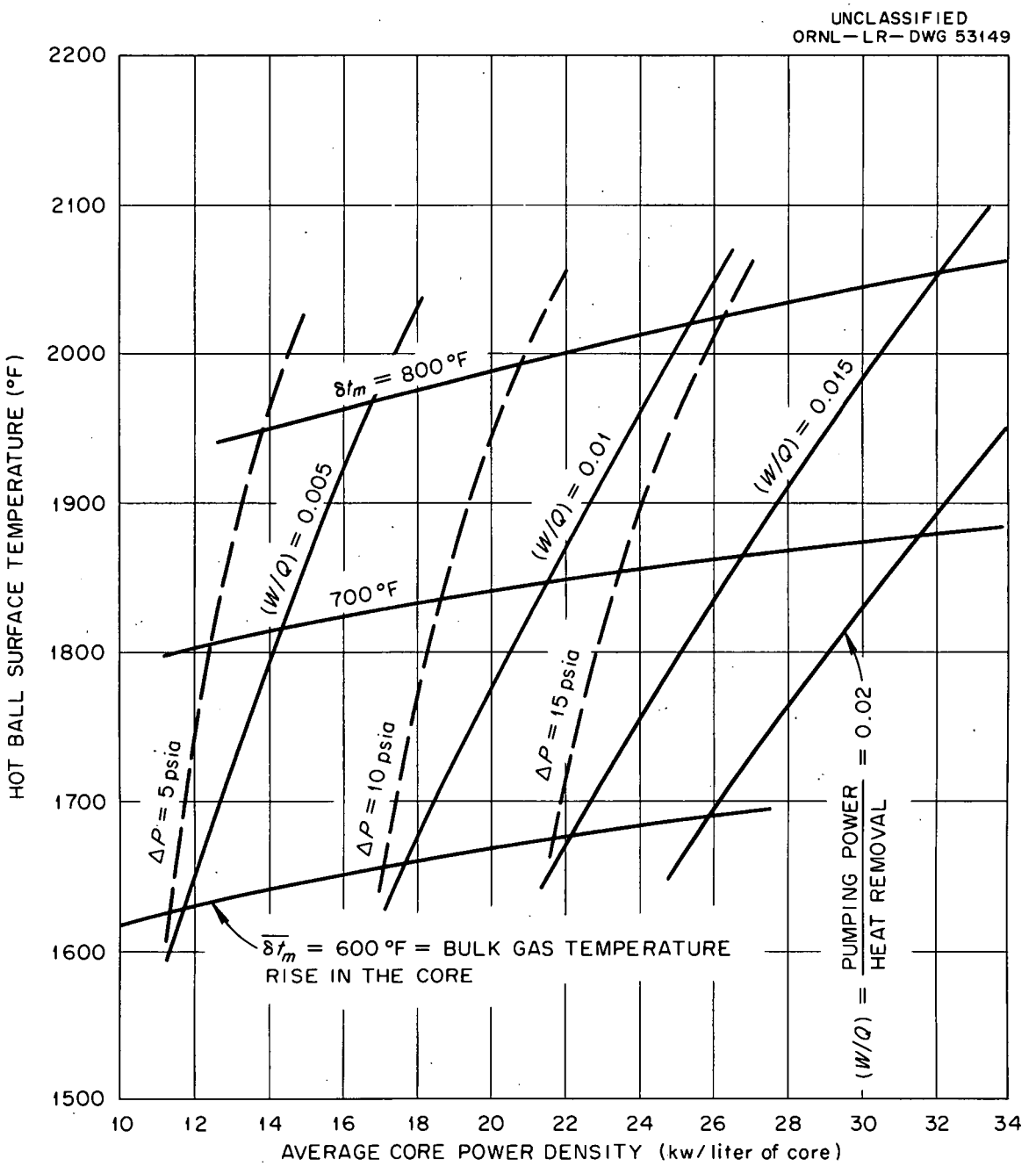

Fig. 10.3. Hot Ball Surface Temperature Versus Core Power Density Assuming a Chopped Cosine Axial Power Distribution and a Hot Spot in the Wake of a Closely Packed Cluster.

and both the gas and ball surface temperature distribution throughout the core were calculated. It was found that the maximum values for both the gas and the ball surface temperature were obtained at the core outlet. The solid curves of Fig. 10.4 present these values. The assumed void distribution is also shown.

The temperature differential between adjacent annuli near the core perimeter seemed to be excessive. Rough estimates of the effects of radial mixing in the spaces between layers of balls indicated that in an 18-in.-diam, 8-ft-high core radial mixing would remove roughly 75% of the difference between the mean and the local gas temperature given by this first approximation. The dotted curve of Fig. 10.4 was then plotted to show the radial gas temperature distribution assuming this degree of mixing. The extent to which radial mixing can be expected to alleviate hot channel effects will require careful study. It will probably be necessary to devise and conduct special experiments to clarify this vital question.

The hot-spot temperature to be expected in the wake of a closely packed cluster near the outlet of the PBRE core was estimated from the radial gas temperature distribution, with the allowances for radial mixing given in Fig. 10.4. The average film temperature drop for each radial position was multiplied by a factor of 2 and added to the local gas temperature to give the envelope for the hot ball surface temperature presented in Fig. 10.5. It should be emphasized that this curve does <u>not</u> represent the ball surface temperature distribution at the core outlet, but, rather, it indicates the surface temperature that might prevail at any given radial position at the core outlet if a closely packed cluster lay just below the position in question. The estimate includes the effects of an extra 50°F gas temperature rise through such a cluster.

The ball center temperatures implied by the above ball surface temperatures and the local power densities have also been estimated and plotted in Figs. 10.4 and 10.5. The internal temperature drop within

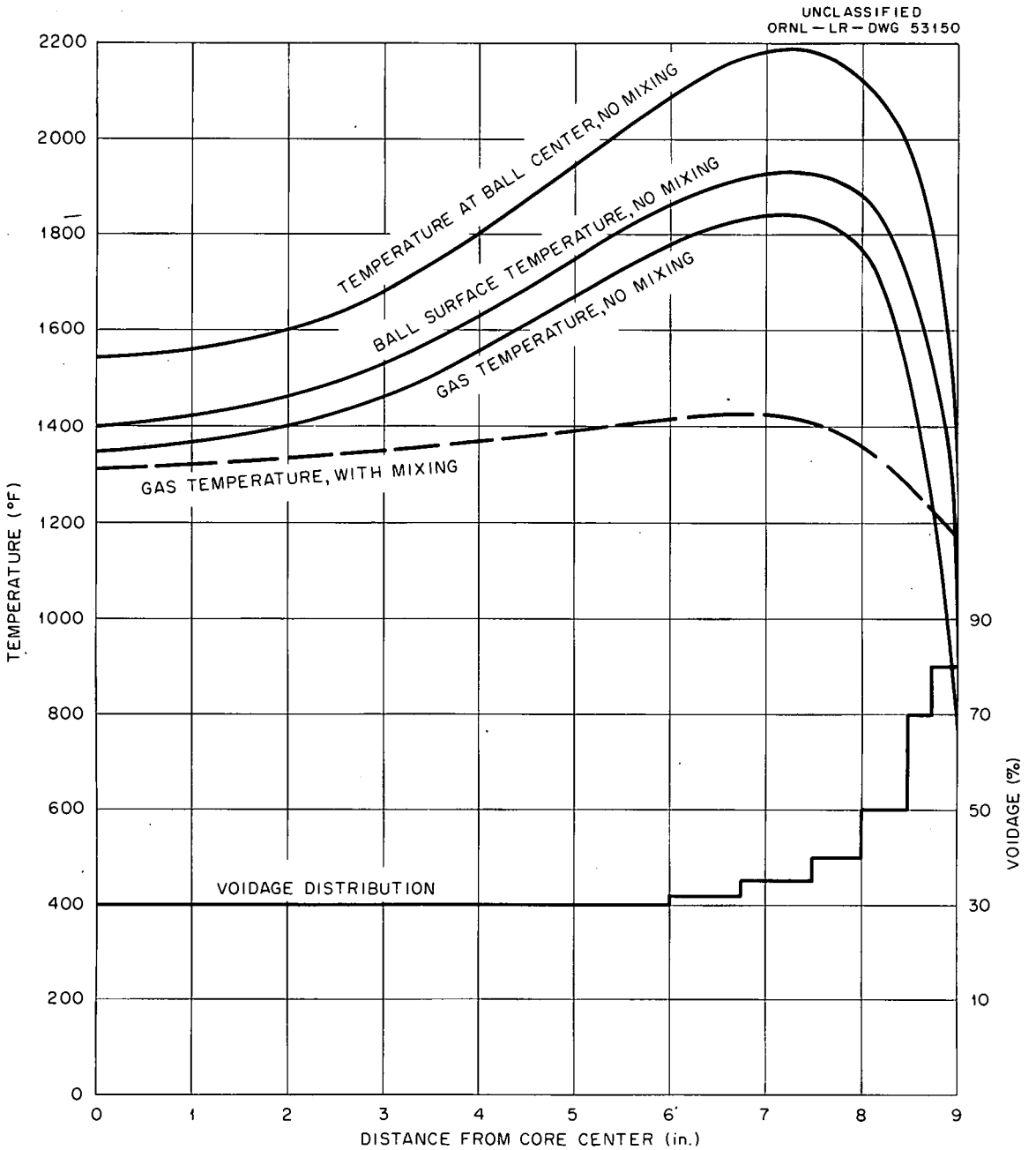

Fig. 10.4. Gas, Ball Surface, and Ball Center Temperatures at the Outlet of Core Assuming No Radial Mixing and No Hot Spots.

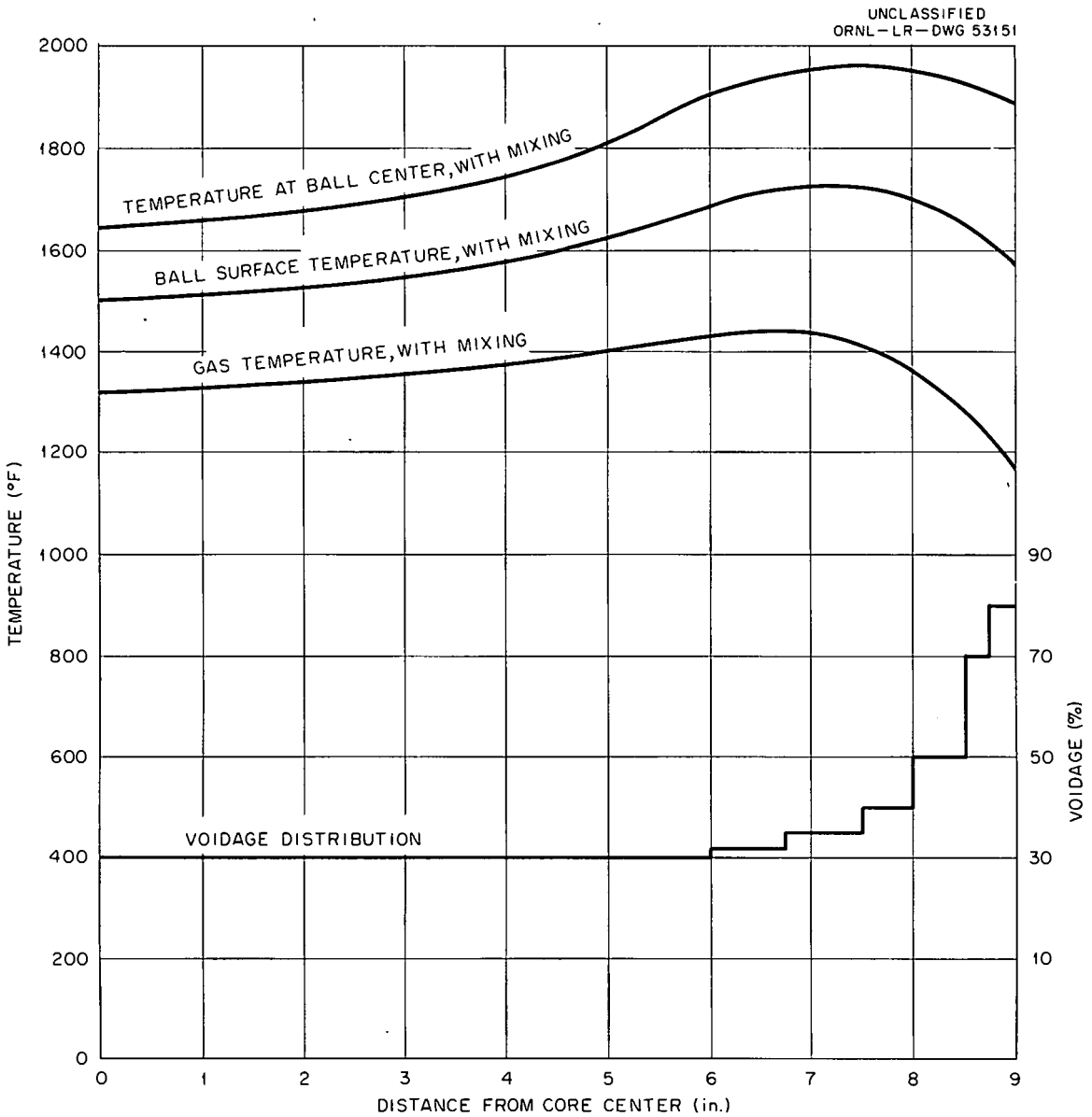

Fig. 10.5. Estimated Maximum Gas, Ball Surface, and Ball Center Temperatures for Hot Spots in the Wakes of Closely Packed Clusters Assuming Strong Radial Mixing.

the balls was multiplied by 1.25 to allow for the effects of irregularities in the heat transfer coefficient over the surface of individual spheres.

In reviewing the above, it appears that the 18-in.-diam, 8-ft-high core selected for the PBRE is a good choice from the hot-spot standpoint. The radial gas flow distribution is well matched to the radial power distribution in that the high power density region near the periphery is somewhat overcooled, thus keeping the film drop from being high. At the same time, the large length-to-diameter ratio promises to make radial mixing effective in flattening what would otherwise be a poor radial gas temperature distribution. On the whole, while the above estimates are rough approximations at best, they indicate that the proposed PBRE core should be less subject to difficulties with hot spots than a full-scale reactor where radial mixing could not be nearly so effective in flattening the radial gas temperature distribution.

11. NUCLEAR CONTROL AND SAFETY SYSTEMS

Safety System

The problem of safe operation of the reactor may be approached by first examining what may be considered safe and what unsafe. For power reactors in general it is usually unsafe to operate the reactor with some part of the lattice at too high a temperature, and it is also sometimes unsafe to operate in a transient which causes the rate of increase of some temperatures to be excessively large. The temperature and rate of change of temperature in question are usually those of one or more fuel elements. Such elements may be considered as perverse elements in that either the power density in the element is too high or the rate of cooling too low. Either of two pieces of information, namely a high temperature or a high positive rate of change of temperature, thus may be considered as the information which actuates the safety system.

Unfortunately, there is no way to measure directly either of these variables in order to actuate the safety system. In lieu of what may be called primary sensory information, "symptomatic" information can be derived as follows: (1) With the coolant flowing at some constant rate, a rise in coolant outlet temperature indicates or is a "symptom" of a rise in the temperatures of the reactor components that are being cooled. Accordingly, a high coolant outlet temperature, T_o, can be used to trip the safety system. (2) A high rate of change of reactor component temperatures comes about because of an unbalance between the nuclear power produced and the power carried off by the coolant. A condition of balance or unbalance between these two quantities is determined by the relation:

$$f(t) = p - aW(T_o - T_i) \quad , \qquad (1)$$

where p is the nuclear power, which can be measured by means of a calibrated ion chamber, W is the mass coolant flow, and T_i and T_o are reactor

coolant inlet and outlet temperatures, respectively. The constant a relates the units of p and $W(T_o - T_i)$ and contains the heat capacity of the coolant. For $f(t) > 0$ the temperature of the reactor elements is rising.

Information for the terms of Eq. (1) is delayed by the time constants of the sensors, and both T_o and T_i, in practice, are displaced timewise from their actual values by a transport lag because T_i is measured before the coolant enters the reactor and T_o is measured after the coolant has left the reactor.

The nature of this symptomatic information suggests immediately that one cannot expect satisfactory safety action from T_o for a fast nuclear excursion or a sudden loss of coolant flow. This is indeed true, and, accordingly, safety action is initiated by a high value of T_o only for situations brought about by a slow drift upward in the system temperature. The outlet temperature, T_o, gives all the safety action needed for the slow drift to high temperatures.

In order to take care of situations involving fast transients, such as nuclear excursions or loss of coolant, faster response times in the sensors are needed, and, since the device which provides safety information for the transients is not needed for the slow drift situation, Eq. (1) can be modified by the addition of a term as follows:

$$F(t) = p - aW(T_o - T_i) - g(t) , \qquad (2)$$

where g(t) is defined by the equation:

$$g(t) = \frac{dg}{dt} + \lambda g = \lambda[p - aW(T_o - T_i)] \quad , \qquad (3)$$

where λ is the reciprocal of a time constant, which is larger than the time constant of any of the sensors for information in Eq. (1). The function F(t) has the property that it vanishes in steady states. In some respects it is similar to the derivative of f(t) in Eq. (1). It is indeed a high-frequency band pass for the information contained in f(t). For a single-ended positive step A in f(t), $F(t) = Ae^{-\lambda t}$.

The function F(t) can be generated from information provided by sensors in the form shown as f(t) by use of three transistorized operational amplifiers of the type used in analog computers. There is no new art involved, except insofar as these combinations of well-known devices constitute new art.

There is some maximum value of F(t), as can be determined by analysis (using analog computing devices), that is safe. All values higher than this maximum are unsafe and accordingly will trip the safety system.

The two trip levels, namely one provided by T_o and the other by F(t), are all the nuclear safety actuators the reactor needs in the range of operation where sensible heating of the fuel elements occurs. Further, safety trip information is needed for the low level or startup regime, and this will be explained later. The two trip levels described will be "armed" at all times, even though they do not provide safety at low levels, since they cannot interfere with the operation at low level nor do they, by definition, interfere with safe operation at any level.

A defense of the safety trip F(t) proposed here is in order. Defense of F(t) comes about by first establishing justification of f(t) as the source of safety information. The heat transfer system here is a linear system and can be described by a set of first-order differential equations with constant coefficients. Accordingly the system's response to a step in p or a step of opposite sign in W will be characteristic of the response of a linear system. If the step is large, the rate of change of a temperature in the system can also be large, and it has been assumed that it is unsafe to have too large a rate of change in temperature. While it is not possible to have a step in any of the variables of f(t), it is entirely credible that fast changes can occur in p, W, and perhaps T_i. In some reactors a fast change can occur in T_o, as, for example, when a rupture in the system mixes cold coolant with hot coolant at the reactor outlet. There is no way to avoid using the expression defining the heat balance to provide information for safety trips in transients, since there is no transient if $f(t) = 0$, and there is always a transient when $f(t) \neq 0$. One could trip on p, on W, on T_o, or on T_i and continuously adjust the levels for all these variables to suit the operating

range of the reactor. This is little more than using f(t) to trip the safety system, but it is using it the hard way.

The justification of the use of F(t) to trip in unsafe transients instead of f(t) is the following: Drift in the sensors measuring p, W, T_o, and T_i could easily make $f(t) \neq 0$ for the steady state. Sufficient drift would give a spurious trip, or, what is worse, if the drift were away from the trip level, fail to give safety when needed. If f(t) is to be used, continuous steady-state calibration or resetting would be required to avoid these two conditions. Since F(t) = 0 for all steady states regardless of the slow drift of the sensors, then the two situations described above cannot come about when the trip is actuated by a high value of F(t).

The transistorized computer amplifiers are extremely reliable and add little to the unreliability of F(t) as compared to f(t). It is proposed to use three such elements in the safety system, independent of each other, to take advantage of the benefits of coincidence and redundancy in providing safety.

In the startup range, i.e., in bringing the reactor up from source level to approximately 10% of design point or to 1 Mw, in this instance, additional safety information is needed for several reasons. At power levels below those where sensible heating of the fuel occurs, the rods may be withdrawn in such a way that the reactor power might change with a very short period without causing any damage. Once the fuel temperature starts rising, because of the Doppler temperature coefficient of reactivity, the excess reactivity begins to decrease until the reactor is driven subcritical again. A damped oscillatory condition persists for some time after rod withdrawal is stopped. The power can reach a relatively high peak, at which time the rate of change of fuel temperature is a maximum. This value can very well exceed the maximum permissible rate of change of the fuel temperature.

It is advisable to bring the reactor up to a level of 1 Mw with a flux trip set at 1.5 Mw to prevent this relatively high power overshoot, with the attendant high rate of increase in fuel temperature. The power

can be leveled off at 1 Mw before operation at higher powers is undertaken. In bringing the reactor up to 1 Mw, rod motion can be stopped or the rods can be reversed on period information. Such use of period information does not involve the safety system but is only a means of control and operation which prevents actuation of the safety system solely because of clumsy operation.

Nuclear Control System

Since the reactor is to be operated over most of its range with variable coolant flow and power with the flow matched to the power, two control systems will be supplied, one to control the coolant flow and one to control the power.

The closed loop flow controller operates with an error signal ϵ_f, given by the expression:

$$\epsilon_f = T_o - T_{o_1 s.p.} \quad , \tag{4}$$

where $T_{o_1 s.p.}$ is the outlet temperature set point which can be varied manually by the operator. For $\epsilon_f > 0$ in the case of a proportional controller or for $\epsilon_f > \left|\frac{\epsilon_1}{2}\right|$ for an on-off controller, the flow is increased. Here ϵ_1 is the dead band for the on-off controller. This controller can be shown to be stable by analog analysis with no more damping than that given by the derivative $d\epsilon_f/dt$.

The power controller operates with an error signal ϵ_p of the form

$$\epsilon_p = m\,F(t) + n(x - x_{s.p.}) \quad , \tag{5}$$

where $F(t)$ is defined in Eq. (2), x represents either p or T_i, depending upon whether one wishes to operate the reactor at constant power and match the load to it or operate the plant in such a way that the reactor power follows the load, $x_{s.p.}$ is the manually controlled set point for

p or T_i, as the case may be, and m and n are optimization constants for stabilizing the controller and making sure the deviation in x about $x_{s.p.}$ is acceptable. For $\epsilon_p > 0$ when a proportional controller is used, or for $\epsilon_p > \left|\frac{\epsilon_2}{2}\right|$ when an on-off controller is used, the rods are inserted. Here ϵ_2 is the dead band. The controller can be shown to be stable for the error signal (5) in either the case where x = p or where x = T_i.

If three parallel servos are used acting on the same rod or rods, then the output of each channel operates two switches in a switching matrix to withdraw rods and two different switches in a different switching matrix to insert rods. This requires use of the on-off type of controller. The switching matrix provides coincidence and redundancy such that rod action occurs only when two channels agree that such action is required.

The quantity F(t) in the error signal ϵ_p can be the same as that of the safety system only if three completely independently derived values of F(t) are used in a "two-out-of-three" safety system that is logically sound in design and is used along with the three parallel closed loop controllers.

Further Analysis

Maximum rod speeds can be determined by means of the startup accident analysis for a 1-Mw reactor. Analog computer analyses of the controllers and safety system information given here have been made for the EGCR, which is dynamically similar to the PBRE. These analyses support the validity of the conclusions related to such items and given in this report.

Failures in other parts of the plant will probably require that the reactor be shut down. If so, information describing the failures could initiate safety action.

Reliable means should be provided for removal of afterheat on loss of coolant. It is preferable that the mechanism for removing afterheat be operable at all times rather than available only on a standby basis.

12. STEAM GENERATOR

General Considerations in the Selection of a Heat-Removal System

The selection of a heat-removal system capable of dissipating up to 10 Mw of heat from a high-pressure high-temperature helium-cooled reactor depends on the objectives of the reactor experiment. Aside from considerations of power generation it was thought prudent to avoid the selection of a heat-removal system for the PBRE that would involve design problems not shared by a full-scale pebble-bed-reactor plant. Thus the use of fluids other than water for primary-system cooling was examined only briefly.

One concept of reasonable simplicity and requiring no cooling water would employ direct cooling of the helium gas by ambient air. The air could be drawn into the containment shell through filters, pass over a helium-to-air heat exchanger, and be discharged up the stack. Because of the direct access of contaminated helium to ambient air and the consequences in the event of a heat exchanger leak, multiple valves would be required on both the inlet- and exit-air ducts. Valve operation would have to be sufficiently rapid so that in the event of a gross heat exchanger rupture the activity released to the stack would be within permissible limits. Valve requirements would be determined by the magnitude of the permissible activity release to the atmosphere. Valves located in the stack could closely control the release rate. The volume in the air system would be sized to prevent pressure buildup even in the event of a gross heat exchanger failure.

Aside from the hazards problems associated with the above system, the design of a gas-to-gas heat exchanger presents no trivial problem. The unit would be required to operate at a high pressure differential, and the design would have to provide for access for repair of heat exchanger leaks. Thus the use of a conventional "sandwich" type of gas heat exchanger does not appear to be satisfactory. In addition, the relatively poor heat-transfer characteristics of low-pressure air and the large thermal gradients complicate the heat exchanger design.

Some of the objections to a direct air-cooled heat-removal system could be overcome through the use of a secondary pressurized-gas cooling system. This scheme would also require a heat exchanger which permitted detection and repair of leaks. A second pressurized-gas system would require additional blowers, expensive container piping, and significant space in the containment shell.

The use of water for cooling the primary gas permits a more compact heat exchanger than does the gas-to-gas system. There is a good background of technology in the design of pressurized gas-to-water heat exchangers for nuclear power plants, and a water-steam system would duplicate, at least in part, some of the problems which are likely to occur in the design, maintenance, and operation of a large pebble-bed-reactor plant. Information on problems such as the detection of steam leaks into the helium system, the repair of tube leaks in the contaminated steam generator, and the transient response of the system to operating perturbations are all important to the success of the large-scale reactor plant. Thus, the decision to employ a steam generator and steam system stemmed from the advantages of water as a coolant and the better simulation that it would give of the large-scale plant.

The decision on whether to utilize generated steam for generation of electrical power is discussed in Chapter 18 of this report.

Design Requirements

The design of a steam generator for a system operating with a contaminated-gas coolant must satisfy a number of prime requirements:

1. The steam generator unit must be capable of producing high-temperature, high-pressure steam.
2. Reliability of the steam generator is of paramount importance.
3. The unit must be repairable in the event of tube leaks.
4. The steam generator should be replaceable.
5. The unit design should enhance removal of afterheat by natural convection.
6. The design should be such as to minimize plant gas piping and shielding requirements.
7. The design should be readily fabricable.

The decision to employ an integral pressure envelope (see chap. 4) incorporating the heat exchanger vessel on top of the pressure vessel helped satisfy requirements 5 and 6 but imposed rather strict boundary conditions within which to achieve a design satisfying all the other requirements.

The necessity for access at the top of the reactor pressure vessel coupled with the problems associated with support of the exchanger from the pressure vessel produces a strong incentive to minimize the heat exchanger vessel diameter. In addition, the desirability of achieving afterheat removal by natural convection, the considerations of lateral shaking forces with respect to the unit height, and the limitations imposed by manufacturing capabilities and maintenance requirements combine to determine acceptable design lengths for the steam generator.

A layout of the heat exchanger and the pressure vessel indicated that a heat exchanger diameter of approximately 2 ft would allow adequate access space at the top of the reactor vessel for control rods, fuel loading, and reactor access. Accordingly, 2 ft was selected tentatively as the inside diameter for the heat exchanger shell.

Steam Conditions and Steam Generator Type

The full-scale pebble-bed reactor should be capable of producing high-temperature high-pressure steam, and a demonstration of this ability in the test reactor is a worthwhile objective if the incremental cost is not large. In the full-scale reactor plant, steam pressures will undoubtedly exceed gas pressures, and tube leaks from the heat exchanger will occur as steam leaking into the gas system. Fortunately, this is much the preferred condition from the hazards standpoint. Further, it is desired to obtain information on the detection of such leaks and the effects of such leaks on the graphite in the core and reflector. Since rough estimates indicated that there would not be a major cost incentive to reduce the steam pressure below 1000 psi, only operating steam pressures above that of the gas were considered.

The requirement for producing high-temperature steam is not so clear. In the final analysis the steam temperature and pressure for the large reactor plant will be determined by a cost optimization procedure which balances plant costs against plant performance. Operating steam temperatures, however, will certainly be in the range of 1000 to 1100°F. The duplication of this temperature range in the test reactor will bring out problems in the steam generator design associated with the thermal expansion of the unit which will be applicable to the large unit. In addition, fission-product deposition is known to be temperature and material sensitive, and thus the distribution of deposition within the steam generator will also be partially simulated. Information related to unit reliability will also be more significant if the unit is operated at high temperatures and pressure. Further, system characteristics such as the thermal capacity of the steam generator and the speed of response of steam temperature and pressure to load changes will be functions of the steam conditions selected. As discussed later in this section, the additional cost of designing the steam generator to operate at high steam temperatures is not great and thus seems to be well justified by the above considerations. Therefore a steam pressure of 1000 psia and a steam temperature of 1000°F were selected for the test reactor.

Two basic types of steam generator were examined for this application: (1) a once-through unit in which the total feedwater flow to the economizer section would enter a set of tubes from which it would leave as superheated steam, and (2) a natural recirculation boiler employing an intermediate steam drum between the boiler and the superheater section. A natural recirculation boiler was selected for this application over the once-through design principally because of the increased latitude the natural circulation unit permits in selecting flow rates on the steam side to give good flow stability in the economizer and boiler region, both at design and off-design conditions. The recirculation boiler suffers from the requirement of an additional intermediate steam drum, with additional tube penetrations of the shell, but it gives better

design control over the steam generator height and a somewhat simplified gas flow path through the heat exchanger unit.

Steam Generator Geometry

A pictorial concept of a natural-recirculation steam generator is presented in Fig. 12.1. Hot gas from the reactor core is directed up a central 6-in. stainless steel pipe to the top of the steam generator unit. Guide vanes at the top of the generator unit then direct the gas flow down across the tube matrix surrounding the upflow pipe. The gas passes across the superheater, boiler, and economizer sections to the top of the pressure vessel leading to the compressor section. Gas for cooling the steam-generator vessel is directed up the cooling annulus and joins the main gas stream at the top of the heat exchanger vessel. Between the vessel-cooling annulus and the tube-matrix section is a barrier of reflective insulation. The design allows the vessel wall temperature to increase from about 600°F at the bottom to approximately 650°F at the top.

The use of high-pressure helium permits high mass velocities and strongly affects the selection of tube surface geometry. At high gas velocities the helium heat transfer coefficients are sufficiently high and fin efficiencies are sufficiently low that there is little incentive for using extended surfaces. An additional consideration is that the heat exchanger height was in part determined by a desire to achieve natural convection on shutdown and thus there is little advantage to reducing the steam generator height to less than that required for this purpose. For these reasons bare tubing was used in all sections of the heat exchanger. No detailed cost comparison with an extended surface design was carried out, but rough estimates indicate that bare tubes give the least expensive unit.

The small heat exchanger diameter and the height considerations discussed above led to the selection of an axial counterflow design for the tube matrix, giving the arrangement shown in Fig. 12.2. The tubes

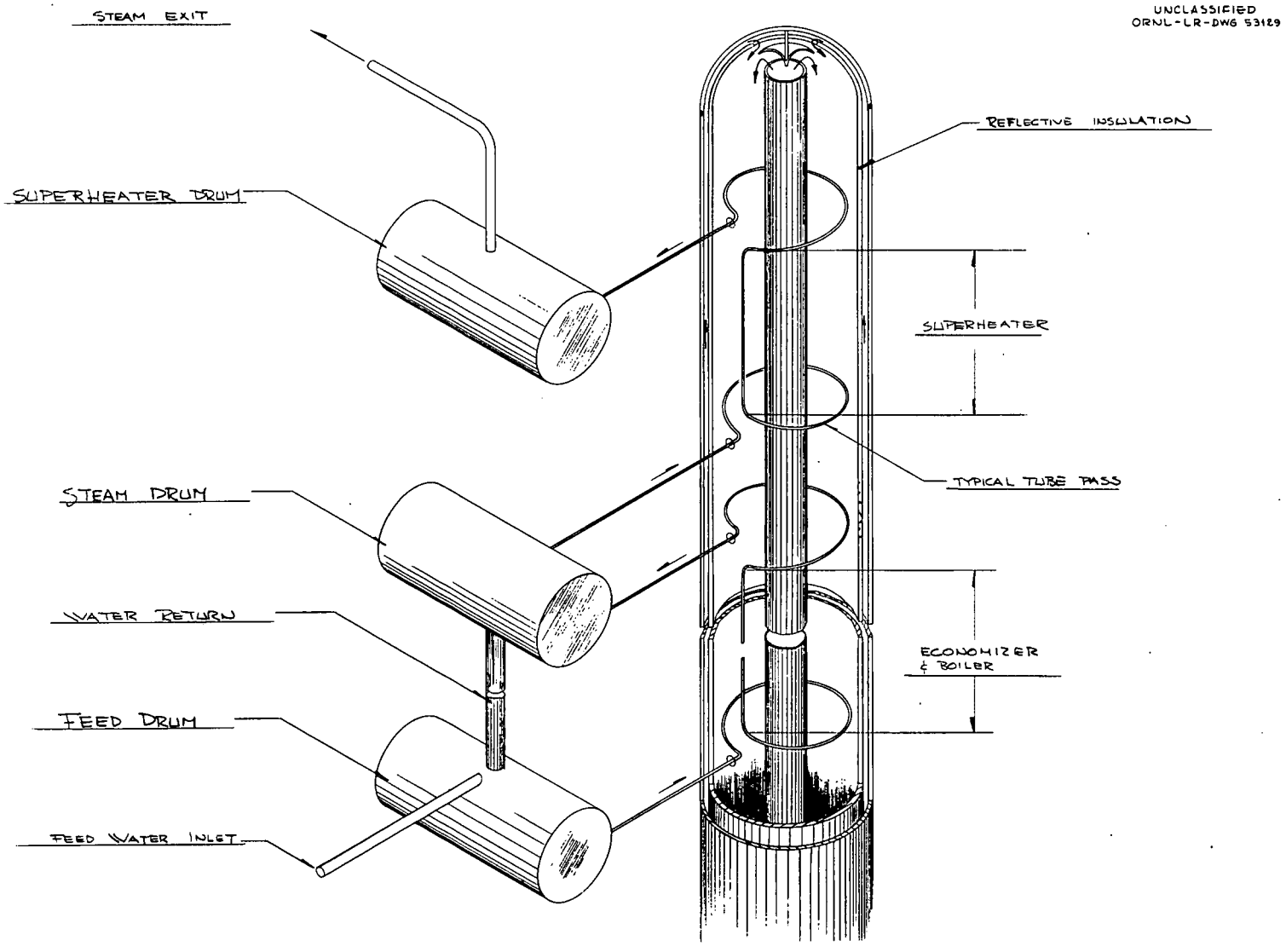

Fig. 12.1. Natural-Circulation Steam Generator.

UNCLASSIFIED
ORNL-LR-DWG 53140

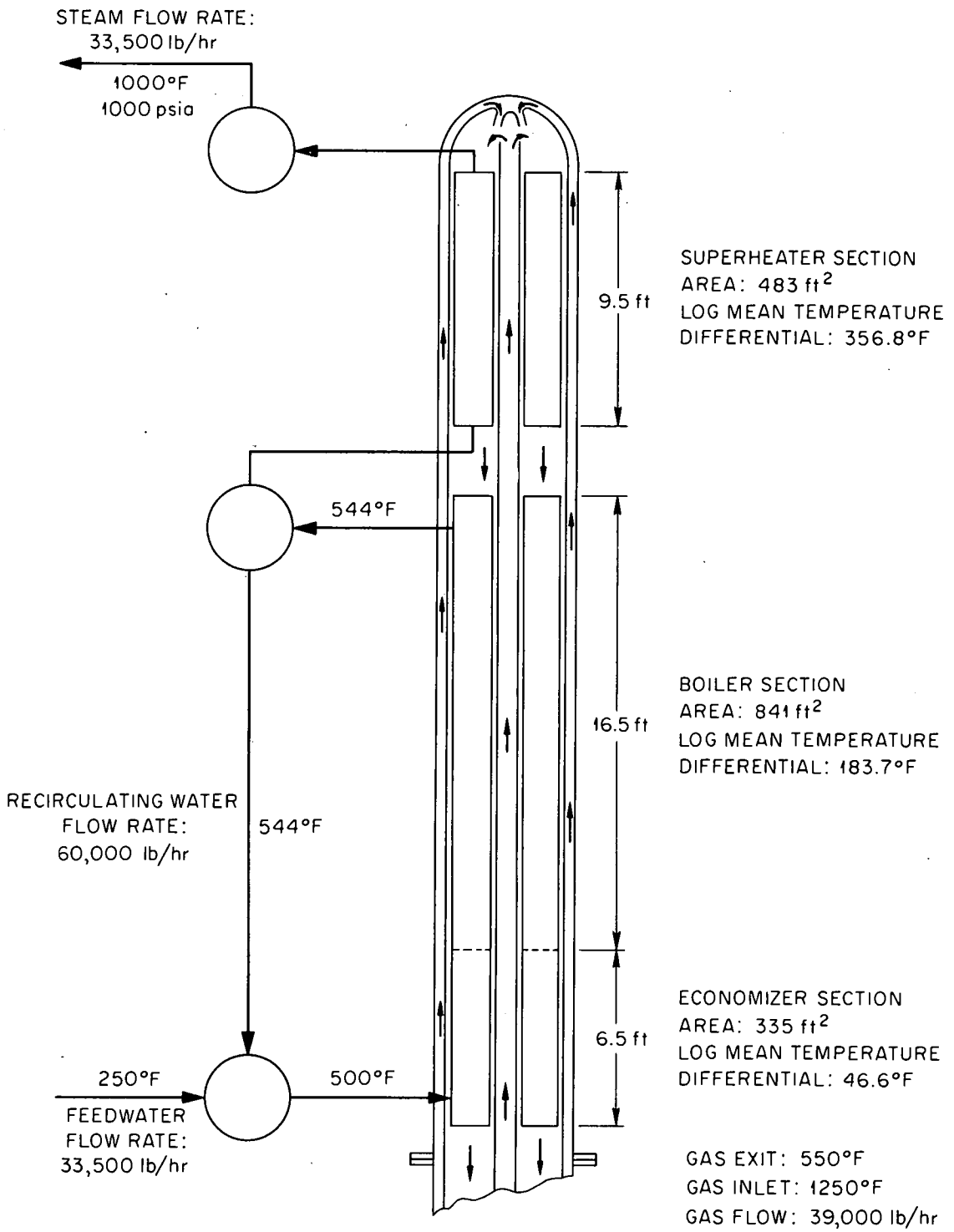

Fig. 12.2. Schematic Diagram of Steam Generator.

are arranged on an equilateral pitch in the annulus between the upflow stack and the reflective thermal barrier. A number of tube diameters and tube-spacing arrangements were examined, and data for an arrangement capable of satisfying the heat transfer, water flow stability, and gas pressure drop requirements are given in Table 12.1. Figure 12.3 presents the steam generator gas flow rate and gas temperatures, together with the steam flow rate (neglecting blowdown) and steam system temperatures and pressures.

The acceptable gas pressure drop through the heat exchanger would normally be determined by balancing the pumping power cost against the steam generator capital charges. In the present case the ability to remove heat by natural convection offered an incentive to reduce the total system pressure drop, and the maximum allowable gas pressure drop through the steam generator was estimated to be approximately 30% of the estimated total system drop. The gas pressure drop for the proposed unit is 3 psi, which is comfortably below the maximum allowable for good thermal convection.

Although calculations based on area considerations indicate that approximately 195 tubes can satisfactorily be accommodated with the 2-ft shell, a detailed layout may require an adjustment of a few inches in the shell diameter.

The requirement of steam generator repairability can be satisfied most expeditiously by plug-welding of leaking tubes. This procedure necessitates that individual tubes or bundles of tubes terminate in a header which is accessible for determination of the leaking tube and plug welding of the tube entrance. To accomplish this, all header drums have been fitted with flanged openings and have been placed outside the primary steam generator shielding but within shielded cubicles, as partially shown in Fig. 21.1 of Chapter 21. (Note that the layouts of Figs. 6.3 and 6.4, chap. 6, were prepared for a preliminary design for a once-through unit with a different header drum arrangement.)

Detail Design Considerations

Two principal problems which must be considered in the steam generator design are provisions for thermal expansion and methods of

Table 12.1. Steam Generator Design Data

	Economizer	Boiler	Superheater	Total
Flow scheme	Axial counterflow gas outside tubes			
Tube outside diameter, in.	1.0	1.0	1.0	
Tube inside diameter, in.	0.875	0.875	0.875	
Number of tubes				195
Tube arrangement and spacing	Equilateral spacing on 1.375-in. centers			
Shell side area, ft^2	335	841	483	1660
Straight height of section, ft	6.5	16.5	9.5	
Over-all estimated exchanger height, ft				45
Gas mass velocity, $lb/ft^2 \cdot sec$				9.44
Gas pressure drop, psi				3
Gas pressure (design), psia				1000
Gas flow, lb/hr				39 000
Water inlet temperature, °F	500			
Steam exit temperature, °F			1000	
Net steam flow, lb/hr				33 500
Steam exit pressure, psia				1000
Log mean temperature differential, °F	46.6	183.7	356.8	
Heat load, Btu/hr	1.84×10^6	21.77×10^6	10.49×10^6	34.1×10^6
Percentage of total heat load	5.4	63.8	30.8	
Gas-side heat transfer coefficient, $Btu/hr \cdot ft^2 \cdot °F$				150

Table 12.1 (Continued)

	Economizer	Boiler	Superheater	Total
Tube-side heat transfer coefficient, Btu/hr·ft^2·°F	700	5000 (assumed)	160 (average)	
Heat flux, Btu/hr·ft^2 (outside area)	5500	25 900	21 700	
Over-all heat transfer coefficient, Btu/hr·ft^2·°F	118	141	71	

tube support. The present concept envisions expansion loops on the tubes, as shown in Fig. 12.1, to accommodate differential thermal expansion between the tubes and the pressure shell. Sufficient provision for expansion at tube bends must be made to permit larger relative tube movements when a tube has been plugged off and consequently is at a temperature well above the temperature of adjacent tubes. It is estimated that approximately 2.5 ft of shell height will be required for tube bending and expansion at the end of each section. Thus, the over-all height of the steam generator unit is estimated at approximately 45 ft above the welded joint at the top of the transition piece extending downward to the reactor pressure vessel. The central upflow pipe can be hung from the top dome, and a sleeve with a slip fit can be used at the lower end to permit thermal expansion of this pipe. Superheater tubes will be supported from the top end of the heat exchanger vessel, and the boiler-economizer section can be supported from an intermediate perforated plate or grid welded to the exchanger shell between the boiler and superheater sections.

Tube spacers must be designed so that gas flow will be directed through the tube bundle in such a manner as to promote a small degree of gas swirl and prevent channeling and temperature stratification in the gas flow. This will be particularly important if there are any plugged tubes. The perimeter of the upflow pipe and the reflective insulation baffle must be fluted to avoid excessive gas bypass.

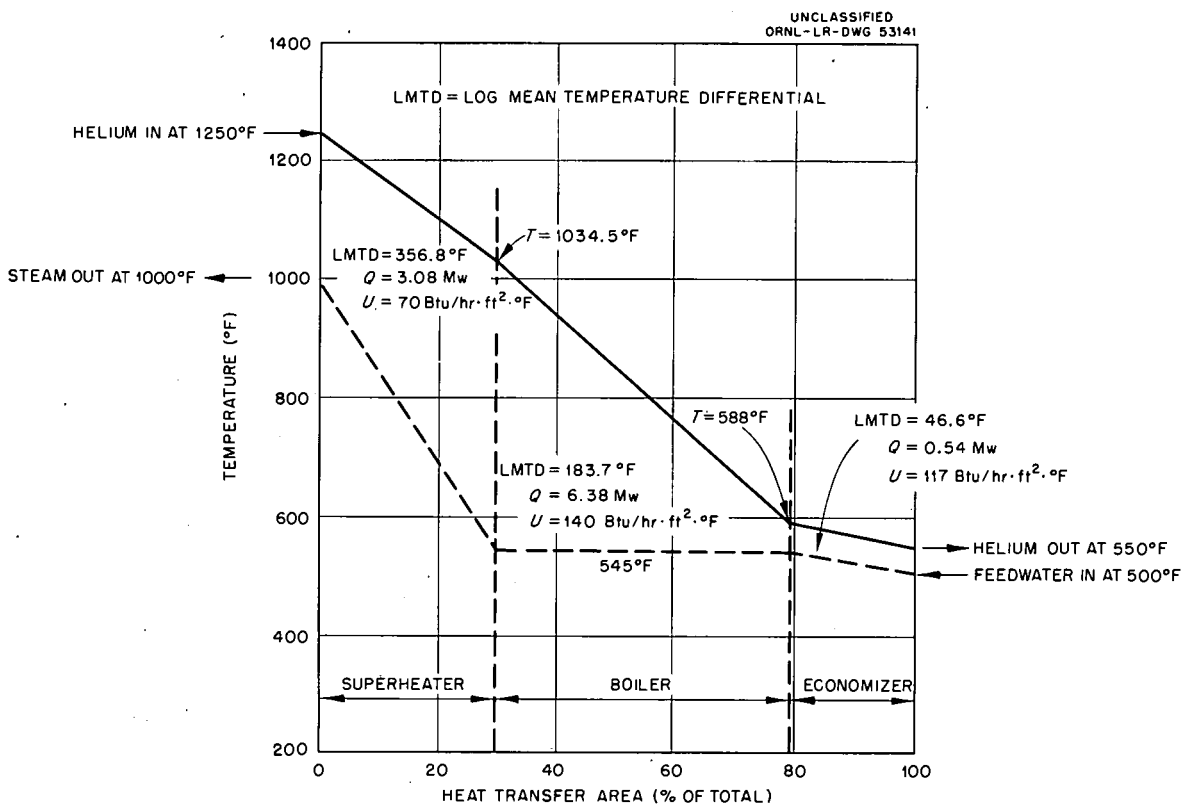

Fig. 12.3. Helium and Steam Characteristics of PBRE Steam Generator.

One important additional design requirement for the steam generator entails the removal of afterheat from the reactor core during reactor shutdown. In the event of a heat exchanger tube leak to the gas system, it is desirable to valve off the water supply to the steam generator to prevent excessive steam leakage to the primary system. To permit this procedure with the present design, the heat exchanger will be divided into two independent sections. Two sets of feed rums, steam drums, and superheater drums will be employed. The tubes from each section will be arranged within the heat exchanger to insure adequate cooling of the gas on shutdown if one heat exchanger is inoperative.

Leak Detection and Maintenance Procedures

A non-trivial problem associated with the above arrangement is the determination of which heat exchanger section is leaking. If the sections are homogeneously arranged within the shell, determination of the leaking system presents real difficulty. A possible solution would be to introduce in one steam system special tracer elements having a characteristic activity not duplicated or masked by the activity expected to be present in the gas coolant. Another possibility would involve a degree of heterogeneity in the arrangement of the sections within the shell to permit the detection of leaks and to permit identification of the leaking section. This arrangement must avoid nonuniform cooling in the event one section is shut down, perhaps by providing periodic mixing points for overcoming nonuniform shutdown cooling.

Still another possible solution to the leak identification problem would utilize a small (perhaps 5% capacity) auxiliary cooling unit capable of handling shutdown requirements and thus affording protection in the event of a main heat exchanger leak. Such an auxiliary unit would be located within the heat exchanger vessel and would permit safe shutdown in the event of a steam leak in the main unit.

As previously discussed, tube leaks would be repaired by plug welding the end of the leaking tube. Since the header drums are isolated

from the steam generator by shielding, detection and repair can be carried out directly in the fashion proposed for the GCR-2 reactor.[1]

The need for replacement of a steam generator might possibly arise. Although it is anticipated that such an occurrence is very unlikely, provisions have been made to handle this requirement, since the alternative might be the complete shutdown of the reactor experiment.

In order to replace the steam generator it will first be necessary to decontaminate it. Two methods for carrying out the decontamination procedure are apparent. If a suitable liquid seal can be accomplished between the heat exchanger and the reactor to permit liquid filling of both the tube matrix and the upflow pipe, decontamination can be carried out as discussed in Chapter 17. Fill nozzles and liquid drain lines would be provided in the heat exchanger. A monitored sampling line would be utilized to determine the activity level in the effluent. One method of providing the required liquid seal would utilize inflatable bladders inserted through the top of the reactor pressure vessel into the pipes or areas to be sealed. The bladders would be inflated after positioning. If this scheme is chosen, it should be checked out before the reactor is started up. If it does not work, the steam generator could be provided with spray nozzles at the top of the vessel and at intermediate points above the boiler economizer section. Decontaminant running down the outside tube surfaces could be directed to a drain sump located at the base of the heat exchanger-pressure vessel transition piece. Temperature requirements for decontamination could be met by providing heat from the steam system through use of a small auxiliary heater located in the steam line leading to the generator unit. The process of decontaminating the steam generator components would require extensive effort, but the required frequency and the alternative to this process make the effort attractive.

---

[1]Oak Ridge National Laboratory, "The ORNL Gas-Cooled Reactor," Part 3, ORNL-2500.

Costs

The cost of the steam generator described above is estimated to be $100 000 for a unit employing six header drums. This cost is equivalent to $100 per kw of capacity, which is comparable to the $83/kw cost of the EGCR steam generators. Of this, about $40 000 is associated with the superheater tubing and superheater drums. Therefore, if the superheater section could be replaced with equivalent area in the boiler section (thus producing saturated steam only) and if the area requirements were adjusted for differences in heat transfer coefficients and log mean temperature difference, it appears that a net saving of $ 30 000 to $35 000 might accrue from elimination of the superheater section from the present design. This reduction may be more apparent than real, however, since temperature differences at the top of the boiler inherent in such a design could give serious trouble by driving this region into the film-boiling region and thus severely threatening the reliability of the unit.

13. BLOWERS

The coolant flow for the PBRE is to be supplied from two independently driven single-stage centrifugal blowers. In addition to meeting the operating conditions summarized below, the blower housings are to provide two of the three support points for the reactor pressure vessel:

Flow rate per blower	
Maximum	6 lb/sec (975 cfm)
Minimum	1 1/2 lb/sec
Design pressure	1000 psia
Suction temperature	550°F
Head required	30 psi, 11 700 ft
Compression ratio	1.03

A further requirement is that the variation in flow rate should be obtained by varying the speed of rotation of the blower. This method has the advantage of simplifying the process system in that valves and/or bypass lines are not required. It also has the advantage over an adjustable diffuser-vane compressor in that leakage points in the casing are eliminated and maintenance requirements should be reduced. These requirements imply a blower of relatively low flow rate and high discharge head and can only be met in a single-stage machine by going to high rotative speeds.

The impeller design required for these operating conditions will probably be of the following dimensions:

Impeller outside diameter	16 in.
Impeller outlet width	1/4 in.
Specific speed at 14 400 rpm	400
Estimated impeller efficiency	85%

The over-all efficiency of the blower is expected to approach 70%, probably about 67%, and thus will require about a 200-hp blower drive.

In order to achieve the operating speed of 14 400 rpm and still vary the flow rate over a range of at least a factor of 4 by changing the rpm (down to 3600), the drive system should be similar to one of the following two types:

1. a 3600-rpm motor fed from a conventional 60-cycle source driving through an adjustable fluid clutch and gear speed increaser of 4-to-1 ratio,
2. a two-pole a-c motor driven from a variable-frequency source, such as an M-G set, with its motor coupled to the generator through a fluid clutch.

A maximum generated frequency of 240 cycles/sec would be required.

It is expected that system 1 would be less expensive but would require much more maintenance than system 2, and this extra maintenance would be required in an area where the radiation dose level would be high. Further studies should be made before a final decision is reached, but for purposes of this report system 2 was chosen.

The primary problem foreseen with this design is the achievement of a long-life, low-leakage shaft seal for the 1000-psi system pressure, with a shaft speed of over 14 000 rpm. It is believed that a modification of the type of seal being developed for the EGCR with oil lubrication instead of water would be satisfactory, although some development effort would be required. To minimize contamination of the seal oil, clean helium from the bypass cleanup system should be returned to the main gas stream through an annulus at the oil seal on the blower shaft. A labyrinth seal should be provided between this annulus and the impeller to minimize back diffusion along the shaft from the contaminated main stream.

The impeller, shaft, bearing, and seal assembly would be mounted in a flanged plug to facilitate removal and replacement of the moving parts. As in the ART fuel pumps, the assembly would incorporate a heat dam so that the oil flowing through the seal and bearings would keep the outer end of the assembly cool. An O-ring seal would be provided in the mounting flange for this assembly.

14. FUEL-HANDLING SYSTEM

The simplicity of the fuel-handling system has been one of the most widely claimed and generally accepted advantages of the pebble-bed reactor concept. This being the case, the first step taken toward developing a mechanical arrangement for the fuel-handling system was to study and evaluate the existing concepts and the design information which demonstrate and give substance to this advantage. Sanderson & Porter have stated that the scope of their pebble-bed work to date has excluded design or development effort on the mechanical components of the fuel-handling system, such as valves, ball flow cutoff, ball counting, and other devices. Thus it is important to recognize that this advantage of fuel-handling simplicity is founded wholly upon the general truth that beds of uniformly sized spheres will flow under certain conditions and, as a consequence of this flow, will or should be transferable to and from a reactor without the use of a mechanism designed to enter the core, seek a specific location, and remove or install each individual "fuel assembly." From the fuel-handling point of view, it can only be concluded at this date that this advantage is real, and on the basis of this conclusion the design effort has been directed toward its development. It must be recognized at this point that implicit in the conclusion that the fuel handling advantage is real is the assumption that fuel spheres will be developed that will remain intact, will maintain adequate strength, and will resist fusing into multiple-ball clusters.

Design Precepts

One of the first decisions to be made in designing the refueling system for a gas-cooled power reactor is whether to design for refueling at power, during a shutdown at full operating pressure and temperature, or with the reactor shut down and depressurized but at elevated temperature. This decision involves considerations such as the frequency and duration of the refueling operations. Since it would be advantageous to avoid depressurizing the system or even reducing the power unless

these moves make an important difference in the costs or hazards associated with the fuel-handling operations, attention was directed primarily at a system for refueling at power.

Four fundamental design precepts were adopted at the outset. These are as follows:

1. to make the most of the possibilities of a pebble-bed reactor, the fuel flow should be downward through the core,
2. while dumping balls into or out of the core in batches might be advantageous, for good control of the reactor each ball admitted to or removed from the core should be counted,
3. the system design should have the greatest possible reliability,
4. the system must be maintainable, and at least two different means must be available to cope with jammed fuel balls anywhere in the system.

Sanderson & Porter have developed some design precepts in the course of their investigations of the general characteristics of ball flow from a reservoir into and through a drain tube, means for starting and stopping such flow, and the relative axial velocities of balls through cylindrical cores as a function of the radial position. The first of these precepts is that uniformly sized spheres flowing from a large-diameter reservoir into an essentially vertical, round, drain duct will occasionally bridge and cease to flow if the diameter of the drain duct is less than five ball diameters. In actual practice, the drain-duct diameter should be made slightly larger than exactly five ball diameters. Balls flowing "single file" through a round duct will flow without jamming or locking for duct diameters up to 1.7 ball diameters but may jam in ducts between 1.7 and 5 ball diameters. Finally, there is no known way to converge from a five ball diameter duct to "single file" flow of balls without bridging and jamming of ball flow unless a mechanical agitating device is used.

Fuel-Discharge System

The Sanderson & Porter work on arrangements for starting and stopping ball flow has been concerned primarily with the ball-removal port at the exit from the reactor core. The first design concept for the unloading valve was a bulk unloader. The valve consisted of a refractory tube driven on its vertical axis by a rack and pinion. In the upper position the tube was above the bottom grate, and fuel elements were prevented from entering by a graphite or refractory conoid head over the unloading tube. Apertures

around the bottom of this hood allowed fuel elements to rise to just below the level of the unloading valve in its top position. As the unloading valve was lowered, fuel elements rolled over its upper rim and dropped through the valve into a holdup vessel or discharge line.

A model of this valve has been built and operated and the design principles have been demonstrated. The valve operates under pressure, since it is contained within the reactor vessel. A daily charge of fuel elements can be held up by discharge into a holdup vessel and/or holding them in the unloading valve. The valve was designed for bulk unloading, but single-file flow through a tube leading to a reprocessing or storage cell may be possible. It is of simple design, but there is a sliding part in the core. It can handle sound and broken elements and elements of mixed sizes.

The second design concept of an unloading valve was a star plate feeder at the bottom of a tubular extension of the core. It was designed to get moving parts out of the core and to deliver the elements one at a time, i.e., in single file, to a tube leading to a reprocessing room. This valve is a simple, single-plate star feeder incorporating a shutoff plate above the star wheel, making it possible, in a full-scale device, to shut off the flow of balls from the bed and remove the valve for replacement.

A model of this valve has been built and operated at Sanderson & Porter. It has the following characteristics: (1) The valve operates under pressure, since it is self-contained within the reactor system and is pressure-balanced. (2) A daily charge of fuel elements can be held up in the discharge tube leading from the core to the valve, the valve being external to the reactor. (3) Flow from the valve is in single file. (4) The valve is of relatively simple mechanical design. There are no moving parts in the core and it can be removed from the reactor. (5) As presently designed, it will handle a single-size sound ball.

The feasibility of a third type of valve is being investigated to overcome the deficiency of the star unloader with respect to its inability to handle broken and/or mixed-size fuel elements. This is a vibratory feeder, similar to a Syntron Vertical Vibratory Parts Feeder, which can be arranged as shown in Fig. 14.1. The feeder consists of a bowl supported by heavy springs placed at an angle with respect to the vertical axis. An external

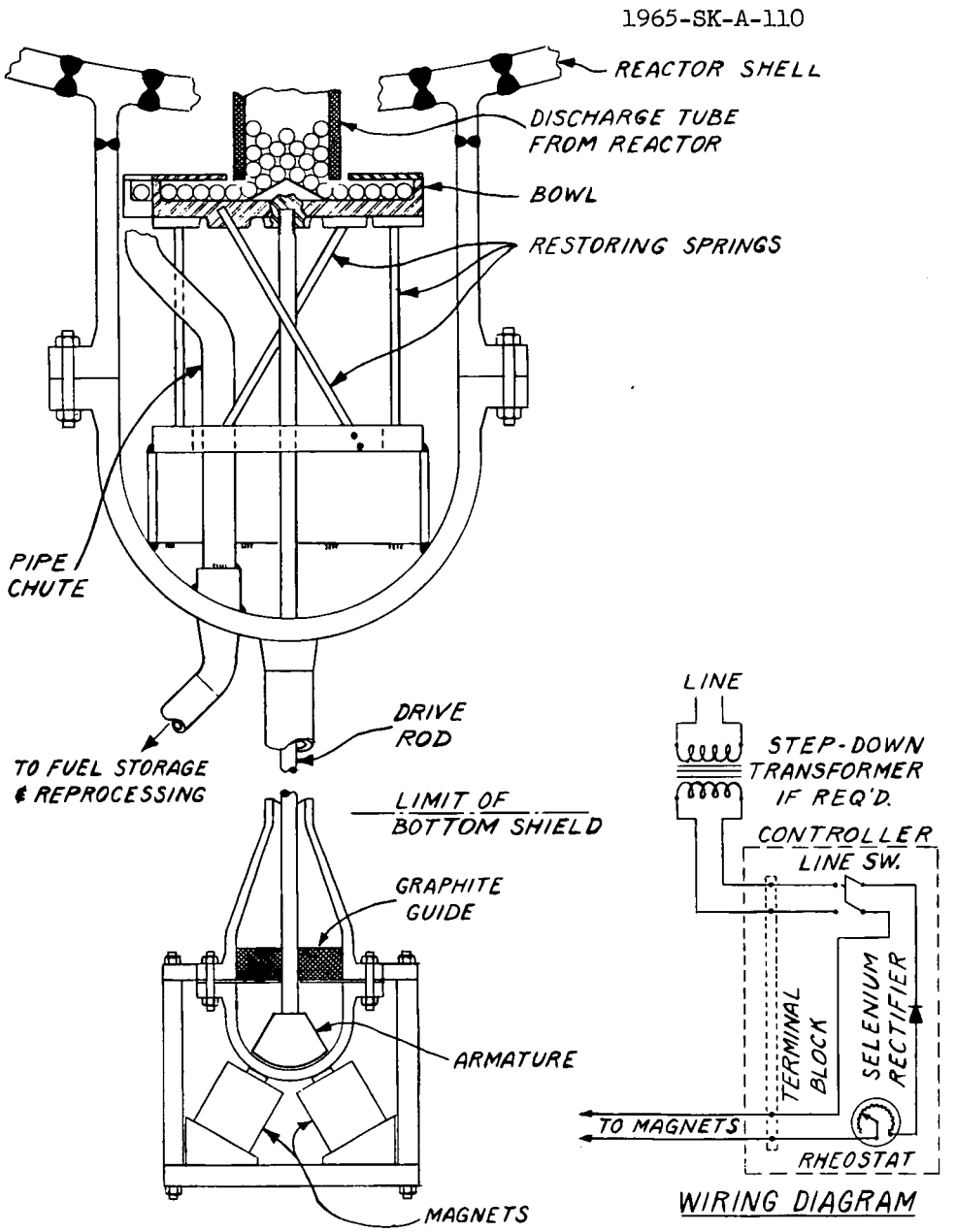

Fig. 14.1. Vibratory Unloading Valve.

force is impressed on the bowl by a rod driven through a diaphragm by means of an electrical magnet external to the pressure vessel, which causes the bowl to oscillate a few thousandths of an inch. The supporting springs are distorted by this action. Being set at an angle, as described, they resist the action and, on return to their original position, create rotating movement of the bowl. This movement causes balls in the bowl to move spirally outward and be discharged at a suitable spot on the bowl rim. The rate of feed can be adjusted by varying the voltage to the driver. Balls are fed into the bowl directly from the core through a centrally located discharge tube which terminates about one and one half ball diameters above the bowl.

A commerical 5-in.-bowl parts feeder (Syntron Model EB-00) has been purchased and used successfully at Sanderson & Porter with a flow model handling 3/16-in. balls. Alternate bowls are being designed and constructed to determine the most feasible design for this application. A bowl having an inside diameter equal to 15 ball diameters is desired. Based on studies and experiments to date, the system has the following characteristics: (1) The valve operates under pressure, since it is self-contained within the system and is pressure-balanced. (2) Flow from the valve is in single file. There are no moving parts in the core and the actuating mechanism is external to the reactor. (3) The valve will handle sound, broken, or mixed fuel elements so long as they will pass under the feedpipe above the bowl.

The design study shown in Fig. 14.1 uses a bottom drive to avoid problems associated with thermal expansion of the reactor pressure vessel, which would cause misalignment problems with a horizontal drive. The bowl, support springs, and drive rod are sealed within the reactor gas system. The drive rod, which can be any reasonable length, is enclosed in a tube, the lower end of which is fitted with a stainless steel, nonmagnetic cap surrounding a soft-iron plunger centered by a graphite bushing. Heat loss through the tube would be sufficient to reduce the temperature at the driving end to ambient. The magnetic driver is completely external to the reactor and can be made replaceable.

The most serious disadvantages of these arrangements are the large inventory of spent fuel held up in the drain duct, the problems of cooling and shielding this column of fuel, the indeterminate number of balls in the tray, the rather large-volume enclosures required (which would be at full system pressure), and the large amount of shielding required for the large ball hold-up in the ducts and trays.

Whatever the particular operational requirements of the system may be, reliability and maintainability are the sine qua non of nuclear fuel-handling systems. In order to evaluate these characteristics for a typical system and to establish space requirements in the facility for maintenance operations, a new fuel-handling system has been conceived which shows promise of offering advantages over the Sanderson & Porter systems, while fitting within the space envelope that the latter would require. This fuel handling system is shown in Fig. 14.2 and is described below. While it is a concept rather than a detailed design, it does represent the end product of a selective process which, for the specific design and operational objectives established, places maximum emphasis on both reliability and maintainability. Additional design objectives included elimination of the hood over the fuel-exit port, minimization of the inventory of fuel balls retained in the fuel-removal duct, provision for one-at-a-time ball entry to the removal duct, mild agitation of the fuel bed in the vicinity of the exit port during fuel removal, simplicity of mechanical design, provision for use of a ball-flow-channel clearing ram or auger, and provision for removal of the entire fuel withdrawal mechanism and reactor fuel charge in the event of unforeseen difficulties.

As mentioned above, every ball-removal system proposed to date appears to require some mechanical motion at the point of ball exit from the system. The arrangement developed in this study and presented in Fig. 14.2 provides for a round ball drain duct from the bottom center of the core structure. This duct has a diameter slightly greater than five ball diameters and is fitted with a round, graphite, fuel-removal plug equal in height to the bottom core support and reflector structure. The top end of this fuel-removal plug is to be truncated at an angle which can only be determined experimentally but which may be visualized as roughly 65 deg from the axis of the plug. When properly positioned in the duct, the lowest point on the inclined top surface of the fuel-removal plug is to be at the same elevation as the adjacent intersection

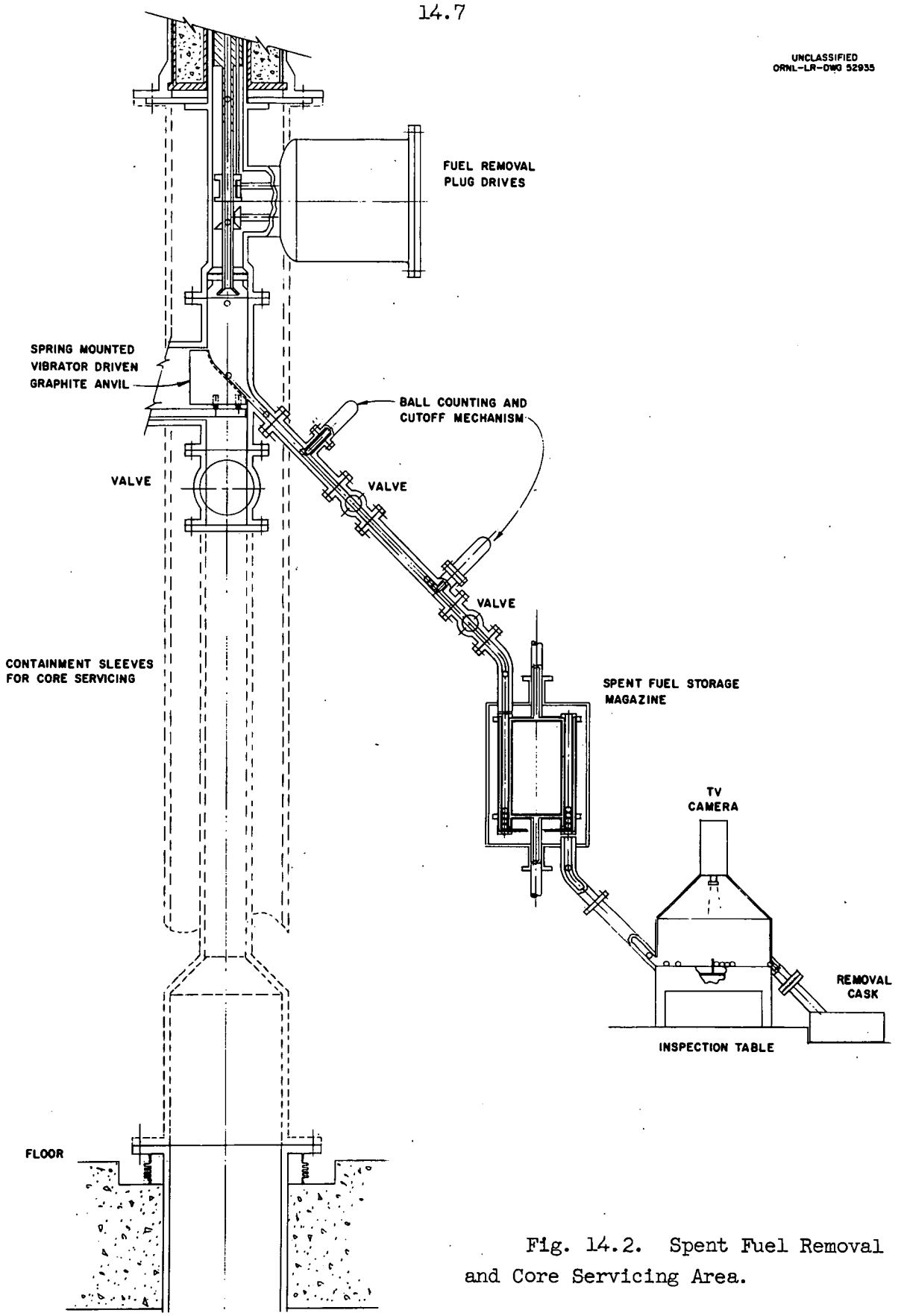

Fig. 14.2. Spent Fuel Removal and Core Servicing Area.

of the duct and core support structure. The highest point, diametrically opposite, will extend possibly 3 in. or more above the intersection of the duct and core support structure. Just below this highest point and in the cylindrical wall of the fuel-removal plug is a hole sized and located to permit entry of fuel balls into the plug from the core. Removal of fuel is accomplished by retraction of a ball cutoff gate just inside the ball port and by rotation of the fuel-removal plug. Balls entering the plug will be ducted down the center of the vertical drive shaft which supports and drives the fuel-removal plug. The need for the ball cutoff gate is questionable. It is unlikely that more than one or two balls will be discharged from the reactor after plug rotation is stopped. However, it is shown to emphasize the need for accurate, positive control of fuel movement into and out of the reactor.

This concept obviates both the hood and the inventory of balls outside the core proper, provides for "single file" flow of balls through the exit duct, provides moderate agitation of the fuel ball bed adjacent to the exit port during fuel removal, and requires what appear to be only simple mechanical motions. These are all considered both real and important advantages of the proposed concept, but the claim of mechanical simplicity must be qualified. The slow rotation of the fuel-removal plug and the up-and-down motion of the ball cutoff gate are indeed simple basic motions, but it must be expected that the design of the actual mechanisms will become somewhat more complex than is implied by these descriptive phrases. Some elaboration upon the drive for these mechanisms is required. Provisions for use of a ball-flow-channel clearing ram or auger and emergency removal of the fuel-withdrawal system and the reactor fuel charge are described as service-machine functions.

The drive mechanism for the fuel-removal system is located outside the biological shield where it would be accessible for maintenance. The drive-system components may be installed outside the pressure envelope to afford direct access, or they may be totally enclosed within the pressure envelope, possibly by incorporation in the shield plug. The

latter arrangement is more desirable for this application, because it requires no sealed rotating-shaft penetrations of the pressurized system. Helium leakage must be regarded as one of the major problems in the design of this plant; pressures and temperatures are high, and the helium is contaminated. The proposed arrangement places motors, gears, bearings, switches, and other components in the high-pressure helium system. The major portion of these components can be partially isolated from the spent-fuel cooling-gas stream by seals between the drive housing and the spent-fuel shaft. This isolation will permit operation of the drive motors and most of the other drive components at temperatures below the gas inlet temperature to the reactor. The major problems are lubrication of gears and bearings and electrical breakdown in ionized helium. Some gears and bearings will be required to operate either unlubricated or with dry-film lubrication. The horizontal drive shafts which carry the bevel gear and eccentric cam follower for operation of the fuel-removal plug and ball cutoff gate, respectively, must be retractable to permit removal of the fuel-removal plug.

The fuel balls removed from the core are guided through the hollow fuel-removal-plug drive shaft and dropped on a spring-mounted vibrator-driven graphite anvil, from which they enter an inclined tube which guides them past a ball-counting and ball-flow cutoff device into a length of inclined tube isolated by two valves. A controlled number of balls is admitted into the chamber between the two valves, with only the upper valve open. The upper valve is closed, and the lower valve is opened to deliver the balls into a vertical storage tube in a revolving multi-chambered holding and cooling magazine. Each vertical magazine tube is sized to accommodate the number of fuel balls which can be transferred in one operation through the valved gas lock. The lower valve in the gas lock is the extreme limit of the high-pressure helium system. The magazine is to be at atmospheric pressure and could be designed for water jacket cooling of each storage tube, enclosed cooling with air recirculated over the stored balls, or both.

The valves in the system must afford a full-flow cross section to pass fuel balls, and either gate or ball valves may be considered. The valve problems arising from graphite dust and chips may be expected to be severe, and a valve development program will be required. Maximum use must be made of double valving and blind cover flanges with clean helium buffer gas between double gaskets to avoid leakage of contaminated gas, and a continuous helium-recovery system will be required to maintain leakoff volumes at controlled pressures. Fully enclosed valve actuators supplied with high-pressure helium as a buffer gas should be used to avoid leakage of contaminated gas around valve stems.

Balls stored in the magazine may be removed by successive rotations of the individual storage tubes over the exit port and release of the latches to deliver the fuel balls to an enclosed mechanical inspection stage where they may be remotely viewed and delivered into shipping casks. The spent fuel in transit through the removal system will require cooling. Helium cooling must be used for the fuel within the main reactor coolant envelope, and cooling with recirculated air and by other means such as water-jacketed magazine tubes may be used. Details of the coolant piping have not been developed, but a system of helium pipes, valves, and possibly filters and pumps will be required.

The arrangement at the bottom of the reactor provides a single nozzle penetration of the reactor pressure-vessel head. For normal plant operation the fuel-removal equipment is attached to the lower end of the 28-in.-diam nozzle where it emerges from the reactor shield. The proposed fuel-removal equipment is designed for remote operation. The shielding afforded by the reactor shield, the shield plug in the nozzle passage, and that around the fuel-removal equipment should permit personnel access to the fuel-removal chamber directly below the reactor when no fuel balls are in the discharge line. This requires that the shielding around that part of the fuel-removal equipment directly under the reactor pressure vessel nozzle be removable to the extent necessary to permit removal of this portion of the equipment. This operation would be required

only when the reactor is shut down and depressurized. The design provides for two operations, in addition to normal fuel removal, that can be carried out without removing the fuel-removal equipment from the nozzle: (1) introduction of a ram or auger to clear the fuel-removal tube and (2) replacement of the fuel-removal plug. These two operations would only be carried out with the reactor shut down and depressurized and would be carried out only in the event of serious trouble. The length of the fuel-removal plug drive shaft requires that it part into an upper and lower section, the lower section to be removed and stored first and then the upper section. This would be followed by the fuel charge if that were still in the reactor. The fuel-removal plug would be lowered until it admitted fuel into the inclined fuel-removal system. It might prove desirable either to provide a device for breaking up ball aggregates to insure removal or to replace the small-diameter inclined ball-removal tube with a larger duct for this operation. The detailed design of these devices must be undertaken before such a system can be evaluated.

It is evident that both the mechanisms and the rooms within which they are operated must be designed to permit decontamination. To this end, the spent-fuel-handling rooms are to be lined with mild-steel sheet painted with a chemically resistant paint. Floor drains, equipment connections, solution and drain tanks, pipes, valves, pumps, and other appurtenances for decontamination will be required.

Fuel-Loading System

The fuel-loading system for a pebble-bed reactor might be a simple feed hopper connected to the reactor core by a valved ball duct. If the loading operation were to be carried out at power, control considerations indicate that the core should be kept full at all times. If a spent ball is removed from the bottom, it should be replaced by a fresh ball at the top. One way to assure this is to employ a ball feed device capable of pushing fresh fuel balls into the core. This would also permit refueling at full power with an upward coolant flow through the reactor sufficient

to raise the fuel bed firmly against the top grid structure. One possibility is the screw feed device shown in Fig. 5.1. Another arrangement suggested is based upon gravity delivery of balls to a fuel-loading plug located at the top of the core. Within this plug, a ball could be aligned with a plunger which would be activated to drive the ball down into the core. Either this device or the screw feeder would be designed to "stall" when the core became full to prevent admission of additional balls. The stalling action would provide a means of determining when the core is full. The effects of a forced-feed device on ball "ratcheting" and the resulting stresses in the graphite sleeve containing the ball bed can be determined only from experiments.

The problems of delivering new fuel balls into the feed system from a magazine include those of valving, shielding, helium leakage, and space allocation. At the feeding device just above the core, there appear to be additional problems. Some means should be provided to indicate that each ball introduced into the feed system actually enters the core. If balls are introduced one at a time, the force feeder travel or actuating torque might provide this information. This method, while it might provide the required operating information, requires one operation of the gas-lock valves for each ball fed. The arrangement could be improved by providing a magazine loaded with new fuel balls from which individual balls could be released to the force feeder. Introduction of the loaded magazine into the reactor pressure system would obviate the requirement for operation of the gas-lock system for each fuel ball admitted and yet would permit recovery of all new fuel balls in the magazine not delivered to the core.

The arrangements required at the top of the reactor for a ball-feed mechanism operated by a rotary shaft include a single central point of ball entry without special provisions for equal ball distribution to all quadrants. The fuel-feed system would fit within a cylindrical envelope concentric with the reactor core and extending upward from the top of the core through the upper plenum, the shield plug, and the top nozzle

closure to a magazine and drive system at the top. A space allocation problem involving the control-rod and fuel-feed systems will require careful attention.

15. SERVICING EQUIPMENT AND PROCEDURES

The advantages of all-ceramic gas-cooled reactors have been recognized from the time of the Manhattan project. A major objection to this type of system has always been that particulate activity in the form of fine dust would present difficult maintenance problems. Since one of the best measures of the effectiveness of a reactor test facility is the ratio of operating time to down time for inspection, maintenance, or system modification, great care was taken in the design of the PBRE facility to provide adequate space and equipment to carry out these operations expeditiously. Although the fuel-ball development program is being directed toward a high degree of fission-fragment retention and may produce fuel with very low fission-product escape rates, it was though best to design for a much more serious contamination level. This approach seemed particularly in order since it may prove necessary to cope with some unforeseen accident which could contaminate the system to a very much higher level than would ordinarily prevail.

The amount of particulate activity to be expected in an all-ceramic gas-cooled reactor presents one of the greatest uncertainties in the design. In the system proposed, 1% of the main system gas flow will be bypassed through a cleanup system, which should remove most of the reactive volatiles and particulate matter and much of the rare gas from the bypass stream. This, coupled with the full-flow filter at the top of the reactor, which should take out particulate matter down to 0.3 μ, should keep the level of particulate activity throughout the system to as low a value as it is practicable to obtain with any given fuel element design. It is difficult to predict to what extent the remaining activity in the main gas system will tend to adhere to the walls or to what extent it may be present in the form of a fine dust that would collect in crevices and would become airborne upon withdrawal of such items as a shield plug. While experience with the aqueous homogeneous reactor indicates that the activity is firmly plated out on the walls in that system, and while the amount of activity to be expected in the PBRE is down by orders of magnitude from that in an aqueous homogeneous

reactor, it is in the nature of the gas-cooled ceramic-fuel system that much of the activity may tend to condense out in the form of flocculant snowflake-like dust particles in the submicron size range.

Design Precepts

On the basis of the considerations outlined above, a number of design precepts were adopted as a guide in the preparation of the preliminary design of the core servicing equipment and space requirements. While some of these may seem arbitrary, they indicate the bases on which the facility design was developed:

1. All core servicing operations, exclusive of normal fuel transfer, will be carried out with the reactor shut down and depressurized.

2. Access to the reactor core will be provided through vertical nozzles concentric with the core in both the top and bottom heads of the reactor vessel. These nozzles will be sized to accommodate the graphite core lining sleeves.

3. The basic service machine functions will be removal and replacement of the fuel drain system and core components. (These functions exclude normal fuel transfer operations.)

4. All mechanisms, piping, and other equipment exposed to particulate activity or other sources of contamination will be arranged to confine this activity within the smallest reasonable perimeter and to permit its removal by decontamination processes. As a further precaution, the main servicing and fuel storage rooms will be steel lined and painted with a chemically resistant paint to permit decontamination in the event of an activity release from fuel-handling or servicing equipment.

5. The design of the servicing equipment will, to the fullest extent possible, provide for removal of core components into metal containers which can be fully enclosed and sealed and will minimize operations which permit direct communication between internal reactor system surfaces and the atmosphere unless the region has been hydraulically isolated

and decontaminated. Full use of purging and enclosure with plastic bags or boots is intended when an operational step requires breaking a connection prior to making up the joint to a transfer container.

6. Free personnel access to the fuel-removal and core-servicing area will be provided except during operation of the service machine to remove badly contaminated components. The design should provide for emergency entry into this area, with temporary shielding, during such operations. The service machine is to be capable of remote operation, and the option of shielding the containment sleeves to permit personnel entry when they contain an irradiated core component may be exercised.

7. The bulk of the servicing operations will be carried out from the bottom of the reactor where the lower access tube opens into the main servicing area, which will be designed so that it can be used as a hot cell.

8. Servicing operations in the reactor will be confined insofar as possible to inspection or to insertion or removal of subassemblies which can be installed and locked in place by a simple operation, such as inserting and twisting, as in the case of rifle bolts, gun breeches, or bayonet joints. (This requires that the design of both the core and the servicing equipment proceed concurrently with much feedback from one to the other.)

9. Operations within the reactor will be designed to create a minimum of dust, i.e., there will be no sawing, battering, or crushing if such can be avoided.

10. A ram will be provided beneath the lower access tube to facilitate insertion or removal of the shield plug, the graphite sleeves, or other items, including elements of the fuel-discharge system.

11. A mobile remote-handling machine, such as a Mobot (Fig. 15.1) should be provided in the main service area so that the room can be used as a hot cell.

UNCLASSIFIED
PHOTO 51927

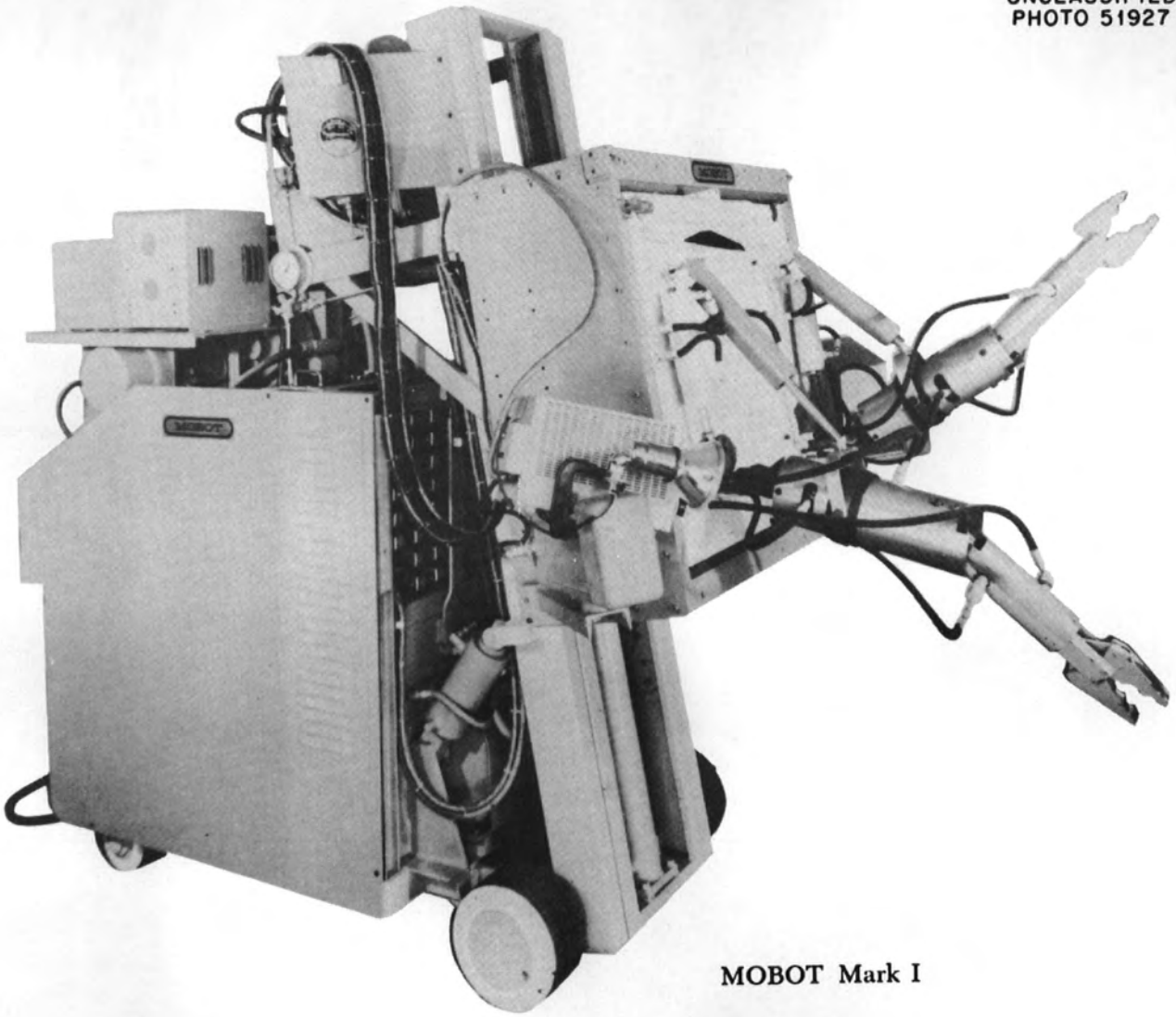

MOBOT Mark I

Fig. 15.1. Mobile Remote-Handling Machine – MOBOT Mark I. (Photograph reproduced from sales brochure of Hughes Aircraft Company.

Servicing Equipment

Careful studies of problems of reactor servicing in connection with both the EGCR and advanced gas-cooled reactors, particularly the BeO reactor described in ORNL-2767 (ref. 1), have shown that the major servicing operations are best carried out with a vertical ram driven by roller chains carried on sprockets. Such a ram can be built with two independent sets of chains supporting it, and these can be designed to operate at a small fraction of their capacity so that a high degree of reliability can be assured.

Because of the shield thickness and the clearances required during construction, both around and within the reactor, it is difficult to reduce the distance between the shield face and the reactor reflector face to less than about 14 ft. At the same time, differential thermal expansion between the reactor vessel and the concrete makes the precise location of heavy equipment outside the shield relative to components within the reactor somewhat uncertain. The difficulty is compounded by deflections if a bending moment is imposed on the arm or ram used to enter the reactor. Such a bending moment can be minimized or avoided by the use of direct vertical access tubes. It should be noted that an arm or ram gives the operator positive control of the positioning of his grapple or other device, so that, while it is more complex, it is much more versatile than a unit suspended from a cable.

Remote-handling equipment is required in the main service area so that it can be used as a hot cell. This equipment should be mobile, and should be suitable for moving the carriages required for casks, special servicing heads for the ram, etc. Several such devices are available. One of them, the Mobot, is a remote-handling machine mounted on a lift-truck chassis (Fig. 15.1). The basic piece of equipment makes use of two arm-and-hand manipulators mounted on shoulders which can be raised and lowered on the lift truck. Also provided are two TV cameras

---

[1] "GCR Quar. Prog. Rep. June 30, 1959," ORNL-2767, p. 6.

which can be turned in almost any direction independently of each other. The Mobot is coupled by a long triaxial cable to a reel, probably mounted well above the floor. The triaxial cable serves both to provide power through transformers and rectifiers and to transmit information from the instruments and the TV cameras. The operator would be at a control panel supplied with two TV screens and the necessary controls and instrumentation for moving the Mobot about and carrying out manipulations.

Special long-handled tools and other equipment would be required for servicing the blowers, the control rods and drives, and other items. This equipment would include a remotely operable hoist in the large tank mounted over the reactor around the control-rod drives. A Mobot could be moved from the hot cell to this enclosure to provide for remote handling of equipment when needed.

Servicing Operations

While firm designs will require much study to develop, some idea of the equipment requirements is given by reviewing some typical servicing operations. The basic arrangement of the service machine area has been presented in Figs. 6.3, 6.5, and 14.2. The fuel-removal equipment is shown installed at the bottom of the reactor vessel nozzle in the main service room with the top of the service machine in the floor of this room. Two sizes of containment sleeves are dotted in place in Fig. 14.2: a large-diameter sleeve between the service machine floor nozzle and the bottom of the reactor nozzle and a small sleeve between the service-machine floor nozzle and the bottom of the valve at the base of the fuel-removal column. The floor nozzle can be rigidly attached to the floor structure and is shown with a bellows seal at floor level to indicate leaktight continuity with the steel lining of the room. The service machine is located below the floor in a vertical tank. This tank would not be designed for system pressure and would only be required to contain helium and/or air at pressures below 15 psig and at temperatures below 150°F. The basic mechanism within the service machine is a ram capable of elevation through a sleeve into the reactor core.

The small-diameter containment sleeve has been shown to suggest one method for introducing a fuel drain tube clearing ram or auger and for lowering the fuel-removal plug to withdraw the reactor fuel charge in the event of an emergency such as fuel balls sintering into clusters. Such an operation might be carried out with a fuel-drain-tube clearing ram mounted within the service machine. The valve at the bottom of the fuel-removal column would permit attachment and use of this tool following reactor shutdown and depressurization. An alternate design based upon a flexible or articulated ram should be studied. Such a device could be mounted within a separate vessel in the fuel-storage room rather than in the service machine. This would have the advantages of simplifying the service machine design and catching any fuel particles removed during the clearing operation in a smaller and more readily decontaminated container. Still other arrangements may be found preferable. If, as in Fig. 6.3, the service machine is track-mounted to permit movement to a position under the ceiling hatches for servicing by the high-bay crane, the drain-tube clearing ram might be mounted beside the service machine in a separate vessel.

The withdrawal of the fuel-removal plug to clean out fragments from the graphite sleeves or fused-fuel-ball clusters would require that the service machine ram be raised through a containment sleeve and through the valve at the base of the fuel-removal column to engage the combined bayonet lock and thrust-bearing assembly immediately above the flared ball exit port at the bottom of the drain tube. After retracting the two drive shafts into the fuel-removal plug drive housing, the fuel-removal plug could be lowered to bring the top surface of the plug opposite the entrance to the inclined fuel-removal tube. A device for breaking up ball clusters or graphite fragments could be introduced to replace the spring-mounted anvil, and the design could permit attachment of a larger-diameter inclined fuel-removal tube which would bypass the magazine and inspection table and deliver fuel directly into a cask. The great length of the fuel-removal plug assembly might require that it be lowered in sections rather than all in one operation, as described

above. This provision requires development of design detail and would represent one of the more difficult design problems.

The functions of the service machine would include removal of the reactor-nozzle shield plug, the bottom core-support grid structure, and the graphite core-lining sleeves. For each of these operations the reactor system would have to be shut down and depressurized and the fuel-removal column withdrawn. The first steps for these operations would be removal of fuel from the reactor and withdrawal of the fuel-removal plug as described above. Following this, the fuel-removal column, consisting of the fuel-removal-plug drive assembly, the housing for the graphite anvil, the valve, and a section of inclined spent-fuel duct, would be removed. Since no valve closure has been shown at the lower end of the reactor nozzle, this operation would require the use of plastic boots to contain particulate activity while coupling the large-diameter containment sleeve. No valve was shown because of the large size of this opening and its exposure to full reactor system pressure.

In removing the shield plug, a plastic bag would be telescoped in accordion style and positioned over the access flange where it would be secured by hoops which would clamp it to cylindrical surfaces provided for the purpose. The shield-plug-removal head would be positioned over the ram. The ram would be engaged to the head and secured with a simple locking device which could be operated by the Mobot, and the ram and shield-plug-removal head would be raised and engaged with the attaching device provided at the shield plug. The shield plug would be broken free with an impact-wrench device incorporated in the shield-plug-removal head, rotated with the ram to disengage it from the breech-lock type of joint provided in the access tube, and lowered to the shield-plug-removal head carriage, which would rest on the floor. The extended plastic bag would be pinched off above the shield plug and sealed with a hot ironing device manipulated by the Mobot. The plastic bag would then be cut, probably in the sealing operation, along the sealed seam. The shield plug would then be moved to a convenient spot in the hot

cell and another service head mounted on the ram for the next operation. The Mobot would be used as a locomotive to draw the carriage carrying the shield plug and shield-plug-removal head.

Cost Estimates

Rough estimates of the cost of the various items of equipment for the servicing procedures outlined above are as follows:

Service machine	$250 000
Mobot	80 000
Steel wall lining (10 000 ft^2)	30 000
Remotely operable hoist	50 000
Long-handled tools and special devices	50 000
Lead casks and storage containers for contaminated material	100 000
Decontaminating equipment	20 000
Total	$580 000

The cost of the servicing equipment appears to be reasonable when compared with the cost of the service machine equipment for the EGCR, which was designed for operation at high power.

A review of the plant layouts presented in Chapter 6 indicates that an appreciable part of the cost of the facility should be charged to the service machine. The greater part of this stems from the provisions made for the ram beneath the lower reactor access tube. A chain-driven ram of the sort described will require about 40 ft of vertical height below the hot-cell floor. In the layouts presented in Chapter 6, this ram is mounted on a carriage which would traverse a canyon below the hot cell. This arrangement was chosen to facilitate removal of the ram and its drive mechanism for servicing. Preliminary estimates indicate that the extension of the containment shell and concrete foundation to the extra depth required for this ram will add

around $300 000 to the cost of the facility, a large price to pay for easy maintenance of the ram and drive assembly. A careful review of the servicing functions indicates that the ram would be extremely valuable and would probably justify this $300 000 added cost for the facility. However, the reliability of the ram drive mechanism seems sufficiently high that a less generous allocation of space for servicing it should be acceptable. An obvious alternative is to locate the ram and its drive mechanism in a well perhaps 12 ft in internal diameter, since it appears that the entire assembly could be kept within a diameter of 4 ft. This would require that the ram and surrounding room be sufficiently decontaminated so that direct personnel access would be acceptable. The mechanism could then be removed by conventional rigging operations in the unlikely event that the servicing could not be carried out in situ. To facilitate this operation, the 12-ft-diam well could terminate at the bottom of the containment vessel as shown in Fig. 21.1. Above this level a canyon perhaps 30 ft long by 15 ft wide could be provided to extend out into the hot cell. Floor slabs and steel sheets over this canyon would have to be removed if the ram and drive assembly were to be removed for servicing. However, it seems likely that all the servicing operations could be carried out in situ during the life of the facility, since the number of hours of operation required of the ram drive assembly would be relatively small in the life of the plant.

The most important shortcoming of this approach is that it would require good decontamination of the hot cell before servicing work could be carried out on the ram drive assembly. This contingency seems to be a small and quite reasonable price to pay for a marked reduction in the cost of the facility.

Another approach that deserves investigation is to shorten the length of the ram and drive assembly by using a telescoping ball jack screw. In a plant application requiring ram entry into the reactor system at power, this type of mechanism would become complex because all the grappling, locking, and other motions required at the ram head

would be transmitted up the telescoping ram sections from drive motors down in or near the service machine. The core servicing functions of this service machine and ram would be carried out with the reactor shut down and depressurized, which might permit installation of pneumatic or electric actuators near the ram head and hence reduce the complexity of the telescoping ram structure.

16. HELIUM PURIFICATION SYSTEM

The purification system for the helium coolant includes provisions for removing gaseous and particulate impurities, both radioative and nonradioactive. A sidestream of helium is withdrawn from the circulating loop at the discharge of one of the helium compressors, and it re-enters the main stream at the compressor suction, thus taking advantage of the pressure rise through the compressor to drive the gas through the cleanup system. The sidestream flow is about 1% of the main coolant flow. In sizing the cleanup system, it was assumed that the surface available for graphite oxidation by impurities in the helium was essentially that of the core wall and that the total amount of graphite which could be allowed to burn up in a two-year period of 300 operating days per year was 1% of the total amount, exclusive of the fuel spheres. This is equivalent to about 700 lb of carbon. The maximum allowable inleakage of water from the main coolant heat exchanger was assumed to be 0.1 lb/day. The purification system consists of a fission-product delay trap, a chemical purification train, and particle filters.

System Components

Fission-Product Delay Trap

The fission-product delay trap consists of charcoal which either removes or simply delays the iodine, xenon, and krypton. The iodine is essentially irreversibly removed by the charcoal,[1] and krypton and xenon will be delayed as they pass through the trap as a result of dynamic adsorption of the gases by the charcoal.[2]

Chemical Purification Train

The nonradioactive gaseous contaminants of interest are carbon monoxide, hydrogen, hydrocarbons, carbon dioxide, and traces of water.

---

[1]R. E. Adams and W. E. Browning, Jr., "Removal of Radioiodine from Air Streams by Activated Charcoal," ORNL-2872 (1960).

[2]W. E. Browning, R. E. Adams, and R. D. Ackley, "Removal of Fission Product Gases from Reactor Off-Gas Streams by Adsorption," ORNL CF-59-6-47 (1959).

All oxidizable gases are converted to carbon dioxide and water, and then the carbon dioxide and water are removed by sorption processes. Copper oxide is used as the oxidizing agent, since early experimental work indicated that it precludes the possibility of getting oxygen contamination into the purified gas.[3]

Particle Filters

Particulate matter is removed from the coolant stream by high-temperature filters in the main coolant stream and by a low-temperature filter in the purification sidestream. The filter in the purification system is downstream from all other components to protect the main stream coolant from solids generated by attrition in the purification process.

Although there are no experimental data directly applicable to the PBRE operating conditions, the maximum carbon dioxide contamination level in the coolant can be estimated on a very conservative basis by assuming that all moisture and carbon monoxide reacts with the graphite to form carbon dioxide. It is known that carbon dioxide will react with graphite to form carbon monoxide, and if this reaction is reversible at the lower temperatures encountered at the cool end of the heat exchanger, there will be a cyclic mass transport of carbon from the graphite to the relatively cool parts of the system which will continue steadily during reactor operation. The rate at which this chemical attack on the graphite will occur is not well known, but it is believed that mass transport through the porous solids at an intermediate temperature and mass transport of the reacting gas and carbon dioxide across the relatively stagnant gas film between solid surfaces and the main gas stream are probably the controlling mechanisms. Assuming that the control of the carbon-carbon dioxide reaction is by mass transfer of the carbon dioxide through the gas film, it is possible to calculate the equilibrium concentration of carbon dioxide which corresponds to the graphite loss rate of 700 lb in two operating years. This

[3]C. D. Scott, "Oxidation of Hydrogen and Carbon Monoxide in Helium by Use of CuO. I. Preliminary Results," ORNL CF-60-7-26 (1960).

concentration comes out to be about 20 ppm by volume, assuming that the carbon dioxide concentration leaving the purification train is set at 30% of the total sidestream flow. The remaining 70% of the flow will go directly to the fission-product delay trap, thus allowing separate and independent use of either or both purification sections.[4-8]

System Flowsheet

A flowsheet of the proposed system is shown in Fig. 16.1. The helium sidestream is split, and the greater part of the flow goes to a gas cooler, where the temperature is reduced to about 85°F before admission to the charcoal fission-product delay trap. The gas cooler consists of a double-pipe heat exchanger with a water-cooled longitudinally finned inner tube (1.5 in. i.d., 24-20 BWG, 0.5-in. fins) inside of a 3-in.-IPS pipe. The temperature of the water is assumed to rise from 75 to 150°F. The total length of the heat exchanger is 60 ft. The size of the delay trap was arbitrarily chosen to provide an average retention time of 30 min for krypton and 6 hr for xenon and to remove 99.9% of the iodine. A trap consisting of 65 ft of 6-in.-diam pipe packed with 405 lb of charcoal (packing density 31.2 lb/ft^3) satisfies the design specifications for operation at 100 psi. The operating temperature is about 85°F, and the pressure drop is estimated to be 3 psi. The estimated effectiveness of the trap in reducing the amount of the various gaseous isotopes in the main gas system is indicated in Table 16.1.

---

[4]J. E. Antill and K. A. Peakall, "Coolant Purity in the HTGCR," AERE-R-3070 (1959).

[5]D. D. Eley, P. W. Selwood, and P. B. Weisz (eds.), "Advances in Catalysis and Related Subjects," Vol. XI, p. 133–221, Academic Press, New York (1959).

[6]D. A. Plautz and H. F. Johnstone, A.I.Ch.E. Journal, Vol. 1, No. 2, p. 193–9 (1955).

[7]C. N. Scatterfield, H. Resnick, and R. L. Wentworth, Chem. Eng. Prog., Vol. 50, No. 9, p. 460–6 (1954).

[8]B. C. Finney, J. C. Suddath, and C. D. Scott, "The Helium Purification System for the Proposed Pebble-Bed Reactor Experiment," ORNL CF-60-10-31 (to be issued).

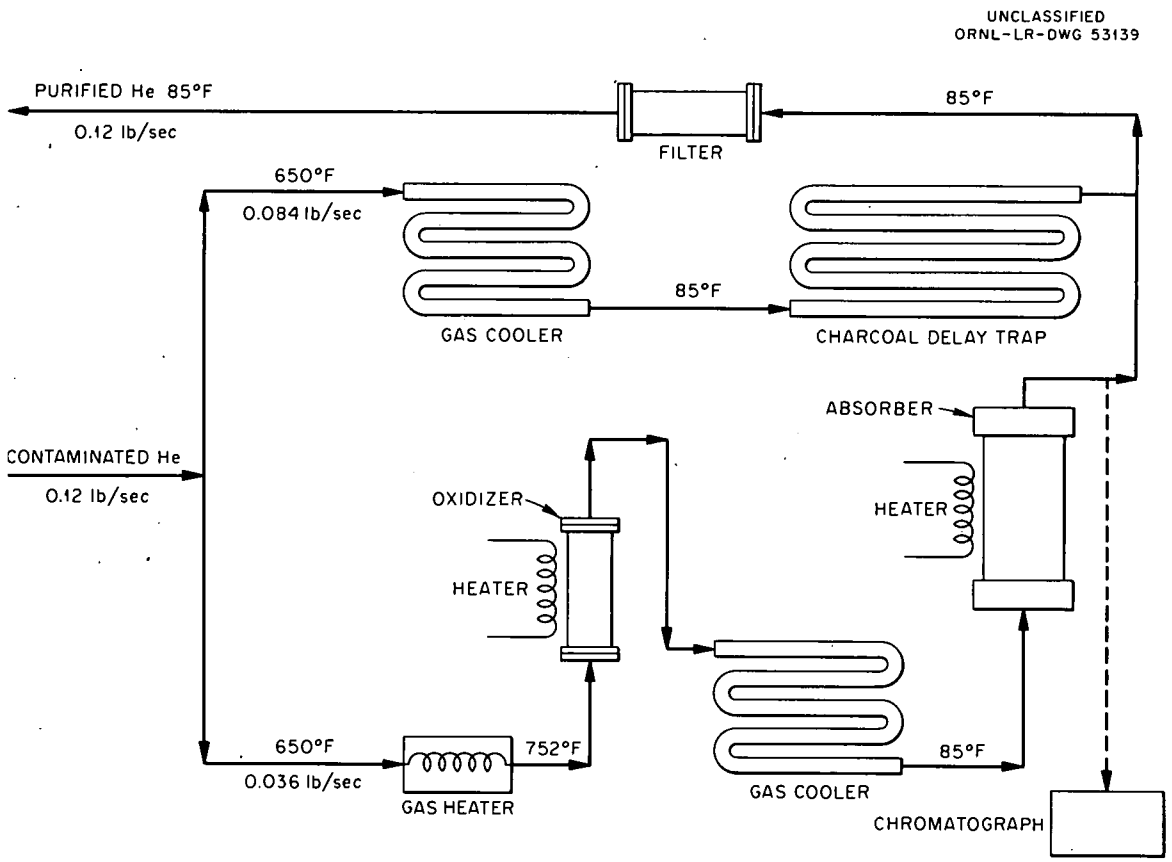

Fig. 16.1. Coolant Purification System Flowsheet.

Table 16.1. Estimated Decontamination Factors for the Fission-Product Delay Trap

Isotope	Half-Life	Loop Activity Without Purification (curies)	Loop Activity With Purification (curies)	Decontamination Factor
Kr^{85}	10.3 yr	1.3×10^3	1.3×10^3	1
Kr^{87}	78 m	3.1	1.66	1.86
Kr^{88}	2.77 hr	20	10.4	1.92
Xe^{131m}	12 d	126	9.3	13.5
Xe^{133m}	2.3 d	24	2	12
Xe^{133}	5.27 d	2.79×10^3	214	13
Xe^{135}	9.13 hr	87.2	8.5	10.3
I^{131}	8.05 d	2.2×10^3	4	5.56×10^2
I^{132}	2.4 hr	1.4×10^3	175	8
I^{133}	20.7 hr	2.4×10^2	3.9	61
I^{135}	6.68 hr	57	2.8	20.1
Total activity		8247	1767	

After leaving the delay trap, the gas stream recombines with the stream from the chemical purification system and passes through a low-temperature filter for the removal of particulate material before returning to the main system. A flow velocity of 6 fpm through absolute filters is recommended for high efficiency. Pleated filters that are 8 in. in diameter and 4 in. deep would be sufficient.

The fraction of the sidestream that is to be chemically purified is first raised to 752°F in a gas heater consisting of an 8-in.-diam coil of 1 1/2-in.-i.d. tubing heated by an electrical furnace of about 7.5-kw capacity. The total heating surface necessary is 10.4 ft^2, or 18 turns of the coil, which would result in about 24 in. of coil length. The over-all dimensions of the unit, including the electrical furnace, are about 2 ft o.d. by 2 ft long.

The gas leaving the heater passes through the oxidizer containing pellets of copper oxide. The oxidizer is designed for seven days of continuous service without regeneration. Assuming that 50% of the copper oxide content will be utilized, the amount of copper oxide

required is 22 lb. At a specific gravity of 1.7 for the copper oxide pellet, the fixed bed of copper oxide is about 0.2 ft^3 in volume. This can be contained in a 6-in.-i.d. vessel 12 in. long. Adding 2 in. of free space to the top and bottom would make the vessel 16 in. long. Since the vessel must be maintained at 752°F, additional electrical heating of about 5 kw is required with 2 in. of insulation.

From the oxidizer the hot gas is cooled to 85°F by passage through a double-pipe heat exchanger consisting of a 3/4-in.-IPS water-cooled inner tube with eighteen 0.024-in.-thick by 0.5-in. axial fins inside of a 2 1/2-in.-IPS pipe. The total length of the heat exchanger is 42 ft.

The cooled gas then passes directly into a molecular-sieve absorber, which is also designed for seven days of continuous operation. The dynamic loading of the molecular sieve should not exceed one-half of the equilibrium loading.[9,10] (Loading is defined as pounds of water or carbon dioxide absorbed per 100 lb of the molecular sieve.) The equilibrium loading on a type 5a molecular sieve for water at less than 0.5 ppm is approximately 10 lb per 100 lb of sieve, and the equilibrium loading for carbon dioxide at 5 ppm is 2.7 lb per 100 lb of sieve.[9] On this basis, the absorber will need 20 lb of molecular sieve for each pound of water and 74 lb of sieve for each pound of carbon dioxide absorbed. Thus a total of 310 lb of type 5a molecular sieve is needed. A vessel 1 1/2 ft i.d. and 5 ft long would be suitable for the fixed bed. Sufficient electrical heating must also be supplied to raise the bed temperature up to 600°F for regeneration (approximately 7.5 kw), and 2 in. of insulation would be required on the outside.

From the absorber the purified gas joins the stream from the delay trap and goes directly to the particle filter. The effectiveness of

---

[9]Linde Company, Bulletin F-1026, "Dry Gas? Use Linde Molecular Sieves."

[10]Linde Company, Bulletin Form 9690-C, "Molecular Sieves for Selective Adsorption, Water Data Sheets" (1957).

the chemical purification system is monitored by means of a gas absorption chromatograph connected just downstream of the absorber.

Operation and Maintenance

An advantage of the proposed sidestream purification system is the simplicity of operation. Since there are no moving components, it is expected that the system will be essentially maintenance-free. However, it would probably be necessary to regenerate the copper oxide oxidizer and molecular sieve after each seven days of reactor operation. In order to accomplish this, the oxidizer is removed from service and regenerated with air for approximately 8 hr at operating temperature, and the absorber is regenerated by purging with dry air at atmospheric pressure and 600°F for approximately 8 hr. The life of the delay trap will depend on the poisoning effect of the iodine and solid daughter products of the fission gases, for which no experimental data are available at the present time. However, it is estimated that the life of the charcoal in the delay trap will exceed two years.

17. DECONTAMINATION PROCEDURES AND FACILITIES

The feasibility of maintaining an all-ceramic gas-cooled reactor plant depends in large measure on the effectiveness with which equipment can be decontaminated in situ before beginning maintenance operations. The procedures described here are those recommended by the ORNL personnel who have developed procedures for decontaminating equipment used in the homogeneous reactor system. These procedures have been applied to a piece removed from an in-pile loop used for testing a gas-cooled ceramic fuel element and have been found to be effective. It is believed that the process recommended would virtually eliminate the problems associated with particulate activity and would drastically reduce dose levels around equipment, such as the blowers, so that, even after severe contamination of the equipment, contact rather than semiremote or remote maintenance procedures could be employed. A major objective of the pebble-bed reactor experiment would be to investigate the effectiveness of these decontamination procedures.

Chemical Treatment

The fission products contaminating metal surfaces exposed to the circulating helium in the PBRE will include volatile elements such as iodine, tellurium, cesium, cerium, and ruthenium, with minor amounts of less volatile elements such as barium, strontium, zirconium, and niobium, together with their daughters. There will also be daughters of the rare gases krypton and xenon. If a uranium carbide—graphite fuel element is used, the rare-earth fission products must be expected in significant quantities. Graphite dust, finely divided enough to be tightly adherent to metal surfaces, will probably be present and will be badly contaminated. There may be some dusting of the fuel microspheres, but the particle size should be large enough for easy removal by hot detergent solution. If the fuel comprises alumina-coated UO_2

particles, any unclad UO_2 powder will be dissolved by oxalate-peroxide, and deposition of the liberated fission products from such material should be negligible.

The oxalate-peroxide reagent that has been found to be the most effective of those tested for the noncorrosive decontamination of stainless or plain carbon steel consists of an aqueous solution of 4% sodium oxalate with 3% hydrogen peroxide and 0.7% oxalic acid at a pH of 5.0. The pH tends to rise with time, however, and, within an hour or less at 95°C in a steel vessel, rapid decomposition of the peroxide may result, with evolution of oxygen. The pH must therefore be monitored at least every half hour and adjusted to 4.5 to 5.0 by the addition of oxalic acid. In the laboratory the solution has been stable for over 2 hr at 95°C without pH adjustment, but it will probably be less stable in contact with miscellaneous dusts in large-scale plant equipment. The solution is stable at room temperature for several days. Mild steel corrosion at a pH of 5 and a temperature of 95°C was 0.0025 mil/hr, at a pH of 4 it was 0.005 mil/hr, and at a pH of 3 it was 0.01 mil/hr. Decontamination is improved with a lower pH at the expense of slightly increased corrosion on mild steel. The maximum stability of the solution is at a pH of about 4.5. At 95°C a mixture of oxalic acid and H_2O_2 at a pH of zero or less rapidly dissolves mild steel but is essentially noncorrosive to type 347 stainless steel (approximately 0.001 mil/hr). Oxalate-peroxide mixtures between pH zero and 5 are superior decontaminating agents and excellent solvents for UO_2.

An alkaline permanganate reagent consisting of an aqueous solution of 2% $KMnO_4$ with 2% NaOH has been found to be effective in removing some fission products, such as ruthenium and cerium, when significant amounts of these materials have remained after scrubbing surfaces with oxalic acid.

Decontamination Procedures

The procedures outlined in this section are tentatively recommended for the decontamination in situ of components of the pebble-bed reactor.

These procedures have been laboratory tested on type 347 stainless steel and on carbon steel. No large-scale tests have been made. The recommended steps are the following:

1. The component should be prepared for treatment by isolating it hydraulically from the rest of the system. To follow the progress of decontamination, remote probes for a scintillation gamma-ray spectrometer should be placed at various locations on the equipment to be decontaminated. A gross gamma-ray monitor should be installed on the solution drain line.

2. Decontamination may be accomplished by either the liquid-fill method or by the liquid-spray method, depending on the equipment size. In both methods the liquid or spray must contact all contaminated surfaces, and complete drainage must be possible. Heating may be accomplished by steam sparging with the liquid-fill method and by using a steam jet to aspirate the decontaminating solutions with the spray method.

3. The component should first be sprayed or filled with a solution of hot nonfoaming detergent to remove water-soluble contamination and wash away graphite dust. The rise and fall of the waste-line gamma activity should be monitored if the spray method is used, and spraying should be discontinued when the activity drops to about 10% of its peak value. In the fill method, the temperature should be maintained at 95 to 100°C for 20 min and then the solution should be drained.

4. If the decontamination is adequate, the apparatus should be rinsed with water. If not, decontamination should proceed with step 5.

5. The equipment should be sprayed or filled with oxalate-peroxide solution at a pH of 4.5 to 5.0 at 95 to 100°C, with the contact time adjusted as for the detergent solution.

6. If decontamination is adequate, the component should be rinsed with water. If not, the oxalate treatment of step 5 should be repeated.

7. If further decontamination is required, the solutions used will depend on the remaining fission products as indicated by a gamma scan with the spectrometer. Neutron activation peaks, such as from Co^{60} and Fe^{59}, in the structure of the metal cannot be reduced. Ruthenium

and cerium may be decontaminated further by alkaline permanganate treatment at 95 to 100°C for 20 min, followed by a water rinse, and an oxalate-peroxide treatment. A broad spectrum of fission products might indicate residual dust containing irradiated fuel either in inaccessible places or tightly adhering to metal surfaces and insoluble in non-corrosive reagents because of the coating.

8. The decontamination cycle should be concluded with water rinsing until samples from the drain line are free of chemical residues. The equipment should then be dried to prevent rusting.

Decontamination by this procedure should reduce the amount of activity by a factor of 50 to 10 000, depending on the initial activity level and on the effectiveness with which all the contaminated surfaces are contacted by the cleaning solutions.

Equipment Required

Maintenance work will be greatly simplified if the component to be decontaminated can be isolated hydraulically from the rest of the system. Since valves in the hot ducts are to be avoided if possible, and since any valves that could be obtained would probably not be hydraulically leaktight, the most promising method for isolating a component appears to be insertion into the duct to be blocked of a rubber bladder similar to that of a basketball. The bladder can then be inflated to seal off the duct. An aperature can be provided in the duct wall through which such a bladder can be inserted. A 3/4- or 1-in. tube leading to a pressure gage might serve this purpose, in which case, little additional complication of the system would be required for insertion of the bladder-type "valve."

The principal items which must be provided in the installation to permit decontamination will be the contaminated fluid storage tanks, the plumbing system to provide drainage of fluid to these tanks, and related pumps and valves.

18. STEAM SYSTEM

It was requested that this study include consideration of both a simple heat dump cooled by either air or river water and the use of a 3-Mw(e) turbine-generator unit that could be made available from the ORGDP steam power plant. A total of ten different variations on these basic suggested arrangements have been considered, and the results are summarized in this section.

A variety of heat transfer and system control considerations indicated that it would be desirable to make use of rather high-pressure high-temperature steam conditions. Because of this and because there seemed to be an incentive to demonstrate the feasibility of producing high-temperature high-pressure steam with the pebble-bed reactor, the steam generator design work was directed initially at producing 1450-psi 1000°F steam with the feedwater at 400°F. In an effort to reduce costs, the pressure was reduced to 1000 psi and the feedwater temperature to 250°F. The background on the choice of steam conditions is presented in the section on the steam generator.

Used Equipment Available

Several 3000-Mw(e) turbine-generator units designed to produce 120-cycle a-c current are available in the ORGDP steam power plant. These units are in sound mechanical condition, but their performance has probably deteriorated somewhat because of wear in the 16 years since they were installed. The arrangements considered for the use of this equipment are described in the following section.

Arrangements Considered

Several different ways of using one of these turbine-generator units were considered. First, one of the units could be installed as it is to produce 120-cycle current, and an electrical-resistance grid could be used to convert the energy into heat and dump it to cooling air. Second, one of the generators could be rewound to give 60-cycle

current, and the power could be delivered to the grid. A third arrangement, similar to the first, would employ a cooling tower rather than river water to cool the condenser so that the turbine-generator unit could be bypassed in the event of operating difficulties and the reactor could operate independently of the turbine. In a fourth system, similar to the third, the generator would be rewound to give 60-cycle power so that the unit could be coupled to the grid. The fifth and sixth systems considered were also similar to the third, except that an air-cooled condenser would be used in place of a cooling tower. In a seventh system, the turbine-generator unit would be eliminated, and a condenser from one of the ORGDP units would be used to dissipate heat to cooling water pumped up from the river. The eighth system considered was similar to the seventh, except that a cooling tower would be employed in place of river water. The ninth system would make use of a new heat exchanger to serve as the condenser and would eliminate the feedwater heater. The tenth system would be similar to the ninth, except that a cooling tower would be used in place of river water. The ninth and tenth units would include a new heat exchanger in place of a used condenser from the ORGDP plant. The estimated costs for these ten systems, including material and the labor for their installation, are summarized in Table 18.1. The details for the cost estimates for items 2 and 9 of this table are presented in Tables 18.2 and 18.3 to indicate the major cost items for these two typical systems. Flow sheets for these systems (2 and 9) are presented in Figs. 18.1 and 18.2.

Recommended System

The least expensive and simplest system of the eight considered is that shown in Fig. 18.2. It has the further advantage that it would require the least attention and the smallest crew for normal operation and maintenance.

The space requirements for this system would be essentially those shown in the basement floor plan of Fig. 18.3, except that the feedwater

heaters and the lube oil cooler could be eliminated. This layout also provides services for the building, including the standby diesel-generator set, a boiler for building heating, and air compressors, in a floor space approximately 44 by 66 ft.

Table 18.1. Costs of the Steam Systems Considered for the PBRE

1.	3000-kw turbine-generator unit, river-water cooling, 120-cycle generator	$620 000
2.	3000-kw turbine-generator unit, river-water cooling, 60-cycle generator*	770 000
3.	3000-kw turbine-generator unit, cooling tower, 120-cycle generator	639 000
4.	3000-kw turbine-generator unit, cooling tower, 60-cycle generator	789 000
5.	3000-kw turbine-generator unit, air-cooled condenser, 120-cycle generator	645 000
6.	3000-kw turbine-generator unit, air-cooled condenser, 60-cycle generator	795 000
7.	Dump condenser (from ORGDP plant), river-water cooling	418 000
8.	Dump condenser (from ORGDP), cooling tower	437 000
9.	New heat exchanger, no return feedwater heating, river-water cooling	393 000
10.	New heat exchanger, no return feedwater heating, cooling tower	414 000

*A new 60-cycle generator would cost $230 000; alterations to convert 120-cycle to 60-cycle would cost $150 000.

Table 18.2. Cost Estimate for a 3000-kw Turbine-Generator Unit with the Generator Altered to Give 60-Cycle Current and with River-Water Cooling

	Labor	Material	Total
Desuperheaters	$ 3 000	$ 15 000	$ 18 000
Bypass control	5 000	15 000	20 000
Turbine generator	30 000	Transfer	15 000
Turbine generator conversion to 60-cycle		15 000	15 000
Condenser		Transfer	
Pressure reducing station	2 000	5 000	7 000
Hotwell (condensate) pumps (transfer 1)	1 000	4 000	5 000
Air ejector	1 000	Transfer	1 000
Deaerator	3 000	5 000	15 000
Boiler feed pumps	2 000	36 000	38 000
Piping	10 000	20 000	30 000
Foundation (turbine generator and condenser)	5 000	10 000	15 000
Building and services (including crane)	50 000	100 000	150 000
Circulating water pumps	2 000	8 000	10 000
Pump house (most favorable location)	3 000	7 000	10 000
Demineralized water plant	1 000	5 000	6 000
Condensate tank	1 000	2 000	3 000
Demineralized water tank	1 000	2 000	3 000
Desuperheater pumps	2 000	12 000	14 000
Instrumentation and controls	20 000	80 000	100 000
Gland seal tank	1 000	1 000	2 000
Switchgear and wiring	20 000	100 000	120 000
Electrical grid (resistance load)	5 000	20 000	25 000
Total	$169 000	$601 000	$770 000

Table 18.3. Cost Estimate for a System Employing a New Heat Exchanger with No Return Feedwater Heating and River-Water Cooling

	Labor	Material	Total
Desuperheaters	$ 3 000	$ 15 000	$ 18 000
Deaerator	3 000	5 000	15 000
Boiler feed pumps	2 000	36 000	38 000
Piping	8 000	15 000	23 000
Building and services (including crane)	25 000	50 000	75 000
Circulating water pumps	2 000	8 000	10 000
Pump house (most favorable location)	3 000	7 000	10 000
Demineralized water plant	1 000	5 000	6 000
Condensate tank	1 000	2 000	3 000
Demineralized water tank	1 000	2 000	3 000
Desuperheater pumps	2 000	12 000	14 000
Instrumentation and controls	15 000	60 000	75 000
Switchgear and wiring	10 000	50 000	60 000
Heat exchanger	10 000	40 000	50 000
Total	$ 86 000	$307 000	$393 000

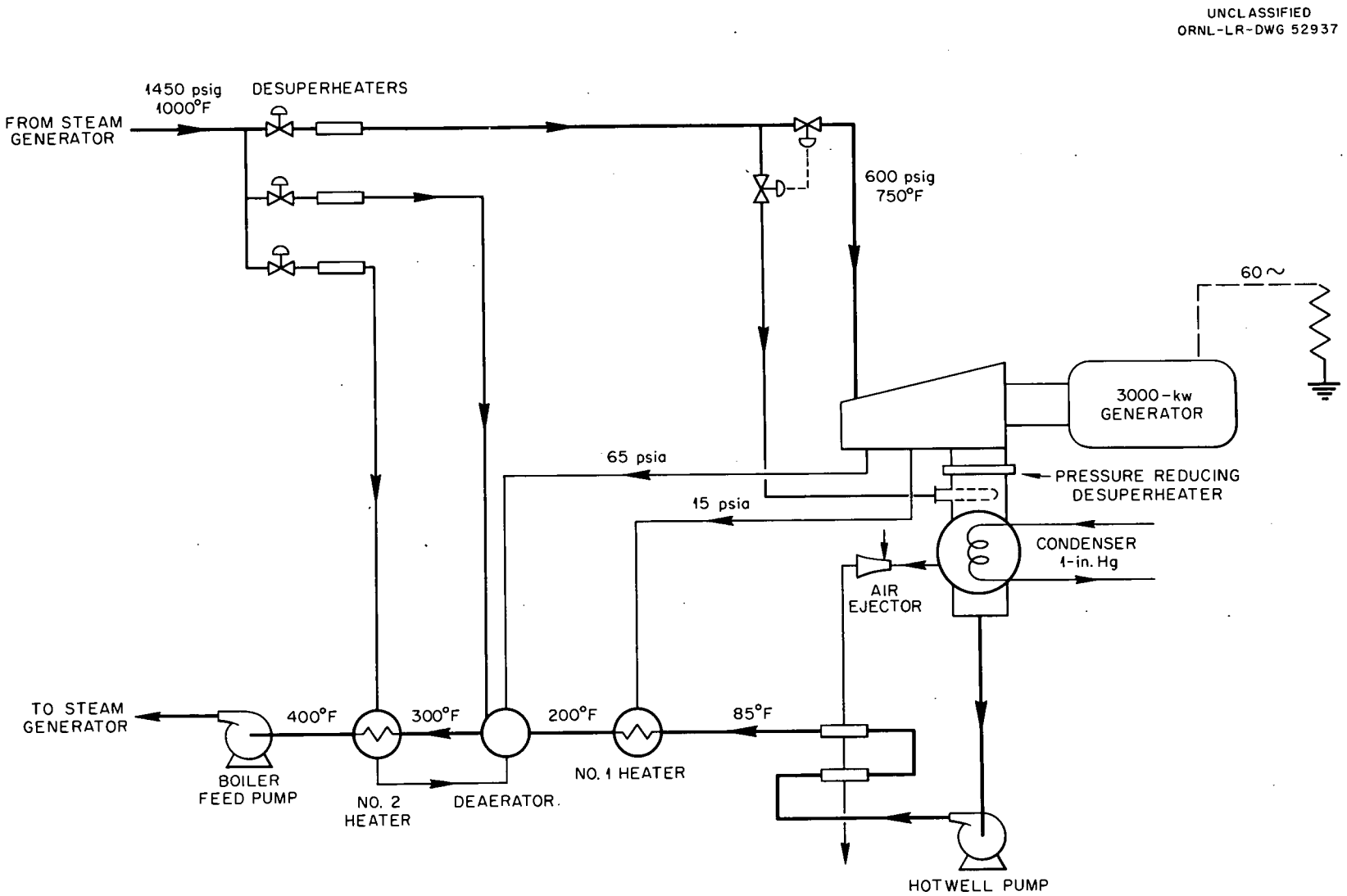

Fig. 18.1. Flowsheet for a 60-Cycle Turbine-Generator Installation with River-Water Cooling of the Condenser.

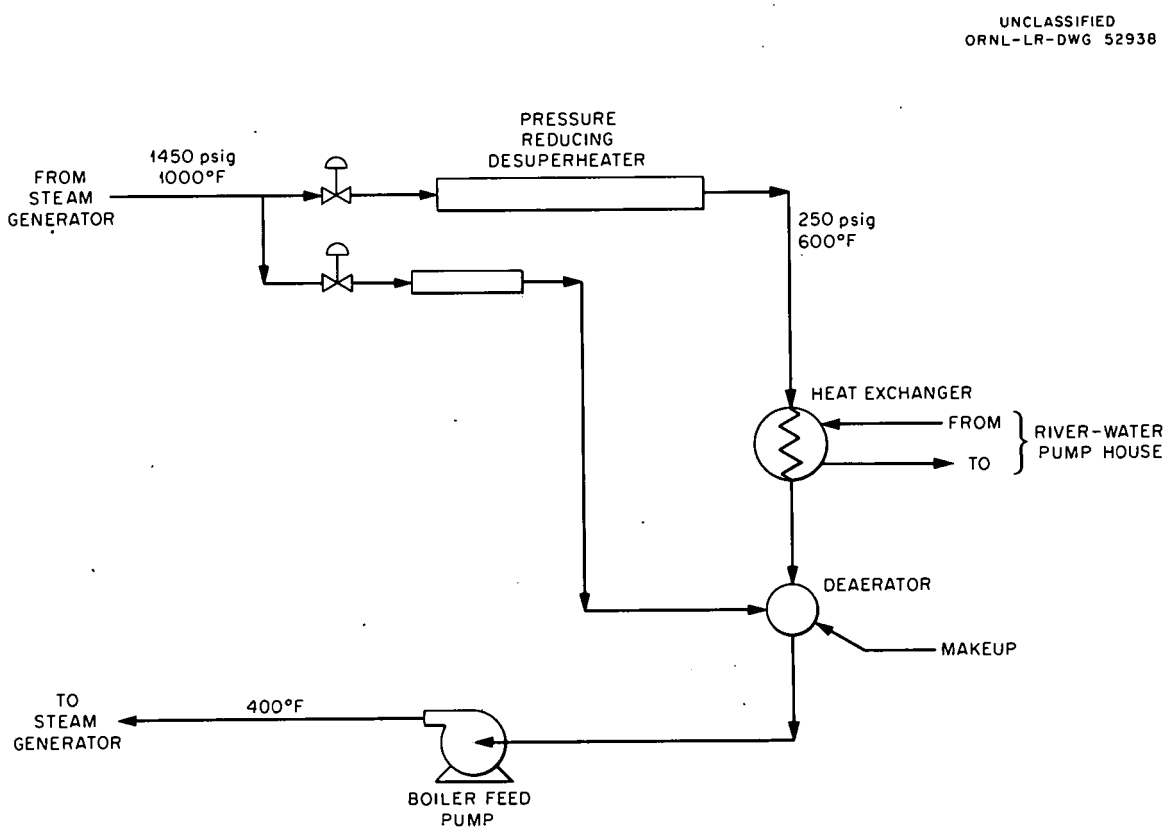

Fig. 18.2. Flowsheet for a Heat Dump System Employing a Heat Exchanger Cooled by River Water and No Feedwater Heater.

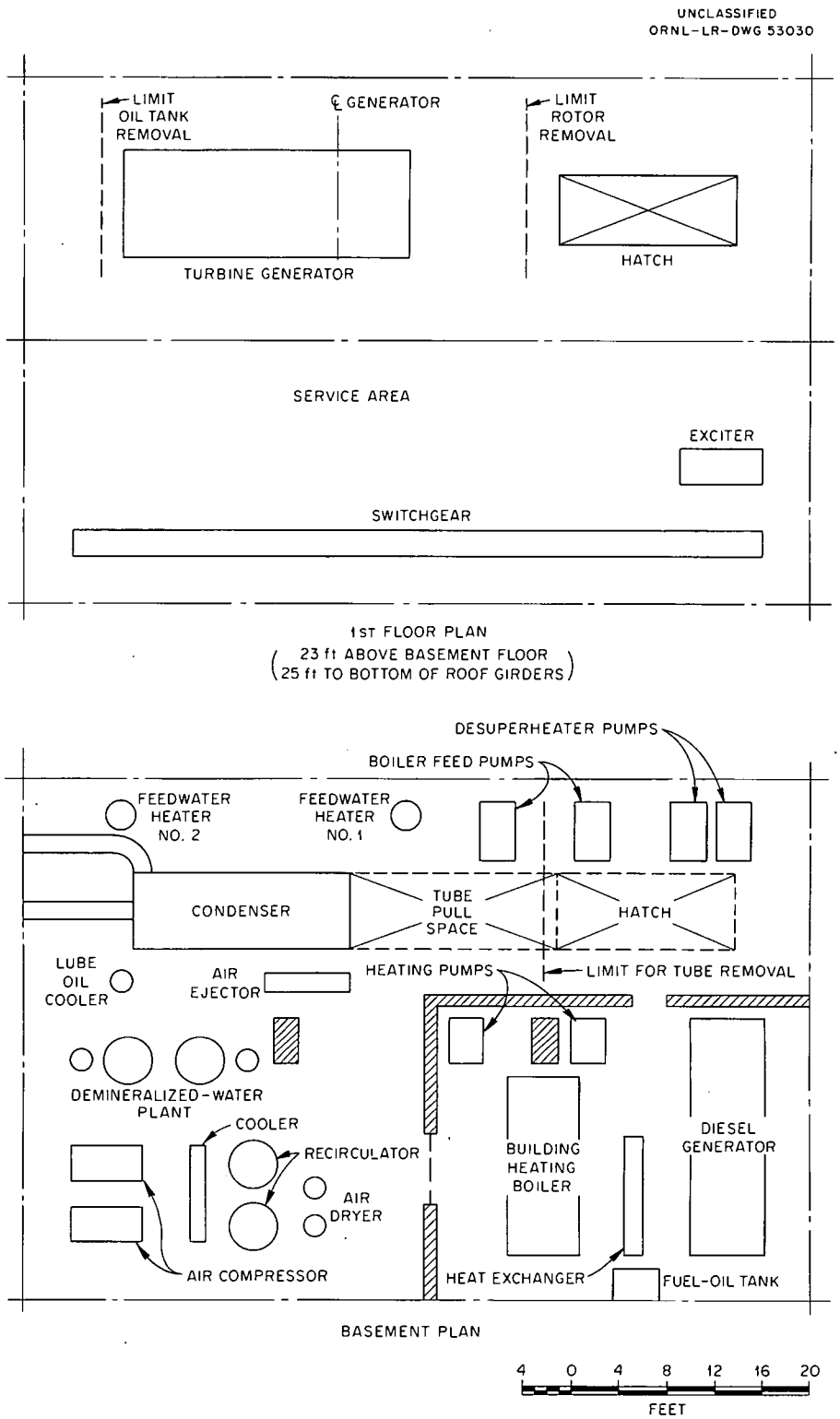

Fig. 18.3. First Floor and Basement Plans for PBRE Steam System.

19. HAZARDS ANALYSIS

Escape of Fission-Product Activity from the Fuel Element

The hazards associated with the operation of the PBRE will, to a large degree, be dependent on the amount of activity circulating or deposited in the coolant system. Based on presently available information, it appears that fission products escaping from the fuel are likely to be the dominant activity source in the coolant.

As discussed in Chapter 8, little is known about the ability of graphite fuel elements to retain fission products under power reactor conditions. Although fission-product release rates from both alumina-coated UO_2 particles and pyrolytic graphite-coated UC_2 particles have been found to be low in experiments involving little fuel burnup, the only experience with coated particles at high burnup is that obtained from the irradiation test of an alumina-coated-particle element now in progress in the BMI reactor.

For the estimation of fission-product escape rates, it would be conservative to assume uncoated UO_2 particles, but to do so means ignoring the recent experience with coated particles. For lack of a better method, the most recent data from BMI have been applied in this study to estimate the escape of all fission products of interest from alumina-coated UO_2 particles dispersed in graphite. The procedure followed was first to extrapolate the data for Kr^{87} and Kr^{88} in Fig. 8.2 to a burnup of 4.8%. The logarithms of the fractional escape values for Xe^{133}, Kr^{85m}, Xe^{135}, Kr^{88}, and Kr^{87} at 4.8% burnup were then plotted versus the logarithms of the decay constants, as shown in Fig. 19.1. With the exception of the Kr^{85m} value, which falls appreciably above the curve, the escape fraction shows a distinct correlation with the decay constant. A relationship of this type would be expected if the mechanism of escape for all the fission products considered were the same, since the amount of time available for escape before decay to another species is a function of the decay constant. Continuing this

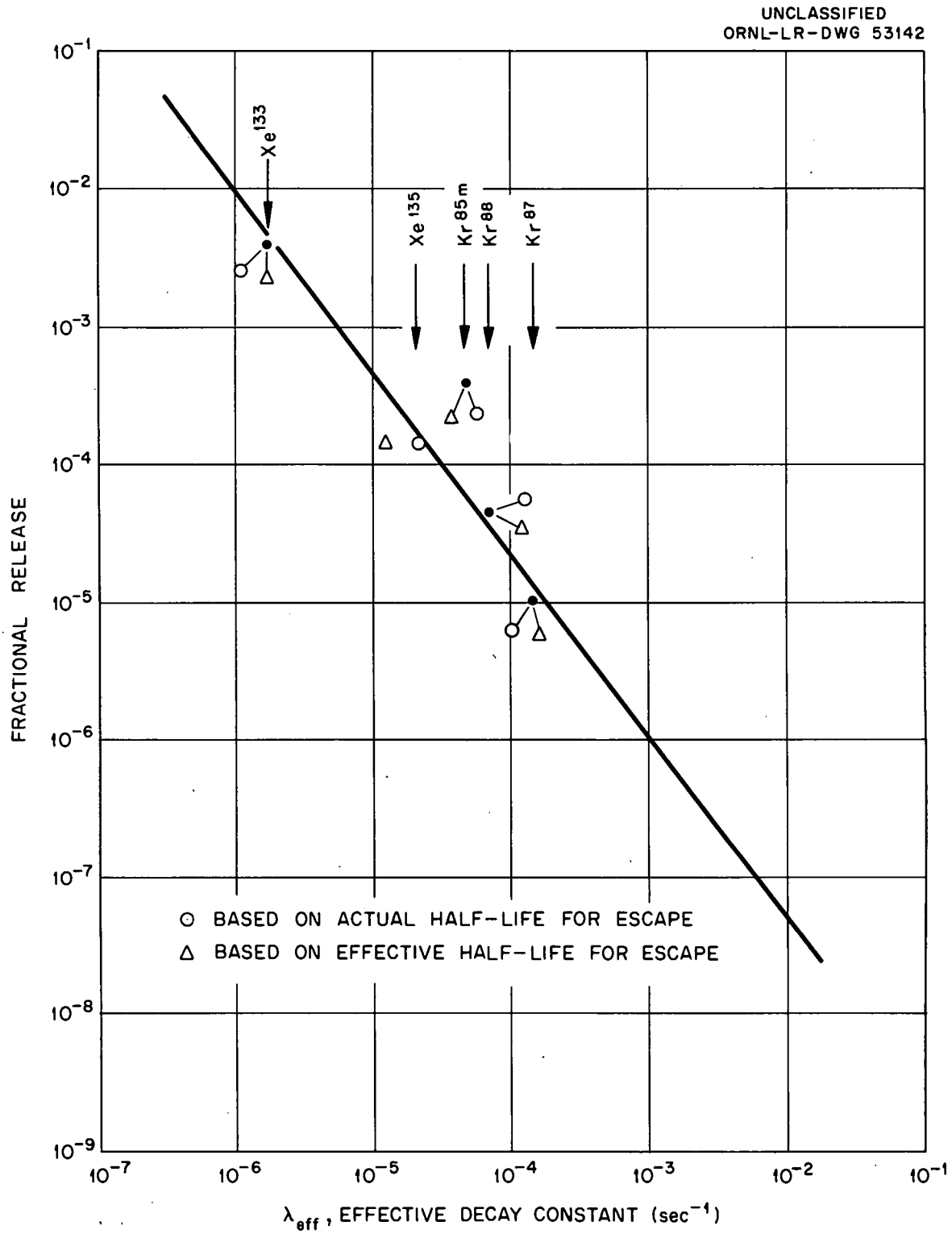

Fig. 19.1. Fractional Fission-Product Release from Alumina-Coated UO_2 Particles Based on BMI Experiment for Uranium Burnup of 4.8%.

argument, however, it would also be expected that the amount of time available for escape of a nuclide would include the times available to all mobile members which precede it in its decay chain. For example, in the chains in which iodine precedes xenon, the amount of xenon which appears external to the fuel is affected by both the iodine and xenon half-lives.

Based on experience with UO_2 at Westinghouse and at Chalk River,[1] only the noble gases, the halides, and the alkali metals would be expected to escape in appreciable quantities by diffusion from UO_2 at the temperature levels in the PBRE. All nuclides can escape by recoil, however, and about 5% of the fission products will recoil out of a spherical particle having a diameter of 150 μ. The fragments which recoil from the UO_2 would be brought to rest in the alumina coating. If the alumina enclosing the fission fragment were intact, escape of the fission product would be thought to be by solid-state diffusion. Some of the fission products which recoil into the alumina may come to rest, however, at locations that permit ready escape from the solid. Regardless of the mechanism by which the fission products escape into the gas phase, they must migrate to the surface of the graphite sphere by gas-phase diffusion before entering the coolant stream. Further, in order to escape into the gas phase, the fission product must be volatile at the conditions in the fuel.

The fission products which evidence indicates have some mobility in UO_2, i.e., xenon, krypton, iodine, barium, cesium, and rubidium, are also those which are volatile at the temperatures of interest. For this reason the fraction of escape from the fuel was assumed to be governed by the average time a fission product and its precursors are in one of the six mobile forms. In addition, tellurium was added as one of the volatile species because it has been found to escape from UO_2; it was detected in the "daughter trap" run of the BMI experiment.

---

[1]W. B. Cottrell, H. N. Culver, J. L. Scott, and M. M. Yarosh, "Fission-Product Release from UO_2," ORNL-2935, September 13, 1960.

The effective half-life of two or more nuclides in series, from the time of birth as the first member of the series to the time the last member decays, can be shown to be the sum of the half-lives of the individual members. Thus in plotting the release rate data one might logically use as the abscissa the effective decay constant which governs the escape of the nuclide, λ_{eff}, where

$$\lambda_{eff} = \frac{0.693}{(t^{1/2})_1 + (t^{1/2})_2 + \ldots} \quad . \qquad (1)$$

This was done for the BMI data. As may be seen by the data of Fig. 19.1 based on the effective half-life for escape, only the λ values for Xe^{133} and Xe^{135} were appreciably changed.

For this study the curve in Fig. 19.1 was employed to estimate the escape rates of all fission products of interest. The decay constant used for estimating the escape of a particular nuclide was that obtained using Eq. (1) and the half-lives of the mobile nuclides in the chain.

The procedure used for estimating fission-product release rates is subject to criticism both as being too pessimistic and too optimistic. It may be pessimistic in that the behavior of the first fuel element of this form ever tested at high burnup is being used to represent the behavior of the fuel which will be developed after at least two more years of intensive effort. The fuel particles used in the SP-5 capsule are from one of the first batches of that type to be prepared. An improvement in performance after further work seems likely.

On the other hand, the results of a test in which the fuel temperature probably did not exceed 1600°F are being used to estimate escape rates from a core in which some of the fuel may be above 2000°F. Where solid-state diffusion is controlling, the escape rate goes up rapidly with temperature. The rate at which the noble gases diffuse from UO_2 might be expected to increase about 9-fold between 1500 and 1800°F and 16-fold between 1500 and 2000°F. In contrast, little temperature dependence would be expected if the controlling step were gas-phase diffusion of particles which had escaped from the solid by recoil.

Unfortunately, the mechanism by which fission products are escaping the SP-5 capsule is not known, and there are no significant data on the effect of temperature on the escape rate.

The results of a study by Cottrell et al.[2] are of interest with regard to the mechanism of fission-product escape in another fuel. The behavior of fission products in a reactor (HGCR) fueled with an admixture of uncoated 200-μ-diam UO_2 particles in graphite was analyzed in detail. Fission products were considered to escape from UO_2 both by diffusion and by recoil. Those which recoiled from the UO_2 were presumed, however, to enter the graphite grains from which they escaped by diffusion. Strontium, barium, tellurium, and yttrium, in addition to the noble gases, halides, and alkali metals, were considered to diffuse from graphite. For the conditions assumed (with 33% of the fuel above 1600°F and 12% above 1800°F), the HGCR estimates show that only in the case of 26.6-y Cs^{137} was there more escape from the UO_2 by diffusion than by recoil. This indicates that, in the PBRE, diffusion is not likely to be as important as recoil in determining the escape rate from UO_2. Whether diffusion of the recoiled fission fragments from alumina is the controlling step cannot be stated at present.

In the HGCR study, about 11% of the Cs^{137} was estimated to escape from the fuel. The only other escape fraction exceeding 1% was that of Y^{90}, which was 5% (because of allowance for the mobility of 28-y Sr^{90} in graphite). In carrying out computations for the PBRE, the escape fraction was not permitted to exceed the recoil fraction of about 5%, since coated particles would be expected to give better fission-product retention than bare particles.

In this study, only those nuclides which might be important with respect to radiation or inhalation were included. Generally the nuclides considered were the hard gamma producers that are volatile or have a volatile precursor and that have chain yields exceeding 0.1%. All the halides having yields above 0.1% were included because of the greater

---

[2]W. B. Cottrell et al., "The HGCR-1, A Design Study of a Nuclear Power Station Employing a High-Temperature Gas-Cooled Reactor with Graphite-UO_2 Fuel Elements," ORNL-2653, July 14, 1959.

hazard associated with their escape. The nuclides considered are listed in the first column of Table 19.1, and their half-lives are listed in the second column. In the third column are the activities which would exist in the reactor after five years of steady operation at 10 Mw if no fission products were removed. The values in this table represent the equilibrium concentrations for most of the nuclides. Column 4 gives the effective decay constants for escape from the fuel, as obtained from Eq. (1). In column 5 are the fractional escape values obtained from Fig. 19.1 in the manner discussed earlier. Column 6 gives the activity which would exist in the reactor external to the fuel if there were no purification or escape of fission products; the values in column 6 are products of those in columns 3 and 5.

Column 7 presents the decontamination factors obtained assuming the purification system described in Chapter 16 with a 1% bypass flow. The purification factors for the alkali metals and those nuclides which are products of alkali metals were obtained by assuming that cesium and rubidium would remain gaseous in the coolant primary system and would be fractionally removed by complete trapping in the purification side stream. The tellurium activity was estimated in the same way, but the activities of the tellurium daughters were computed on the assumption that all the tellurium remained in the primary system. These assumptions are conservative with respect to normal leakage from the primary system. The saturation vapor pressure of cesium at the lowest operating temperature in the primary system (~500°F) is so high that more than a year of reactor operation (at full power) is required to reach the point of condensation from the helium. Thus, if there should be no mechanism other than condensation for its deposition in the primary system, cesium would pass into the purification system and be completely removed at the low temperatures encountered there. The likelihood that some cesium will be adsorbed on the loop surfaces, however, requires that cesium, as well as tellurium, be assumed to remain in the primary system when estimating shielding requirements.

Table 19.1. Estimated Fission-Product Escape Rates From Fuel and Resulting Activity Levels in Primary System

1	2	3	4	5	6	7	8	9	10
Nuclide	Half-Life	Total Activity In Reactor (curies)	Effective Escape, λ (sec^{-1})	Fractional Release Based on BMI Data	Loop Activity Without Purification (curies)	Purification Factor	Loop Activity With Purification (curies)	Fractional Release, HGCR Basis	Loop Activity With Purification, HGCR Basis (curies)
Br^{83}	2.4 h	4.0×10^{4}	8.02×10^{-5}	2.8×10^{-5}	1.1	6	0.2		
Br^{84}	30 m	9.2×10^{4}	3.85×10^{-4}	3.5×10^{-6}	0.32	2	0.2	7.25×10^{-4}	33
Kr^{83m}	114 m	4.0×10^{4}	4.45×10^{-4}	6.0×10^{-5}	2.4	1.9	1.3		
Kr^{85m}	4.36 h	1.3×10^{5}	4.41×10^{-5}	6.1×10^{-5}	8.0	2.0	4.0		
Kr^{85}	10.6 y	8.9×10^{3}	2.14×10^{-9}	5.0×10^{-2}	450	1	450		
Kr^{87}	78 m	2.4×10^{5}	1.48×10^{-4}	1.3×10^{-5}	3.1	1.9	1.7	1.8×10^{-3}	230
Kr^{88}	2.77 h	3.2×10^{5}	6.95×10^{-5}	3.4×10^{-5}	11	1.9	5.7	2.5×10^{-3}	420
Rb^{87}	4.5×10^{10} y	2.6×10^{-5}	3.54×10^{-19}	5.0×10^{-2}	$<10^{-5}$				
Rb^{88}	17.8 m	3.2×10^{5}	6.95×10^{-5}	3.4×10^{-5}	11	1.6	7	3.0×10^{-3}	610
Rb^{89}	15.4 m	4.1×10^{5}	6.2×10^{-4}	1.9×10^{-6}	0.77	1.5	0.5	9.0×10^{-4}	250
Sr^{90}	28 y	5.2×10^{4}	3.6×10^{-3}	1.9×10^{-7}	9.8×10^{-3}	1			
Y^{90}	64.5 h	5.2×10^{4}	3.6×10^{-3}	1.9×10^{-7}	9.8×10^{-3}	1		5.6×10^{-2}	2900
Sr^{91}	9.7 h	5.2×10^{5}	8.25×10^{-4}	1.3×10^{-6}	0.67	1	0.7	4.1×10^{-3}	2100
Y^{91m}	51 m	2.0×10^{5}	8.25×10^{-4}	1.3×10^{-6}	0.27	1	0.3	3.5×10^{-3}	700
Y^{91}	58 d	5.0×10^{5}	8.25×10^{-4}	1.3×10^{-6}	0.66	1	0.7	5.2×10^{-3}	2600
Y^{92}	3.6 h	4.8×10^{5}	8.35×10^{-4}	6.4×10^{-8}	3.1×10^{-2}	1		2.3×10^{-3}	1100
Y^{93}	10 h	5.7×10^{5}	(0.347)	$<10^{-9}$				4.0×10^{-4}	230
Y^{94}	16.5 m	5.7×10^{5}	(0.495)	$<10^{-9}$		1		2.0×10^{-4}	110
Zr^{95}	65 d	1.1×10^{4}	(≥ 1)	$<10^{-9}$	$<10^{-5}$			1.0×10^{-5}	
Nb^{95}	35 d	7.0×10^{4}	(≥ 1)	$<10^{-9}$	$<10^{-4}$			1.0×10^{-5}	
I^{131}	8.05 d	2.5×10^{5}	9.96×10^{-7}	8.6×10^{-3}	2200	560	4.0	5.1×10^{-3}	2.3
I^{132}	2.4 h	3.9×10^{5}	2.24×10^{-6}	2.7×10^{-3}	1000	8	130	6.0×10^{-4}	29
I^{133}	20.8 h	5.7×10^{5}	9.25×10^{-6}	4.3×10^{-4}	240	61	3.9	1.8×10^{-3}	17
I^{134}	52.5 m	6.7×10^{5}	1.19×10^{-4}	1.7×10^{-5}	11	2.8	3.9	3.0×10^{-5}	7.2
I^{135}	6.68 h	5.2×10^{5}	2.89×10^{-5}	1.1×10^{-4}	57	20	2.8	9.0×10^{-4}	23
I^{129}	1.72×10^{7} y	1.8×10^{-2}	1.28×10^{-15}	5.0×10^{-1}	8.9×10^{-3}				
I^{136}	86 s	2.7×10^{5}	8.06×10^{-3}	6.7×10^{-8}	1.8×10^{-2}				
Xe^{131m}	12 d	2.5×10^{3}	6.68×10^{-7}	5.0×10^{-2}	130	13	9.3		

Table 19.1 (continued)

1	2	3	4	5	6	6	8	9	10
Nuclide	Half-Life	Total Activity In Reactor (curies)	Effective Escape, λ (sec^{-1})	Fractional Release Based on BMI Data	Loop Activity Without Purification (curies)	Purification Factor	Loop Activity With Purification (curies)	Fractional Release, HGCR Basis	Loop Activity With Purification, HGCR Basis (curies)
Xe^{133m}	2.3 d	1.4×10^4	2.5×10^{-6}	2.6×10^{-3}	37	12	3.0		
Xe^{133}	5.27 d	5.6×10^5	1.33×10^{-6}	5.8×10^{-3}	3200	13	250		
Xe^{135m}	15.6 m	1.6×10^5	2.8×10^{-5}	1.5×10^{-6}	0.24	1.6	0.1	1.5×10^{-3}	150
Xe^{135}	9.13 h	5.4×10^5	1.2×10^{-5}	3.3×10^{-4}	180	10	18	4.1×10^{-3}	220
Xe^{137}	3.9 m	5.2×10^5	2.70×10^{-3}	2.8×10^{-7}	0.14	1	0.1		
Xe^{138}	17 m	4.8×10^5	6.79×10^{-4}	1.7×10^{-6}	0.820	1.6	0.5		
Xe^{139}	41 s	4.1×10^5	1.6×10^{-2}	2.8×10^{-8}	1.2×10^{-2}				
Xe^{140}	16 s	3.2×10^5	4.3×10^{-2}	8.0×10^{-9}	2.6×10^{-3}				
Cs^{135}	3.0×10^6 y	0.63	7.3×10^{-15}	5.0×10^{-2}	3.1×10^{-2}				
Cs^{137}	26.6 y	6.8×10^4	8.27×10^{-10}	5.0×10^{-2}	3400	4.9×10^5			
Ba^{137m}	2.6 m	6.2×10^4	8.27×10^{-10}	5.0×10^{-2}	3100	4.9×10^5		1.1×10^{-1}	
Cs^{138}	32 m	5.1×10^5	2.36×10^{-4}	6.7×10^{-6}	3.4	2.1	1.6	1.8×10^{-3}	440
Cs^{139}	9.5 m	5.2×10^5	1.62×10^{-3}	5.4×10^{-7}	0.28	1.3	0.2		
Ba^{139}	85 m	5.2×10^5	1.62×10^{-3}	5.4×10^{-7}	0.28	1	0.3	1.0×10^{-3}	520
Cs^{140}	66 s	5.3×10^5	1.22×10^{-2}	3.9×10^{-8}	2.1×10^{-2}				
Ba^{140}	12.8 d	5.3×10^5	1.22×10^{-2}	3.9×10^{-8}	2.1×10^{-2}			4.0×10^{-3}	2100
La^{140}	40.2 h	5.3×10^5	1.22×10^{-2}	3.9×10^{-8}	2.1×10^{-2}			4.0×10^{-3}	2100
Cs^{142}	1 m	3.0×10^5	1.62×10^{-2}	2.7×10^{-8}	8.1×10^{-3}				
Ba^{142}	6 m	3.0×10^5	1.62×10^{-2}	2.7×10^{-8}	8.1×10^{-3}				
La^{142}	74 m	3.0×10^5	1.62×10^{-2}	2.7×10^{-8}	8.1×10^{-3}			1.8×10^{-3}	530
Te^{133m}	63 m	4.0×10^5	1.83×10^{-4}	9.1×10^{-6}	3.7	3.4	1.1		
Te^{133}	2 m	5.3×10^5	5.78×10^{-3}	1.0×10^{-7}					
Te^{134}	44 m	5.9×10^5	2.63×10^{-4}	5.7×10^{-6}	3.4	2.6	1.3		
Te^{135}	2 m	3.7×10^5	5.78×10^{-3}	1.0×10^{-7}					
Te^{127m}	90 d	4.9×10^3	8.82×10^{-8}	5.0×10^{-2}	250	4800			
Te^{127}	9.3 h	2.2×10^4	2.07×10^{-5}	1.6×10^{-4}	3.6	21	0.2		
Te^{129m}	33 d	3.0×10^4	2.43×10^{-7}	5.0×10^{-2}	1500	1700	0.9		

Table 19.1 (continued)

1	2	3	4	5	6	7	8	9	10
Nuclide	Half-Life	Total Activity In Reactor (curies)	Effective Escape, λ (sec^{-1})	Fractional Release Based on BMI Data	Loop Activity Without Purification (curies)	Purification Factor	Loop Activity With Purification (curies)	Fractional Release, HGCR Basis	Loop Activity With Purification, HGCR Basis (curies)
Te^{129}	72 m	9.0×10^{4}	1.60×10^{-4}	1.1×10^{-5}	1.0	3.5	0.3		
Te^{131m}	30 h	3.9×10^{4}	6.42×10^{-5}	3.7×10^{-5}	1.4	63			
Te^{131}	24.8 m	2.5×10^{5}	4.66×10^{-4}	2.8×10^{-6}	0.7	1.9	0.4		
Te^{132}	77 h	3.9×10^{5}	2.50×10^{-6}	2.6×10^{-3}	1000	160	6.2		

The nuclides other than the noble gases, halides, and alkali metals were assumed to be unaffected by processing, as indicated by values of unity in column 7. Column 8 gives the primary loop activity which would occur with processing of the coolant at the rate assumed. Values are given in column 8 for only those nuclides whose activity was high enough to be significant.

It is of interest to obtain release rates using a different set of assumptions to see how the activity levels compare with those obtained above. This has been done by taking the fractional release values computed by Cottrell et al.[2] for uncoated UO_2 particles in the HGCR and applying them to the conditions of the PBRE. The values for HGCR were used directly without attempting adjustment for the difference in temperature distributions in the two systems, since an estimate of the fractions of the fuel volume within various temperature ranges for the PBRE gave values fairly similar to those used for HGCR. Column 9 of Table 19.1 shows the fractional release estimated for the HGCR for the nuclides listed. Column 10 gives the activity which would be present in the PBRE with the release rates shown in column 9.

The loop activity estimated for the uncoated particles is much greater for many of the nuclides than the activities obtained for coated particles by using the BMI data. This is particularly true for the nuclides of barium, yttrium, and strontium, which were themselves considered to be mobile (in graphite and in the gas phase) in the HGCR studies, but were considered to be mobile only through their volatile precursors in using the BMI data. There is considerable uncertainty as to the manner in which these materials would actually behave at the PBRE temperatures. The authors of the HGCR report were required by lack of other data to extrapolate high-temperature results down to the temperature range of interest. Large amounts of nonvolatile materials deposited in the primary loop would be particularly troublesome with regard to maintenance if lodged in or near troublesome equipment, but they probably would not be important with regard to the activity escape

which accompanies helium leakage under normal conditions. As with tellurium, the longer lived species would be removed by processing if they remained suspended in the main gas stream, and, if not, they would not escape from the gas system at low helium leakage rates.

Hazards Associated with Gas Leakage

In assessing the hazards associated with the activity present in the reactor coolant, two conditions have been examined: (1) the activity release which accompanies normal leakage of helium from the primary system, and (2) the activity released in the event of a rupture of the primary system. The escape rate of activity from the reactor has been computed assuming a helium leakage rate from the reactor of 0.1% of the primary system helium inventory per day, and the results are tabulated in Table 19.2 for the significant nuclides. The activity was assumed to escape in proportion to the amount estimated to be present after allowances for purification, as listed in column 8 of Table 19.1. Included in Table 19.2 are the activities of A^{41} and H^3. The A^{41} activity is produced in the shield cooling air by neutron capture in A^{40}, and the generation rate was estimated to be one-fourth of the 400 curies/day computed for the EGCR at 84 Mw(t).[3] The activities of 7.3-s N^{16} and 29-s O^{19} were neglected because of their short half-lives. The tritium activity level was based on an estimate by Sanderson & Porter[4] for a larger reactor and was reduced from their computed value in proportion to the power level.

In order to keep the activity which escapes under normal conditions from contaminating the atmosphere in the containment vessel, the shield cooling air and the air introduced into the vessel for other purposes would be withdrawn in the vicinity of the reactor and discharged from there up the stack. Thus the air movement within the containment vessel should always be toward the reactor. The air flow rate through the containment vessel was assumed to be at a rate sufficient to replace the

---

[3]"Experimental Gas-Cooled Reactor Preliminary Hazards Summary Report," ORO-196 (supplement), May 1959.

[4]Progress Report, Pebble Bed Reactor Program, NYO-2373.

Table 19.2. Activity Levels Resulting from Helium Leakage Under Normal Operating Conditions[a]

1	2	3	4	5	6	7	8
Nuclide	Half-Life	Activity Escape Rate from Reactor with 0.1%/day Leakage (curies/day)	Activity Concentration at Stack Entrance ($\mu c/m^3$)	Occupational MPC ($\mu c/m^3$)	Fraction of Occupational MPC at Stack Entrance	Maximum Ground Concentration ($\mu c/m^3$)	Fraction of Non-occupational MPC[b] at Maximum Ground Concentration
Kr^{85}	10.6 y	1.3	2.4	3.0	0.8	6.4×10^{-4}	2.0×10^{-3}
I^{131}	8.05 d	4.0×10^{-3}	7.5×10^{-3}	3.0×10^{-3}	2.5	2.0×10^{-6}	7.0×10^{-3}
I^{132}	2.4 h	0.17	0.33	0.08	4.1	8.6×10^{-5}	1.1×10^{-2}
I^{133}	20.8 h	3.9×10^{-3}	7.3×10^{-3}	0.01	0.7	1.9×10^{-6}	2.0×10^{-3}
I^{135}	6.68 h	2.8×10^{-3}	5.3×10^{-3}	0.04	0.1	1.4×10^{-6}	3.0×10^{-4}
Te^{127m}	90 d	5.1×10^{-5}	9.6×10^{-5}	0.05	2.0×10^{-3}	2.5×10^{-8}	5.0×10^{-6}
Te^{129m}	33 d	8.8×10^{-4}	1.7×10^{-3}	0.01	0.17	4.3×10^{-7}	4.3×10^{-4}
Te^{132}	77 h	6.3×10^{-3}	1.2×10^{-2}	0.04	0.3	3.1×10^{-6}	8.0×10^{-4}
H^3	12.3 y	0.73	1.4	5.0	0.3	3.6×10^{-4}	7.0×10^{-4}
A^{41}	1.83 h	50	94	0.4	240	2.5×10^{-2}	0.62

[a]Assumes removal of circulating activity, including cesium and tellurium, by coolant purification.

[b]10% of occupational MPC.

air in the vessel once per hour. The activity at the stack entrance with this flow rate is given in column 4 of Table 19.2.

To provide a frame of reference for judging the importance of the activity shown, column 5 of Table 19.2 gives the MPC (maximum permissible concentration) of the nuclides listed under occupational exposure conditions.[5] Column 6 gives the fraction of MPC which would exist at the entrance to the stack. The values in columns 4 and 6 represent the equilibrium concentrations which would exist in the containment vessel if the air in the vessel were completely mixed before discharge. The level of airborne activity outside the shield, however, should actually be very much less than that based on complete mixing, since air movement would be toward the reactor vessel. On the other hand, the fission-product escape rate could be considerably higher than that shown in Table 19.2 if the fuel retained fission products less well than assumed, or if the leak rate from the primary system were, say, 1%/day rather than 0.1%. However, the air flow pattern designed to keep fission products from circulating outside the shield would still be effective in limiting activity levels in the containment vessel. The possibility of an abnormal release of activity, of course, is another matter which affects the advisability of designing for personnel to be in the containment vessel when the reactor is at power or at full pressure.

To estimate the maximum ground concentration which would exist under normal conditions, the dilution computed for EGCR under a condition of a strong inversion was assumed. The EGCR analysis, as described in the preliminary hazards report,[3] was based on a stack height of 200 ft above ground level and a wind velocity of 4.9 ft/sec. The maximum ground concentration was estimated to occur at a distance downwind of 7900 ft. For this condition the activity is computed by the following equation:

$$\chi_{max} = \frac{Q}{2.38 \times 10^4} , \qquad (2)$$

[5]"Maximum Permissible Body Burden and Maximum Permissible Concentrations of Radionuclides in Air and in Water for Occupational Exposures," U. S. Dept. of Commerce, NBS Handbook 69, June 5, 1959.

where χ_{max} is the activity concentration in $\mu c/m^3$ and Q is the activity release rate in $\mu c/sec$. In this computation, the activity escape rate was again that given in column 3 in Table 19.2. No credit was taken for removal of activity from air entering the stack by filtration or iodine absorption. Column 7 is the maximum ground concentration under normal conditions of activity escape as computed using Eq. (2). Column 8 gives the maximum ground concentration as a fraction of nonoccupational MPC (10% of the value given in column 5).

As shown by Table 19.2, the estimated activity release under normal conditions would not exceed the MPC for any of the nuclides considered. Further, a factor of 100 increase in either the escape rate from the fuel or the leakage rate from the reactor, or a combination of these, would still not bring the estimated maximum ground concentration above the permissible level for any nuclide except I^{132}. Since the fractional release used for I^{132} was 0.37%, it is very unlikely that the actual escape rate from the fuel would be over ten times that assumed. To bring the estimated maximum ground concentration above the MPC would require that a tenfold increase in the escape fraction be coupled with a tenfold increase in leakage rate from the reactor. Even if the escape rates from the reactor were much higher than assumed, stack filters could be provided to reduce the release rates to tolerable levels.

Hazard Associated with Rupture of Primary System

The second condition considered in assessing hazards is that associated with a rupture of the primary system. Such an accident, however unlikely, could lead to combustion of the graphite fuel balls by the oxygen present in the containment vessel. The surface temperature of much of the fuel is high enough for rapid combustion, the surface-to-volume ratio is high, and most of the fission-product heat would be released in the fuel. These conditions are all more severe than those which exist in a graphite-moderated reactor, such as the EGCR, in which the fuel is separated from the moderator.. Whether the fuel would

be exposed to sufficient oxygen to produce rapid combustion before it could be cooled below the ignition point is a question requiring extensive analysis.

It may well be that, as discussed in Chapter 8, the graphite spheres will have to be coated to prevent their oxidation by the small amount of CO_2 which contaminates the helium under normal conditions. At the moment there appears to be no technique for applying nonpermeable silicon-carbide coatings at temperatures acceptable for alumina-coated particles dispersed in graphite. However, application of low-permeability coatings that would greatly reduce oxidation rates may be possible. A coating having this property would permit the bed to be cooled without extensive oxidation, even in the presence of air.

Another approach is to exclude the possibility of oxygen getting to the core in the event of a rupture by providing an inert atmosphere, such as nitrogen, in the containment vessel. Although it may not be reasonable to have the entire vessel filled with nitrogen, having an inert-gas-filled inner container surrounding the contaminated parts of the reactor might be feasible. This container could be fitted with pressure-relief devices to permit rapid equalization between it and the rest of the vessel so that it would not have to withstand a pressure difference. Its leaktightness would only have to be such as to keep the oxygen content of the gas blanket fairly low. Even in the event the inner container were penetrated by a missile, the oxygen concentration in the blanket gas would be low for a time, and the concentration in the core would be still lower (particularly if the reactor rupture were a single-ended failure).

If the possibility of combustion of the fuel cannot otherwise be excluded, it may be possible to provide for quenching a fire or preventing one by injection of steam or water or an oxidation-inhibiting chemical, such as chlorine.

The consequences of extensive combustion of graphite may be severe. The containment vessel has an air content that is sufficient to oxidize 5100 lb of graphite to CO_2. If a rupture of the reactor and the heat

exchanger were followed by complete reaction of the oxygen with graphite, the final pressure in the system would be about 20 psig and the temperature about 700°F. In performing this computation, all the graphite and steel in the system (including the containment vessel) were considered to come to temperature equilibrium with the gas, but no allowance was made for heat storage in the concrete shield. If all or part of the 880 lb of fuel were consumed, there would obviously be a substantial release of activity to the containment vessel. The leaktightness requirement imposed on the containment vessel by the possibility of a large activity release is discussed later.

A rupture of the reactor without oxidation of the graphite would not result in a significant pressure increase in the containment vessel. Escape of the helium at 1000 psig and an average temperature of 900°F would increase the containment vessel pressure only 1.0 psi and raise the gas temperature 17°F (assuming no heat transfer from the gas to the structure). Rupture of the steam system would increase the pressure only an additional 0.3 psi and the temperature only 5°F. Hence, the conditions following rupture of both steam and helium systems (without heat loss) would be a pressure of 1.3 psig and a temperature rise of 22°F above the initial temperature.

In the event of a rupture, even if both blowers continue to function, the heat removal capability of the system will be greatly reduced because of the reduced density of the coolant. An analysis of this condition would depend on knowledge of the blower characteristics, but the circulation rate of either air or helium at atmospheric pressure will probably be sufficient to prevent excessive temperatures in the core. If both blowers fail, however, natural thermal-convection cooling will not be sufficient at a system pressure near atmospheric to prevent the fuel temperature from increasing. Should the temperature become high enough for a rapid reaction of the alumina and graphite (approximately 3000°F), a significant fission-product release would occur, and, if the melting point of UO_2 were reached, the release would be even greater.

The maximum credible accident would be a rupture of the reactor which would lead to melting or oxidation of the fuel. If oxidation of the graphite cannot be excluded as a possibility, the containment vessel will have to be capable of withstanding the maximum temperature and pressure that are credible. Design of a vessel which will retain its integrity at 20 psig and 700°F, the values estimated for reaction of all oxygen present to produce CO_2, is not unreasonable.

An estimate was made of the leaktightness requirement imposed on the containment vessel by the possibility of UO_2 meltdown or oxidation. Leakage from the container at ground level was assumed, and the limiting emergency dose at the perimeter of a 1000-ft-radius exclusion area was taken as 25 rem in an 8-hr period. The activity release was obtained by assuming that 100% of the noble gases would be released from the fuel along with 50% of the other volatile nuclides (halogens and alkali metals) and 5% of the nonvolatile nuclides. Dose rates were estimated by adjustment of values in the EGCR preliminary hazards report to the conditions assumed for the PBRE. The results indicated a permissible leakage rate of 0.4%/day of the gas in the containment vessel. The permissible leakage was computed to be limited by the internal dose rate from radioactive iodine.

Radiation Levels with Shielding

The presence of fission-product activity in the helium coolant and the possibility of activity depositing on surfaces which are outside the core requires heavy shielding around all pipes and components which contain contaminated gas. Estimates of dose levels which would exist at the external surface of a 3-ft-thick concrete shield were made to determine whether the shielding specified for the reactor components is adequate.

The results for the nuclides of importance with regard to gamma radiation are summarized in Table 19.3. Column 3 gives the total gamma

Table 19.3. Hard-Gamma Radiation Dose Rates Near Reactor System With and Without Shielding

1	2	3	4	5	6
Nuclide	Half-Life	Total Gamma Energy Per Disintegration (Mev)	Dose Rate at Shield Surface with No Purification (mr/hr)	Unshielded Surface Dose Rate During Operation[a] (mr/hr)	Unshielded Dose Rate 24 hr After Shutdown[a] (mr/hr)
Br^{84}	30 m	2.21	1.1×10^{-3}	17	
Kr^{87}	78 m	1.07	1.5×10^{-3}	66	
Kr^{88}	2.77 h	1.65	1.7×10^{-2}	790	2
Rb^{88}	17.8 m	0.955	6.2×10^{-3}	300	
I^{131}	8.05 d	0.080	5.5×10^{-6}	15	14
I^{132}	2.4 h	2.01	0.85	1.6×10^{4}	1.3×10^{4}
I^{133}	20.8 h	0.555	1.5×10^{-4}	100	55
I^{135}	6.68 h	1.92	7.2×10^{-3}	250	20
Ba^{137m}	2.6 m	0.661	8.3×10^{-5}	9.4×10^{4}	9.4×10^{4}
Ba^{139}	85 m	0.272	4.0×10^{-6}	8	
La^{140}	40.2 h	2.10	5.3×10^{-6}		
Xe^{135}	9.13 h	0.024	3.9×10^{-8}	10	1
Cs^{138}	32 m	2.14	2.1×10^{-3}	21	

[a]Assumes removal of circulating activity, except for tellurium and cesium, by coolant purification.

energy accompanying decay of the nuclides. The values in Column 4 represent the dose rate at the surface of the 3-ft-thick shield from radiation originating in a 1-ft-diam pipe. The activity in the pipe was estimated by assuming that all the activity in the primary system would be distributed uniformly throughout its volume. This assumption is obviously not valid with regard to nonvolatile nuclides which deposit preferentially at points throughout the system. No further treatment was made of the barium and lanthanum activities for the shielded system, since, even with a thousandfold increase, they would still not represent important sources. The I^{132} is the major radiation source, contributing 50 times as much to the dose rate as Kr^{88}, the next largest source. Over a hundredfold increase in I^{132} activity would be required to make the dose rate exceed 100 mr/hr, and well over a thousandfold increase would be required for any other nuclide. A hundredfold increase in I^{132} activity does not seem reasonable, since the fractional release used to compute the activity level is already 0.37%, although the surface adsorption of iodine throughout the system would increase the doses from iodine over the amounts shown here. However, iodine is believed to remain volatile, and furthermore the I^{132} activity would be less than that computed if its 77-h Te^{132} precursor were removed by processing. With processing of the coolant, the dose rate from I^{132} would be reduced to 0.11 mr/hr (still assuming that tellurium is not affected by processing), and the dose rate from Kr^{88} would be reduced to 0.01.

Radiation Level Without Shielding

An indication of the radiation level which would exist near components of the primary system without shielding was obtained because of its effect on the possibility of direct maintenance. The hard-gamma dose rate at the surface of a bare 1-ft-diam pipe containing activity in proportion to its fraction of the total volume was estimated. The dose rates are given in column 5 of Table 19.3 for the activity levels

which would exist with coolant purification but with the assumption that only tellurium and cesium deposit in the primary system. The conditions which would exist at full power and 24 hr after shutdown are shown in column 6. The unshielded dose rate is quite high because of the radiation from I^{132} and Ba^{137m}. These activity sources would be considerably reduced if the tellurium and cesium parents of iodine and barium were removed from the system by coolant purification. The source would be intensified, however, if iodine were adsorbed on the system surfaces or if preferential adsorption of cesium at some point in the system resulted in a concentration of the Ba^{137m}. Ba^{137m}, whose effective half-life is determined by that of its 26.6-y Cs^{137} precursor, does not decay rapidly enough for the computed activity level to decrease appreciably with time.

The unshielded radiation levels given in Table 19.3, if encountered in practice, are sufficiently high to discourage direct maintenance of components in the primary system. There is a possibility, however, that tellurium and cesium remain in the vapor phase long enough to be affected by processing. Alternatively, their preferential deposition in the heat exchanger might leave the dose level in other components appreciably lower than indicated by Table 19.3. Successful removal of the important radiation sources by decontamination would, of course, also completely alter the situation with regard to direct maintenance.

The dose rates listed in Table 19.3 are only those from hard-gamma-emitting nuclides. Without shielding, the gamma rays less energetic than those considered here could be an important radiation source. This has not been examined in detail, but, in general, the nuclides emitting weak gamma rays (less than 0.4 Mev) decay more rapidly than those emitting hard gamma rays. In addition, relatively light portable shielding would be effective in reducing the dose level from weak gamma sources.

Natural-Circulation Cooling

The PBRE has been designed with the intention that natural circulation of helium will be adequate for cooling the core in the event both

blowers cease to operate. This capability would exist only if the helium pressure remained near its design value. Thermally induced circulation would not be adequate for cooling at atmospheric pressure.

The height required to remove various fractions of the design power has been estimated for specified helium exit temperatures. In all cases the gas was assumed to return to the core at 550°F. The pressure drop through the core was obtained using Eq. (7) of Chapter 10. This relation is still applicable at the flow rates associated with natural-circulation. The flow resistance external to the core was based on a design that under normal conditions would cause a pressure drop of 3.5 psi. Allowance was made for the change to laminar flow in the heat exchanger at low circulation rates.

The results of the natural-circulation calculations are presented in Fig. 19.2. The decrease in fission-product energy release rate with time is also shown. The "effective height" of the ordinate is that height to be used in computing the buoyancy driving force with the densities taken as those at the core and heat exchanger exits; it is approximately the vertical distance from the center of the core to the center of the heat exchanger.

Assuming that the control rods are inserted soon after loss of power to the blowers, blower coast-down could provide adequate flow for the first 2 1/2 min. (Presumably loss of power is the only event which would stop both blowers; any accident of a type which would stop a blower from coasting is unlikely to affect both simultaneously.) After 2 1/2 min, natural circulation must remove about 3% of the power at which the reactor has been operating. The exit gas could leave the core at about 1500°F without damaging the piping or the heat exchanger. As shown in Fig. 19.2, an effective height of about 26 ft would be required to remove 3% of full power with a core exit temperature of 1500°F and with the system at 900 psia.

The height required for a given power removal capability and a given exit gas temperature is inversely proportional to the square of the

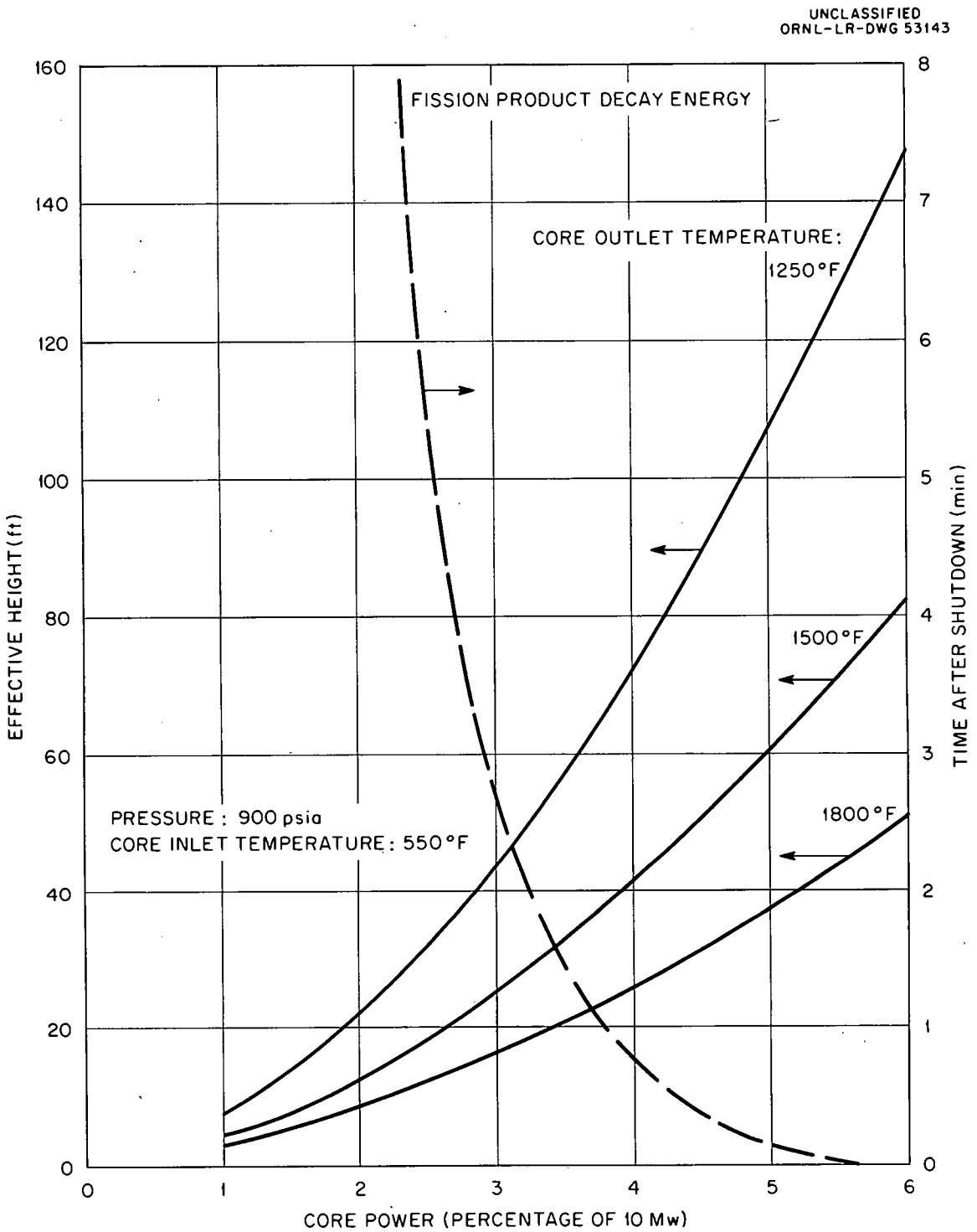

Fig. 19.2. Required Elevation of Heat Exchanger Above Core for Natural-Circulation Cooling.

absolute pressure. Thus, if the pressure were only 450 psia, the required height would be four times as great as that required at 900 psia.

Heat Exchanger Tube Rupture

The reactor secondary system would be operated to maintain the pressure of steam in the heat exchanger greater than the pressure of helium in the core. Hence a heat exchanger tube rupture would result in the leakage of steam into the primary system. The operations performed following detection of moisture in the helium are discussed in Chapter 12.

Two consequences of a tube rupture have been considered briefly: (1) the addition of reactivity which would result from moisture entering the core, and (2) the reaction of steam with graphite in the core. The reactivity addition was computed by assuming that all the void volume of the core contained steam at a pressure corresponding to saturation at 550°F (37.6 g per liter of void). A value of 2.6% $\Delta k/k$ was obtained. This is substantially smaller than the reactivity which can be controlled by the poison rods, since the cold, clean shutdown margin is 6% $\Delta k/k$.

The surface temperature of the fuel in the PBRE core will be high enough for a reaction to occur between steam and any uncoated graphite. This reaction is endothermic, with an energy adsorption of 32 400 cal/g·mole. Hence the reaction will cool the graphite and, if sufficient water is available, will eventually reduce its temperature to below that at which the reaction rate is significant (above 1000°F).

Neglecting fission-product decay heat, about 6% of the graphite, which is initially at 1800°F, would be gasified in reducing the temperature to 1000°F. Allowing for the fission-product heat generated in 10 min, about 10% of the graphite would react. If the bed were being cooled by convection, as well as by the reaction, less graphite would be oxidized than is indicated by the above numbers.

The hydrogen and carbon monoxide products of the carbon-water reaction are both combustible. No oxygen would be available to produce an explosive mixture, however, unless there was a subsequent rupture of the primary system.

Hazards Summary and Conclusions

The amounts of fission-product activity released from the PBRE under normal conditions and following the maximum credible accident have been estimated. From the results one may conclude that the highest ground concentration of activity normally released from the stack will not exceed the maximum permissible concentration. Further, if the reactor system is housed in a conventional containment vessel, the exposure to the public from the maximum credible accident will be well below the acceptable limit of 25 rem. In contrast to these conclusions regarding hazards to the public, the dose rate to be expected for personnel performing maintenance operations on the reactor can be stated with little certainty. The results obtained for these and other conditions are summarized below.

Maximum Credible Accident

The containment vessel design criterion for the PBRE is predicated upon a rupture of the primary coolant system which results in oxidation or melting of the fuel material. If allowance is made for reaction of all the oxygen within the container with graphite, the design temperature and pressure are 20 psig and 700°F, respectively. Melting or oxidation of the fuel was assumed to release 100% of the noble gases, 50% of the volatile products (notably iodine), and 5% of the nonvolatile products to the containment vessel. With leakage of 0.4%/day of the container volume at ground level, the resulting exposure 1000 ft downwind for an inversion condition would not exceed 25 rem in an 8-hr period.

Normal Activity Release

About 900 curies of fission-product activity was estimated to circulate in the primary system at equilibrium conditions with chemical processing of the coolant. The individual activities comprising this total were used in evaluating the activity leakage from the reactor

and its disposal from the containment vessel. A leakage rate of 0.1%/day of the helium in the primary system was used in estimating fission-product escape from the reactor.

The release rates of fission products from the alumina-coated UO_2 fuel particles were based on the data obtained for several xenon and krypton isotopes in the experiment presently in progress at BMI. The data employed in the analysis correspond to a uranium burnup of 4.8%, which approaches the value expected in the PBRE. The average fuel temperature in the reactor may, however, be several hundred degrees above that of the fuel in the BMI test. Unfortunately, sufficient experimental data do not exist to permit a quantitative estimate of the increase in release rate with temperature.

In estimating the activity escape from the fuel, release rates of the halides (iodine, bromine), alkali metals (cesium, rubidium), and tellurium were assumed to follow the same release vs decay constant dependence as that exhibited by the noble gases. All nonvolatile nuclides were assumed to exist in the gas only as a result of decay from a gaseous precursor.

The activity released from the fuel circulates with the primary coolant from which it may be removed by the following processes: (1) filtration in a total-stream filter, (2) filtration in the bypass cleanup system, (3) deposition and adsorption on the system surfaces, and (4) decay and leakage. Unfortunately, the removal efficiencies of mechanisms 1 and 3 are not known with much certainty. It may be shown, however, that even if these mechanisms do not remove activity from the gas, operation of the bypass cleanup system will provide an upper limit on the activity concentration in the circulating coolant. This limiting concentration was the basis for the estimate of activity leakage from the reactor under normal conditions.

The estimated fission-product release rates involve considerable uncertainty, particularly with regard to the effects of greater uranium burnup and higher fuel temperature. Hence the fission-product escape rates based on these values cannot be considered conservative with

regard to present knowledge. It is not unreasonable, however, to expect that before completion of the PBRE additional work on fuel materials may effect further improvements in their ability to retain fission products. In any case, the computed activity release rates for normal conditions are low enough that a hundredfold increase would be required to exceed the maximum permissible concentrations.

Direct Radiation Dose Rates from Reactor Components

Even if there were no purification of the coolant, the dose rate at the surface of the 3-ft-thick shield would be within tolerable limits. Dose rates from unshielded piping, however, may exceed 100 rem/hr 24 hr after shutdown. The dose rate estimate is particularly dependent on the assumptions made regarding the deposition or adsorption of tellurium and cesium on surfaces in the primary system. If these elements are deposited in favorable locations or removed by the coolant purification system, the reduced activities of their I^{132} and Ba^{137m} daughters may lower the dose level appreciably below the 100-rem value quoted. The same effect would, of course, be achieved by decontamination of the system before maintenance is attempted. A higher local dose rate than 100 rem/hr could exist, however, if there were preferential adsorption of the important nuclides on the component to be handled. Thus lack of knowledge about activity deposition and adsorption makes it impossible to predict accurately the conditions which will exist with regard to maintenance operations.

Other Conditions

Two other conditions which were examined are heat removal in case of blower failure and the consequences of a heat exchanger tube rupture. Natural circulation appears to be adequate for cooling the fuel in the event of simultaneous blower failures, as long as the helium pressure remains near its design value. Temperatures in the reactor would not be limited, however, to reasonable values by natural circulation if the pressure fell much below 900 psi.

A heat exchanger tube leak would admit steam into the primary system that would react with graphite in the core. Fortunately, this reaction is endothermic and would result in a lowering of the graphite temperature until a level were reached at which the reaction rate would cease to be significant.

20. RESEARCH AND DEVELOPMENT

As indicated in the previous chapters, and particularly in the discussion on the fuel element (chap. 8), there are a number of serious problems to which favorable solutions must be found before a pebble-bed reactor can be properly designed and built. A preliminary estimate of the research and development program required is presented here.

Fuel Element Development

The major questions that must be resolved before the fuel elements for a pebble-bed reactor core loading can be obtained with confidence are, first, the rate of fission-gas release as a function of temperature and burnup for, not only Al_2O_3-coated UO_2 particles, but also BeO-coated UO_2 and pyrolytically carbon-coated UC_2, all dispersed in a graphite matrix. Second, information is needed with respect to the oxidation of graphite by impurity gases, primarily CO_2 and H_2O, in the coolant stream. The rates of these reactions are complex functions of temperature, pressure, gas flow rate, gas composition, graphite characteristics, and probably radiation. The need for an oxidation-resistant surface coating must be carefully assessed because the temperatures required to apply Si-SiC, the most promising coating for this purpose, would preclude the use of Al_2O_3- or BeO-coated UO_2 as the fuel particles. At the 3500 to 3600°F coating-application temperature, both of these compounds react excessively with graphite.

The fuel element development program should be designed to take full advantage of the extensive coated-fuel-particle work now being sponsored at Battelle by the Atomic Energy Commission. The funds allotted for this program are $500 000 for the balance of fiscal year 1961 and $1 million for each of the fiscal years 1962 and 1963. The project is divided into the following five tasks:

Task I. Al_2O_3-coated UO_2 dispersed in graphite

Task II. BeO-coated UO_2 dispersed in graphite or BeO

Task III. Pyrolytic-carbon-coated UO_2 or UC_2 dispersed in graphite

Task IV. Optimum coated particle fuel element

Task V. Evaluation of coated particles developed by other organizations

Both process development and product evaluation, including irradiation tests, are to be performed under the first four tasks listed. Under Task V, promising particle coatings developed by other organizations will be evaluated. Companies now known to be working on fuel-particle coatings are the following:

Oxide coatings	Minnesota Mining and Manufacturing Company Nuclear Materials and Equipment Company
Pyrolytic carbon coatings	American Metal Products Company High Temperature Materials, Inc. Minnesota Mining and Manufacturing Company National Carbon Company

The fabrication experience of the various companies who have participated in the Sanderson & Porter fuel element development program should also be used as extensively as possible. The information available from other related programs, such as the General Atomic HTGR, OEEC Dragon, and the National Carbon Company fuel cycle program, should also be of great help. The experimental phase of the fuel element development effort should include an evaluation of coated particles, fuel sphere fabrication and evaluation, and the development of fuel processing techniques.

Coated Particle Evaluation

It is anticipated that much of the basic coating-evaluation work will be performed under the AEC contract at Battelle. The purpose of an experimental program would be to extend the data, where necessary, to meet specific PBRE operating requirements.

The most promising coated particles could be obtained from Battelle and private manufacturing companies and evaluated by metallographic

techniques, by oxidation or HNO_3 leaching tests, by thermal cycling, by extended high-temperature heat treatment, by testing for compatibility with graphite, and by examination and testing following neutron activation. The information thus obtained could be relayed to the producer with suggestions for product improvement where appropriate.

Fuel Sphere Fabrication and Evaluation

For the fabrication work to be significant, careful control and recording of process variables will be required, since properties such as thermal conductivity, thermal expansion, impact and abrasion resistance, oxidation resistance, and dimensional stability under irradiation can be expected to vary with the type and quantity of filler and binder, baking cycle, and temperatures used in fabricating the spheres.

Comprehensive evaluation tests would be required. Metallography techniques could be used to determine condition and distribution of the coated fuel particles and to determine the proportions of carbon and graphite, and structure of the matrix. X-ray diffraction examinations could be made to determine lattice parameters and crystallite size. Nondestructive tests, such as radiography, could be used, and "hot oil" immersion density determinations could be made on coated spheres. Mechanical and thermal examinations would include thermal shock, impact, compression, and abrasion testing. Thermal conductivity and expansion measurements would be made. Oxidation tests would be used to determine the extent of reactions with minor amounts of impurities in the coolant to ascertain need for sphere surface coatings. Fission-gas retention and radiation damage would be determined following extensive exposure.

A reasonable number of specimens to permit thorough evaluation of the fuel would be approximately 1000 balls. The cost of preparing these balls, along with the cost of evaluating coated particles and balls, is estimated to run between $300 000 and $400 000. Two types of irradiation test are being considered: (1) miniature-capsule tests to evaluate the basic fuel particle—graphite matrix, and (2) full-scale element tests. The cost of about 30 miniature capsule tests is estimated at

$1 200 000 to $1 500 000, and the cost of 20 to 30 full-scale tests might be between $2 700 000 and $4 000 000.

Fuel Reprocessing

Although the development of fuel-reprocessing procedures is not a prerequisiste to the design of a reactor experiment, an economic chemical recovery process for the spent fuel will have to be developed if the PBR or any other semihomogeneous reactor is ever to be an important long range reactor concept. Consequently work should be done on the following items along with the development of the fuel: (1) graphite disposal, (2) preparation of the residual material in a form for processing in, for example, the Thorex plant at ORNL, (3) conversion of the uranium and thorium back to the oxides or carbides and ball refabrication under fairly radioactive conditions. Further, an estimate should be made of the cost of this process in comparison with other fuel-reprocessing schemes.

The cost of developing the required fuel-reprocessing method is extremely uncertain because current AEC fuel-reprocessing technology does not encompass such a method. Disposal of the graphite ball matrix does not appear to be unreasonably difficult. Crushing or treatement with fuming nitric acid have already been used successfully in the laboratory, and if the uranium and thorium compounds are physically accessible to the leaching solution, there does not seem to be a serious problem in recovering the fuel in a form for wet processing according to established techniques. However, dense alumina is about as refractory a material as is ever encountered, and there are no known reagents which will dissolve it and which also can be contained in available equipment. Thus, if the alumina coating on the fuel particles is not damaged in the reactor, it probably will be necessary to crush such particles before leaching. While the laboratory work required to establish the steps in the process might be done for about $250 000, the engineering development of the remote mechanical and chemical systems required to operate under hot-cell conditions would cost at least $1 000 000 and perhaps as much as $3 000 000.

Pyrolytic graphite coatings might be easier to dispose of than alumina coatings, but no assurance can be given at this stage that the final costs would be different.

Development of Graphite Components

The major problem with respect to the graphite components for the PBRE is the fabrication of the large sleeves for the pebble-bed container and coating of these sleeves with an oxidation-resistant coating. Solutions to both aspects of this problem can be achieved only by manufacturing companies with extensive experience in graphite fabrication and coating.

It may be necessary to fabricate one of these sleeves in order to establish reasonable dimensional tolerances, the amount of distortion to be expected during coating, and feasible means for attaching the graphite sleeves to their steel sockets. Tests should also be made to determine whether the contemplated 1-in. taper in 8 ft is adequate to provide for easy withdrawal of one sleeve relative to another. Costs may run from $50 000 to $100 000.

Graphite Shrinkage Cracking

An extensive study of graphite shrinkage and creep is under way in connection with other reactor programs, so there is no advantage to initiating a new program for the PBRE. There is a possibility, however, that the geometry or installation of the graphite sleeves for the inner layers of the reflector could be modified in such a way as to increase their lives in the reactor before cracking begins. Structural tests would be required to evaluate the effectiveness of such modifications. If the results of this work prove favorable, it might be possible to increase the expected life of the PBRE graphite sleeves by a factor of 2. The cost of this study might run from $10 000 to $50 000.

Core Cooling Problems

Matching the gas flow distribution to the power distribution will probably require both model and full-scale tests. Schemes to be tested

would include fluting or ribbing of the inner surface of the reflector. This work should also include a statistical investigation of the void fraction distribution. The gas flow distribution radially across the core can be determined by air flow tests at room temperature with a good simulation of the full-scale Reynolds number. A variety of geometries of the top and bottom of the core should be tested to investigate the feasibility of keeping the bed free of bobbing or spinning balls under pressure drops up to double that which causes bed flotation.

It may be worthwhile to run an extended endurance test to investigate the amount of abrasion that might occur from ball bobbing or spinning under upflow conditions with some elements of the bed floating. Such a test would also give some idea of the extent to which filter clogging may prove to be a problem. The effects of various end grate geometries on ball flow through the core should also be investigated. Costs for studying gas flow distribution and developing holddown techniques are estimated to run from $100 000 to $200 000.

If the radial gas flow distribution can be matched reasonably well to the nuclear power distribution, it would be important to get some idea of the extent to which radial mixing of the cooling gas will alleviate an excessive gas temperature rise in a hot annulus. This might be done by heating the core model isothermally to perhaps 400°F with no coolant flow and then measuring the transient temperature behavior of thermocouples buried in representative balls dispersed throughout the bed as flow is resumed with cold gas. The resulting ball temperature distribution can be compared with the gas radial velocity and temperature distribution to give a good indication of the effects of mixing. Costs for this study might be $10 000 to $50 000.

Helium Containment and Fuel Handling

Containment of the helium within the high-pressure system is more than a routine design problem because (1) there has been little experience

with containment of helium at both high temperature and high pressure, particularly where closures of one sort or another are involved, and (2) much more than conventional leaktightness is required because of the contained radioactivity (including tritium). If one is to consider transporting fuel into and out of the reactor, even at reduced pressure, an elaborate system of pressure-buffered locks is required to keep the external contamination under control. Elastomeric materials cannot be used because of both the high temperature and the high radiation dose rates, and no hard-seated valves are known which can be operated repeatedly and yet give this degree of leaktightness, or anywhere near it, especially with gritty materials passing over the valve seats. The operating sequence of the locks calls for a rather intricate system of mechanical or electrical interlocks as a guarantee against operator error. The operation must be conducted in sealed chambers, and the spent fuel discharging must be done completely remotely behind heavy shielding. Finally, the equipment must be successfully checked for tightness after each operation.

Along with development of a leaktight fuel transport system it is essential to demonstrate that the ball feed mechanism assures proper distribution and flow across the core without exceeding the ball jacket impact limits. The ball-removal mechanism below the core must demonstrate positive ball movement, adequate ball cooling, and freedom from jamming.

There is no way to design a satisfactory system on paper, because the experience upon which the designer must draw does not exist. Design work will have to be accompanied by model tests to check out proposed components. When a suitable system design has been evolved, a full-scale model should be built and tested under simulated conditions of gas pressure, remote manipulation, and contamination. The testing of many modifications must be expected in the course of the work on both the small and the full-scale models. The cost of this may be from $400 000 to $1 000 000.

Helium Purification

The purity of the circulating helium must be maintained in order to limit the spread of radioactive contamination and to prevent chemical

attack on the graphite. The purification system proposed in this study is modeled to a large extent after the one designed for the EGCR, but it appears that the cleanup requirements for the PBRE are considerably more stringent. In this connection, more complete information is needed on the dynamic absorption of krypton, xenon, and iodine on charcoal at relatively high pressures (1000 psi), including the effect of iodine poisoning. Information is also needed on the kinetics of co-sorption of H_2O and CO_2 by molecular sieves at high pressures and low H_2O and CO_2 levels. More precise information is needed on the effect of the impurities on fuel-ball integrity, fission-product retention, and graphite mass transfer and dusting in the event of jacket failure. More extensive studies are required of the kinetics and reaction mechanism of the graphite-gas reactions and of the kinetics of graphite mass transfer at pressures and temperatures of interest. In particular, the maximum tolerable level of carbon-gas impurities should be determined in advance of PBRE final design, especially if the tolerable level is extremely low.

A less critical problem involves removal of particulate material from the gas stream. The PBRE design includes full-flow filters at the reactor outlet, but such devices may not be practical in large power reactors. Nonetheless, the particle filtering requirements appear to be associated with fuel-ball integrity and, hence, with chemical cleanup conditions. The development work required may cost from $50 000 to $100 000.

Maintenance Procedures

Although the maintenance procedures will not, in general, be complicated by requirements of helium containment or contaminated fuel-ball handling, the problems of personnel shielding and contamination control will be severe. Any operation for which the pressure vessel closures or ball-handling equipment must be opened will require, first, that adequate seals be established for coupling to the maintenance

equipment containers or that the work be accomplished under hot-cell conditions. Maintenance work under such conditions is complicated because there must be a physical barrier between the operator and the equipment. In some cases it will be practical to provide windows for viewing, but in other cases the work must be done entirely remotely. Cases in point are replacement of control rods and drives, replacement of fuel-discharge mechanism components, and removal of the core graphite sleeves. Costs are likely to run from $200 000 to $500 000.

The direct access to the blowers assumed in this study is based on the fission-product release being very small and the possibility of removing any activity that lodges in the blower casings by wet decontamination. The proposed program for the PBRE in-pile loop will aid considerably in determining the equilibrium activity levels in the helium stream, possible methods of lowering the activity, and the amount, location, and nature of deposited fission products. This work could profitably be augmented and correlated with work under way at ORNL with ORR loop No. 2 and with the General Atomic in-pile work at the GETR. In any event, it remains to be demonstrated that the scheme presented for hydraulically isolating the blower casings is feasible and that all trash and decontaminating solution residue can be prevented from leaking into the rest of the system. It would be very desirable to test those decontaminating procedures on components, such as blowers, which can be obtained from in-pile loops used for testing ceramic fuel elements not contained in metal capsules. The cost of conducting these tests and evaluating the results is likely to run from $100 000 to $150 000.

Summary of Research and Development Costs

The cost estimates are summarized below:

Fuel element development			
Ball fabrication and testing	$ 300 000	to $	400 000
Irradiation testing	3 900 000	to	5 500 000
Coating of large graphite pieces	50 000	to	100 000

Structural tests of graphite sleeves	$ 10 000	to	$ 50 000
Core cooling problems			
Gas flow distribution and bed holddown	100 000	to	200 000
Radial gas mixing and temperature distribution	10 000	to	50 000
Helium containment and fuel handling	400 000	to	1 000 000
Helium purification	50 000	to	100 000
Maintenance procedures			
Mechanical operations	200 000	to	500 000
Decontamination techniques in situ	100 000	to	150 000
Total	$5 120 000	to	$8 050 000

The total cost of the research and development required in order to provide a firm Title II design of the PBRE and to assure reasonably satisfactory operation of the reactor for a number of years is thus estimated to be in the range $5 000 000 to $8 000 000. (If a firm design of a fuel reprocessing facility is also desired, an additional cost of from $1 million to $3 million may be required for research and development.) This estimate is based on the probable effort required to solve the problems that are clearly foreseen. However, it has been general experience that difficulties and complications always arise from the problems that are <u>not</u> foreseen, and, in a project of the magnitude and complexity of an experimental version of an advanced power reactor, estimates of the required research and development are usually understated by sizeable amounts.

21. CONSTRUCTION COSTS

While the preliminary nature of the design work to date makes firm cost estimates out of the question, the preliminary designs presented in this report are sufficient to give some idea of the cost of the facility for a pebble-bed reactor experiment. The cost estimates were prepared by tabulating the quantity and cost data available for the EGCR, estimating quantities of material or surface area for the corresponding components of the PBRE, and scaling the costs according to the quantities involved. Tables 21.1 and 21.2 summarize these estimates. There are substantial uncertainties in these costs that stem in part from the preliminary character of the PBRE design and in part from the fact that many of the EGCR estimates are not yet supported by actual cost experience.

In reviewing the cost data of Tables 21.1 and 21.2, it is apparent that major savings relative to the EGCR should accrue from the much smaller power output of the PBRE. Further savings accrue from utilization of some of the services and facilities already provided for the EGCR, including the access road, water main, and electric power lines. Other factors which help to reduce costs are elimination of a number of major items, including the turbine and generator, with its related switchgear and control equipment, the experimental cells of the EGCR, and much of the floor space for special activities.

Reactor Building

The cost of the reactor building for the PBRE is about half that of the EGCR. While it might be thought that reducing the reactor power rating by a factor of 10 should reduce the cost by more than a factor of 2, the building diameter is quite insensitive to reactor power output. The pressure vessel must be protected from fast-neutron radiation by a thickness of roughly 3 ft of graphite and thermal shielding material; at least 3 ft of space for construction work must be provided between the pressure vessel and the shield; and the thickness of the shielding

Table 21.1. Summary of Cost Data and Estimates for the EGCR and PBRE

Cost Code	Description	EGCR		PBRE	
		Quantity	Cost	Quantity	Cost
21.210	Access road and water main	0.876 mi	180 000	0.1 mi	45 000
21.211	General yard improvements	120 000 ft^2	660 000	40 000 ft^2	160 000
21. 212	Reactor service building	512 000 ft^3 17 500 ft^2	432 000	250 000 ft^3	250 000
	Turbine building	665 000 ft^3	611 000	90 000 ft^3	90 000
	Control building	358 000 ft^3 25 200 ft^2	373 000	150 000 ft^3	150 000
	Guard, stack, chlorine, etc., buildings	800 ft^2	300 000		95 000
	River pumping station	30 000 gpm	527 000	5000 gpm	100 000
21.213	Reactor building		3 902 000		1 960 000
21.214	Experimental cells	7000 ft^2	930 000		
22.220	Reactor equipment		3 527 000		777 000
22.221	Heat transfer system		2 249 000		624 000
22.222	Fuel handling and storage		2 358 000		600 000
22.224	Radioactive waste treatment		93 000		100 000
22.225	Instrumentation and controls		1 812 000		800 000
22.226.7	Steam system		533 000		200 000
23	Turbine generator unit	25 Mw	1 267 000		
24	Accessory electrical equipment		1 235 000		310 000
25	Miscellaneous power plant equipment		128 000		60 000
	Transmission plant		198 000		30 000
	Miscellaneous		146 000		70 000

Table 21.1 (Continued)

Description	EGCR Cost	PBRE Cost
Total direct costs	$21 461 000	$6 421 000
Indirect costs (general and administrative, at 12% of direct)[a]		770 000
Total direct and indirect costs		7 191 000
Engineering, design, and inspection (at 15%)[a,b]		1 078 000
Total direct + indirect + engineering		8 269 000
Contingency (at 10% of direct + indirect + engineering)[a]		827 000
Total	$21 461 000	$9 096 000

[a]Charges assigned are based on those used in the USAEC "Civilian Power Reactor Program, Part 3, Status Report on Gas-Cooled Reactors," 1959.

[b]Actual indirect, engineering, design, inspection, and contingency figures are not yet available for the EGCR.

Table 21.2. Approximate Quantity and Cost Estimates for the Reactor Building and Reactor for the EGCR and the PBRE

Cost Code	Description	EGCR		PBRE	
		Quantity	Cost	Quantity	Cost
21.213.1	Excavation and gunniting	53 250 yd^3	120 000	26 000 yd^3	50 000
.3	Concrete	23 200 yd^3	1 565 000	12 500 yd^3	800 000
.4	Containment shell and related items	2 600 000 lb	1 761 000	1 300 000 lb	880 000
.6	Building services and miscellaneous		456 000		230 000
21.213	Total reactor building		3 902 000		1 960 000
22.220.1	Reactor vessel and internals	700 000 lb	1 600 000	150 000 lb	320 000
.2	Control rods and drives	21	480 000	6	137 000
.4	Cooling facilities		400 000		40 000
.6	Graphite	313 000 lb	887 000	64 000 lb	200 000
	Miscellaneous		160 000		80 000
	Total		3 527 000		777 000
22.221.11	Main blowers and drives	6200 hp	465 000	500 hp	200 000
.12	Main coolant piping and valves		237 000	3500 lb	3 500
.31	Steam generators	88.1 Mw	700 000	10 Mw	100 000
.32	Attemperators		132 000		
.4	Coolant charging and discharging	244 000 ft^3	184 000	20 000 ft^3	50 000
.5	Coolant purification equipment		193 000		200 000
.6	Burst slug detection system		162 000		
	Miscellaneous		176 000		70 000
22.221	Total heat transfer system		2 249 000		624 000

around the reactor must be at least 8 ft. These requirements lead to a minimum outside diameter for the reactor shield of 30 ft for a core diameter of 18 in., whereas on the same basis the shield diameter would be only about 45 ft for a 1000-Mw(t) reactor having a 15-ft-diam core. Similar considerations lead to a height for a small reactor experiment which is not far from that for a large power plant, since removal of the afterheat by thermal convection requires about 50 ft of vertical height between the mid-planes of the reactor and the steam generator. Access to the top of the steam generator and the bottom of the core require minimal distances which come out to be much the same for both experimental and full-scale reactors. Fortunately, the weight of the containment vessel varies as the square of the diameter, since structural stability considerations ordinarily determine the thickness of the containment shell. As a result, the 80-ft-diam PBRE containment vessel requires only about half as much steel as the 115-ft-diam EGCR vessel.

Reactor

In examining the reactor costs it is apparent that the reduced output of the PBRE is responsible for marked reductions in costs. The reactor pressure vessel is much smaller and hence weighs much less. In addition, the design is such that no complex machining operations are required. The number of control rod drives is greatly reduced, as are the weight of the graphite, the size and power requirements for the blowers, the steam generator capacity, and the helium pumping and storage capacity. The compact configuration chosen largely eliminates the piping, with its associated bellows, required for the EGCR main gas system. The burst-slug detection system is completely eliminated. The fuel-handling system is much less complex and hence should be much less expensive. Facilities for handling radioactive wastes are likely to be much the same for the two installations. The instrumentation and control requirements will probably be much the same, except that the burst-slug detection system will be eliminated from the PBRE, and hence a large saving in the cost can be effected.

Possible Reductions in Construction Costs

As discussed in the section on servicing equipment and procedures, the plant layout proposed in Chapter 6 included generous space allocations to facilitate servicing and maintenance operations. A preliminary review of the design indicates that several modifications might be made which ought to reduce the cost of the reactor building. The most obvious change is that discussed in the section on servicing equipment and operations, i.e., the bottom of the containment shell could be raised 38 ft relative to the reactor and the service machine ram could be located in a 12-ft-i.d. well extending down from the bottom of the containment shell, as shown in Fig. 21.1. This would reduce the depth of the excavation, the amount of concrete required in the reactor building, and the amount of steel in the containment shell. The space lost in this fashion for installation of equipment would be partly offset by utilization of the space gained in the ends of the service canyon (shown in Fig. 6.6) for the service machine ram and its drive mechanism. The helium storage tanks could be located to one side of the ram and reactor in the upper part of what had been the ram service canyon, while the storage tanks for the radioactive fluid from decontamination operations could be located in what had been the other end of this canyon. The incremental cost of the well for the service machine ram would be about $40 000.

This modification should result in a net saving in excavation costs of about $15 000, a reduction in the cost of concrete of about $185 000, and a reduction in the containment shell cost of about $90 000, for a total saving of approximately $290 000.

Some reduction in construction costs might be effected through moving the control rooms for the service machine and fuel-handling equipment to the main reactor control room. This might be advantageous in that it would place the operating personnel outside the containment shell during these operations and thus provide greater safety for them. If this were done, much of the concrete in what is the ground floor of Fig. 6.3 could be eliminated, along with a set of hatches to the hot cell. With this floor eliminated, it would then seem appropriate to

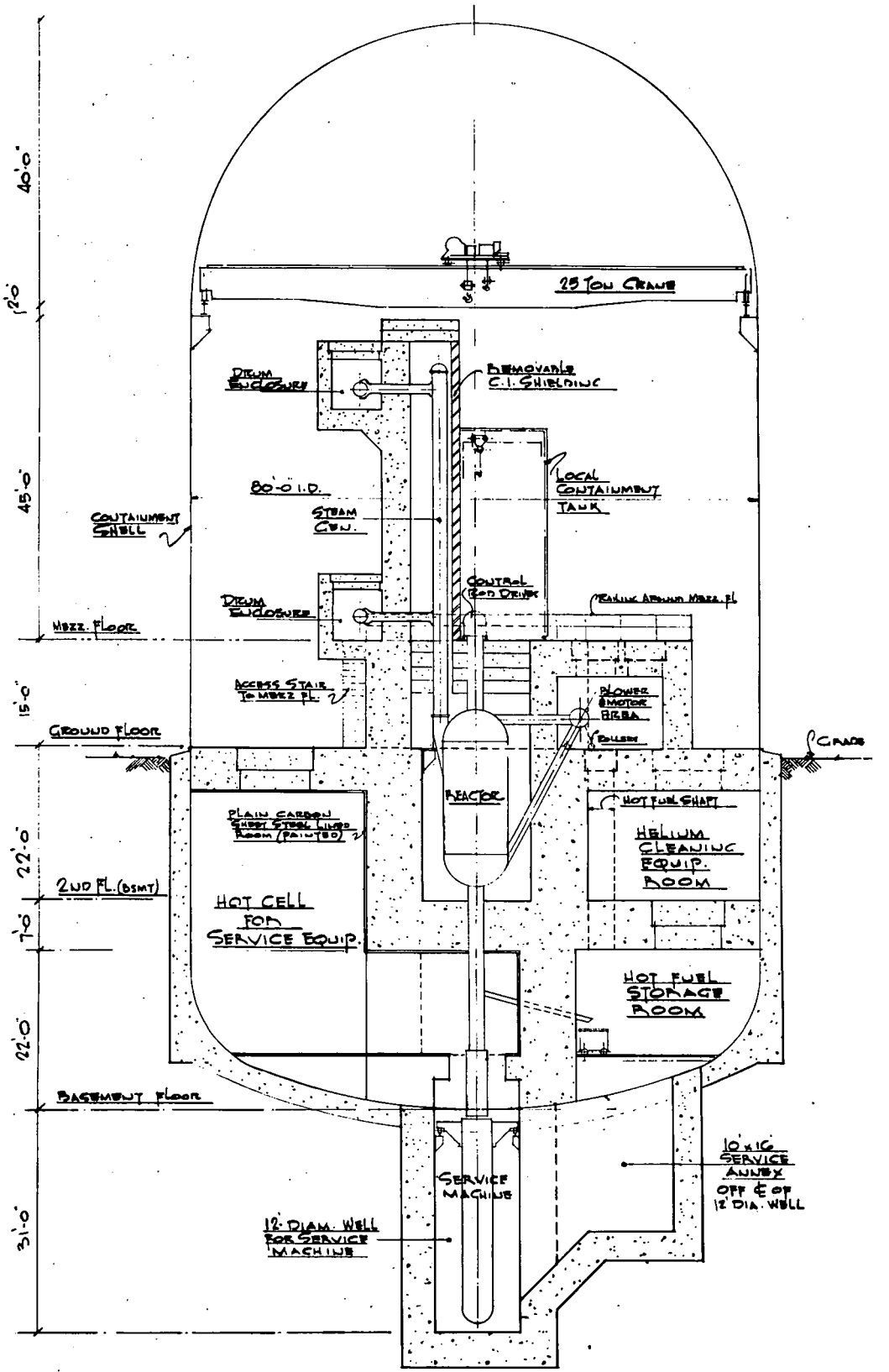

Fig. 21.1. Section Through Alternate Containment Vessel Layout.

move the ground level line to the top of the ceiling over the hot cell. This would reduce the excavation cost by perhaps $10 000 and should cut the cost of the concrete by about $90 000 to give a net saving of about $100 000 for this modification. It would have the further advantage that it would raise the bottom of the containment shell above the water level of Melton Hill Dam when it is completed if the suggested site were used.

The cost of the containment shell could be reduced if the top of the shell were lowered 10 ft so that the crane would clear the top of the steam generator shield by 2 ft. The saving in the containment shell should be about $20 000. The crane shown in the design presented in Chapter 6 could be removed and replaced with a gantry crane which could be moved about on the ground floor of the reactor building. If this were done, the top of the containment shell could be lowered sufficiently to save another $25 000. However, this latter change would not only reduce both the headroom and the utility of the crane, and thus the flexibility of operations after completion of the facility, but it would probably result in increases in construction costs during the installation of major items of equipment. Thus this last modification seems definitely unwise.

In summary, it appears that possibly $400 000 in the cost of the reactor building could be saved by reducing the depth of the containment vessel and placing the service machine ram in a well, lowering the ground level to the top of the hot cell, and lowering the top of the containment shell to give a 2-ft clearance between the crane bridge and the top of the steam generator shield. These modifications have all been incorporated in the revised vertical section through the reactor facility shown in Fig. 21.1

The building for reactor control and servicing operations also may be larger than necessary. It is possible that its size might be reduced by as much as 35%, in which case its cost (including contingencies, etc.) might be reduced by about $150 000. This, coupled with a possible reduction of $400 000 in the cost of the reactor building, together with the associated top charges, could reduce the cost estimate for the complete facility by about $780 000 to give a total cost of $8 316 000.

These modifications and their consequences should be studied carefully before a decision is made as to whether they should be incorporated in subsequent designs. Particular attention should be given to various servicing operations that might be required and the detailed equipment and facilities needed to carry them out expeditiously. A careful study should also be made of space requirements for equipment in the reactor building. Hot cell operations should be examined to determine whether a room should be provided beside the hot cell so that personnel could work with long-handled tools through a concrete wall only a few feet thick for servicing the spent fuel-handling system or other contaminated components.

While there is no doubt that reductions in the size of the reactor building would reduce the cost of the steel and concrete, it is entirely possible that these savings might be more than offset by higher engineering costs for the design of servicing equipment for operation in cramped quarters, not to mention the increased cost of more complex equipment or the higher operating costs associated with longer shutdowns to accomplish a given job. It may be that further study will show that the space provided in the layouts of Chapter 6 is somewhat inadequate rather than overly generous and that the facility will require modifications which will increase rather than decrease its cost relative to the estimates in Tables 21.1 and 21.2.

Fuel Fabrication Costs

The facility construction costs given in Table 21.1 do not include the cost of the fuel. An estimate of the fabrication cost of the fuel element spheres for the first core loading represents an extrapolation from present experience. While only 8500 spheres would be required to fill the core, about that many more might be required to fill the supply and drain lines. Two estimates were obtained on the fabrication of 20 000 fuel elements of a reference design, i.e., 1 1/2-in.-diam Si-SiC-coated graphite spheres containing 5 g of 100 to 200 μ spherical UC_2 particles each coated with 30 to 50 μ of pyrolytic carbon. The two cost estimates were summarized in Table 21.3.

Table 21.3. Cost Estimate for Fabricating 20 000 Fuel Element Spheres

Cost of fissionable material excluded

	Estimate A	Estimate B[a]
Fabricating UC_2 spherical particles	$ 75 000	$100 000
Coating of UC_2 particles	24 000	30 000
Fabricating fueled spheres	30 000	15 000
Applying Si-SiC surface coating	20 000	80 000
Total	$149 000	$225 000

[a]Estimate originally based on 10 000 spheres.

Neither of these estimates makes any allowance for scrap or other loss of material during processing. The major differences between the two estimates lie in the cost of the Si-SiC surface coating of $1 vs $4 per ball. While estimates were not available for the cost of alumina in place of pyrolytic graphite coatings on the particles, it appears likely that the coating process might cost $100 000 rather than $24 000 to $30 000.

BIBLIOGRAPHY

Sanderson & Porter Reports

1. S&P 1965-17, Current Fuel Element Developments and Their Effects on the Pebble Bed Reactor Porgram, May 10, 1960.
2. S&P 1965-20, Progress Report for May 1960.
3. S&P 1965-22, Progress Report for June 1960.
4. S&P 1965-23, Progress Report for July 1960.
5. NYO-9058, Quarterly Progress Report, February 1, 1960-April 30, 1960.
6. S&P 1964-18, Progress Report for April 1960.
7. S&P 1964-20, Progress Report for May 1960.
8. S&P 1964-22, Progress Report for June 1960.
9. S&P 1964-23, Progress Report for July 1960.
10. NYO-9060, Subsurface Coatings for Fueled Graphite Spheres.
11. NYO-2708, Concerning Several Methods for the Removal of Fission Products from a Gas Cooled Reactor.
12. NYO-9059, Thorium Oxide Infiltration of Graphite Spheres.
13. NYO-9068, Adsorption of Radioactive Gases on Activated Carbon.

ORNL Reports and Memoranda

1. A. M. Perry et al., A Study of Graphite-Moderated Th-U^{233} Breeder Systems, ORNL-2666, January 18, 1960.
2. W. B. Cottrell et al., The HGCR-1, A Design Study of a Nuclear Power Station Employing a High-Temperature Gas-Cooled Reactor with Graphite-UO_2 Fuel Elements, ORNL-2653, rev., July 14, 1959.
3. H. L. Falkenberry et al., A Preliminary Study of a Direct-Cycle Steam-Cooled Reactor for Merchant Ship Propulsion, ORNL-2759, September 8, 1959.
4. W. Häfele and M. Tsagaris, The Fast Multiplication Effect of Beryllium Oxide in Reactors, ORNL-2849, November 30, 1959.
5. A. P. Fraas, Beryllium Oxide Development Tests, CF-59-12-5, rev., February 10, 1960.

6. A. M. Perry, Gas-Cooled Breeder Reactors, CF-59-10-116, October 29, 1959.

7. A. M. Perry, Economic Effects of Gas-Cooled Reactor Parameters, CF-59-12-40, December 9, 1959.

8. M. N. Ozisik and R. B. Korsmeyer, Dependence of Core Power Density on Reactor Parameters in a Gas-Cooled Reactor, CF-60-1-65, January 27, 1960.

9. R. S. Carlsmith, Power Density in Ceramic-Fuel-Element Gas-Cooled Reactors, CF-59-8-87, August 14, 1959.

10. M. N. Ozisik and R. B. Korsmeryer, The Core Power Density in a Gas-Cooled Reactor with Parallel Plate Fuel Assemblies, CF-60-4-5, April 4, 1960.

11. R. S. Carlsmith, Nuclear Characteristics of BeO-Moderated Cores vs Graphite-Moderated Cores, CF-60-1-43, January 15, 1960.

12. R. S. Carlsmith, Protactinium Losses in a BeO-Moderated Reactor, CF-60-1-108, January 27, 1960.

13. R. S. Carlsmith, Pressure Vessel Exposure to Fast Neutrons, CF-60-1-75, January 21, 1960.

14. A. P. Fraas, Flow Stability in Heat Transfer Matrices under Boiling Conditions, CF-59-11-1, November 1, 1959.

15. G. C. Robinson, Containment Vessel Cost and Buckling Considerations, CF-59-9-52, September 15, 1959.

16. A. P. Fraas and M. N. Ozisik, Relative Capital Charges and Fuel Cycle Costs for All-Ceramic Gas-Cooled Reactors, CF-60-7-41, July 20, 1960, to be issued.

17. W. B. Cottrell et al., Fission-Product Release from UO_2, ORNL-2935, September 13, 1960.

18. A. P. Fraas, Nuclear Gas Engine, CF-58-9-12, November 28, 1958.

19. A. P. Fraas and A. M. Perry, Summary of Advanced Design Work on Gas-Cooled Reactors at ORNL, 1958 to 1960, CF-60-7-40, July 15, 1960.

20. A. P. Fraas, Preliminary Designs for Two Integrated Gas-Cooled Reactor Core and Steam Generator Units, ORNL-2752 (rough draft dated June 1, 1960).

References on Heat Transfer and Pressure Drop in Packed Beds of Spheres

1. W. E. Renz, Friction and Transfer Coefficients for Single Particles and Packed Beds, Chem. Eng. Prog., 48, No. 5, May 1952, p. 247.

2. E. B. Baumeister and C. O. Bennett, Fluid-Particle Heat Transfer in Packed Beds, AIChE Journal, 4, No. 1, March 1958, p. 69.

3. L. R. Galloway, W. Komarnicky, and N. Epstein, Effect of Packing Configuration on Mass and Heat Transfer in Beds of Stacked Spheres, Can. J. Chem. Eng., Dec. 1957, p. 139–150.

4. D. Thoenes, Jr. and H. Kramers, Mass Transfer from Spheres in Various Regular Packings to a Flowing Fluid, Chem. Eng. Sci., 8 (1958), p. 271–83.

5. T. Shirai, Fluid Flow through Fixed Beds, Representation of the Fluid Friction with the Drag Coefficient of Single Particle, C_d, Kagaku Kikai, 20 (1956), p. 434.

6. S. Yagi, D. Kunii, and Y. Shimomuira, Studies on Heat Transfer in Packed Bed with Fluid Flow, Kagaku Kikai, 21 (1957), p. 342.

7. C. M. Thatcher, Local Rates of Mass Transfer in a Packed Bed of Spheres with Orifice Entry of Air, University microfilms publication No. 19722, p. 231, University of Michigan, Ann Arbor.

8. J. Weisman, Effect of Void Volume and Prandtl Modulus on Heat Transfer in Tube Banks and Packed Beds, AIChE Journal, 1 (1955), p. 342.

9. W. O. Smith et al., Packing of Homogeneous Spheres, Phys. Rev., 34, Nov. 1, 1929, p. 1271.

10. S. S. Kwong and J. M. Smith, Radial Heat Transfer in Packed Beds, Ind. Eng. Chem., 49, No. 5, May 1957, p. 894–906.

11. D. A. Garton and F. Sterry, Hydraulically Packed, Inverted Sphere Beds, AERE-ED/R-1882.

12. E. McCoy and A. J. Townnend, Heat Transfer in Static Granular Beds, Information Bibliography IGRL-IB-CA, No. 23, 1957, A.E.A. Risley.

13. M. Ristić and Z. Zarić, Packed-Bed Fuel Assembly for a Gas-Cooled Heterogeneous Reactor, Vol. 7, p. 746, 1958, Second United Nations International Conference on the Peaceful Uses of Atomic Energy.

14. W. H. Denton, C. H. Robinson, and R. S. Tibbs, The Heat Transfer and Pressure Loss in Fluid Flow through Randomly Packed Spheres, Part I. HPC-35, June 28, 1949.

15. L. H. S. Roblee, R. M. Baird, and J. W. Tierney, Radial Porosity Variation in Packed Beds, AIChE Journal, Dec. 1958, p. 460.

16. S. Ergun, Mass-Transfer Rate in Packed Columns, Chem. Eng. Prog., 48, 1952, p. 227.

17. J. C. Chu, G. Kalil, and W. A. Wetteroth, Heat Transfer in a Fluidized Bed, Chem. Eng. Prog., 49, 1953, p. 141.

18. J. J. Martin, W. L. McCabe, and C. C. Monrad, Pressure Drop through Stacked Spheres, Effect of Orientation, Chem. Eng. Prog., 47, No. 2, Feb. 1951, p. 91–4.

19. D. A. Plautz and H. F. Johnstone, Heat and Mass Transfer in Packed Beds, AIChE J., 1, No. 2, June 1955, p. 193–9.

20. M. B. Glaser and G. Thodos, Heat and Momentum Transfer in the Flow of Gases through Packed Beds, AIChE Journal, 4, No. 1, March 1958, p. 63–68.

21. G. M. Anderson, Temperature Distribution in Spherical Pellets, AECD-4109, May 1953.

22. W. H. Denton, The Packing and Flow of Spheres, AERE-E/R-1095, Jan. 1953.

23. E. J. Cairns and J. M. Pransnitz, Velocity Profile, Tis. Ex. Che., 51, No. 12, Dec. 1959, p. 1441–4.

24. T. Akehata and K. Sato, Flow Distribution in Packed Beds, Kagaku Kikai, 22 (1958), p. 430.

ORNL
Central Files Number
60-10-63

Distribution

1. S. A. Beall
2. M. Bender
3. A. L. Boch
4. R. B. Briggs
5. R. S. Carlsmith
6. C. E. Center (K-25)
7. W. R. Chambers
8. R. A. Charpie
9. J. H. Coobs
10. W. B. Cottrell
11. F. L. Culler
12. E. P. Epler
13. D. E. Ferguson
14. J. Foster
15. A. P. Fraas
16. B. L. Greenstreet
17. T. Hikido
18. W. O. Harms
19. R. B. Korsmeyer
20. P. G. Lafyatis
21. R. N. Lyon
22. H. G. MacPherson
23. W. D. Manly
24. E. R. Mann
25. H. C. McCurdy
26. A. B. Meservey
27. M. N. Ozisik
28. P. Patriarca
29. A. M. Perry
30. R. C. Robertson
31. M. W. Rosenthal
32. G. Samuels
33. H. W. Savage
34. A. W. Savolainen
35. O. Sisman
36. M. J. Skinner
37. I. Spiewak
38. J. C. Suddath
39. J. A. Swartout
40. D. B. Trauger
41. C. S. Walker
42. A. M. Weinberg
43. M. E. Whatley
44. C. E. Winters
45. M. M. Yarosh

46-49. ORNL – Y-12 Technical Library Document Reference Section
50-99. Laboratory Records Department
100. Laboratory Records Department, ORNL R.C.
101-103. Central Research Library